A MICROPROCESSOR-BASED SYSTEM FOR PROTECTION OF POWER TRANSFORMERS

A Thesis

Submitted to the College of Graduate Studies and Research

in Partial Fulfilment of the Requirements

for the Degree of

Doctor of Philosophy

in the

Department of Electrical Engineering

University of Saskatchewan

by

TARLOCHAN SINGH SIDHU

Saskatoon, Saskatchewan

September 1989

The author claims copyright. Use shall not be made of the material contained herein without proper acknowledgement, as indicated on the copyright page.

COPYRIGHT

The author has agreed that the Library, University of Saskatchewan, may make this thesis freely available for inspection. Moreover, the author has agreed that permission for extensive copying of this thesis for scholarly purposes may be granted by the Professor who supervised the thesis work recorded herein or, in his absence, by the Head of the Department or the Dean of the College in which the thesis work was done. It is understood that due recognition will be given to the author of this thesis and to the University of Saskatchewan in any use of the material in this thesis. Copying or publication or any other use of this thesis for financial gain without approval by the University of Saskatchewan and the author's written permission is prohibited.

Requests for permission to copy or to make any other use of the material in this thesis in whole or in part should be addressed to:

Head of the Department of Electrical Engineering,
University of Saskatchewan,
Saskatoon, Canada S7N 0W0.

ACKNOWLEDGEMENTS

The author would like to express his gratitude and appreciation to Drs. M.S. Sachdev and H.C. Wood for their guidance and consistent encouragement throughout the course of this work. Their advice and assistance in the preparation of this thesis is thankfully acknowledged.

Special thanks are due to his wife, Sarabjit, for understanding and encouragement throughout the course of this work.

The author takes this opportunity to acknowledge the encouragement and moral support provided by his parents, and all other family members.

The author is thankful to Mr. Lloyd Litwin for his help in fabrication of the printed circuit boards. Special thanks are extended to Mrs. Parmjit Grewal and Mr. Virinder Grewal for their help in the prepration of the thesis.

Financial assistance provided by the NSERC and the University of Saskatchewan is thankfully acknowledged.

UNIVERSITY OF SASKATCHEWAN

Electrical Engineering Abstract 89A318

A MICROPROCESSOR-BASED SYSTEM FOR PROTECTION OF POWER TRANSFORMERS

Student: T.S. Sidhu Supervisors: Dr. M.S. Sachdev
Dr. H.C. Wood

Ph.D. Thesis Submitted to the
College of Graduate Studies and Research
September 1989

ABSTRACT

Differential, overcurrent and ground fault relays are used for protecting transformers in electric power systems. Several algorithms, that perform these functions and are suitable for implementation on microprocessors, have been proposed in the past.

This thesis describes and evaluates an improved technique for modelling inverse-time overcurrent relay characteristics. This technique, which is used in a digital overcurrent relaying algorithm, is simple and requires a modest amount of computer memory. The proposed algorithm performs most computations in an off-line mode and, therefore, requires few on-line computations. The performance of the algorithm is evaluated using computer simulations. Some test results are reported in the thesis.

Digital algorithms that can detect winding faults in power transformers are described in the thesis. The algorithms use non-linear models of a transformer to determine its health. The algorithms take the non-linearity and hysteresis of the transformer core into account, however, these do not explicitly become part of the algorithms. They are suitable for protecting transformers whose winding currents can not be measured at the terminals. The performance of the algorithms is studied for a variety of operating conditions simulated on a digital computer using the Electro-Magnetic Transient Program (EMTP). Some results of the simulation studies are reported in the thesis.

The proposed algorithms for overcurrent relaying and transformer winding protection are implemented in a microprocessor-based system. The design, implementation and testing of the system are presented in the thesis. The system includes a man-machine interface for changing relay settings and relay software, and for uploading the relay signals for further analysis. The performance of the system was checked in the laboratory. The testing procedure and some test results are also presented.

Table of Contents

COPYRIGHT i
ACKNOWLEDGEMENTS ii
ABSTRACT iii
TABLE OF CONTENTS v
LIST OF FIGURES ix
LIST OF TABLES xvii

1. INTRODUCTION 1

1.1. Background 1
1.2. Protection of Power Systems 1
1.3. Transformer Protection and Monitoring Using Microprocessors 3
1.4. Objectives of the Thesis 4
1.5. Outline of the Thesis 5

2. TRANSFORMER PROTECTION AND MONITORING 8

2.1. Faults in a Power Transformer 8
2.2. Transformer Protection 9
2.2.1. Fuses 10
2.2.2. Overcurrent protection 10
2.2.3. Differential protection 11
2.2.3.1. Voltage restraint 16
2.2.3.2. Harmonic restraint 17
2.2.3.3. Percentage bias 18
2.2.4. Ground fault protection 18
2.2.5. Other relays 19
2.3. Instrumentation and Alarms 20
2.4. Off-line Gas Analysis 22
2.5. Economic Considerations 23
2.6. Summary 23

3. DIGITAL PROTECTION AND MONITORING OF TRANSFORMERS 25

3.1. Digital Algorithms for Differential Protection 25
3.1.1. Waveshape identification technique 26
3.1.2. Harmonic restraint algorithms 26
3.1.2.1. Fourier algorithms 27
3.1.2.2. Least error squares technique 28
3.1.2.3. Finite impulse response technique 31
3.1.2.4. A recursive filtering approach 32

3.1.2.5. Other technique 33
3.1.3. Flux-restraint algorithm 33
3.1.4. Algorithms using transformer models 35
3.2. Discussion of the Algorithms for Differential Relays 40
3.3. Ground Fault Algorithms 41
3.4. Overcurrent Relay Algorithms 43
3.4.1. Modelling time-current characteristics 43
3.4.2. Previously proposed algorithms 48
3.5. Microprocessor-Based Relays for Transformer Protection 50
3.6. Microprocessor-Based Monitoring 52
3.7. Summary 54
4. THE PROPOSED ALGORITHM FOR A DIGITAL OVER-CURRENT RELAY 55
4.1. Introduction 55
4.2. Modelling of the Relay Characteristics 56
4.2.1. The technique 57
4.2.2. Evaluation of the proposed technique 61
4.3. Computing the RMS Value 66
4.4. The Algorithm 69
4.4.1. Development of the algorithm 69
4.4.2. Selection of the target number 72
4.4.3. Reset characteristics 74
4.4.4. Functions of the algorithm 76
4.4.4.1. Off-line computations 77
4.4.4.2. On-line operations 78
4.5. Test Results 79
4.6. Summary 80
5. PROPOSED ALGORITHMS FOR TRANSFORMER WINDING PROTECTION - VERSION-I 86
5.1. Introduction 86
5.2. Detecting Faults in a Single-Phase Transformer 87
5.2.1. The algorithm 90
5.3. Detecting Faults in Three-Phase Transformers 91
5.3.1. Wye-wye tranformers 92
5.3.1.1. The algorithm 94
5.3.2. Delta-wye transformers 96
5.3.2.1. The algorithm 103
5.4. Testing of Algorithms 106
5.4.1. Generating input signals 108
5.4.2. Simulating low-pass filters 108
5.4.3. Test results - a single-phase transformer 110
5.4.4. Test results - three-phase transformers 111
5.4.4.1. A wye-wye transformer 111
5.4.4.2. A delta-wye transformer 117
5.5. Summary 124

6. PROPOSED ALGORITHMS FOR TRANSFORMER WINDING PROTECTION - VERSION-II 131

6.1. Introduction 131
6.2. Detecting Faults in a Single-Phase Transformer 132
6.2.1. The algorithm 133
6.3. Detecting Faults in Three-Phase Transformers 133
6.3.1. Wye-wye tranformers 134
6.3.1.1. The algorithm 135
6.3.2. Delta-wye transformers 135
6.3.2.1. The algorithm 139
6.4. Testing the Algorithms 140
6.4.1. Test results - a single-phase transformer 140
6.4.2. Test results - three-phase transformers 143
6.4.2.1. A wye-wye transformer 143
6.4.2.2. A delta-wye transformer 149
6.5. Comparison of Version-I and Version-II 154
6.6. Summary 155

7. DESIGN, IMPLEMENTATION AND TESTING OF THE PROTECTION AND MONITORING SYSTEM 157

7.1. Design Requirements 158
7.2. Design Of the System Hardware 158
7.2.1. Isolation and analog scaling 160
7.2.2. Data acquisition system 162
7.2.3. Microcomputer 168
7.3. The System Software 169
7.3.1. Data acquisition software 170
7.3.2. Application software 173
7.3.2.1. Overcurrent relaying software 173
7.3.2.2. Winding protection software 174
7.4. Testing the Protection System 175
7.4.1. Testing overcurrent relays 177
7.4.2. Testing the transformer protection scheme 179
7.5. Summary 195

8. SUMMARY AND CONCLUSIONS 201

8.1. Summary and Conclusions 201
8.2. Suggestions for Future Work 205

REFERENCES 207

Appendix A. DETERMINITION OF MODELLING COEFEICIENTS 213

Appendix B. ESTIMATION OF THE RMS VALUE 216

B.1. Introduction 216
B.2. Mathematical Background 216

Appendix C. SIMULATION OF TRANSFORMER CONDITIONS 219

Appendix D. DESIGN OF THE LOW-PASS DIGITAL FILTER 223

Appendix E. CIRCUIT DIAGRAM OF I/O BOARD 225

Appendix F. DETERMINITION OF TRANSFORMER WINDING PARAMETERS 228

F.1. Procedure and Results 228

Appendix G. RESULTS FROM TESTING OF THE WINDING PROTECTION SCHEME 232

List of Figures

Figure 2.1:	Circuit diagram of a differential protection relay for a delta-wye transformer.	12
Figure 2.2:	Magnetizing characteristics of a typical single-phase power transformer.	13
Figure 2.3:	Magnetizing inrush phenomenon in a power transformer.	14
Figure 2.4:	Circuit diagram showing the arrangement of the restraining and operating coils in a voltage-restrained differential relay.	17
Figure 2.5:	Circuit diagram for a ground fault relay for delta-wye transformers.	19
Figure 3.1:	Equivalent tee circuit of a single phase two winding transformer.	38
Figure 3.2:	Equivalent pi circuit of a single-phase three-winding transformer.	39
Figure 3.3:	Time-current characteristics of the Westinghouse CO-7 type overcurrent relay. (Source: Westinghouse Doc. No. I.L. 41-100F, Curve No. 418247)	44
Figure 3.4:	Time-current characteristics of the Westinghouse CO-9 type overcurrent relay. (Source: Westinghouse Doc. No. I.L. 41-100F, Curve No. 418249)	45
Figure 4.1:	Operating time vs time dial setting characteristic of the Westinghouse CO-7 relay at 5.0 times the pick-up current.	58
Figure 4.2:	Calculated values of $\frac{K\Delta T}{t_r}$ for the Westinghouse CO-7 overcurrent relay.	72
Figure 4.3:	Linear reset characteristics provided by Equation 4.14.	76
Figure 4.4:	Exponential reset characteristics provided by Equation 4.15.	77
Figure 5.1:	A circuit diagram of a two-winding single-phase transformer.	88
Figure 5.2:	The proposed error vs primary-volts characteristic of the relay.	91
Figure 5.3:	A circuit diagram of a two-winding three-phase wye-wye transformer.	93

Figure 5.4:	A circuit diagram of a two-winding three-phase delta-wye transformer.	97
Figure 5.5:	Magnitude response of the low-pass filter.	109
Figure 5.6:	Phase response of the low-pass filter.	110
Figure 5.7:	Instantaneous values of the primary and secondary voltages and the primary current for a magnetizing inrush condition in the single-phase transformer. The transformer was connected to the supply at time 0.0 s.	113
Figure 5.8:	Errors and values of the trip index for a magnetizing inrush condition in the single-phase transformer. The transformer was connected to the supply at time 0.0 s.	114
Figure 5.9:	Errors and values of the trip index for an external fault condition in the single phase transformer. The fault was applied at time 0.0 s.	114
Figure 5.10:	Errors, values of the trip index and the trip command for a ground fault in the primary windings of the single-phase transformer. The fault was applied on time 0.0 s.	115
Figure 5.11:	Errors, values of the trip index and the trip command for a low-level fault in the secondary windings of the single-phase transformer. The fault was applied on time 0.0 s.	116
Figure 5.12:	Instantaneous values of the primary currents for a magnetizing inrush condition in the wye-wye transformer. The transformer was connected to the supply at time 0.0 s.	118
Figure 5.13:	Instantaneous values of the primary and secondary voltages for a magnetizing inrush condition in the wye-wye transformer. The transformer was connected to the supply at time 0.0 s.	119
Figure 5.14:	Errors and values of the trip indices for (a) phase A, (b) phase B and (c) phase C during a magnetizing inrush condition in the wye-wye transformer. The transformer was connected to the supply at time 0.0 s.	120
Figure 5.15:	Errors and values of the trip indices for (a) phase A, (b) phase B and (c) phase C during a fault external to the wye-wye transformer. The fault was applied at time 0.0 s.	121
Figure 5.16:	Errors and values of the trip indices for (a) phase A, (b) phase B and (c) phase C. during an internal fault in the wye-wye transformer. (d) Trip command issued by the algorithm vs time. The fault was applied at time 0.0 s.	122
Figure 5.17:	Instantaneous values of the primary currents for a	125

magnetizing inrush condition in the delta-wye transformer. The transformer was connected to the supply at time 0.0 s.

Figure 5.18: Instantaneous values of the primary and secondary voltages for a magnetizing inrush condition in the delta-wye transformer. The transformer was connected to the supply at time 0.0 s. 126

Figure 5.19: Errors and values of the trip indices for a magnetizing inrush condition in the delta-wye transformer when (a) phase A, (b) phase B or (c) phase C is used as the "Reference Phase". The transformer was connected to the supply at time 0.0 s. 127

Figure 5.20: Errors and values of the trip indices for a fault external to the delta-wye transformer when (a) phase A, (b) phase B or (c) phase C is used as the "Reference Phase". The fault was applied at time 0.0 s. 128

Figure 5.21: Errors and values of the trip indices for an internal fault in a delta-wye transformer when (a) phase A, (b) phase B or (c) phase C is used as the "Reference Phase". (d) Trip command issued by the algorithm vs time. The fault was applied at time 0.0 s. 129

Figure 6.1: Errors and values of the trip index for a magnetizing inrush condition in the single-phase transformer. The transformer was connected to the supply at time 0.0 s. 141

Figure 6.2: Errors and values of the trip index for a fault external to the single phase transformer. The fault was applied at time 0.0 s. 141

Figure 6.3: Errors, values of the trip index and the trip command for a ground fault in the primary windings of the single-phase transformer. The fault was applied at time 0.0 s. 142

Figure 6.4: Errors, values of the trip index and the trip command for a low-level fault on the secondary windings of the single-phase transformer. The fault was applied at time 0.0 s. 143

Figure 6.5: Errors and values of the trip indices for (a) phase A, (b) phase B and (c) phase C during a magnetizing inrush condition in the wye-wye transformer. The transformer was connected to the supply at time 0.0 s. 146

Figure 6.6: Errors and values of the trip indices for (a) phase A, (b) phase B and (c) phase C during a fault external to the wye-wye transformer. The fault was applied at time 0.0 s. 147

Figure 6.7:	Errors and values of the trip indices for (a) phase A, (b) phase B and (c) phase C during an internal fault in the wye-wye transformer. (d) Trip command issued by the algorithm vs time. The fault was applied at time 0.0 s.	148
Figure 6.8:	Errors and values of the trip indices for a magnetizing inrush condition in the delta-wye transformer when (a) phase A, (b) phase B or (c) phase C is used as the "Reference Phase". The transformer was connected to the supply at time 0.0 s.	151
Figure 6.9:	Errors and values of the trip indices for a fault external to the delta-wye transformer when (a) phase A, (b) phase B or (c) phase C is used as the "Reference Phase". The fault was applied at time 0.0 s.	152
Figure 6.10:	Errors and values of the trip indices for an internal fault in the delta-wye transformer when (a) phase A, (b) phase B or (c) phase C is used as the "Reference Phase". (d) Trip command issued by the algorithm vs time. The fault was applied at time 0.0 s.	153
Figure 7.1:	A block diagram of the microprocessor-based protection system.	159
Figure 7.2:	The isolation and analog scaling circuit for an input voltage signal.	161
Figure 7.3:	The isolation, analog scaling and conversion circuit for a input current signal.	162
Figure 7.4:	A block diagram of the data acquisition module.	164
Figure 7.5:	A circuit diagram showing the connections of the buffer, analog filter and sample and hold components of a channel of the data acquisition system.	166
Figure 7.6:	A circuit diagram showing the connections of the multiplexer and A/D converter of a module.	167
Figure 7.7:	Organization of the application software.	175
Figure 7.8:	Magnetizing inrush currents recorded by the microprocessor-based system. The transformer was connected to the supply at 0.0167 s.	188
Figure 7.9:	The primary and secondary voltages recorded by the microprocessor-based system during a magnetizing inrush condition. The transformer was connected to the supply at 0.0 s.	189
Figure 7.10:	Errors and values of the trip indices for a magnetizing inrush condition when (a) phase A, (b) phase B or (c) phase C is used as the "Reference Phase". The transformer was connected to the supply at time 0.0167 s.	190
Figure 7.11:	Errors and values of the trip indices for an external	191

	fault involving phases A and C when (a) phase A, (b) phase B or (c) phase C is used as the "Reference Phase". The fault was applied at 0.0167 s.	
Figure 7.12:	The primary and secondary voltages recorded by the microprocessor-based system for an internal fault on the secondary side involving phases A and C. The transformer was connected to the supply at 0.0 s and the fault was applied at 0.0167 s.	192
Figure 7.13:	The primary currents recorded by the microprocessor-based system for an internal fault on the secondary side involving phases A and C. The transformer was connected to the supply at 0.0 s and the fault was applied at 0.0167 s.	193
Figure 7.14:	Errors and values of the trip indicies for a two-phase internal fault when (a) phase A, (b) phase B or (c) phase C is used as the "Reference Phase". The fault was applied at 0.0167 s.	194
Figure 7.15:	The primary and secondary voltages recorded by the microprocessor-based system when the transformer is switched with an internal fault on the secondary side that involves phase C. The transformer was connected to the supply at 0.0167 s.	197
Figure 7.16:	The primary currents recorded by the microprocessor-based system when the transformer is switched with an internal fault on the secondary side that involves phase C. Transformer was connected to the supply at 0.0167 s.	198
Figure 7.17:	Errors and values of the trip indicies when the transformer is switched on with a single phase internal fault when (a) phase A, (b) phase B or (c) phase C is used as the "Reference Phase". The transformer was connected to the supply at time 0.0167 s.	199
Figure 7.18:	Errors and values of the trip indicies for a single phase internal fault when (a) phase A, (b) phase B or (c) phase C is used as the "Reference Phase". The fault was applied at 0.0167 s.	200
Figure C.1:	Model of an N-winding single-phase transformer.	220
Figure C.2:	A combination of windings equivalent to a partly short-circuited winding in the transformer model.	221
Figure C.3:	Current-flux characteristics of the model transformer.	222
Figure E.1:	Circuit diagram of the piggy-back I/O board.	226
Figure G.1:	Errors and values of the trip indices for a magnetizing inrush condition when (a)phase A, (b)phase B or (c)phase C is used as the "Reference phase". The transformer was connected to the supply at 0.0167 s.	233

Figure G.2: Errors and values of the trip indices for a magnetizing inrush condition when (a)phase A, (b)phase B or (c)phase C is used as the "Reference phase". The transformer was connected to the supply at 0.0167 s. 234

Figure G.3: Errors and values of the trip indices for a magnetizing inrush condition when (a)phase A, (b)phase B or (c)phase C is used as the "Reference phase". The transformer was connected to the supply at 0.0167 s. 235

Figure G.4: Errors and values of the trip indices for a magnetizing inrush condition when (a)phase A, (b)phase B or (c)phase C is used as the "Reference phase". The transformer was connected to the supply at 0.0167 s. 236

Figure G.5: Errors and values of the trip indices for a magnetizing inrush condition when (a)phase A, (b)phase B or (c)phase C is used as the "Reference phase". The transformer was connected to the supply at 0.0167 s. 237

Figure G.6: Errors and values of the trip indices for an internal fault on the secondary side that short circuits phases A, B and C through a resistance of 1.2 ohms and when (a)phase A, (b)phase B or (c)phase C is used as the "Reference phase". Trip command issued by the system is shown in (d). The fault was applied at 0.0167 s. 238

Figure G.7: Errors and values of the trip indices for a condition when the transformer is switched on with an internal fault on secondary side that short circuits phases A and B through a resistance of 1.2 ohms and when (a)phase A, (b)phase B or (c)phase C is used as the "Reference phase". Trip command issued by the system is shown in (d). The transformer was connected to the supply at 0.0167 s. 239

Figure G.8: Errors and values of the trip indices for a condition when the transformer is switched on with an internal fault on secondary side that short circuits phases A, B and C through a resistance of 1.2 ohms and when (a)phase A, (b)phase B or (c)phase C is used as the "Reference phase". Trip command issued by the system is shown in (d). The transformer was connected to the supply at 0.0167 s. 240

Figure G.9: Errors and values of the trip indices for a condition when the transformer is switched on with an internal fault on primary side that short circuits phase A through a resistance of 1.2 ohms and when 241

(a)phase A, (b)phase B or (c)phase C is used as the "Reference phase". Trip command issued by the system is shown in (d). The transformer was connected to the supply at 0.0167 s.

Figure G.10: Errors and values of the trip indices for an internal fault on the primary side that short circuits phases A and C through a resistance of 1.2 ohms and when (a)phase A, (b)phase B or (c)phase C is used as the "Reference phase". Trip command issued by the system is shown in (d). The fault was applied at 0.0167 s. 242

Figure G.11: Errors and values of the trip indices for a condition when the transformer is switched on with an internal fault on the primary side that short circuits phases A and B through a resistance of 1.2 ohms and when (a)phase A, (b)phase B or (c)phase C is used as the "Reference phase". Trip command issued by the system is shown in (d). The transformer was connected to the supply at 0.0167 s. 243

Figure G.12: Errors and values of the trip indices for an internal fault on the primary side that short circuits phases A and B through a resistance of 1.2 ohms and when (a)phase A, (b)phase B or (c)phase C is used as the "Reference phase". Trip command issued by the system is shown in (d). The fault was applied at 0.0167 s. 244

Figure G.13: Errors and values of the trip indices for an internal fault on the secondary side that short circuits phases B and C through a resistance of 1.2 ohms and when (a)phase A, (b)phase B or (c)phase C is used as the "Reference phase". Trip command issued by the system is shown in (d). The fault was applied at 0.0167 s. 245

Figure G.14: Errors and values of the trip indices for an internal fault on the secondary side that short circuits phase A through a resistance of 1.2 ohms and when (a)phase A, (b)phase B or (c)phase C is used as the "Reference phase". Trip command issued by the system is shown in (d). The fault was applied at 0.0167 s. 246

Figure G.15: Errors and values of the trip indices for an external fault that involves phases A and ground when (a)phase A, (b)phase B or (c)phase C is used as the "Reference phase". The fault was applied at 0.0167 s. 247

Figure G.16: Errors and values of the trip indices for a three phase external fault when (a)phase A, (b)phase B or 248

(c)phase C is used as the "Reference phase". The fault was applied at 0.0167 s.

Figure G.17: Errors and values of the trip indices for a condition when the transformer is switched on with an external fault involving phases A and B and when (a)phase A, (b)phase B or (c)phase C is used as the "Reference phase". The transformer was connected to the supply at 0.0167 s. 249

Figure G.18: Errors and values of the trip indices for a condition when the transformer is switched on with an external fault involving phase C and ground and when (a)phase A, (b)phase B or (c)phase C is used as the "Reference phase". The transformer was connected to the supply at 0.0167 s. 250

List of Tables

Table 4.1:	Coefficients of the polynomial described by Equation 4.1 for modelling the Westinghouse CO-7 overcurrent relay at 1.5 to 20 times the nominal relay current.	59
Table 4.2:	Coefficients of the polynomial described by Equation 4.1 for modelling the Westinghouse CO-9 overcurrent relay at 1.5 to 20 times the nominal relay current.	60
Table 4.3:	Differences (in cycles of 60 Hz) between the relay operating times calculated by using Equation 4.1 and the published operating times for the CO-7 relay.	62
Table 4.4:	Differences (in cycles of 60 Hz) between the relay operating times calculated by using Equation 4.1 and the published operating times for the CO-7 relay.	63
Table 4.5:	Differences (in cycles of 60 Hz) between the relay operating times calculated by using Equation 4.1 and the published operating times for the CO-9 relay.	64
Table 4.6:	Differences (in cycles of 60 Hz) between the relay operating times calculated by using Equation 4.1 and the published operating times for the CO-9 relay.	65
Table 4.7:	Coefficients of the least error square filters for calculating the real and imaginary components of the fundamental frequency components.	67
Table 4.8:	Values of the the coefficients for calculating the rms value of a phasor using the two-region approximation approach.	68
Table 4.9:	Differences (in cycles of 60 Hz) between the operating times of the simulated CO-7 overcurrent relay and the published times for time dial settings of 0.5, 1.0, 2.0, 3.0, 4.0 and 5.0.	82
Table 4.10:	Differences (in cycles of 60 Hz) between the operating times of the simulated CO-7 overcurrent relay and the published times for time dial settings of 6.0, 7.0, 8.0, 9.0, 10.0 and 11.0.	83
Table 4.11:	Differences (in cycles of 60 Hz) between the operating times of the simulated CO-9 overcurrent relay and the published times for time dial settings of 0.5, 1.0, 2.0, 3.0, 4.0 and 5.0.	84
Table 4.12:	Differences (in cycles of 60 Hz) between the operating	85

times of the simulated CO-9 overcurrent relay and the published times for time dial settings of 6.0, 7.0, 8.0, 9.0, 10.0 and 11.0.

Table 5.1: Values of the trip indices during internal faults in a wye-wye transformer. 96

Table 5.2: Criteria used by the decision-logic module for detecting internal faults. 107

Table 5.3: List of transformer conditions used to test the performance of the proposed algorithms. 112

Table 5.4: Maximum values of the trip indices for magnetizing inrush, overexcitation and external fault conditions in the wye-wye transformer. 112

Table 5.5: Time required by the trip indices to exceed the threshold for internal fault conditions in a wye-wye transformer. 117

Table 5.6: Maximum values of the trip indices for magnetizing inrush, overexcitation and external fault conditions in the delta-wye transformer. 123

Table 5.7: Time required by the trip indices to exceed the threshold for internal fault conditions in the delta-wye transformer. 123

Table 6.1: Maximum values of the trip indices for magnetizing inrush, overexcitation and external fault conditions in the wye-wye transformer. 144

Table 6.2: Time required by the trip indices to exceed the threshold for internal fault conditions in the wye-wye transformer. 145

Table 6.3: Maximum values of the trip indices for magnetizing inrush, overexcitation and external fault conditions in the delta-wye transformer. 149

Table 6.4: Time required by the trip indices to exceed the threshold for internal fault conditions in the delta-wye transformer. 150

Table 6.5: Number of arithmetic operations required to implement Version-I and Version-II of the algorithms. 156

Table 7.1: A list of the Input/Output signals for the data acquisition system. 168

Table 7.2: Calibration of the isolation and analog scaling, and data acquisition blocks. 177

Table 7.3: The published operating times, emulated operating times and their differences for the Westinghouse CO-7 relay when the relay current is 2.5 and 4.0 times the pick-up value. 180

Table 7.4: The published operating times, emulated operating times and their differences for the Westinghouse CO-7 relay when the relay current is 7.0 and 10.0 times the pick-up value. 181

Table 7.5:	The published operating times, emulated operating times and their differences for the Westinghouse CO-7 relay when the relay current is 15.0 and 20.0 times the pick-up value.	182
Table 7.6:	The published operating times, emulated operating times and their differences for the Westinghouse CO-9 relay when the relay current is 2.5 and 4.0 times the pick-up value.	183
Table 7.7:	The published operating times, emulated operating times and their differences for the Westinghouse CO-9 relay when the relay current is 7.0 and 10.0 times the pick-up value.	184
Table 7.8:	The published operating times, emulated operating times and their differences for the Westinghouse CO-9 relay when the relay current is 15.0 and 20.0 times the pick-up value.	185
Table 7.9:	A list of conditions used to test the performance of transformer winding protection system.	186
Table C.1:	Winding resistance and leakage inductance of a single-phase transformer model.	221
Table E.1:	Description of the interconnections between the output port and data acquisition system.	227
Table E.2:	Description of the interconnections between the input port and data acquisition system.	227
Table F.1:	Transformer voltage and current phasors during the short-circuit test.	230
Table F.2:	Resistance and inductance of the primary and secondary windings of the test transformer.	231

1. INTRODUCTION

1.1. Background

A power system generates, transmits and distributes electrical energy. The system includes facilities, such as, generating stations, switching stations, transmission lines and distribution networks. These elements occasionally experience faults resulting from insulation failures. These failures are either due to aging of insulation, or due to over voltages caused by atmospheric disturbances and switching surges. Occurrence of a fault can cause damage to equipment, severe drop in voltage, loss of synchronism and substantial loss of revenue due to interruption of service. A system element should, therefore, be protected from damage due to faults and abnormal operating conditions.

1.2. Protection of Power Systems

Electrical equipment, such as generators, transformers and transmission lines are protected by relays. Their function is to detect the presence of faults, determine their locations and initiate opening of circuit breakers to isolate the faulted section from the system. Generally, a power system is divided into protection zones; each zone is protected by a set of relays [1]. In the event of a fault in a zone, protective relays of that zone open circuit breakers which disconnect the zone from the remaining system. This prevents further damage and consequent shut down of the power system.

A protection zone normally consists of a generator, a transformer, a transmission line, a distribution line or a load. Several different type of protective relays are used for generator protection. These include differential,

rotor earth fault, negative sequence current, overvoltage, overcurrent, loss of excitation and reverse power relays. A transmission line is protected by overcurrent, pilot, distance or differential relays or by a combination of these relays. In case of transformers, differential, earth fault, overcurrent and Bucholz relays are used. Distribution lines are protected by fuses and overcurrent, directional overcurrent and distance relays.

In early developments of power systems, fuses were used to protect generators, transformers and lines. A significant improvement in system protection was achieved with the development of electromechanical relays which could initiate tripping of a circuit breaker or circuit breakers [2]. Sensitive, selective and high speed relays were developed as the complexity of power systems increased. The development of solid state electronic relays started in the 1950's. These relays were not generally accepted by the users because of the high failure rates of electronic components, and inadequacy of their designs. Later developments used newer semiconductor technology and improved designs. Today, several kinds of solid state relays are being used in power systems [3].

Rapid advances in digital processor technology have prompted the application of microprocessors in protective relays [4, 5]. The use of real-time computations for system protection was proposed in 1966 by Last and Stalewsky [6]. In a pioneering paper, Rockefeller [7] proposed an overall philosophy for using a digital computer to protect the entire equipment in a substation. The concept of using a single computer alongwith its back up for protection of a substation has been discarded in favour of using individual microprocessors for each major relaying task. Many researchers are of the view that the long range economic trend favours the use of digital processors for protection.

Transformer protection and monitoring is a challenging area of power system protection using microprocessors. This area has, therefore, received

attention from many researchers [4, 5]. In 1969, Rockefeller [7] proposed a method for differential protection of transformers. Since then several schemes have been reported in the literature.

1.3. Transformer Protection and Monitoring Using Microprocessors

A major emphasis of research in the area of microprocessor-based protection of transformers has been the development of suitable algorithms. These algorithms perform differential, earth fault and overcurrent protection tasks. Initial designs of algorithms for digital differential protection were conceptually similar to the designs of conventional relays [8, 9, 10, 11, 12]. They used second harmonic components of the difference currents to restrain relay operation during a magnetizing inrush condition. During internal faults, they calculated the fundamental frequency phasors representing through and difference currents and compared them. Digital filtering and correlation techniques were used to calculate the phasors. The operating voltages of power systems and lengths of transmission lines have increased substantially during the last twenty years. This has increased the possibilities of the differential currents during internal transformer faults containing large amounts of harmonic components. This condition, if it occurs, can cause a relay to restrain even during an internal fault. The security of differential relays using the harmonic restraint principle is, therefore, a matter of concern. Recently, some algorithms have been reported in the literature that do not rely on the harmonic components for restraining relays during magnetizing inrush conditions [13, 14, 15, 16]. These algorithms use currents in transformer windings and transformer parameters for making appropriate decisions. Terminals of delta connected windings are not usually brought out of a transformers tank. The winding currents are, therefore, not available for use in protective relays.

Three digital algorithms for overcurrent relays have been suggested in the past [17, 18, 19]. These algorithms are conceptually similar to each

other except that they use different techniques for modelling relay characteristics and for computing of the relay currents. Also, they require considerable amount of real-time computations.

On-line monitoring of transformers using microprocessors is still in early stages of development. Microprocessor-based systems that can monitor parameters of a transformer have been reported in the literature [20, 21]. However, a microprocessor-based system that monitors transformer parameters and performs analysis to determine the health of a transformer has recently been reported by Poyer [22, 23]. Design and testing of three prototype microprocessor-based relays for transformer protection have been reported by researchers [12, 17, 24]. These relays provide differential, earth faults and overcurrent protection.

It seems that the existing digital algorithms for transformer protection have limitations and, therefore, improved digital algorithms are needed. Research reported in this thesis was aimed at developing appropriate digital algorithms and implementing them in a microprocessor-based system.

1.4. Objectives of the Thesis

The major objectives of the work reported in this thesis were to

1. develop digital algorithms for detecting winding faults in single-phase and three-phase transformers,
2. develop a technique for modelling time-current characteristics of overcurrent relays, and then use the technique for developing a digital algorithm for overcurrent relays, and
3. design, implement and test a microprocessor-based system for protection and monitoring of power transformers.

1.5. Outline of the Thesis

The thesis is organized in nine chapters and seven appendices. The first chapter introduces the subject of the thesis and describes its organization. Chapter 2 reviews the faults which affect power transformers and the relays which are used to detect those faults. The phenomenon of magnetizing inrush experienced by transformers is explained. This illustrates the significance of including a feature to restrain relays during magnetizing inrush conditions. Chapter 2 also describes the instruments that are used for measuring and monitoring transformer parameters.

Chapter 3 reviews the previously proposed algorithms for differential, ground fault and overcurrent protection of transformers. Limitations of these algorithms are identified. Three microprocessor-based relays for transformer protection, reported in the literature, are briefly described. A recent development in the application of microprocessors for monitoring transformer parameters is also presented.

A technique for modelling time-current characteristics of overcurrent relays is proposed in Chapter 4. This technique is then used to develop a digital algorithm for overcurrent protection. The algorithm requires only a few on-line computations because most of the calculations are done in the off-line mode. The performance of the algorithm was checked using digital computer simulations. Some results obtained from the simulation studies are included.

Chapter 5 proposes digital algorithms that can detect winding faults in single-phase and three-phase transformers. The algorithms are based on a non-linear model of a transformer instead of using harmonic components of the differential currents. The algorithms can protect three-phase delta-wye transformers even if currents in the delta winding can not be measured. The non-linearity and hysteresis of the transformer core are taken into account but they do not become part of the algorithms. The algorithms were

tested on a digital computer by using data generated by the Electro-Magnetic Transient Program (EMTP). Some results are also included in Chapter 5.

Chapter 6 describes Version-II of the algorithms for digital protection of transformer windings. These algorithms are conceptually similar to those proposed in Chapter 5 except that the winding resistances are neglected and the rectangular rule is used for numerical integration. These algorithms were tested using the same data as was used to test Version-I of the algorithms. Some test results are included in Chapter 6. The performance of Version-I and Version-II of the algorithms was compared and the results of the comparisons are also included.

Chapter 7 describes the design, implementation and testing of a microprocessor-based system for protection and monitoring of transformers. The system uses algorithms of Chapters 4, 5 and 6 to protect a transformer during external faults and winding faults. The system also has facilities for monitoring transformer parameters. The design requirements of the proposed system are identified. Hardware and software that meet the specified requirements are described. The proposed system was implemented and its performance was checked in the laboratory. The implementation and testing procedures are described. Test results demonstrating the performance of the system are included.

Chapter 8 includes a summary and conclusions drawn from the work reported in this thesis. A list of references is given in Chapter 9.

This thesis contains seven appendices. Appendix A describes a procedure for calculating the coefficients of a polynomial for modelling time-current characteristics of overcurrent relays. Appendix B presents a technique that estimates the rms value of a fundamental frequency component from its real and imaginary components. Appendix C lists the parameters of

a transformer used to model internal and external faults on the EMTP. The procedure for simulating faults and operating conditions is also described. A procedure to transform the transfer function of a fourth-order Bessel-type low-pass analog filter to its equivalent digital filter is described in Appendix D. Appendix E provides the design and interface details of an I/O board designed for use in the microprocessor-based system. Appendix F describes a procedure to determine the resistance and inductance of the windings of the transformer used to test the microprocessor-based system. Appendix G presents several cases which illustrate the performance of the winding protection scheme of the microprocessor-based system.

The specific contributions made by this project include the following:

1. An improved technique for modelling overcurrent relay characteristics has been developed. The technique is described in Chapter 4.

2. A digital overcurrent relaying algorithm that uses the proposed modelling technique is also reported in Chapter 4.

3. Two versions of a new digital relaying algorithm for detecting winding faults in single-phase and three-phase transformers have been developed. Version-I is described in Chapter 5, and Version-II is presented in Chapter 6.

4. A microprocessor-based system for protecting single-phase and three-phase transformers has been designed, implemented, and tested. The details are reported in Chapter 7.

2. TRANSFORMER PROTECTION AND MONITORING

Power system protection and developments in protection and monitoring of power transformers are briefly presented in Chapter 1. Power transformers experience a variety of faults and abnormal operating conditions which are briefly discussed in this chapter. Relays for detecting faults in transformers and isolating the affected transformer from the remaining system are briefly reviewed. Slowly developing electrical faults in oil-filled transformers can be detected by using gas analysis and this aspect is discussed in this chapter. Economic considerations in applying protection to power transformers are then outlined. Instruments generally used for monitoring the health of power transformers are also described in this chapter.

2.1. Faults in a Power Transformer

Faults affecting a power transformer can be divided into two categories, faults outside the protection zone of the transformer classified as through faults and faults in the protection zone of the transformer classified as internal faults.

Some external faults are short circuits which are limited practically by the transformer reactance only. The fault currents are very high because the reactance of a transformer is usually small. If these fault currents are allowed to persist, they can extensively damage the transformer. In such cases, the transformer must be disconnected to avoid damage. It is not essential to disconnect a transformer from the system if the fault currents flowing in a transformer are not excessive or do not persist for a long time.

Internal faults can be divided into two categories; incipient faults and short circuits, such as, phase to phase, phase to ground and inter-turn faults. Phase to phase faults on the terminals or in the transformer are rare. However, a transformer equipped with a tap changer usually experiences single phase to ground faults in the tap changer which sometimes develop into phase to phase faults. Single-phase to ground winding faults are mainly due to bushing failures and flash over in the transformer tank. Bushing failures generally occur due to flashover caused by surges, ageing, contamination, cracking, moisture, low oil level and external short circuits caused by birds. The severity of these faults depends on the system parameters, the method of grounding the system neutral and the transformer design.

Most internal faults involving transformer windings are inter-turn faults. These faults are caused by localised burning of conductors and breakdown of the inter-turn insulation of a coil. Initially, turn-to-turn insulation failure does not involve a large enough part of the winding to draw sufficient current from the system. Therefore, it is difficult to detect an inter-turn fault until it extends to involve a large section of the winding.

Majority of incipient faults which are also internal faults include core failure due to insulation breakdown or shorted laminations. Other incipient faults include deterioration of the transformer oil, oil leakage and auxiliary system failures. Most incipient faults do not pose immediate danger to a transformer. However, if they are left undetected, they can develop into major faults.

2.2. Transformer Protection

Different approaches are used to protect a transformer. Even identical transformers, applied differently in a power system, are protected using different philosophies. The philosophy of protection used is influenced by the size and importance of the transformer. Small transformers are usually protected by fuses and, overcurrent and instantaneous earth fault relays. Dif-

ferential, and gas accumulator and oil surge detection relays are used for protecting large power transformers [2].

2.2.1. Fuses

Fuses are commonly used to protect transformers of upto 5 MVA capacity. Fuses protect transformers from internal and in some cases from external faults. Fuses are economical, require little maintenance and do not need a dc power supply. Blowing of one fuse on a three phase transformer does not isolate it from the remaining two phases. This operating mode is detrimental to the connected loads. Therefore, special protection must be added to avoid single-phasing. Protection from internal faults provided by fuses is, however, limited. Sensitive devices for protecting from internal faults are, therefore, provided.

2.2.2. Overcurrent protection

An external fault can damage a transformer if it is allowed to persist. The resulting overload can cause overheating of the winding and, ultimately, insulation failure. Overcurrent relays are often used to disconnect a transformer from the faulted system before it is damaged. These relays can also protect small transformers from internal faults. Inverse-time overcurrent (o/c) relays are generally used for this purpose. The pick-up current of an o/c relay is selected to take advantage of the overload capabilities of the transformer. Fast relay operation is, therefore, not necessary. Because the inverse-time overcurrent relays provide limited protection from internal faults, instanteous overcurrent units are used for clearing major internal faults. These units are set to pick-up at currents higher than the maximum through fault current.

2.2.3. Differential protection

Current differential relays are commonly used for protecting 10 MVA and larger power transformers. These relays are connected to current transformers in such a manner that net operating currents in the relay are the differences between the currents entering and leaving the protection zone, all currents referred to a common base. Differential relays compare the outputs of the current transformers installed on the primary and secondary sides of a transformer. Figure 2.1 shows a typical differential protection arrangement for a two-winding delta-wye three-phase transformer. In this case, the primary and secondary line currents are not in phase, they are displaced by 30 electrical degrees. To eliminate the phase shift, the primary ct's are connected in wye and secondary ct's are connected in delta.

The transformer primary and secondary currents are in phase and are equal in magnitude during normal operating conditions and external faults. Therefore, the operating coil of the differential relay does not carry any current. An internal fault upsets this balance and causes currents to flow in the operating windings of the relay.

An internal transformer fault is not the only cause for the presence of differential currents. Non-linear phenomena are experienced which result in operating currents in the differential relay even when the transformer is not faulted. These are; magnetizing inrush, differences in the characteristics of ct's used on the primary and secondary sides of the transformer and the ratio mismatch of the ct's used. These phenomena are briefly described in this section. The objective is to illustrate the significance of including a restraint feature to avoid tripping when these phenomena occur.

Magnetizing inrush

Consider a single-phase transformer whose magnetizing characteristics are shown in Figure 2.2. When this transformer is switched off, the mag-

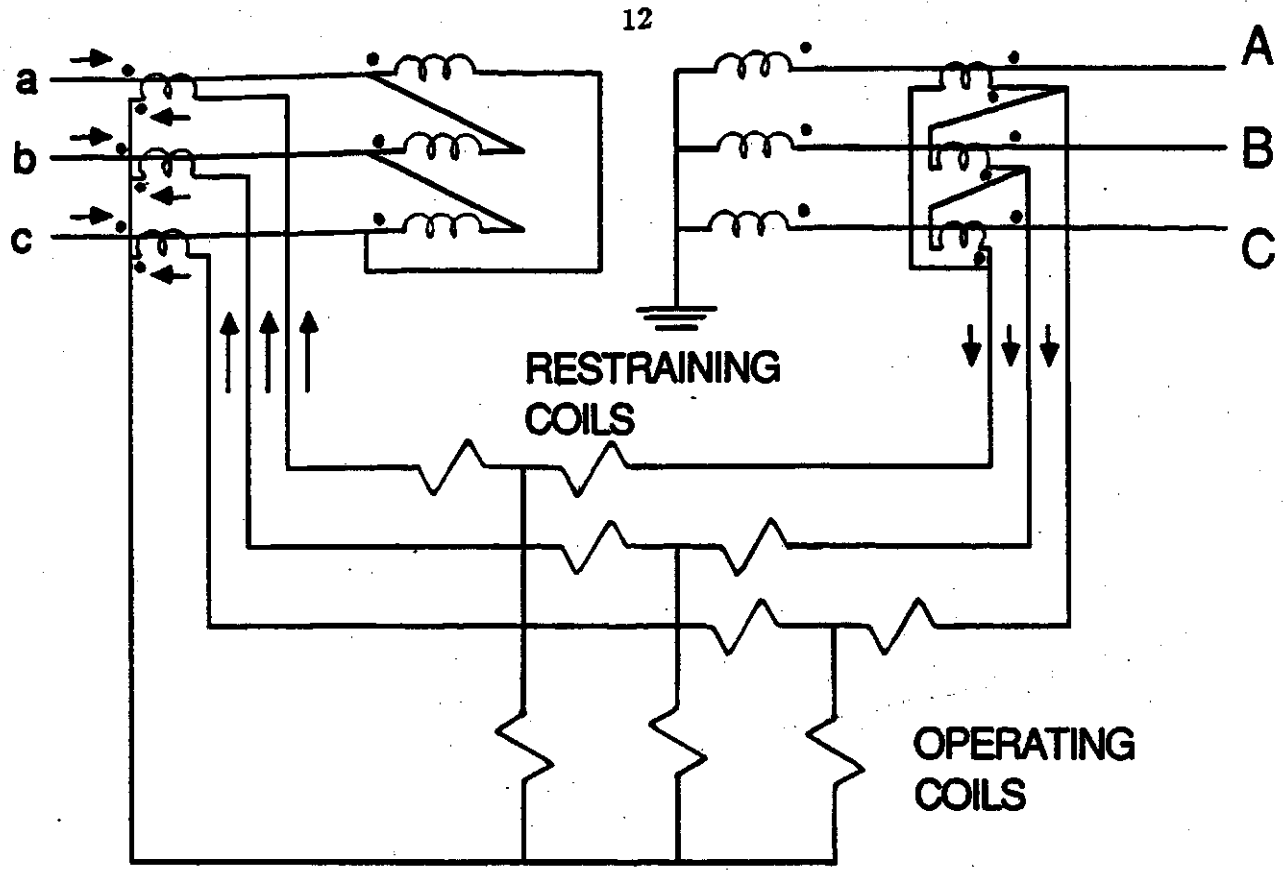

Figure 2.1: Circuit diagram of a differential protection relay for a delta-wye transformer.

netizing current follows the hystersis loop to zero when the flux density is $+B_r$ as shown in Figure 2.2. The magnetizing current, i_2 and the flux density, B_2 at the instant of switching-off, t_1, are shown in Figure 2.3. At this instant, the current passes through zero when the flux density is $+B_r$. If the transformer was not switched off, the current and flux density waveforms would have followed the dotted curves.

Assume that the transformer is re-energised at instant, t_2, when the flux density would normally be $-B_{max}$. Since the magnetic flux can not be instantly created or destroyed, the flux density starts at the end of curve B_2 with the residual value B_r and traces curve B_3 instead of starting with its normal value ($-B_{max}$ in this case). This curve is a sinusoid riding a dc offset. As a result, the transformer core saturates. The magnetizing current required to produce the flux is drawn from the power system. The current,

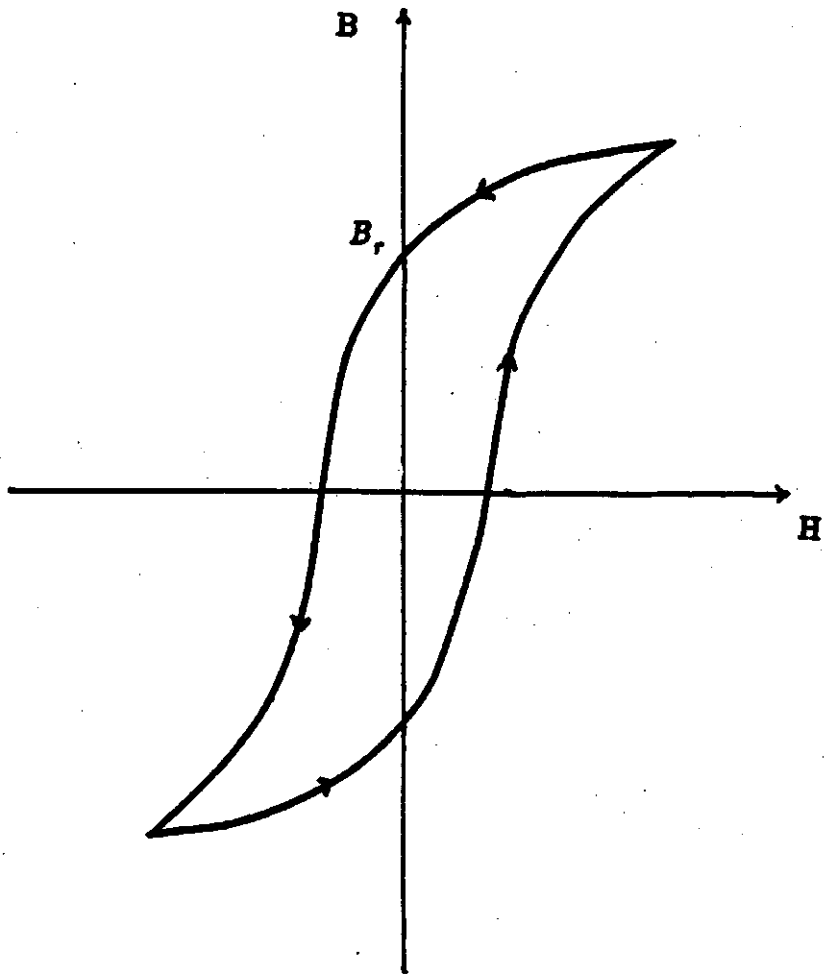

Figure 2.2: Magnetizing characteristics of a typical single-phase power transformer.

corresponding to the flux density waveform B_3, is also shown as i_3 in Figure 2.3. This current is substantially greater than the normal magnetizing current, i_1, also shown in Figure 2.3.

The magnetizing inrush current in a transformer can have peak values several times the rated full load current. The peak inrush current depends on the transformer core characteristics, residual flux and instant at which the voltage is applied.

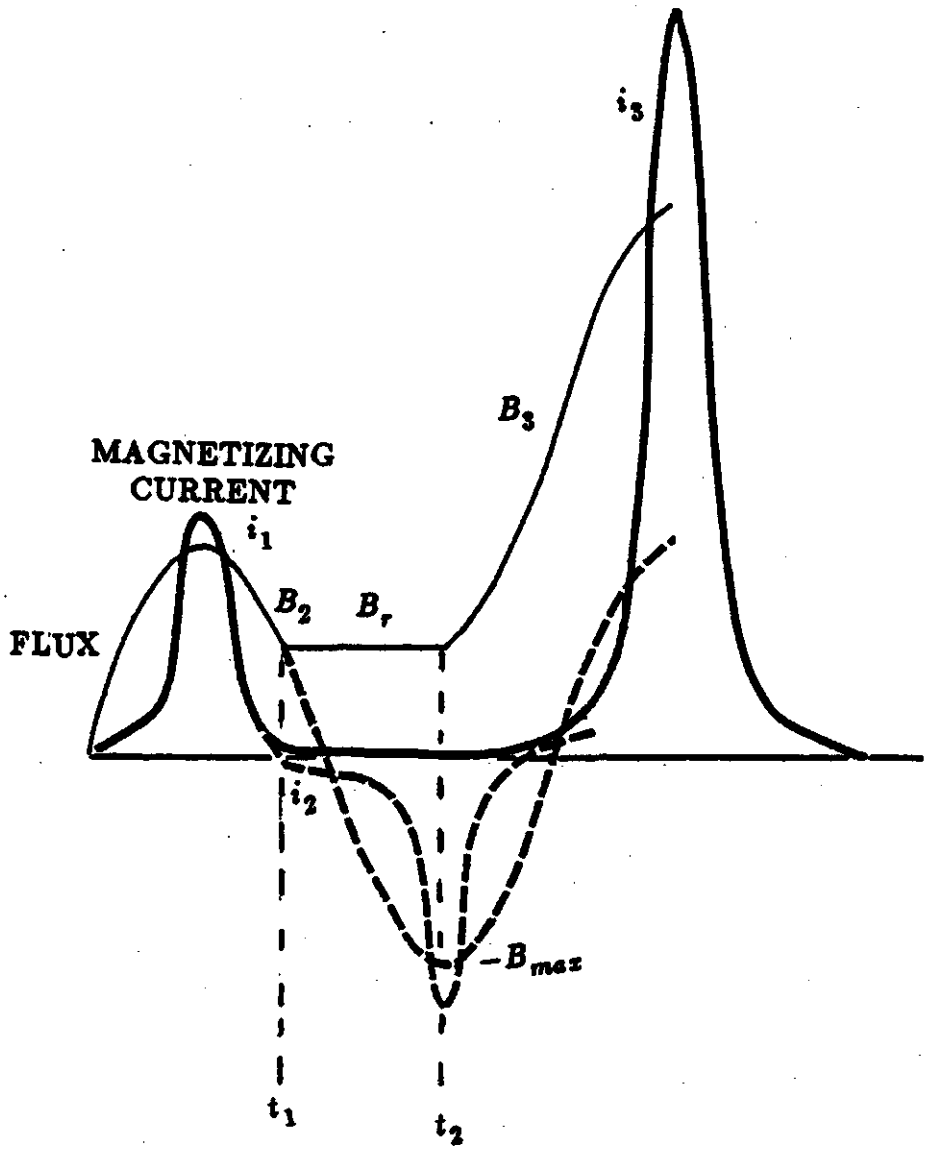

Figure 2.3: Magnetizing inrush phenomenon in a power transformer.

Magnetizing inrush is a complicated phenomenon in three phase transformers [25]. It is difficult to switch on all three phases at an instant when no inrush would result. Inrush currents are, therefore, experienced in at least two phases. Also, the levels of inrush currents in different phases are different; they depend on the connections of the windings and the magnetic coupling between the windings.

The waveshape of an inrush current is not sinusoidal; it is distorted due to the saturation of the transformer core. Since inrush currents flow in either the primary or the secondary windings of a transformer, a differential relay sees them as operating currents.

Differences in ct characteristics

Matching of the characteristics of the primary and secondary side ct's is difficult because of the differences in the designs of ct's used at different voltage levels. The lengths of the leads connecting the primary and secondary ct's to the relay are usually not equal. The VA burdens of the primary and secondary ct's are, therefore, not equal. The differences cause the ct's to operate at different ratio errors which, in turn, results in currents in the operating elements of the differential relay.

Ratio mismatch

Another phenomenon that causes currents to flow in the operating coils of a differential relay is the mismatch of the ratios of the ct's and the power transformer. Most power transformers are equipped with automatic on-load tap changers. The operation of a tap changer changes the turns ratio between the primary and secondary windings of the transformer. The ct ratios are usually selected to match for operation at the nominal tap setting. The outputs of the primary and secondary ct's, therefore, do not balance when the transformer operates at an off-nominal tap setting.

To avoid relay operation during magnetizing inrush, either voltages or harmonic components of the differential currents are used to restrain the relay. However, to avoid trippings due to ratio mismatch and/or differences in the ct characteristics, differential relays are provided with a percentage-bias feature.

2.2.3.1. Voltage restraint

A voltage-restraint differential relay uses in each phase one undervoltage relay with time-delay pick-up and reset to block operation during magnetizing inrush. The contacts of the undervoltage relays, connected in series with a low resistance, shunt the operating coil of the differential relay. This is shown schematically in Figure 2.4. The undervoltage relays are energised from the potential transformers that measure the secondary voltages of the power transformer. When the transformer is de-energised, the undervoltage relay resets and short circuits the operating coil of the differential relay. When the transformer is energised, the undervoltage relay does not pick up for a short time because of the designed time delay. This desensitizes the differential relay during the magnetizing inrush period. However, after the set time delay, the undervoltage relays reset opening their contacts and inserting the operating coil of the differential relay in the circuit. An obvious disadvantage of using undervoltage relays with time delay pick-up is that they can delay trippings when internal faults occur during magnetizing inrush.

An improved arrangement consists of using three high-speed voltage relays to control the tripping of a differential relay. These relays are connected between phases or between individual phases and the neutral. All three voltage relays pick up during magnetizing inrush indicating that either the transformer is in good health or the fault currents are very low. These relays start a timer that disables the tripping circuit of the differential relay for a designed time. This avoids the tripping on magnetizing inrush. However, an internal fault reduces at least one system voltage. As a result the timer does not start and tripping occurs immediately.

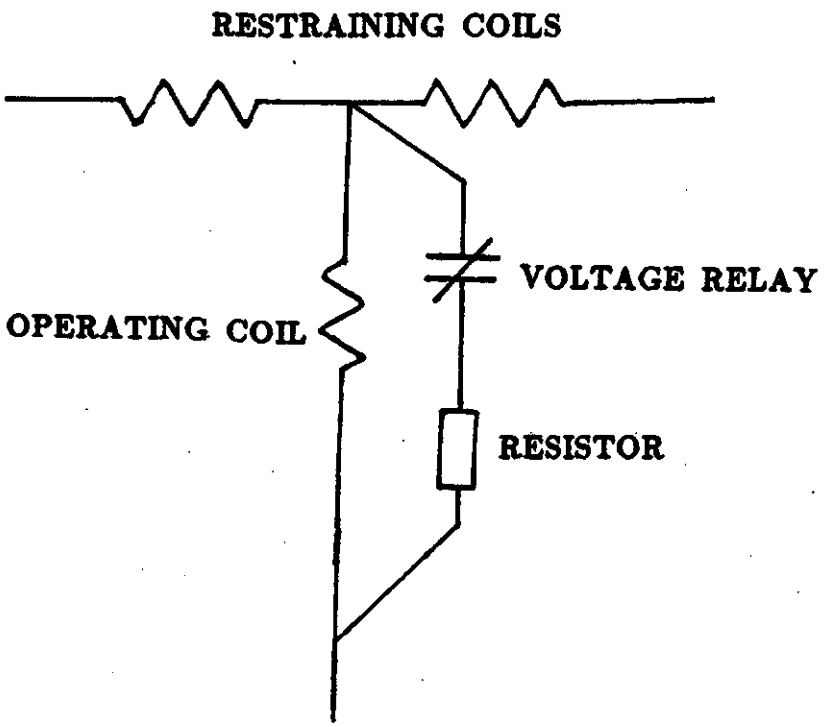

Figure 2.4: Circuit diagram showing the arrangement of the restraining and operating coils in a voltage-restrained differential relay.

2.2.3.2. Harmonic restraint

Harmonic restraint is incorporated in differential relays to avoid undesired trippings due to magnetizing inrush currents. These currents contain components of second and higher harmonic frequencies. Analyses of typical inrush currents indicate that the second harmonic component predominates [26]. This component is extracted from the differential currents using frequency selective circuits and is used to restrain the operation of the relay. Some designs use other harmonics, in addition to the second harmonic, to restrain the relay. The basic objective of these designs is to restrain the relay operation for all levels of magnetizing inrush but permit operation for internal faults.

2.2.3.3. Percentage bias

To avoid trippings due to ratio mismatch and differences in ct characteristics, a percentage bias is used in differential relays. This is achieved by requiring that the differential current to operate the relay be a prespecified percentage (or more) of the through current. This ratio is referred to as the percentage slope of the relay characteristics. The restraint can be fixed, adjustable or variable.

Percentage-biased differential relays permit increased speed and security with reasonable sensitivity at low fault currents. This is because the operating currents far exceed the restraining currents when the fault is internal.

2.2.4. Ground fault protection

A transformer differential relay has only a limited ability to operate in the event of a ground fault [27]. The presence of a resistor in the grounding circuit reduces ground fault currents. These currents are approximately proportional to the distance of the fault from the neutral end of the winding. Large portions of the windings are, therefore, not protected from ground faults. This necessitates the use of ground fault relays for protecting major transformer installations.

A typical ground fault relay applied to a delta-wye transformer is shown in Figure 2.5. This relay can detect a ground fault on any of the wye connected windings of the transformer. In this relay, the three line currents are balanced against the current in the transformer neutral. For a line to ground fault, outside the zone of the ground fault relay, the neutral current is sum of the currents at the transformer terminals. Current in the operating coil of the ground fault relay is, therefore, zero. However, in case of a phase to ground fault in the protected zone, the neutral current is not equal to the sum of currents at the transformer terminals. A current, therefore, flows in the operating coil of the relay which consequently operates.

This relay does not respond to two phase and three phase faults in the protected zone.

Ground faults in the delta windings are detected by a relay which is connected to three line ct's connected in parallel. This scheme responds to earth faults in the delta connected windings but does not operate for earth faults on the wye side of the transformer.

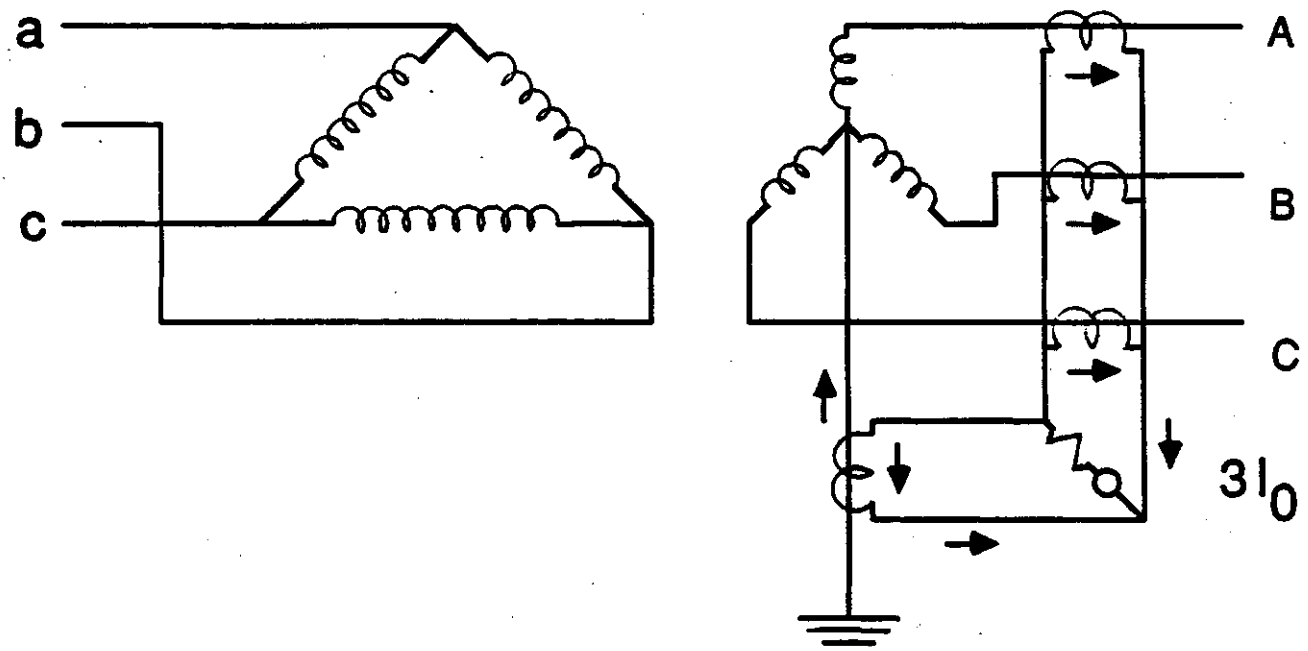

Figure 2.5: Circuit diagram for a ground fault relay for delta-wye transformers.

2.2.5. Other relays

Other relays used for transformer protection are

- gas accumulator relay,
- gas-pressure relay and

- oil-pressure surge relay.

A gas accumulator relay also known as Buchholz relay can be applied to a transformer that is equipped with a conservator tank. The relay is placed in the pipe connecting the conservator tank to the main transformer tank. It traps gases, produced due to a fault in the transformer over a period of time and, thus, operates for low level faults also. Because a gas accumulator relay can detect a small volume of gas, it can detect arcs of low energy. This relay is usually applied to supplement the differential protection of a transformer.

A gas-pressure relay can be applied to a gas-cushioned oil immersed transformer. It is mounted at the top end of the transformer. It monitors the rate of rise of the gas pressure in the transformer and operates when the pressure increases rapidly. It does not operate if the gas pressure changes slowly due to changes in loading and ambient temperature. High energy arcs produce large quantities of gases which cause the relay to operate in a short time.

An oil-pressure surge relay can be applied to an oil immersed transformer. It is mounted on the transformer tank below the oil level. This relay monitors the rate of rise of the oil pressure in the transformer tank and operates for internal faults that produce rapid changes in oil pressure. It, however does not operate on slow changes in oil pressure.

2.3. Instrumentation and Alarms

In addition to the protective relays discussed in the previous sections of this chapter, power transformers are equipped with several instruments [28]. These instruments measure transformer parameters, issue alarms in the event of an abnormal operating condition and, in some cases, issue trip commands. These instruments include

- level gauges,
- pressure gauges,
- Oil, water and gas temperature measuring devices,
- hot spot estimator and
- combustible limit relay.

A fluid level gauge indicates the level of oil in an oil-filled transformer. It is equipped with low-level and/or high-level alarm contacts. Low level alarm signals a condition that can result from a failure to fill the transformer initially or from excessive leakage of the oil during operation. The alarm is set to operate before it becomes unsafe to operate the transformer.

A vacuum pressure gauge monitors the gas pressure in a transformer with sealed tank construction. The pressure fluctuates between a lower (vacuum) and an upper limit (positive pressure) during major load cycles. It is equipped with limit alarms that provide warnings in the event of excess vacuum or positive pressure that could cause deformation or rupture of the transformer tank.

Oil-filled transformers are equipped with devices which are appropriately located to monitor the hottest part of the oil. These temperature measuring devices are often equipped with contacts which close at selected temperatures to start fan motors and ultimately to issue an alarm. A gas temperature thermometer performs a similar function in a sealed gas-filled transformer. However, the temperature range extends to about $200^{o}C$ to accommodate the higher operating temperatures of sealed gas-filled transformers. Transformer oil and gas have much longer thermal time constants than the windings and, therefore, these temperature monitoring devices are more sluggish than changes in the winding temperature due to load changes.

Hot spot temperature estimation reflects the thermal condition of a

transformer. A common method of measuring the hot spot temperature is to measure the temperature of oil at the top of the tank and supplement it with the heating effect of the winding currents. A thermostat element is immersed in the transformer oil. This element is also heated by an electric heating element which is supplied with a current proportional to the winding current. The thermostatic element, therefore, measures the temperature which the hot spot of the winding attains. This arrangement often indicates higher temperature for a heavy overload that exists only for a short time and, therefore, is not suitable for detecting deterioration of the transformer insulation. A thermal overload relay is used for this purpose. This relay introduces a time lag in its temperature registration thus accounting for the fact that insulation deterioration is a function of the duration of high temperature. Otherwise, the relay design is similar to that of the thermostatic element arrangement described earlier in this paragraph.

Combustible limit relay is used in oil-filled transformers that use controlled inert gas method for keeping the oil from deterioration. Combustible gases are produced as the oil breaks down or the insulating material decomposes due to a fault in the transformer. The relay indicates, records or even transmits the composition of the combustible gases on an hourly, daily or weekly intervals. It can also actuate an alarm if the content of the combustible gases reaches a predetermined level.

2.4. Off-line Gas Analysis

Electrical faults in oil-filled transformers usually generate combustible gases. Many transformer faults, in their early stages, are incipient in nature and the deterioration is gradual. However, sufficient quantities of combustible gases are usually formed to permit detection at a very early stage. A sample of the gas from a transformer is usually analysed periodically. The interval between consecutive tests depends on the size, importance and loading of the transformer. The results of the analysis are evaluated. Evaluation procedures vary from utility to utility and are influenced by their pre-

vious operating experience, the transformer location and its importance. However, a general classification of the gas analysis readings is suggested in Reference [29].

2.5. Economic Considerations

Different approaches are used for transformer protection. Even identical transformers, applied at different locations in a power system, are protected with different devices. Individual engineering analysis determines the most cost effective scheme. There are usually many alternatives that are technically feasible; each alternative offers different degrees of sensitivity, speed and selectivity. The selected scheme balances these factors against overall economics. The following factors are generally considered for this purpose.

- Cost of repairing damage.
- Cost of lost production.
- Adverse effects of losing the transformer on the power system.
- Spreading the damage to the nearby equipment.

2.6. Summary

A brief description of faults in power transformers has been presented in this chapter. Concepts of protecting power transformers using fuses, overcurrent relays, differential relays, ground fault relays and gas relays have been discussed. It has been emphasized that the design of a differential relay must include a restraint feature to avoid tripping during magnetizing inrush. The schemes used by conventional relays to avoid tripping due to magnetizing inrush are then discussed.

Instruments that measure operating parameters of a power transformer, actuate alarms and issue trip commands have been described in this chapter. Application of off-line gas analysis for detecting slowly developing faults in a

power transformer have been outlined. Finally, the importance of economics in applying protection to power transformers has been emphasized.

3. DIGITAL PROTECTION AND MONITORING OF TRANSFORMERS

Faults affecting power transformers and systems used for their detection have been described in Chapter 2. Instruments for monitoring transformer parameters have also been briefly discussed. Protection and monitoring of power transformers using microprocessors has been an area of active research for the last fifteen years. Emphasis has been on the development of digital algorithms for transformer protection. Algorithms suggested in the past are for differential, ground-fault and overcurrent protection of power transformers. These algorithms are reviewed and discussed in this chapter. Three microprocessor-based relays for power transformer protection, reported in the literature, are also described briefly. Lastly, a recent development in microprocessor-based monitoring of power transformers is presented.

3.1. Digital Algorithms for Differential Protection

An important requirement of a digital algorithm for differential protection of power transformers is that it should correctly identify magnetizing inrush, overexcitation and, internal and external faults. Several algorithms reported in the literature claim to fulfil this requirement. These algorithms can be classified into four categories based on their underlying principles which are

- waveshape indentification,
- harmonic restraint,
- flux restraint and
- transformer models.

Major features of these algorithms are briefly describes this section.

3.1.1. Waveshape identification technique

As discussed in Chapter 2, substantial differential current flows in a relay circuit when a fault occurs in the protected zone. However, magnetizing inrush, ratio mismatch and unequal levels of current transformer saturation during external faults also manifest as differential currents. The presence of differential current under these circumstances is not due to a fault in the protected zone. Rockefeller [7] suggested that successive peaks of a magnetizing inrush current occur at intervals of either 4 or 16 ms but the successive peaks of a fundamental frequency fault current occur 7.5 to 10 ms apart. Also, the peak value of the fault current is within 75% to 125% of its previous peak value and two successive peaks are of opposite signs. Rockefeller, therefore, suggested that the magnetizing inrush phenomenon can be identified by examining the pattern of the waveforms of the currents.

3.1.2. Harmonic restraint algorithms

These algorithms use harmonic components of the differential currents to restrain a differential relay during magnetizing inrush. Magnetizing inrush currents contain large amounts of harmonic components whereas fault currents do not contain these components. This fact is used in developing harmonic restraint algorithms. Digital differential relays sample the currents at regular intervals of time and calculate the peak values of their fundamental frequency and harmonic components. If the harmonic components in the differential currents exceed a pre-specified percentage of the fundamental frequency components, it is concluded that magnetizing inrush is being experienced. Some algorithms use the second harmonic components whereas others use a combination of several harmonics in the differential currents. The algorithms utilize different digital filtering techniques to estimate the magnitudes of the fundamental and harmonic frequency components of the primary and secondary side currents. Some of the filtering techniques are briefly described in the paragraphs that follow.

3.1.2.1. Fourier algorithms

These algorithms assume that the waveform of a current, $i(t)$, has a finite energy in the interval $(0,T)$ and can be expressed as

$$i(t) = A_0 + \sqrt{2}A_1 sin(2\pi t/T) + \sqrt{2}A_2 cos(2\pi t/T) + \sqrt{2}A_3 sin(4\pi t/T) + \sqrt{2}A_4 cos(4\pi t/T) + \cdots . \quad (3.1)$$

In this equation, $A's$ are the Fourier coefficients and T is the time period of the fundamental frequency component. The peak values of the fundamental and second harmonic components of $i(t)$ can be computed from Fourier coefficients as

$$I_1 = \sqrt{2}(A_1^2 + A_2^2)^{0.5} \ and \quad (3.2)$$

$$I_2 = \sqrt{2}(A_3^2 + A_4^2)^{0.5} \quad (3.3)$$

where,

I_1 is the peak value of the fundamental frequency component and

I_2 is the peak value of the second harmonic component.

Researchers proposed different approaches for obtaining the Fourier coefficients. Malik et al. [8] suggested that the Fourier coefficients be estimated by correlating $i(t)$ with sine and cosine waveforms of unit peak value.

Thorp and Phadke [11] employed non-recursive Discrete Fourier Transform (DFT) to extract fundamental, second harmonic and fifth harmonic frequency components of the differential current. They developed an algorithm for protection of three-phase three-winding transformers. The algorithm uses five signals, one trip signal and four restraining signals. The trip signal is the magnitude of the fundamental frequency component of the differential current. The first restraint signal is the through current to prevent tripping during heavy external faults. The second restraint is to prevent tripping the

transformer when it is operating with the primary circuit breaker open. The third and fourth restraint signals are the second and fifth harmonic components of the differential currents. They prevent tripping during magnetizing inrush and overexcitation respectively.

3.1.2.2. Least error squares technique

Luckett et al. [30] proposed the use of the least squares approach for computing amplitudes and phase angles of voltages and currents. Brooks [31] also used the least squares approach and assumed that a current is composed of a dc component and a fundamental frequency component. Sachdev and Baribeau [32] reported further developments in this approach. They demonstrated a procedure for modelling the decaying dc component for including in the design process. They also demonstrated that most of the computations can be done off-line. Later, Sachdev and Shah [10] applied this technique for differential protection of transformers. They assumed that a differential current contains a decaying dc component and components of the fundamental frequency and the second and third harmonics. Therefore, they expressed a current as

$$i(t) = I_0 e^{-t/\tau} + \sum_{m=1}^{3} I_m \sin(m\omega_0 t + \theta_m) \qquad (3.4)$$

where,

I_0 is the magnitude of the decaying dc component at t=0,

τ is the time constant of the dc component,

I_m is the magnitude of the $m-th$ harmonic component,

θ_m is the phase angle of the $m-th$ harmonic component.

Approximating the exponential by the first two terms of its Taylor series expansion and replacing $\sin(m\omega_0 t+\theta_m)$ by $cos\theta_m sin(m\omega_0 t) + sin\theta_m cos(m\omega_0 t)$, the following equation was obtained.

$$i(t) = I_0 - (I_0/\tau)t + \sum_{m=1}^{3} (I_m cos\theta_m) sin(m\omega_0 t) + (I_m sin\theta_m) cos(m\omega_0 t) \quad (3.5)$$

At time $t = t_1$, the current was, therefore, represented as

$$i(t_1) = I_0 - (I_0/\tau)t_1 + (I_1 cos\theta_1) sin(\omega_0 t_1) + (I_1 sin\theta_1) cos(\omega_0 t_1) + (I_2 cos\theta_2) sin(2\omega_0 t_1) + (I_2 sin\theta_2) cos(2\omega_0 t_1) + (I_3 cos\theta_3) sin(3\omega_0 t_1) + (I_3 sin\theta_3) cos(3\omega_0 t_1). \quad (3.6)$$

This equation was rewritten in a linear form as

$$i(t_1) = a_{11}x_1 + a_{12}x_2 + a_{13}c_3 + a_{14}x_4 + a_{15}x_5 + a_{16}x_6 + a_{17}x_7 + a_{18}x_8, \quad (3.7)$$

where,

$x_1 = I_0$, $a_{11} = 1$,

$x_2 = -(I_0/\tau)$, $a_{12} = t_1$,

$x_3 = I_1 cos\theta_1$, $a_{13} = sin(\omega_0 t_1)$,

$x_4 = I_1 sin\theta_1$, $a_{14} = cos(\omega_0 t_1)$,

$x_5 = I_2 cos\theta_2$, $a_{15} = sin(2\omega_0 t_1)$,

$x_6 = I_2 sin\theta_2$, $a_{16} = cos(2\omega_0 t_1)$,

$x_7 = I_3 cos\theta_3$, $a_{17} = sin(3\omega_0 t_1)$,

$x_8 = I_3 sin\theta_3$, $a_{18} = cos(3\omega_0 t_1)$.

Because the current $i(t)$ is sampled every ΔT seconds, the next sample was expressed as

$$i(t_1+\Delta T) = a_{21}x_1 + a_{22}x_2 + a_{23}x_3 + a_{24}x_4 + a_{25}x_5 + a_{26}x_6 + a_{27}x_7 + a_{28}x_8. \quad (3.8)$$

For a preselected time reference and sampling rate, the values of the 'a' coefficients are known. For p samples taken at ΔT second intervals, the process was expressed in the form of p equations in eight unknowns [10].

$$\underset{p\times 8}{[A]} \quad \underset{8\times 1}{[x]} = \underset{p\times 1}{[i]} \quad (3.9)$$

For p greater than eight, the vector of unknowns, $[x]$, was determined by using

$$\underset{8\times 1}{[x]} = \underset{8\times p}{[A]^+} \; \underset{p\times 1}{[i]}, \quad (3.10)$$

where,

$[A]^+$ is the left pseudo-inverse of $[A]$ defined by

$$\underset{8\times p}{[A]^+} = \underset{8\times p}{[[A]^T[A]]^{-1}} \underset{p\times 8}{[A]^T} \quad (3.11)$$

The authors of Reference [10] determined the elements of $[A]^+$ in the off-line mode. Equation 3.10 suggests that the values of the real and imaginary parts of the fundamental and second harmonic frequency components of a current can be computed using its sampled values and the elements of third, fourth, fifth and sixth rows of the left-pseudo inverse of $[A]$. The peak values of the fundamental and second harmonic components can then be determined by using

$$I_1 = \sqrt{x_3^2 + x_4^2} \; and \quad (3.12)$$

$$I_2 = \sqrt{x_5^2 + x_6^2} \quad (3.13)$$

The authors of Reference [10] designed othrogonal fundamental and second harmonic frequency filters using a twelve sample window and time reference coinciding with the centre of the data window. They used a sampling rate of 720 Hz. Using this procedure, Reference [10] compared the second harmonic components of the differential currents with their fundamental frequency components. If a second harmonic component was more than 33% of the fundamental frequency component, the algorithm classified the situation as magnetizing inrush.

3.1.2.3. Finite impulse response technique

Schweitzer et al. [9] used Finite Impulse Response (FIR) digital filters for differential protection of transformers. They used four FIR filters; two each for the fundamental frequency and second harmonic components. The weighting functions of these filters were selected to be +1 or -1 which reduced the computations to additions and subtractions of the sampled inputs. The sampling rate used in this work was 480 Hz and the criterion for discriminating the magnetizing inrush from internal faults was based on ξ defined as

$$\xi = \frac{Max(|S_2|,|C_2|)}{Max(|S_1|,|C_1|)}, \tag{3.14}$$

where,

S_1 *and* C_1 are the outputs of the fundamental frequency digital filters that have 'odd' and 'even' weighting functions respectively and

S_2 *and* C_2 are the outputs of the second harmonic digital filters that have 'odd' and 'even' weighting functions respectively.

The theoretical limits of the value of ξ were investigated and were found to be between 0 and 0.146 for internal faults and between 0.334 and 0.586 for magnetizing inrush.

3.1.2.4., A recursive filtering approach

Sykes and Morrison [33] used recursive filters for transformer differential protection. These filters incorporate feedback by using previous outputs as a part of the inputs. The authors sampled a differential current, processed it to estimate its fundamental frequency and second harmonic components. If the magnitude of the second harmonic component exceeded a pre-specified percentage of the fundamental frequency component, they concluded that the transformer was experiencing magnetizing inrush.

The outputs of recursive filters used in Reference [33] are not suitable for comparison of the instantaneous outputs because of the phase displacement between them. The values of the outputs were, therefore, rectified and smoothed before comparison. The authors tested the proposed technique by off-line simulation of faults and magnetizing inrush in a single phase transformer. The test results revealed that the procedure can identify inrush conditions from internal faults. However, the frequency response of the filters indicate that they do not suppress the decaying dc completely.

Another recursive filter used for transformer protection is the Kalman filter. Its output depends on the present inputs and the previous outputs. Sachdev, Wood and Johnson [34] explained the Kalman filtering technique in power system terminology and demonstrated its application for estimating phasors representing voltages and currents. They also demonstrated the procedure for designing Kalman filters that can estimate the fundamental frequency and selected harmonics in a signal. Reference [34] reported an eleven state Kalman filter which can handle a decaying dc and sinusiods of the first to fifth harmonics. Murty and Smolinski [35] applied the Kalman filtering technique for transformer protection. They designed Kalman filters using a five state model which assumes that the transformer currents contain decaying dc and fundamental and second harmonic frequency components only. Later, they used an eleven state model [12] reported in Reference [34]. Reference [12] computed the fundamental frequency, second, fourth and fifth har-

monics in each differential current, and the fundamental frequency component in each through current. The second and fourth harmonic components of the differential currents were used to form the restraint signal to inhibit tripping during magnetizing inrush. The fifth harmonic components of the differential currents were used to inhibit tripping during overexcitation.

3.1.2.5. Other technique

Degens and Langedijk [17] used frequency sampling method to design non-recursive digital filters for differential protection of transformers. This consists of sampling a specified frequency response characteristic at equispaced frequencies and equating the responses with the discrete Fourier transforms of the digital filter coefficients. This procedure provides simultaneous equations from which the filter coefficients are determined using inverse discrete Fourier transform. The authors of Reference [17] designed filters which estimate the fundamental and the second and fifth harmonic frequency components of differential currents. A ratio of the second harmonic and fundamental frequency components greater than 0.16 was interpreted as magnetizing inrush. A ratio of fifth harmonic and fundamental frequency components greater than 0.08 was considered to indicate overexcitation.

3.1.3. Flux-restraint algorithm

The algorithms described in Section 3.1.2 rely on the presence of harmonics in the differential currents to prevent tripping during magnetizing inrush and overexcitation. Phadke and Thorp [13] suggested a differential protection algorithm that uses the flux-current relationship of the transformer to decide if the relay be restrained. The proposed technique expresses the following relationship between a phase voltage at the terminals of a transformer winding, $v(t)$, the current in the transformer winding, $i(t)$, the mutual flux linkage, $\lambda(t)$, and the leakage inductance of the winding, l.

$$v(t) - l(di/dt) = d\lambda(t)/dt \tag{3.15}$$

This equation assumes that the resistance of the transformer winding is neglegible. Integrating Equation 3.15 from time t_1 to t_2 yields

$$\lambda(t_1) - \lambda(t_2) = \int_{t_1}^{t_2} v(t)dt - l[i(t_2) - i(t_1)]. \tag{3.16}$$

Applying the trapezoidal rule of integration, the following equation is obtained.

$$\lambda(t_2) = \lambda(t_1) + \frac{t_2 - t_1}{2}[v(t_2) - v(t_1)] - l[i(t_2) - i(t_1)] \tag{3.17}$$

If the voltage and current are sampled at $k\Delta T$ and $(k-1)\Delta T$ s, Equation 3.17 can be written as

$$\lambda(k\Delta T) = \lambda[(k-1)\Delta T] + \frac{\Delta T}{2}\{v(k\Delta T) - v[(k-1)\Delta T]\}$$

$$- l\{i(k\Delta T) - i[(k-1)\Delta T]\}. \tag{3.18}$$

This equation suggests that the flux linkage of a transformer can be computed using the voltage and current samples. As the differential current of a transformer is equal to the magnetizing current, the samples of the differential current and the flux linkages lie on the open circuit magnetization curve for normal operating conditions, magnetizing inrush and overexcitation. However, this criterion can not be used because the remanance flux is not known. The authors of Reference [13] suggested that this problem can be overcome by considering $d\lambda/di$ rather than λ. The value of $d\lambda/di$ computed by rearranging Equation 3.18 is given by

$$d\lambda/di = \{\lambda(k\Delta T) - \lambda[(k-1)\Delta T]\}/\{i(k\Delta T) - i[(k-1)\Delta T]\}$$

$$= \frac{\Delta T}{2}[\{v(k\Delta T) + v[(k-1)\Delta T]\}/\{i(k\Delta T) + i[(k-1)\Delta T]\}] - l. \tag{3.19}$$

It was suggested that samples of $d\lambda/di$ and i can be used to identify internal faults from other operating conditions. The $[(d\lambda/di), i]$ plane can be divided into two regions; one representing the normal operation a transformer and the other representing internal faults. During an internal fault, the current samples and $d\lambda/di$ samples remain continuously in the fault region. However, during magnetizing inrush, they alternate between the fault and

normal operation regions. An index was, therefore, defined which is incremented each time $[(d\lambda/di), i]$ sample lies in the fault region and is decremented if it lies in the no-fault region. This index grows monotonically for faults but does not reach a specified threshold value for magnetizing inrush. It is suggested in Reference [13] that the threshold should be determined experimentally.

The algorithm was tested off-line to study its performance. The data used for testing the algorithm was obtained by sampling at 720 Hz voltages and currents of a model transformer. Results of 21 cases reported in Reference [13] reveal that the algorithm correctly identifies magnetizing inrush and overexcitation conditions as normal operations. Average tripping time for internal faults is reported to be approximately 11 ms.

3.1.4. Algorithms using transformer models

Another class of algorithms that do not use harmonic components of differential currents to discriminate magnetizing inrush from internal faults have been proposed in the past. They are based on transformer models; three algorithms of this category are described in this section.

Sykes [14] used the saturation of the transformer core to identify magnetizing inrush. He used the following model of the saturated transformer.

$$v_1 = R_1 i_1 + L_{11}(di_1/dt) + L_{12}(di_2/dt) \tag{3.20}$$

$$v_2 = R_2 i_2 + L_{21}(di_1/dt) + + L_{22}(di_2/dt) \tag{3.21}$$

where:

v_1 *and* v_2 — are the voltages of the primary and secondary windings respectively,

i_1 *and* i_2 — are the currents in the primary and secondary windings respectively,

R_1 *and* R_2 are the resistances of the primary and secondary windings respectively,

L_{11} *and* L_{12} are the self and mutual inductances of the primary winding respectively and

L_{22} *and* L_{21} are the self and mutual inductances of the secondary winding respectively.

Assuming that the self and mutual inductances and resistances of the primary and secondary windings are known, the primary and secondary voltages can be computed using sampled values of the winding currents and the right hand sides of Equations 3.20 and 3.21. It was suggested that magnetizing inrush can be distinguished from internal faults by comparing the computed values of the voltages with their measured values. The calculated and measured values of the terminal voltages are close during magnetizing inrush but are substantially different during internal faults.

Jin and Sachdev [15] presented an algorithm that uses the electrical-magnetic interrelation of a transformer considering non-linear magnetization characteristics. They developed an algorithm that can be used to protect a single-phase two-winding transformer using the model shown in Figure 3.1. In this figure, the resistances, R_p and R_s and the leakage inductances, L_p and L_s are parameters of the primary and secondary windings. The shunt branch, R_i and L_m are equivalent resistance and inductance respectively which represent hysteresis and magnetizing characteristics of the transformer core. The values of L_m are functions of the instanteous values of flux and magnetizing current and are derived from the B-H characteristics of the core. Using the transformer model of Figure 3.1, the primary voltage, v_1 can be expressed as

$$v_1 = R_p i_1 + L_p(di_1/dt) + L_m(di_m/dt) \tag{3.22}$$

where,

i_1 is the current in primary winding and

i_m is the magnetizing current.

Since the current in the shunt branch R_i is small, the magnetizing current can be expressed as

$$i_m = i_1 - i_2 \tag{3.23}$$

where,

i_2 is the current is the secondary winding.

For external faults, normal operating conditions and magnetizing inrush, the differential current $(i_1 - i_2)$ is approximately equal to the magnetizing current, i_m. A substitution of the magnetizing current by the differential current, therefore, satisfies Equation 3.22. But, for internal faults, the Equation 3.23 is not valid and, therefore, Equation 3.22 is not satisfied. This fact was used in the algorithm to distinguish internal faults from external faults, magnetizing inrush and overexcitation conditions. Simulation results showed that the algorithm performs well for the protection of a single phase transformer.

Multi-circuit transformers can be represented by a universal equivalent circuit composed of admittances [36]. An n-winding transformer can be represented by an equivalent circuit containing $n(n+1)/2$ admittances. This approach was used by Inagaki et al. [16] to represent a single-phase three-winding transformer by the equivalent circuit shown in Figure 3.2. They called y_{12}, y_{13} and y_{23} in Figure 3.2 as transfer inverse inductances and y_{10}, y_{20} and y_{30} as shunt inverse inductances. Reference [16] showed that the form of the equivalent circuit does not change as the operating conditions change. The values of transfer inverse inductances remain constant for all operating conditions but, the values of the shunt inverse inductances change as the operating parameters change. The values of the shunt inverse inductances for internal faults are different from their values during normal

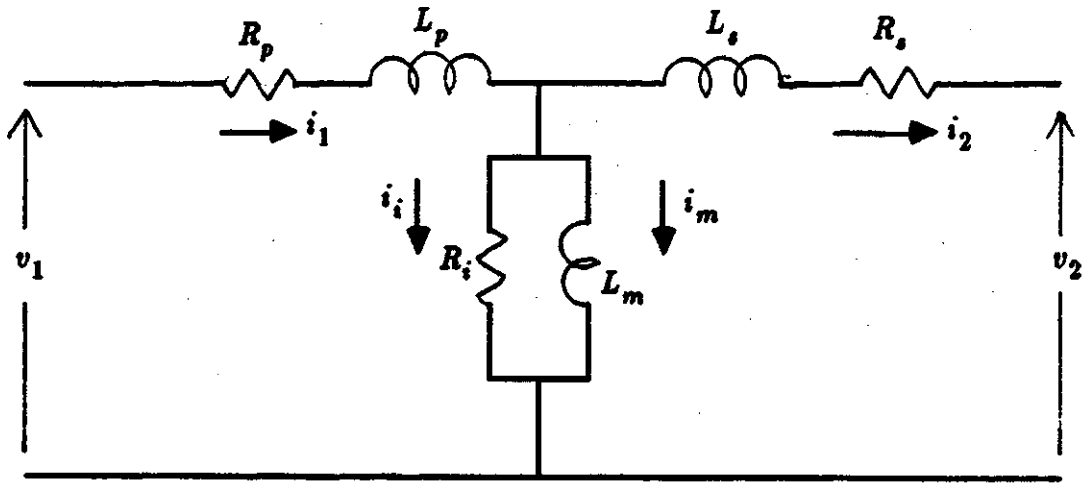

Figure 3.1: Equivalent tee circuit of a single phase two winding transformer.

operating and magnetizing inrush conditions. This fact was used in Reference [16] to distinguish internal faults from other operating conditions. The authors suggested that the shunt inverse inductances can be computed from voltages and currents of the transformer windings. The transfer inverse inductances were calculated using the equations

$$y_{10} = \{i_1 - [(y_{12}\int v_2 dt + y_{13}\int v_3 dt)/\int v_1 dt]\} + y_{12} + y_{13}, \tag{3.24}$$

$$y_{20} = \{i_2 - [(y_{21}\int v_1 dt + y_{23}\int v_3 dt)/\int v_2 dt]\} + y_{21} + y_{23} \text{ and} \tag{3.25}$$

$$y_{30} = \{i_3 - [(y_{31}\int v_1 dt + y_{32}\int v_2 dt)/\int v_3 dt]\} + y_{31} + y_{32}. \tag{3.26}$$

where,

v_1, v_2 *and* v_3 are the voltages of windings 1, 2, and 3 respectively and

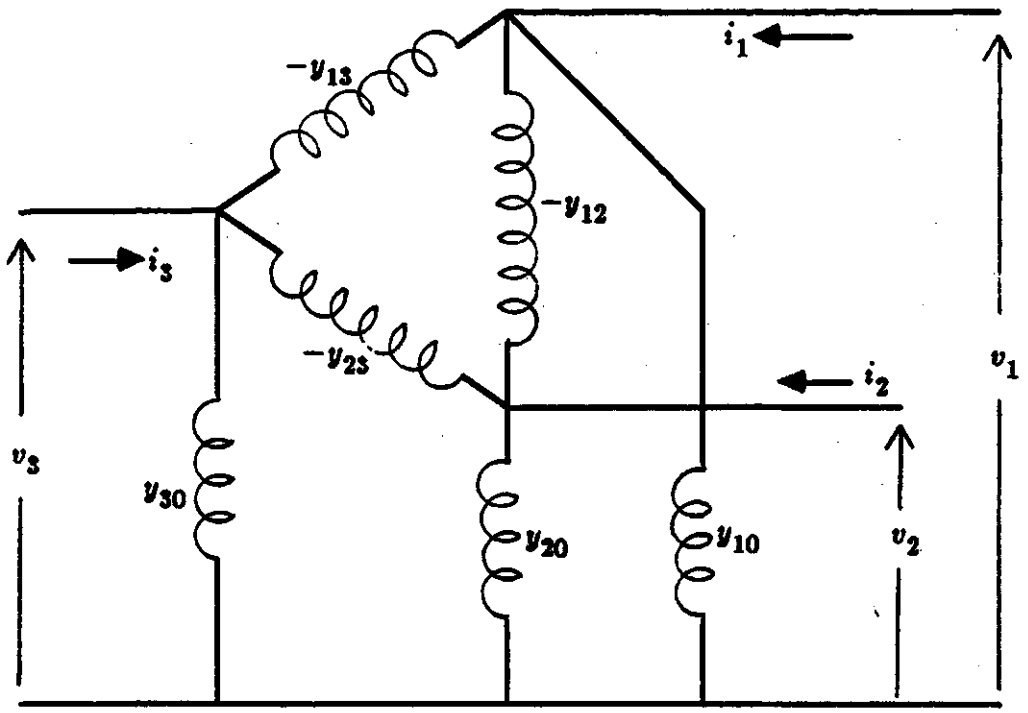

Figure 3.2: Equivalent pi circuit of a single-phase three-winding transformer.

i_1, i_2 *and* i_3 are the currents in windings 1, 2, and 3 respectively.

In a digital algorithm, the values of the shunt inverse inductances can be computed by sampling and digitizing winding voltages and currents at a prespecified rate and using numerical methods for integrating Equations 3.24, 3.25 and 3.26. The values of the transfer inverse inductances can be calculated off-line from short-circuit test data of the transformer [36].

The algorithm was tested using data from digital simulations for a power transformer and experimental data from a single-phase, 2.1 kVA transformer. The results show that the algorithm can recognize an internal fault in about 8 ms after its inception.

3.2. Discussion of the Algorithms for Differential Relays

Algorithms used in differential relays have been reviewed in Section 3.1. This section discusses relative merits and weaknesses of these algorithms.

The harmonic restraint algorithms use harmonic components of differential currents to restrain differential relays during magnetizing inrush conditions. The operating voltages of power systems and lengths of transmission lines have increased substantially during the last thirty years. Because of these factors, differential currents during internal transformer faults can contain large harmonic components. Harmonic components can also be present during internal faults due to arcing and saturation of ct's, especially, during heavy faults. These algorithms can, therefore, restrain a differential relay during internal faults. Also, if a faulted transformer is energized, magnetizing inrush currents and fault currents are experienced simultaneously. The harmonics in the inrush currents can prevent the algorithms from issuing a trip command until the inrush currents have decayed substantially.

The flux-restraint algorithm uses currents in the transformer windings to make appropriate decisions. Terminals of delta connected windings are not usually brought out of the transformer tank. The winding currents are, therefore, not available for use in making relaying decisions. This limits the application of the flux algorithm to single-phase and three-phase wye-wye transformers.

Algorithms based on transformer models also use winding currents to make decisions. All winding currents are not available in three-phase delta-wye transformers. Their application is, therefore, limited to single-phase and three-phase wye-wye transformers.

The algorithm of Reference [14] is based on a linear model of a two-winding single-phase transformer, but the flux-current relationship of the transformer core is non-linear. Therefore, the algorithm experiences large er-

rors during magnetizing inrush. To avoid trippings during magnetizing inrush, the sensitivity of the relay is decreased. Consequently, the algorithm is able to issue trip commands for heavy internal faults only.

Reference [15] uses a tee model consisting of two leakage inductances and a magnetizing inductance. The magnetizing inductance can be calculated from the B-H characteristics of the transformer core. This information is not generally available and, therefore, must be determined experimentally. Also, the extension of this algorithm for protecting three-phase transformers will require further developmental work.

The algorithm suggested by Inagaki et al. [16] achieves the protection of a three-windings single-phase transformer by using an equivalent pi model. An equivalent pi circuit of a single-phase three-winding transformer has six elements. In general, an equivalent pi circuit for n-winding transformer consists of $n(n+1)/2$ elements. For example, the equivalent pi models of three-phase two-winding and three-phase three-windings transformers will have 21 and 45 elements respectively. The algorithms based on these models are complex and require considerable computations. Also, some elements of the equivalent pi circuits of single-phase and three-phase transformers are non-linear; their values depend on the operating conditions of the transformer. This increases the complexity of the algorithm because determining the values of non-linear elements for an entire range of operation is a major problem.

3.3. Ground Fault Algorithms

Digital algorithms for ground fault relaying of transformers are conceptually similar to conventional ground fault relays. Three algorithms have been reported in the literature. The first algorithm published by Sachdev and Shah [10] determines the sampled values of the relay current, i_r, by using the following equations.

$$i_r = i_n - (i_a + i_b + i_c) \tag{3.27}$$

$$i_r = i_a + i_b + i_c \tag{3.28}$$

where:

i_a, i_b *and* i_c are the sampled values of currents in phases a, b, and c respectively and

i_n is the sampled value of current in the transformer neutral.

Equation 3.27 is used for the protection of wye connected neutral-grounded windings. For delta-connected and ungrounded wye connected windings, Equation 3.28 is used. The algorithm uses sampled values of the currents, calculates i_r and then uses least squares digital filters to compute the fundamental frequency component of the relay current. This component is compared with a threshold for relaying purposes. If the relay current exceeds the threshold, a trip counter is incremented. A trip signal is issued once the trip counter exceeds a prespecified value. However, if the relay current is less than the threshold, another counter called decrement counter, is incremented. Both trip and decrement counters are reset if the decrement counter reaches a pre-specified value.

Recently, Murty and Smolinski [12] used an approach similar to the technique of Reference [10] for ground fault protection. However, they used a Kalman filter instead of a least error squares filter to compute the fundamental frequency component of the relay current. A similar procedure for ground fault protection of transformers is reported by Degens and Langedijk [17]. It differs from the algorithm of References [10] and [12]; it uses the instantaneous values of the relay current for comparison with a threshold instead of computing the fundamental frequency component of the relay current.

3.4. Overcurrent Relay Algorithms

As discussed in Chapter 2, overcurrent relays are used to protect transformers from external faults. The relays also act as backup relays for protecting major transformers. There has been a considerable interest in developing digital algorithms for overcurrent relays. Development of a digital overcurrent relay algorithm consists of three parts; the first part is the modelling of current-time characteristics of the relay. The second part is the development of a technique for calculating the fundamental frequency current from sampled values. The third part is the development of a logic for incorporating specified time delays if the current is in excess of a set value. The time delay should correctly emulate the specified time-current characteristics of the relay. This section discusses the previously suggested techniques for representing the relay characteristics. Previously reported microprocessor-based algorithms for overcurrent relays are also described.

3.4.1. Modelling time-current characteristics

Time-current characteristics of inverse-time overcurrent relays are represented by a family of curves which depict contact closing times versus the relay currents. Traditionally, a time dial setting allows to achieve a desired contact closing time for a specified operating current. Time dial settings are continuous and it is, therefore, possible to have an infinite number of characteristic curves. However, the characteristics are usually published as a family of curves for time dial settings of 0.5, 1, 2, 3, 4, 5, 6, 7, 8, 9, 10, and 11 [37]. Figures 3.3 and 3.4 show the time-current characteristics of the Westinghouse CO-7 and CO-9 overcurrent relays.

Mathematical equations representing time-current characteristics of overcurrent relays have been suggested by a number of researchers in the past. A.R. van C. Warrington [27] proposed the following generalised hyperbolic equation for representing the relay contact closing time.

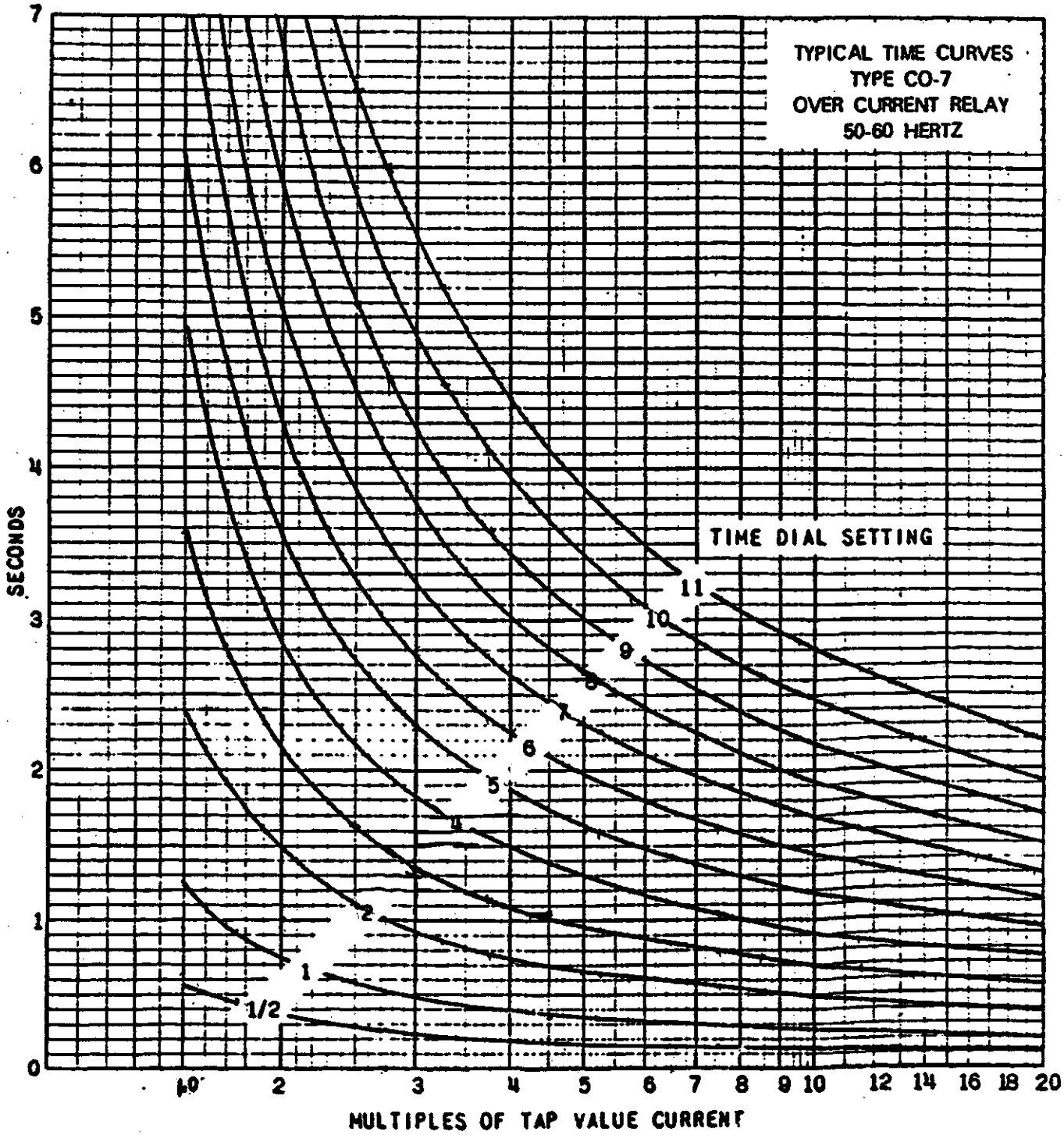

Figure 3.3: Time-current characteristics of the Westinghouse CO-7 type overcurrent relay. (Source: Westinghouse Doc. No. I.L. 41-100F, Curve No. 418247)

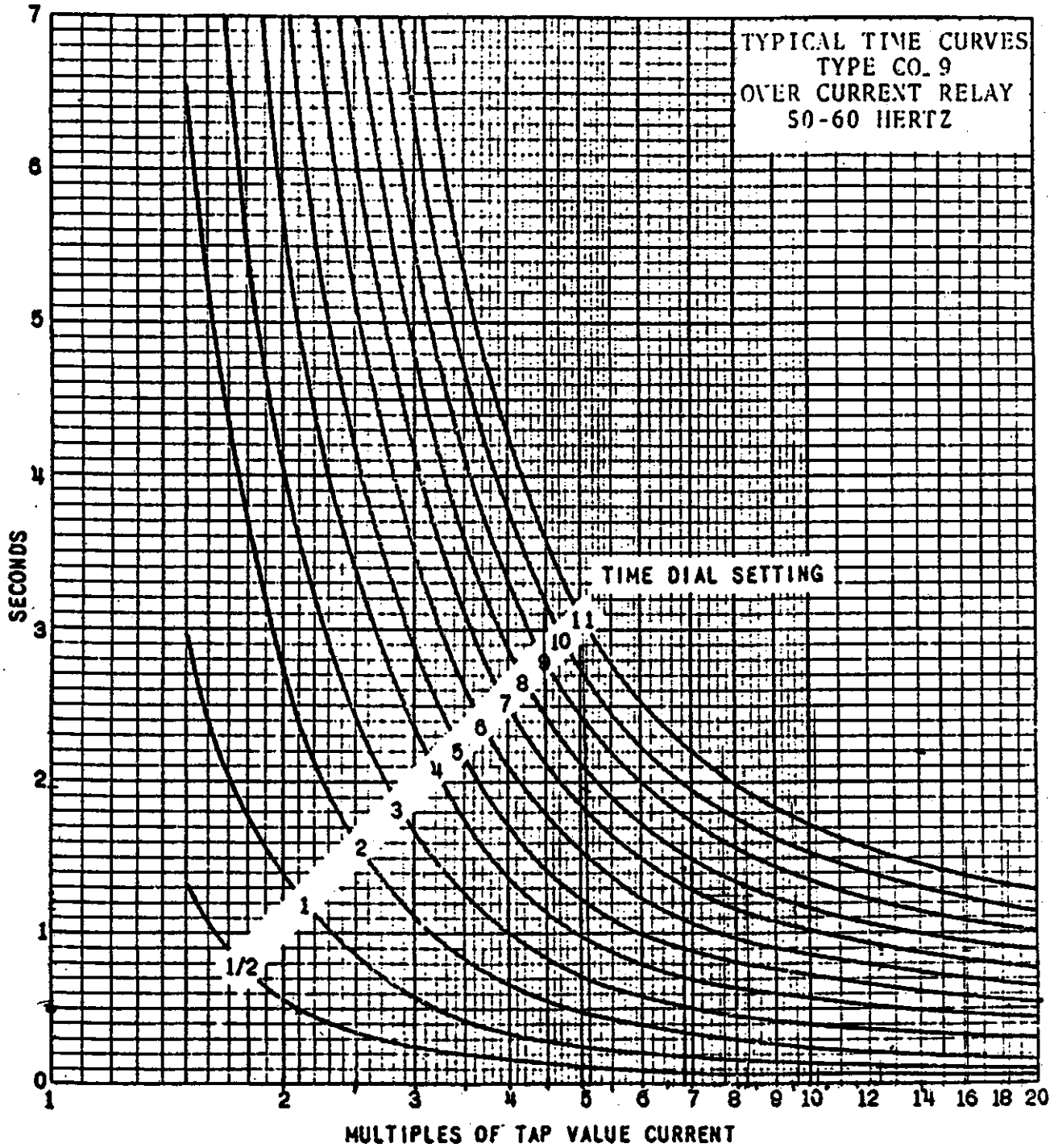

Figure 3.4: Time-current characteristics of the Westinghouse CO-9 type overcurrent relay. (Source: Westinghouse Doc. No. I.L. 41-100F, Curve No. 418249)

$$t_r = a_0 + \frac{a_1 TDS}{(I - I_0)^n - [I_0]^m} \tag{3.29}$$

where:

t_r is the trip contact closing time,

TDS is the time dial setting,

I is the relay current in multiples of tap setting,

I_0 is multiple of tap setting at which pick-up occurs and

a_0, a_1, n *and* m are constants.

It is suggested in the IEC Standard 255.4 [38] that the characteristic curves for inverse-time overcurrent relays correspond to the following formula.

$$t_r = \frac{K_1}{(I)^\alpha - 1} \tag{3.30}$$

where:

K_1 is a constant characterising the relay,

α is an index characterising the algebraic function.

Radke [39] expressed the relay operating times as polynomials of the logarithm of the relay current; the suggested equation is reproduced here as Equation 3.31. Albrecht et al. [40] also expressed the operating characteristics of an overcurrent relay as a polynomial reported as Equation 3.32.

$$Log(t_r - DC) = b_0 + b_1 Log(I) + b_2[Log(I)]^2 + b_3[Log(I)]^3 + b_4[Log(I)]^4 \tag{3.31}$$

$$t_r = [\sum_{j=0}^{M} \sum_{i=0}^{N} c_{ij} (TDS)^j (I)^i]^\beta \tag{3.32}$$

where,

DC is a constant used to improve the model,

b_0, b_1 $\cdots$ are constants,

M and N are integers and

c_{ij} and β are constants.

Sachdev, Singh and Fleming [41] examined five polynomials for representing characteristics of inverse-time overcurrent relays. One of those polynomials is

$$t_r = d_0 + \frac{d_1}{I - 1} + \frac{d_2}{(I - 1)^2} + \cdots \tag{3.33}$$

where,

d_0, d_1, $\cdots$ are constants.

In another paper [18], they described the relay characteristics in the form of Equations 3.34 and 3.35 which are two special cases of Equation 3.29. Degens and Langedijk [17] expressed the contact closing time of an overcurrent relay in the form of Equation 3.36.

$$t_r = \frac{K_2}{(I)^n} \tag{3.34}$$

$$t_r = T_0 + \frac{K_3}{(I)^n - 1} \tag{3.35}$$

$$t_r = \frac{K_4}{(I)^2 - (K_0)^2} \tag{3.36}$$

where:

K_0 and K_2 are constants,

K_3 and K_4 are constants and

T_0 is a constant which accounts for the effects of friction and hysteresis in the magnetic circuits.

Schweitzer and Aliaga [19] proposed that the time-current characteristics for a particular time-dial setting can be modelled as a series of piece-wise continuous segments. They suggested that the relay operating time given by each segment can be expressed as

$$t_r = \frac{K_5}{e_1 I - e_2}. \tag{3.37}$$

In Equation 3.37, K_5, e_1 and e_2 are the constants. e_1 and e_2 have unique values for each segment. Reference [19] also suggests that by varying the value of K_5, the contact closing times at different time dial settings can be achieved.

Equations 3.29 to 3.37 are capable of accurately representing time-current characteristics of inverse-time overcurrent relays. However, the use of these equations for developing microprocessor-based overcurrent relays either require large storage or their implementation is not easy because of their mathematical complexity. The use of Equation 3.30 is limited because the characteristics of overcurrent relays manufactured by North American manufacturers do not correspond to this equation.

3.4.2. Previously proposed algorithms

A digital algorithm for inverse-time overcurrent relays was proposed by Singh et al. [18]. They used Fourier analysis approach to estimate the fundamental frequency component of the current from its samples taken at 240 Hz. The operating time of the relay was computed using either Equation 3.34 or 3.35 depending on the relay characteristics being implemented. Since the current during a fault changes, they suggested that the following criterion be used to determine the instant when a trip command should be issued.

$$\int y(t)dt > K \tag{3.38}$$

where,

$y(t) = 0$ when the current is less than or equal to the pick-up value and

$y(t) = \frac{K}{t_r(t)}$ when the current is greater than the pick up value.

In this equation, K is a threshold and $t_r(t)$ is the operating time of the relay corresponding to the current observed at time t. This time was computed using the mathematical equation representing the relay characteristics. The integration suggested in Equation 3.38 starts when the relay current exceeds the pick up value. Reference [18] used two variations for resetting the relay. In one version, the summation provided by Equation 3.38 is reset to zero as soon as the relay current falls below the pick-up value whereas, in the second version, the summation is reduced at a rate selected by the user.

Another algorithm for digital inverse-time overcurrent relays reported by Degens and Langedijk [17] used the criterion described by Equation 3.38 for determining when a command to trip the circuit breaker be issued. The relay characteristics were modelled using Equation 3.36. A digital filter designed using the frequency sampling approach was used to estimate the rms value of the fundamantal frequency component of the relay current. A sampling rate of 600 Hz was used.

Yet, another algorithm is described by Schweitzer and Aliaga [19]. They also used the criterion of Equation 3.38 for determining when a command to trip the circuit breaker be issued. The authors of Reference [19] used Equation 3.37 to model the relay characteristics and employed FIR digital filters to estimate the rms value of the fundamental frequency component of the relay current from its samples. A sampling rate of 480 Hz was used in the application.

3.5. Microprocessor-Based Relays for Transformer Protection

Researchers used the previously described algorithms to design and implement relays for transformer protection. Three prototype relays reported in the literature are described. A relay designed by Larson et al. [24], provides differential protection for single phase transformers. Other relays [12, 17] includes differential, ground fault and overcurrent protection for three phase transformers. These relays use harmonic restraint to inhibit tripping during magnetizing inrush. The hardware used includes a data acquisition system and a microcomputer; brief details are given in this section.

The first relay [24]

This relay provides differential protection of single phase transformers. The hardware of this relay can be divided into three blocks, analog signal conditioning, analog to digital conversion and microcomputer blocks. The analog signal conditioning block consists of two isolation amplifiers, two low-pass filters, two sample-and-hold amplifiers, a multiplexer and a clock. The second block includes a 12-bit analog to digital converter (A/D) that has a 0-10V analog input range. The third block consists of a microcomputer built around a Motorola MC6800 microprocessor. The microcomputer contains five modules; a CPU, RAM, ROM, communications, and I/O modules. The CPU module contains the microprocessor, the system clock and buffers. The RAM module provides 2 Kbytes of static RAM for storing the relay software. The ROM module contains a program that was used for developing and debugging the software. The communications module provides an interface between the user and the computer. The I/O module facilitates exchange of data between the computer and the peripherals.

The relay uses variable percentage-bias characteristics to avoid tripping due to ratio mismatch and differences between the ct characteristics. Tripping during magnetizing inrush is restrained using the second harmonic com-

ponent of the differential current. The algorithm described in Section 3.1.2.3 of this chapter is used for this purpose.

The relay was tested in the laboratory using a single phase transformer. Magnetizing inrush, internal faults, simultaneous magnetizing inrush and internal faults, and external faults were applied. The reported results show that the magnetizing inrush conditions were correctly identified. The minimum and maximum relay operating times for internal faults were 12.6 and 19.1 ms respectively. However, for simultaneous internal faults and magnetizing inrush, the maximum operating time was 99 ms. During these tests, the transformer was supplying power at unity power factor. It is also reported that the relay did not operate during external faults.

The second relay [17]

This relay protects a two-winding three-phase transformer and provides differential, earth fault and inverse-time overcurrent protection. The relay hardware can be divided in four blocks, an analog signal conditioning block, an A/D converter block, a microcomputer and a digital to analog converters (D/A) block. The analog signal conditioning block consists of seven buffers, seven sample-and-hold amplifiers, and a multiplexer. A 12-bit A/D converter constitutes the second block. The third block is a microcomputer that uses a MOTOROLA MC68000 microprocessor, RAM, ROM and a clock. The clock is used to sample signals at 600 Hz. The fourth block of the relay includes D/A converters which convert digital signals to equivalent analog signals for verifying the operation of the relay.

The relay software, stored in ROM, implements the algorithms of Sections 3.1.2.5, 3.3 and 3.4.2 for differential, earth fault and overcurrent protection respectively. The proposed relay was tested in the laboratory using a 10 kVA, 220/220V, delta-wye connected three-phase transformer. Reference [17] reports that the relay detected earth faults in about 3.4 ms. However,

for inter-turn faults, the trip time range from 20 to 30 ms. The errors between the relay trip time and the theoretical trip time for inverse-time overcurrent protection ranged from 0 to 7.3%. The results for simultaneous internal faults and magnetizing inrush are not reported.

The third relay [12]

This relay uses a data acquisition system, a TMS32010 DSP chip, a digital output port and a power supply. The data acquisition system consists of analog scaling circuits, sample and hold amplifiers, an analog multiplexer, a 12-bit A/D converter and a programmable clock. The relay software is stored in the on-chip ROM of the TMS32010 processor. The software includes programs for controlling data acquisition and implementing algorithms for differential and earth fault protection of transformers. Algorithms described in Sections 3.1.2.4 and 3.3 are used in this relay.

The proposed relay was tested in the laboratory using a 7.5 kVA, 240/240V, delta-wye connected three-phase transformer. Some results showing the performance of the relay are reported in Reference [12]. The relay did not issue any trip commands during magnetizing inrush and overexcitation conditions. However, for heavy internal faults, a trip command was issued in about one-half cycle. Reference [12] does not report the trip times for internal faults accompanied by magnetizing inrush.

3.6. Microprocessor-Based Monitoring

Instruments presently used to measure, display and record the operating parameters of a transformer are described in Chapter 2. They either actuate an alarm or initiate tripping if a parameter exceeds a prespecified value. However, a microprocessor can perform monitoring functions that conventional instruments normally perform. Additionally, they can monitor the health of the transformer by analysing the observed parameters. This can enhance the availability and utilization of a transformer by continuously monitoring and analyzing its operating parameters [22].

A survey of the presently available literature revealed that only one microprocessor-based monitoring and analysis system has been reported [23]. This system uses a single board microcomputer based on an 8-bit NSC800 microprocessor manufactured by the National Semiconductor Corporation. The microcomputer has 16 Kbytes of read/write memory, 32 Kbytes of programmable ROM, an RS-232C interface for communication with the host computer and a digital display. The reported system includes sensors for measuring

- winding currents,
- relative corona,
- top oil temperature and
- gas-in-oil.

The monitoring system has a capability of monitoring 32 status inputs. Facilities for conditioning sensor outputs and converting them to equivalent digital numbers for storage in the microcomputer memory are also provided.

The reported system measures and checks the inputs every ten seconds and issues a trip command if an input is outside its prespecified limit. The parameters and status-input readings are stored in the read/write memory in the form of a circular table. Every 24 hours, the observed data are transferred to a host computer via an RS-232C communication port. The host computer uses diagnostic algorithms for analyzing the data to determine trends and deciding if the transformer is slowly developing a problem or problems.

3.7. Summary

Developments in the area of digital protection and monitoring of transformers are reported in this chapter. Digital algorithms for differential, ground fault and overcurrent protection of transformers are described. The presently used differential protection algorithms have some limitations. The harmonic-restraint differential algorithms can block tripping even during internal faults. Also, the issuing of a trip command can be delayed when the transformer is switched on with an internal fault. The application of algorithms using flux-restraint and transformer models is limited to single-phase and three-phase wye-wye transformers.

The modelling equations used for computer representation of overcurrent relay characteristics are reviewed. Their use in developing digital overcurrent relays either require large amounts of memory to store their coefficients or they are not easy to implement. The previously proposed microprocessor-based relays for transformer protection and a microprocessor-based monitoring system for power transformers are also described in this chapter.

4. THE PROPOSED ALGORITHM FOR A DIGITAL OVERCURRENT RELAY

4.1. Introduction

Previously proposed techniques for modelling characteristics of inverse-time overcurrent relays have been described in Chapter 3. Three algorithms used in digital overcurrent relays are also described in that chapter. The modelling techniques either require large amounts of memory for storing coefficients of equations or the equations are mathematically complex. Also, the algorithms used in overcurrent relays described in Chapter 3 require that a considerable amount of computations be performed in real-time .

This chapter describes and then evaluates another technique for modelling the characteristics of inverse-time overcurrent relays [42, 43]. The objective of this work was to develop a technique that is simple and requires only a modest amount of computer memory. Also described is an overcurrent digital relaying algorithm that uses the proposed modelling technique [42, 43]. The proposed algorithm performs most of the computations in an off-line mode and thus, reduces the on-line computations to a minimum. The algorithm was tested using digital computer simulations. Some results demonstrating the performance of the proposed algorithm are presented in this chapter.

4.2. Modelling of the Relay Characteristics

As already described in Chapter 3, the time-current characteristics of an overcurrent relay are a family of curves of relay currents in multiples of the pick-up current versus operating times. It is possible to achieve an operating time for a specified relay current by changing the time dial setting. The dial settings are continuous and it is, therefore, possible to describe an infinite number of time-current curves for a relay. However, most North American relay manufacturers provide curves for time dial settings of 0.5, 1, 2, 3, 4, 5, 6, 7, 8, 9, 10 and 11. Typical time current curves for the Westinghouse CO-7 and CO-9 overcurrent relays are shown in Figures 3.3 and 3.4 respectively.

This section describes the development of a new technique for modelling characteristics of overcurrent relays. The objective is that the technique should meet the following requirements.

1. The modelling equations should be simple so that their coefficients can be easily determined from the data taken from published time-current curves.

2. The operating times provided by the models should be accurate. Previous researchers [39, 41] considered the equations acceptable if, for a specified relay current, the calculated operating time is either within three cycles or is within five percent of the corresponding value taken from the published curve. However, in this study the technique was considered accurate if, for any current, the absolute difference between the operating time provided by the model and the time read from the published time-current curve does not exceed two cycles of the fundamental frequency.

3. The technique should represent the relay characteristics at all time dial settings without requiring excessive memory.

4. It should be easy to use the proposed technique for developing microprocessor-based overcurrent relays. The proposed equations should not use special functions, such as logarithm, trigonometric and exponential functions, because they are not included in the instruction sets of presently available microprocessors.

4.2.1. The technique

The similarities in the shapes of the time-current curves for different time dial settings suggest that, for each value of current, a relationship might exist between the operating times at different time dial settings [44]. The proposed technique uses this premise to model them for use in a digital overcurrent relay. Operating characteristics of the Westinghouse CO-7 relay were used for investigating the proposed approach. Figure 4.1 shows the relationship between the operating time and time dial settings at 5.0 times the pick-up current. It is plotted using the data taken from the published time-current curves of the relay. Investigations revealed that the operating time can be expressed as a polynomial in the time dial settings.

$$t_r = a_0 + a_1(TDS) + a_2(TDS)^2 + a_3(TDS)^3 + a_4(TDS)^4 + a_5(TDS)^5 \quad (4.1)$$

where,

t_r is the relay operating time,

TDS is the time dial setting and

$a's$ are the coefficients.

The coefficients a_0 to a_5 of the polynomial can be determined using data taken from the published curves and the least squares curve fitting technique. The procedure is illustrated in Appendix A. Further investigations revealed that Equation 4.1 is also suitable for expressing the operating time of the relay as a function of the time dial settings at other relay currents.

Time-current characteristics of the Westinghouse CO-7 and CO-9 overcurrent relays were modelled using the approach described in the previous paragraph. A FORTRAN program was written to determine the coefficients a_0, a_1, a_2, a_3, a_4 and a_5 at different current multiples. The program was executed on a microVAX 3600, which is available at the University of Sas-

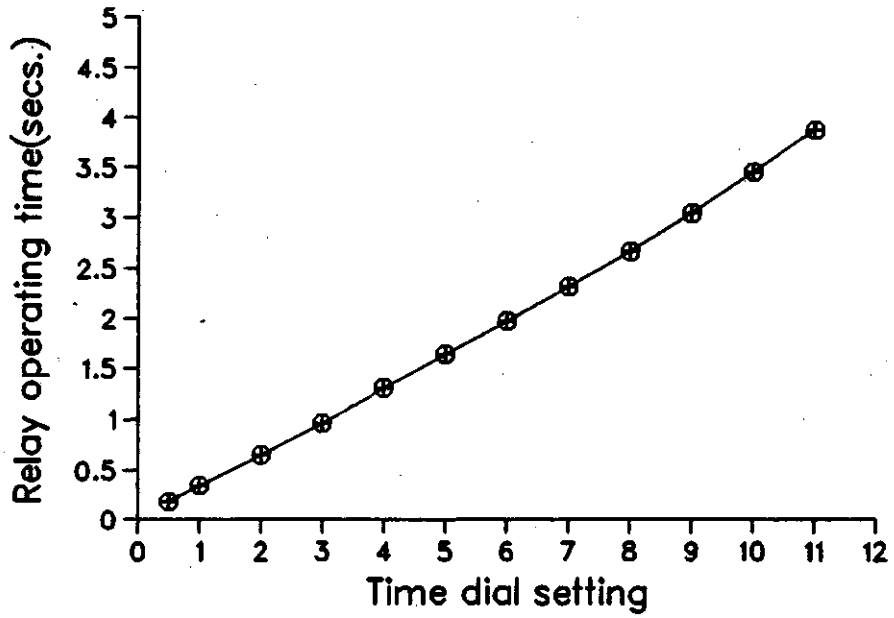

Figure 4.1: Operating time vs time dial setting characteristic of the Westinghouse CO-7 relay at 5.0 times the pick-up current.

katchewan, for calculating the coefficients of the polynomial for twenty four values of current between 1.5 and 20.0 times the pick-up value. The calculated values of the coefficients are listed in Tables 4.1 and 4.2.

The least squares curve fitting technique requires that at least seven data points be taken from the published curves. However, for CO-9 relay, enough data points corresponding to the currents of 1.5 and 2.0 times the pick-up value are not available for the CO-9 relay. In these cases, the order of the polynomial was reduced. At 1.5 times the pick-up current, a second order polynomial was used and, for 2.0 times the pick-up current, a fourth order polynomial was used.

Table 4.1: Coefficients of the polynomial described by Equation 4.1 for modelling the Westinghouse CO-7 overcurrent relay at 1.5 to 20 times the nominal relay current.

Current Multiple	a_0	a_1	a_2	a_3	a_4	a_5
1.50	-0.50170549	2.67026017	-1.34973598	0.52599458	-0.09038127	0.00566988
2.00	-0.09283568	0.92948496	-0.09696809	0.01508130	-0.00079067	0.00000810
2.50	0.03632798	0.54414232	-0.00511216	0.00007560	0.00015610	-0.00000799
3.00	-0.00303191	0.51123456	-0.04312224	0.01154906	-0.00127018	0.00005199
3.50	0.03096797	0.35754539	0.01873126	-0.00247928	0.00008254	0.00000476
4.00	0.05151062	0.30294002	0.03130589	-0.00589312	0.00046445	-0.00001038
4.50	0.03456471	0.32130107	0.00468170	0.00009391	-0.00009655	0.00000800
5.00	0.03879516	0.28733138	0.01192646	-0.00174806	0.00012020	-0.00000139
5.50	-0.00464754	0.35933891	-0.03970564	0.01062333	-0.00115447	0.00004527
6.00	0.02048806	0.29292212	-0.00866005	0.00313799	-0.00037063	0.00001572
7.00	-0.01401317	0.38163779	-0.07336994	0.01772749	-0.00177572	0.00006410
8.00	0.02592358	0.28607476	-0.03223135	0.00923230	-0.00101396	0.00003935
9.00	0.01824297	0.29246388	-0.04939077	0.01410042	-0.00155667	0.00006018
10.00	-0.00311027	0.32124139	-0.06707830	0.01726533	-0.00179660	0.00006652
11.00	0.03205489	0.22309450	-0.01707779	0.00627429	-0.00075179	0.00003068
12.00	0.01363259	0.25560288	-0.04344218	0.01295800	-0.00145995	0.00005707
13.00	-0.00164477	0.26909819	-0.05272161	0.01468836	-0.00159399	0.00006059
14.00	0.02461869	0.19844837	-0.01782865	0.00778841	-0.00102484	0.00004398
15.00	0.00530226	0.21302900	-0.01857143	0.00616683	-0.00074087	0.00003082
16.00	-0.00633983	0.23003461	-0.02558630	0.00710173	-0.00080873	0.00003314
17.00	-0.00825752	0.23807609	-0.03393328	0.00923281	-0.00102306	0.00004042
18.00	-0.01772032	0.26161343	-0.05029023	0.01309325	-0.00141575	0.00005454
19.00	-0.00238724	0.22600609	-0.02708797	0.00710583	-0.00078972	0.00003182
20.00	0.00754069	0.19118477	-0.00093408	-0.00001072	-0.00002177	0.00000319

Table 4.2: Coefficients of the polynomial described by Equation 4.1 for modelling the Westinghouse CO-9 overcurrent relay at 1.5 to 20 times the nominal relay current.

Current Multiple	a_0	a_1	a_2	a_3	a_4	a_5
1.50	-0.25000000	3.00000000	0.20000000	0.00000000	0.00000000	-0.00000000
2.00	-0.50000000	2.34166667	-0.52500000	0.08333333	0.00000000	-0.00000000
2.50	-0.10436216	1.03861012	-0.15307948	0.03827397	-0.00339426	0.00008860
3.00	0.03504518	0.43725946	0.07227383	-0.01439470	0.00126508	-0.00003539
3.50	0.02309296	0.34508244	0.04057259	-0.00764535	0.00064285	-0.00001622
4.00	0.03452176	0.25229669	0.04412877	-0.00915841	0.00089450	-0.00002980
4.50	-0.00314329	0.32167590	-0.04017232	0.01186557	-0.00126405	0.00004741
5.00	-0.01172525	0.27473664	-0.02825793	0.00781172	-0.00074548	0.00002484
5.50	-0.01906332	0.28950601	-0.05705902	0.01478586	-0.00145136	0.00005017
6.00	-0.01969300	0.25749127	-0.04303414	0.01069585	-0.00100880	0.00003385
7.00	0.00341260	0.18339624	-0.01424128	0.00400247	-0.00035965	0.00001141
8.00	-0.00542461	0.15470824	0.00255687	-0.00104307	0.00019701	-0.00000965
9.00	0.01990978	0.08471045	0.03317398	-0.00706383	0.00069044	-0.00002390
10.00	0.01612496	0.07006516	0.03489566	-0.00675172	0.00058789	-0.00001803
11.00	0.03040563	0.03790954	0.04630300	-0.00879280	0.00076288	-0.00002416
12.00	0.03108729	0.03212299	0.04820600	-0.00957980	0.00085650	-0.00002766
13.00	0.03317061	0.02369164	0.04912206	-0.00947451	0.00082061	-0.00002570
14.00	0.02488866	0.03749725	0.03989324	-0.00728119	0.00058557	-0.00001673
15.00	0.02584635	0.03204869	0.04343524	-0.00853137	0.00074388	-0.00002339
16.00	0.03088309	0.02112052	0.04630978	-0.00870148	0.00071369	-0.00002075
17.00	0.01733698	0.05449638	0.02377806	-0.00351537	0.00021364	-0.00000362
18.00	0.02758798	0.02733680	0.04265387	-0.00868751	0.00078961	-0.00002587
19.00	0.01664379	0.05345982	0.02622895	-0.00488320	0.00041150	-0.00001244
20.00	0.01117894	0.06762264	0.01633767	-0.00247559	0.00016233	-0.00000324

4.2.2. Evaluation of the proposed technique

The proposed technique was evaluated to verify if it meets the specifications listed in Section 4.1. This section presents the results showing the accuracy of the proposed technique.

1. The proposed technique is simple because the coefficients of the polynomials can be easily calculated in the off-line mode and stored in the memory of a microprocessor.

2. Equation 4.1 can be used to compute the operating time of the relay at a selected time dial setting and a specified current-multiple if the coefficients (a's) corresponding to the current-multiple are available in the computer memory. To compute the operating time at other time dial settings and other current multiples, linear interpolation can be used.

3. The proposed technique uses the coefficients a_0 to a_5 for twenty four current multiples. This means that 144 coefficients are needed to model the entire relay characteristics. Each coefficient takes two bytes of storage space, therefore, 288 bytes of the microprocessor memory are required to store the coefficients of one relay.

4. The accuracy of the modelling technique was verified by comparing the computed values of the operating times, for different current-multiples at different time dial settings, with the corresponding values read from the published curves. The operating times were calculated using Equation 4.1 and the coefficients listed in Tables 4.1 and 4.2. Tables 4.3 and 4.4 show the absolute differences between the operating times computed by Equation 4.1 and the corresponding times obtained from the published curves for the Westinghouse CO-7 relay. The absolute differences in the operating times for the Westinghouse CO-9 overcurrent relay are listed in Tables 4.5 and 4.6. A review of Tables 4.3 to 4.6 indicates that the differences between the computed and published operating times are less than two cycles of the fundamental frequency, the specified limit.

5. The relay operating time for a specified relay current and a time dial setting can be computed using Equation 4.1 and the values of the 'a' coefficients stored in the microprocessor memory. The calculations require additions and multiplications only. Interpolations, when they become necessary, also require additions, subtractions, multiplications and divisions only. These operations are

available in the instruction sets of most presently available microprocessors.

Table 4.3: Differences (in cycles of 60 Hz) between the relay operating times calculated by using Equation 4.1 and the published operating times for the CO-7 relay.

Current multiple	Differences at time dial settings of					
	0.5	1.0	2.0	3.0	4.0	5.0
1.50	0.22	0.61	1.01	1.21	0.87	0.34
2.00	0.03	0.24	0.81	1.08	0.32	0.20
2.50	0.43	0.87	0.42	0.63	0.74	0.52
3.00	0.19	0.28	0.26	0.85	0.35	0.76
3.50	0.43	0.61	0.44	1.39	0.71	0.09
4.00	0.61	0.88	0.45	1.38	0.28	0.30
4.50	0.38	0.57	0.28	1.04	0.65	0.27
5.00	0.31	0.51	0.06	0.62	0.22	0.25
5.50	0.08	0.03	0.41	0.62	0.11	0.16
6.00	0.01	0.15	0.52	0.29	0.34	0.20
7.00	0.27	0.62	0.53	0.24	0.85	0.22
8.00	0.12	0.12	0.12	0.25	0.97	0.37
9.00	0.07	0.24	0.27	0.28	0.80	0.09
10.00	0.13	0.40	0.45	0.38	1.31	0.64
11.00	0.00	0.22	0.66	0.22	0.70	0.05
12.00	0.17	0.44	0.41	0.30	0.90	0.23
13.00	0.21	0.47	0.32	0.40	0.91	0.30
14.00	0.28	0.72	0.75	0.15	0.86	0.10
15.00	0.13	0.31	0.27	0.23	0.41	0.62
16.00	0.11	0.27	0.22	0.13	0.35	0.00
17.00	0.10	0.25	0.24	0.19	0.69	0.31
18.00	0.18	0.32	0.11	0.20	0.33	0.28
19.00	0.02	0.17	0.51	0.45	0.21	0.33
20.00	0.17	0.13	0.55	0.68	0.50	0.89

Table 4.4: Differences (in cycles of 60 Hz) between the relay operating times calculated by using Equation 4.1 and the published operating times for the CO-7 relay.

Current multiple	Differences at time dial settings of					
	6.0	7.0	8.0	9.0	10.0	11.0
1.50	0.06	-	-	-	-	-
2.00	0.66	1.37	0.86	0.19	-	-
2.50	0.82	0.67	1.89	1.61	0.67	0.12
3.00	0.88	0.11	0.53	0.66	0.38	0.09
3.50	0.06	0.04	0.32	1.27	1.12	0.31
4.00	0.33	0.27	0.22	1.34	1.48	0.43
4.50	0.10	0.73	0.56	0.76	0.97	0.29
5.00	0.03	0.01	0.15	0.18	0.32	0.11
5.50	0.15	0.18	0.13	0.38	0.36	0.10
6.00	0.84	0.16	0.81	0.01	0.43	0.16
7.00	0.56	0.40	0.19	0.33	0.27	0.07
8.00	0.41	0.44	0.90	0.07	0.52	0.18
9.00	0.53	0.26	0.72	0.06	0.30	0.11
10.00	0.14	0.60	0.86	0.08	0.46	0.16
11.00	0.88	0.33	0.73	0.58	0.93	0.29
12.00	0.36	0.14	0.17	0.48	0.52	0.15
13.00	0.42	0.18	0.24	0.16	0.00	0.01
14.00	0.63	0.30	0.13	1.02	0.97	0.26
15.00	1.41	0.65	0.22	0.13	0.09	0.05
16.00	0.22	0.07	0.25	0.55	0.39	0.09
17.00	0.52	0.63	0.24	0.08	0.07	0.02
18.00	0.06	0.47	0.08	0.60	0.54	0.14
19.00	0.16	0.20	0.10	0.32	0.32	0.09
20.00	0.28	0.76	0.48	0.60	0.53	0.16

Table 4.5: Differences (in cycles of 60 Hz) between the relay operating times calculated by using Equation 4.1 and the published operating times for the CO-9 relay.

Current multiple	Differences at time dial settings of					
	0.5	1.0	2.0	3.0	4.0	5.0
1.50	0.00	0.00	0.00	-	-	-
2.00	0.00	0.00	0.00	0.00	0.00	-
2.50	0.67	1.43	0.92	0.82	1.67	0.08
3.00	0.60	1.12	0.16	1.65	1.99	0.54
3.50	0.29	0.50	0.05	0.91	1.13	0.50
4.00	0.34	0.44	0.26	0.39	0.13	0.62
4.50	0.06	0.06	0.34	0.29	1.49	1.04
5.00	0.03	0.11	0.24	0.28	0.32	0.52
5.50	0.11	0.11	0.20	0.01	1.07	1.50
6.00	0.03	0.03	0.22	0.05	1.04	1.45
7.00	0.12	0.23	0.01	0.43	0.31	0.27
8.00	0.15	0.24	0.08	0.43	0.11	0.32
9.00	0.28	0.52	0.05	0.72	0.62	0.20
10.00	0.18	0.31	0.04	0.08	0.28	0.24
11.00	0.29	0.51	0.15	0.04	0.64	0.62
12.00	0.24	0.44	0.26	0.28	0.52	0.10
13.00	0.25	0.46	0.21	0.05	0.08	0.12
14.00	0.16	0.27	0.00	0.19	0.00	0.10
15.00	0.16	0.21	0.20	0.43	0.03	0.16
16.00	0.18	0.28	0.03	0.23	0.05	0.13
17.00	0.07	0.10	0.02	0.08	0.11	0.18
18.00	0.17	0.26	0.11	0.40	0.06	0.16
19.00	0.08	0.13	0.08	0.39	0.29	0.15
20.00	0.05	0.07	0.09	0.40	0.43	0.02

Table 4.6: Differences (in cycles of 60 Hz) between the relay operating times calculated by using Equation 4.1 and the published operating times for the CO-9 relay.

Current multiple	Differences at time dial settings of					
	6.0	7.0	8.0	9.0	10.0	11.0
1.50	-	-	-	-	-	-
2.00	-	-	-	-	-	-
2.50	1.42	1.05	0.24	-	-	-
3.00	0.33	0.44	0.64	0.52	0.14	-
3.50	0.59	1.48	1.06	0.11	0.45	0.14
4.00	0.82	1.29	1.53	0.75	1.37	0.42
4.50	0.05	0.71	0.88	0.36	0.75	0.24
5.00	0.37	0.37	0.77	0.44	0.07	0.01
5.50	0.49	0.50	0.89	0.96	0.59	0.14
6.00	0.47	0.63	0.87	0.63	0.30	0.06
7.00	0.20	0.03	0.56	1.04	0.65	0.14
8.00	0.01	0.06	0.76	1.10	0.58	0.11
9.00	0.34	0.20	0.54	0.67	0.32	0.05
10.00	0.24	0.06	0.61	0.39	0.01	0.03
11.00	0.22	0.04	0.80	0.54	0.01	0.05
12.00	0.30	0.37	0.62	0.16	0.45	0.15
13.00	0.05	0.33	0.27	0.28	0.39	0.12
14.00	0.13	0.33	0.02	0.59	0.55	0.15
15.00	0.07	0.29	0.03	0.76	0.70	0.19
16.00	0.07	0.11	0.11	0.35	0.40	0.12
17.00	0.01	0.02	0.11	0.05	0.04	0.02
18.00	0.13	0.02	0.28	0.09	0.11	0.05
19.00	0.21	0.00	0.03	0.15	0.10	0.02
20.00	0.33	0.07	0.67	0.71	0.33	0.06

4.3. Computing the RMS Value

An overcurrent relay must determine the rms value of the fundamental frequency component of the current. A current may contain, in addition to a fundamental frequency component, transient components, such as, exponentially decaying dc and, harmonic and other high frequency components. This is especially true for currents during a fault. However, it is possible to suppress the transient components of a current and compute the rms value of the fundamental frequency component. Microprocessor-based relays achieve this by using digital filtering techniques. In the work reported in this chapter, the least squares technique was used to design digital filters which compute the real and imaginary components of the current phasors (the procedure used is discussed in Chapter 3). The digital filters used in this work were designed assuming that a relay current is composed of an exponentially decaying dc component and, the fundamental, second and third harmonic frequency components. A data window of twenty samples taken at 1200 Hz was used. The time reference (t=0) was assumed to coincide with the centre of the data window. The decaying dc component was approximated using the first two terms of its Taylor series expansion. Table 4.7 lists the coefficients of the designed filters. Using the coefficients listed in the first column provides estimates of the real components of the phasor and using the coefficients in the second column provides estimates of the imaginary components of the phasor.

The rms value of the fundamental frequency component was computed from the real and imaginary components of the fundamental frequency phasor using two methods. The first method uses the following equation.

$$I_{rms} = 0.707\sqrt{I_r^2 + I_i^2} \qquad (4.2)$$

where:

Table 4.7: Coefficients of the least error square filters for calculating the real and imaginary components of the fundamental frequency components.

Filter for calculating the	
Real part	Imaginary part
0.387272	-0.098768
0.004456	-0.089100
-0.183139	-0.070710
-0.180170	-0.045399
-0.089541	-0.015643
-0.027554	0.015643
-0.041563	0.045399
-0.091886	0.070710
-0.104884	0.089100
-0.046636	0.098768
0.046636	0.098768
0.104884	0.089100
0.091886	0.070710
0.041563	0.045399
0.027554	0.015643
0.089541	-0.015643
0.180170	-0.045399
0.183139	-0.070710
-0.004456	-0.089100
-0.387272	-0.098768

I_{rms} is the rms value of the fundamental frequency component of the relay current,

I_r is the real part of the phasor representing the fundamental frequency component of the current,

I_i is the imaginary part of the phasor representing the fundamental frequency component of the current.

This procedure requires that a square root be taken; this can be achieved either by using special hardware capable of performing this function or by

using a computationally expensive subroutine written as a part of the relay software. The second approach is to use a piecewise linear approximation technique to estimate the rms value of the fundamental frequency component of the relay current [45]. The details of the technique are given in Appendix B. The technique uses the following equation to estimate the rms value of the fundamental frequency current.

$$I_{rms} = x_n a + y_n b \tag{4.3}$$

where:

a	represents the larger of the two values, $\|I_r\|$ and $\|I_i\|$,
b	represents the smaller of the two values, $\|I_r\|$ and $\|I_i\|$,
x_n *and* y_n	are the coefficients for the nth region in which the fraction b/a lies.

In the work reported in this chapter, a two region approximation was used. The values of the coefficients for the two regions are given in Table 4.8.

The procedure involves comparing the values of a and b to find out the region in which the fraction b/a lies. Then, the rms value is computed by using the coefficients for the appropriate region and Equation 4.3.

Table 4.8: Values of the the coefficients for calculating the rms value of a phasor using the two-region approximation approach.

Region	x	y
0 = b/a < 0.25	0.7036	0.0873
0.25 < b/a < 1.0	0.6163	0.3660

4.4. The Algorithm

A technique for modelling overcurrent relay characteristics has been described previously. This technique is suitable for use in digital inverse-time overcurrent relays. This section develops an algorithm for digital overcurrent relays. Three options for resetting the relay are also described. The functions performed by the proposed algorithm are then outlined.

4.4.1. Development of the algorithm

Major functions performed by an overcurrent relaying algorithm include estimating the rms value of the fundamental frequency current and deciding if the current has exceeded a threshold value. If the current is more than the threshold, the relay should issue a command to trip the circuit breaker after a time delay which emulates the time-current characteristics of the relay. Equation 4.1 and the stored coefficients a_0 to a_5 can be used to determine the time delay corresponding to the current in the protected equipment. Since the current during a fault changes with time, Equation 4.1 can be modified to the following form for determining the instant when a trip command should be issued [18].

$$\int y(t)dt > K \tag{4.4}$$

where:

$y(t) = 0$ when the current is less than or equal to the pick-up value,

$y(t) = K/t_r(t)$ when the current is greater than the pick-up value.

In this equation, K is a target number and $t_r(t)$ is the operating time of the relay for the current observed at time t. The integration defined in Equation 4.4 is started at the inception of the fault i.e. when the relay current exceeds the pick-up value. The procedure is continued untill the value of integral, $\int y(t)dt$, exceeds the target number, K, at which time a trip com-

mand is issued. However, if the value of the relay current, after having exceeded the pick-up value, falls below the nominal value, the process to reset the relay is started. This is done by modifying the value of the integral, $\int y(t)dt$, in a manner that achieves the desired reset characteristics.

Because digital relays use values of currents sampled at ΔT seconds, numerical integration can be performed using the equation

$$\sum_{m=1}^{N} (X)_m > K \tag{4.5}$$

where,

$(X)_m = 0$ when the current is less than or equal to the pick-up value and

$(X)_m = \frac{K\Delta T}{(t_r)_m}$ when the current is greater than the pick-up value.

In this equation, m represents the $m-th$ sample after the inception of a fault and $(t_r)_m$ is the relay operating time corresponding to the current estimated on receiving the $m-th$ sample. Let $N\Delta T$ be the time to relay contact closing; ΔT is known but N is not. It is, therefore, necessary to compute the value of $(X)_m$ and check the criterion described in Equation 4.5 after taking each sample of the current. If the current is less than the pick-up value, the relay is reset by reducing the value of the sum, $\sum (X)_m$, in a manner that achieves the desired reset characteristics.

The computations of the values of $(X)_m$ include calculating the tripping time $(t_r)_m$ corresponding to the relay current estimated after taking the $m-th$ sample and the term $\frac{K\Delta T}{(t_r)_m}$. This requires considerable real-time computations. These can be avoided if the relay type, time dial setting, sampling interval, ΔT, and the value of the target number, K are selected by the operator in an off-line mode when the relay is first powered on.

In the relay designed by the author, the microprocessor computes t_r corresponding to current multiples of 1.5, 2.0, 2.5, 3.0, 3.5, 4.0, 4.5, 5.0, 5.5, 6.0, 7.0, 8.0, 9.0, 10.0, 11.0, 12.0, 13.0, 14.0, 15.0, 16.0, 17.0, 18.0, 19.0 and 20.0 in an off-line mode. The processor uses Equation 4.1 and the appropriate coefficients (a's) listed in Tables 4.1 and 4.2 and are stored in the relay memory. The values of $\frac{K\Delta T}{t_r}$ at selected current multiples are then computed using the prespecified values of K and ΔT. The computed values are stored in the form of a look-up table for use in the on-line mode. Figure 4.2 shows the values of $\frac{K\Delta T}{(t_r)}$ computed for the Westinghouse CO-7 relay when K is 70,562,000, ΔT is 1.0/1200.0 and a time-dial setting is 5.0. The time-current characteristics of the relay is also shown in the figure for comparison.

Now, the relay can use the look-up table to compute the values of $\sum (X)_m$ without calculating $\frac{K\Delta T}{t_r}$ in real-time. For currents listed in the table, the values of $(X)_m$ are read from the look-up table, and for other currents, linear interpolation is used. If $(I)_m$ is the relay current for which the value of $(X)_m$ is to be determined, interpolation is performed using the equation

$$(X)_m = (X)_1 + \frac{[(X)_2 - (X)_1][(I)_m - (I)_1]}{(I)_2 - (I)_1} \tag{4.6}$$

where,

$(I)_1$ *and* $(I)_2$ are currents in the look-up table that are lesser and greater than the calculated current respectively and

$(X)_1$ *and* $(X)_2$ are the numbers in the look-up table corresponding to the currents $(I)_1$ and $(I)_2$ respectively.

Once the value of $(X)_m$ is known, the criteria of Equation 4.5 is used to decide when a trip command should be issued.

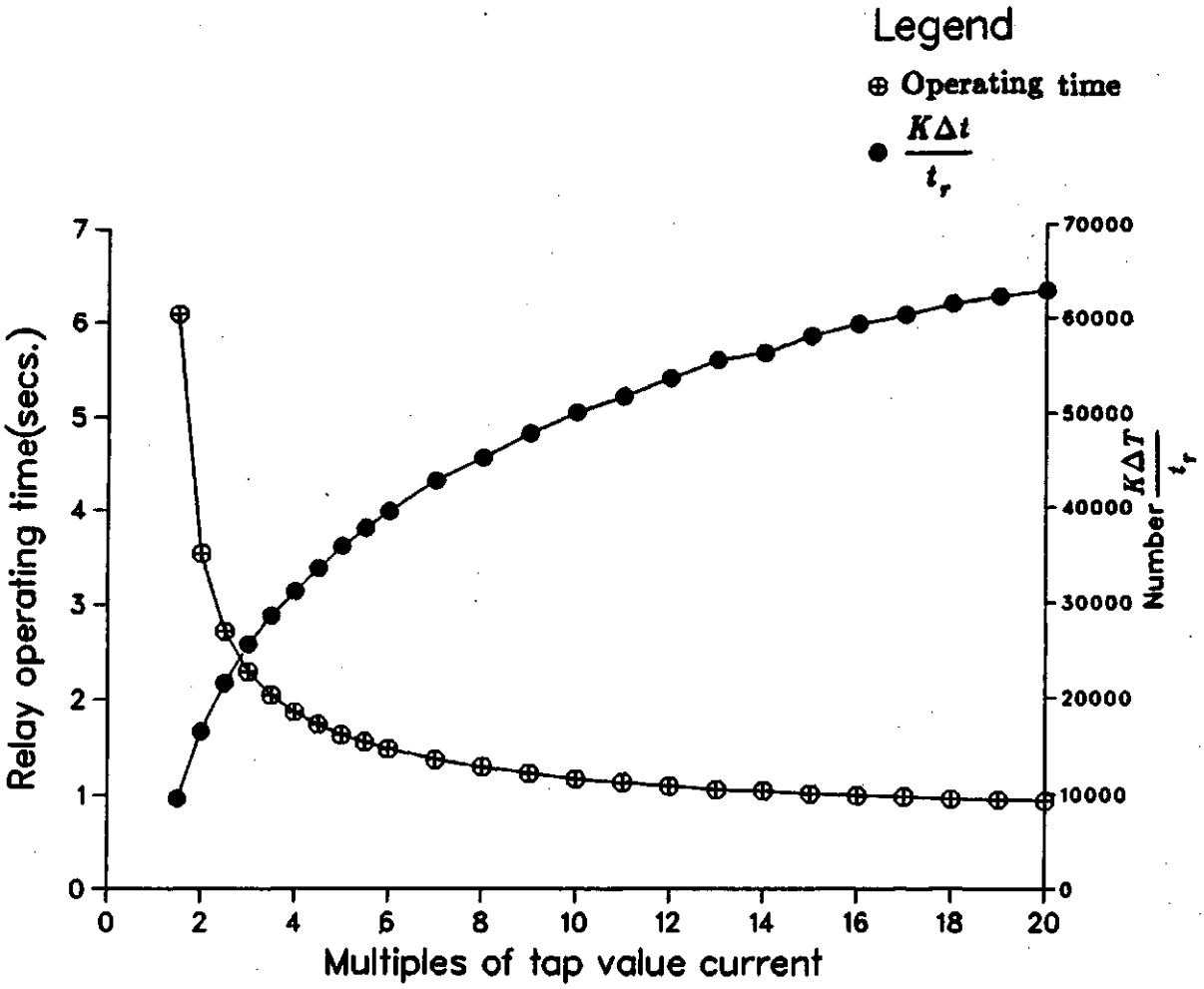

Figure 4.2: Calculated values of $\frac{K\Delta T}{t_r}$ for the Westinghouse CO-7 overcurrent relay.

4.4.2. Selection of the target number

Off-line computations of $\frac{K\Delta T}{t_r}$ require that an appropriate value of K be selected and provided to the algorithm. This value should be such that time delays are accurate. Consider that a trip delay of t_r corresponds to the relay current. Let $\frac{K\Delta T}{t_r}$ corresponding to the relay current be

$$\frac{K\Delta T}{t_r} = X+y \tag{4.7}$$

where,

X is the integer part of the number and,

y is the decimal part of the number.

If the computed number, $X+y$, is used in the criterion of Equation 4.5 to determine the trip time, it will be satisfied in N sampling intervals such that $N\Delta T$ is equal to the trip time, t_r. A selected value of K, will provide accurate trip times if the computations are performed in floating point arithmetic. However, in most microprocessor-based relays, the calculations are performed using integer arithmetic. Therefore, the decimal part of the number is truncated when the criterion of Equation 4.5 is applied. This introduces errors in the tripping times. The errors can be limited to a maximum of one sampling interval if the contribution of the decimal part, y towards the criterion of Equation 4.5 in a period of N sampling intervals is less than the number, X. This can be mathematically expressed as

$$(N)(y) < X. \tag{4.8}$$

In a worst case situation, the value of the decimal part, y can be $0.999\cdots$. Considering it to be approximately 1.0 reduces the Inequality 4.8 to the following:

$$N < X \tag{4.9}$$

It is possible to express N and X in terms of the relay operating time, t_r, the sampling interval, ΔT, and the target number, K as

$$X = INT(\frac{K\Delta T}{t_r}) \text{ and} \tag{4.10}$$

$$N = INT(\frac{t_r}{\Delta T}) \tag{4.11}$$

where,

INT represents an integer value.

Substituting the values of N and X in Inequality 4.9 provides

$$INT(\frac{t_r}{\Delta T}) < INT(\frac{K\Delta T}{t_r}). \tag{4.12}$$

Simplification of this expression provides the following criterion for the selection of the target number, K.

$$K > INT[(\frac{t_r}{\Delta T})^2] \tag{4.13}$$

The selected value of the target number should satisfy this criterion for the entire range of the relay characteristics. The largest value of the trip time should, therefore, be used in the inequality. For example, the largest value of the trip time for the Westinghouse CO-7 relay is 7.0 s. If a sampling rate of 1200 Hz is used, the value of the target number should be greater than 70,560,000.

4.4.3. Reset characteristics

As soon as the currents in a protected circuit fall below the pick-up value, the inverse-time overcurrent relays used to protect the circuit reset. Electromechanical relays reset gradually due to the influence of restraining springs. Some solid state overcurrent relays also reset gradually while others reset without any time delay. In digital overcurrent relays, a variety of reset characteristics can be achieved. It is possible to match reset characteristics of a relay with the cooling characteristics of the protected equipment. In this work, the resetting of the relay was achieved by reducing the value of $\sum(X)_m$ in a prespecified manner and testing if the relay has reset. The relay is assumed to have reset, when the value of the accumulated sum reduces to zero; if the value becomes negative, it is reset to zero.

Three types of reset characteristics were provided in the design. This section describes the characteristics and presents the procedure used to achieve the characteristics.

Linear reset characteristics

If this type of characteristics is selected, the relay resets linearly with time. This is achieved by modifying $\sum(X)_m$, using Equation 4.14.

$$[\sum(X)]_{m+1} = [\sum(X)]_m - L \tag{4.14}$$

where,

L is an integer number used for resetting the relay.

The selected value of L determines the rate at which the relay resets. Figure 4.3 shows five of the possible linear reset characteristics that can be obtained using Equation 4.14. In this figure, $\sum(X)_m$ and L have been normalized by using K as the base value. This has avoided the use of specific numbers in the figure. Also, the time on the x-axis is shown as number of sampling intervals because Equation 4.14 is executed at ΔT intervals in a digital relay.

Exponential reset characteristics

If this type of characteristics is selected, the relay resets exponentially with time. This characteristics is achieved by using the equation

$$[\sum(X)]_{m+1} = E_x[\sum(X)]_m \tag{4.15}$$

where,

E_x is a fractional number.

Figure 4.4 shows five reset characteristics that can be achieved by the

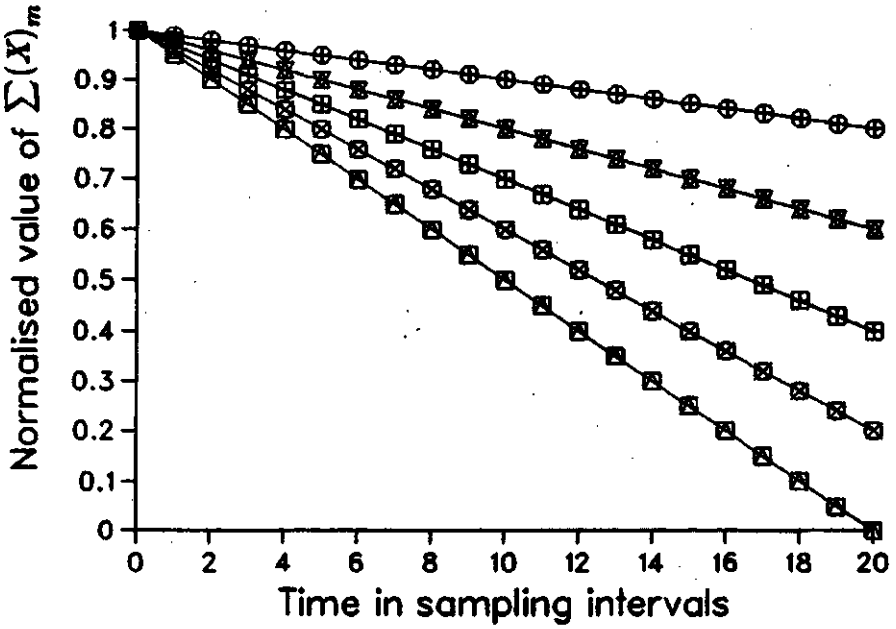

Figure 4.3: Linear reset characteristics provided by Equation 4.14.

described procedure. This figure shows that the relay resetting rate is controlled by value of E_x. In this figure also, $\sum(X)_m$ is normalised by using the target number, K as the base value.

Instantaneous reset characteristics

If this type of characteristics is selected, the relay resets without any time delay. The accumulated value of sum, $\sum(X)_m$ is reduced to zero as soon as the relay current falls below the pick-up value.

4.4.4. Functions of the algorithm

The developed algorithm performs its functions in two parts. The functions in the first part interact with the operator and perform computations off-line . The remaining functions consist of on-line calculations.

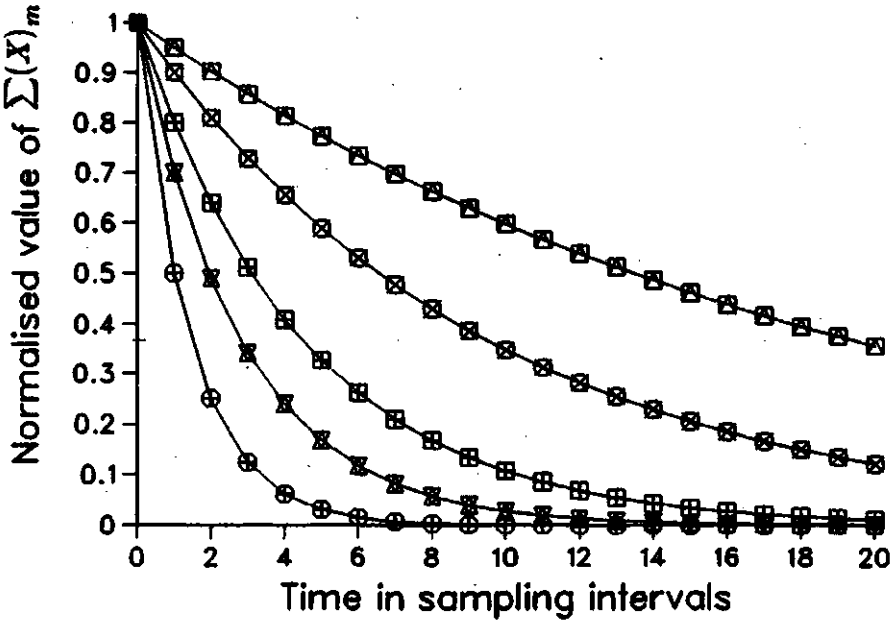

Figure 4.4: Exponential reset characteristics provided by Equation 4.15.

4.4.4.1. Off-line computations

The algorithm interacts with an operator allowing him to select a relay characteristic and relay settings. The algorithm also performs some computations in an off-line mode. The functions performed by the algorithm are as follows.

1. When a relay is powered on, the algorithm displays the available relays. The operator is prompted to select the desired relay type.

2. After selecting the relay type, the operator is prompted to input the desired time dial setting and the pick-up current.

3. The operator is then prompted to select the type of the desired reset characteristics. If the linear reset characteristic is chosen, the operator is prompted to input the value of L. If either exponential or instantaneous reset characteristics are selected, the operator is prompted to enter the value of E_x. For instantaneous reset characteristics, the operator inputs a value of zero.

4. The relay calculates the operating times, (t_r), for selected values of the time dial setting for current multiples of 1.5, 2.0, 2.5, 3.0, 3.5, 4.0, 4.5, 5.0, 5.5, 6.0, 7.0, 8.0, 9.0, 10.0, 11.0, 12.0, 13.0, 14.0, 15.0, 16.0, 17.0, 18.0, 19.0 and 20.0. The relay uses the stored values of the coefficients, a_0 to a_5, and Equation 4.1 to compute the operating times. The relay then calculates the values of $\frac{K\Delta T}{t_r}$ at these current multiples and stores them in the form of a look-up table.

4.4.4.2. On-line operations

In the on-line mode, an input to the relay is a voltage representing a relay current. This voltage is sampled at a specified rate. The sampled data are processed to determine the rms value of the fundamental frequency component by using the least squares filters and the procedure described earlier in this chapter. Equation 4.5 is then used as a criterion for the relay operation. The algorithm implements the criterion by specifically performing the following functions.

1. Set a variable 'SUM' to zero.

2. Obtain a new sample representing the relay current.

3. Determine the rms value of the fundamental frequency component of the current by using least squares filters and two region linear approximation technique described earlier.

4. Compare the computed rms value with the pick-up current.

5. If the rms value exceeds the pick-up current, proceed to step 6, otherwise proceed to step 10.

6. Obtain the number, $(X)_m$ corresponding to the computed value of the current from the look-up table formed in the off-line mode. For values of the current which are not in the table, use the interpolation procedure described by Equation 4.6.

7. Add the number from step 6 to the variable 'SUM'.

8. Check if the updated value of 'SUM' is larger than the target number, K. If it is, issue a trip command.

9. Wait until the intersampling time is expired; revert to step 2.

10. Determine the type of the selected reset characteristics. If it is linear reset characteristics, proceed to step 11. For exponential or instantaneous reset characteristics, proceed to step 12.

11. Modify the variable 'SUM' by subtracting from it the integer number L. Check if the resulting value of 'SUM' is equal to or less than zero. If it is, reset the variable 'SUM' to zero and revert to step 9. Otherwise revert to step 9 without resetting variable 'SUM' to zero.

12. Modify the variable 'SUM' by multiplying it with the number, E_x. Check if the resulting value of 'SUM' is less than $K/128$. If it is, reset the variable 'SUM' to zero and revert to step 9. Otherwise revert to step 9 without resetting variable 'SUM' to zero.

4.5. Test Results

The proposed algorithm was tested off-line using a microVAX 3600 digital computer that is available at the University of Saskatchewan. FORTRAN programs were written to simulate the off-line and on-line operations of the proposed algorithm.

The program for simulating the off-line operation of the algorithm used a target number, K, equal to 70,562,000. This number was selected considering a sampling rate of 1200 Hz and the criteria described earlier in this chapter. The program allows the user to select a time dial setting at which the operation of the relay is to be studied. The program then computes the operating times of the relay at a selected time dial setting for current multiples of 1.5, 2.0, 2.5, 3.0, 3.5, 4.0, 4.5, 5.0, 5.5, 6.0, 7.0, 8.0, 9.0, 10.0, 11.0, 12.0, 13.0, 14.0, 15.0, 16.0, 17.0, 18.0, 19.0 and 20.0. In the next step, the program calculates the values of $\frac{K\Delta T}{t_r}$ at these current multiples and stores them in a look-up table for use by the programs simulating on-line functions of the algorithm.

The simulations of the on-line mode of the algorithm were accomplished

by using two FORTRAN programs. The first program allows the user to input the value of a relay current in multiples of the pick-up value and synthesizes a sinusoidal voltage waveform of the fundamental frequency representing the relay current. The program also discretizes the waveform at intervals of 1/1200 s. The samples are presented to a second FORTRAN program which performs steps 1 to 12 of the on-line functions of the proposed algorithm and determines the operating time.

The programs were executed on the microVAX 3600 digital computer and the relay operating times were computed for relay currents of 2.75, 3.25, 3.75, 4.25, 4.75, 5.25, 5.75, 6.5, 7.5, 8.5, 9.5, 10.5, 11.5, 12.5, 13.5, 14.5, 15.5, 16.5, 17.5, 18.5 and 19.5 times the pick-up value. This was done for both the Westinghouse CO-7 and CO-9 relays at time dial settings of 0.5, 1.0, 2.0, 3.0, 4.0, 5.0, 6.0, 7.0, 8.0, 9.0, and 10.0. The relay operating times obtained from the simulations were compared with the corresponding values read from the published curves and their absolute differences were computed. Tables 4.9 and 4.10 list these differences for the Westinghouse CO-7 relay. Similarly, Tables 4.11 and 4.12 list the differences between the published operating times and the times obtained from the simulation programs for the Westinghouse CO-9 overcurrent relay. An analysis of Tables 4.9 to 4.12 indicate that the operating times provided by the algorithm are within two cycles of the corresponding value obtained from the published curves. This indicates that the proposed algorithm accurately emulates the time current curves of the selected relays.

4.6. Summary

This chapter described a technique for computer modelling of overcurrent relay characteristics. Characteristics of the Westinghouse CO-7 and CO-9 overcurrent relays are modelled to demonstrate the suitability of the proposed technique. Results showing the evaluation of the proposed technique are also presented. The results demonstrate that the proposed technique accurately represents the selected time-current characteristics. The

operating times provided by the modelling technique are within two cycles of the corresponding times of the published curves. The proposed technique is simple and accurate and can be easily used in microprocessor-based overcurrent relays.

The proposed technique has been used for developing microprocessor-based overcurrent relays. A digital overcurrent relaying algorithm that performs most of the computations in an off-line mode is described. The performance of the proposed algorithm was evaluated using simulation programs. The results reported in this chapter show that the algorithm accurately emulates the selected relay characteristics.

Table 4.9: Differences (in cycles of 60 Hz) between the operating times of the simulated CO-7 overcurrent relay and the published times for time dial settings of 0.5, 1.0, 2.0, 3.0, 4.0 and 5.0.

Current multiple	Differences at time dial settings of					
	0.5	1.0	2.0	3.0	4.0	5.0
2.75	0.65	0.00	0.20	0.30	0.00	0.75
3.25	0.45	0.80	0.40	0.15	0.20	0.35
3.75	0.15	0.75	0.05	1.35	0.45	0.05
4.25	0.80	0.60	0.15	1.80	0.35	0.15
4.75	1.25	0.10	0.05	0.70	0.45	0.20
5.25	0.60	0.55	0.25	0.25	0.00	0.35
5.75	0.35	0.25	0.20	0.05	0.05	0.65
6.50	0.50	0.05	0.50	0.05	0.45	0.05
7.50	0.70	0.05	0.10	0.30	0.85	0.10
8.50	0.80	0.55	0.55	0.35	0.20	0.40
9.50	0.50	0.55	0.65	0.20	1.30	0.30
10.50	0.40	0.35	0.30	0.10	0.40	0.05
11.50	0.35	0.55	0.55	0.10	0.15	0.00
12.50	0.10	0.45	0.20	0.35	0.05	0.45
13.50	0.10	0.60	0.70	0.30	0.00	0.10
14.50	0.25	0.65	0.80	0.35	0.30	0.30
15.50	0.05	0.30	0.50	0.30	0.10	0.00
16.50	0.02	0.30	0.35	0.45	0.10	0.45
17.50	0.02	0.00	0.00	0.10	0.40	0.30
18.50	0.07	0.25	0.15	0.15	0.30	0.00
19.50	0.07	0.05	0.20	0.60	0.25	0.00

Table 4.10: Differences (in cycles of 60 Hz) between the operating times of the simulated CO-7 overcurrent relay and the published times for time dial settings of 6.0, 7.0, 8.0, 9.0, 10.0 and 11.0.

Current multiple	Differences at time dial settings of					
	6.0	7.0	8.0	9.0	10.0	11.0
2.75	0.45	1.35	0.00	0.90	0.55	0.60
3.25	0.05	0.50	0.60	0.65	0.05	0.05
3.75	0.35	0.40	0.55	0.90	0.00	0.30
4.25	1.70	1.15	0.30	0.90	1.50	0.30
4.75	0.00	0.05	0.05	0.10	1.45	1.00
5.25	0.40	0.25	0.35	0.25	0.90	0.40
5.75	1.00	0.30	0.30	0.30	1.10	0.10
6.50	0.00	0.20	0.95	0.10	0.55	0.25
7.50	0.15	0.20	0.15	0.00	0.85	0.30
8.50	0.15	0.20	0.05	0.40	0.60	0.40
9.50	0.10	0.10	0.50	0.20	0.50	0.70
10.50	0.60	0.05	0.20	0.25	0.85	1.30
11.50	0.35	0.30	0.65	0.05	1.00	1.00
12.50	0.45	0.05	0.45	0.25	0.40	0.05
13.50	0.05	0.50	0.20	0.25	0.45	0.05
14.50	0.20	0.35	0.40	0.35	0.60	0.50
15.50	0.55	0.00	0.10	0.35	1.75	0.00
16.50	0.50	0.40	0.25	0.30	0.15	0.05
17.50	0.00	0.05	0.25	0.25	0.65	0.05
18.50	0.15	0.45	0.15	0.15	0.05	0.10
19.50	0.35	0.15	0.10	0.10	1.65	0.00

Table 4.11: Differences (in cycles of 60 Hz) between the operating times of the simulated CO-9 overcurrent relay and the published times for time dial settings of 0.5, 1.0, 2.0, 3.0, 4.0 and 5.0.

Current multiple	Differences at time dial settings of					
	0.5	1.0	2.0	3.0	4.0	5.0
2.75	0.90	1.75	0.25	0.00	1.40	0.90
3.25	0.75	0.80	0.60	0.20	1.90	0.05
3.75	0.05	0.15	0.10	0.15	0.45	0.10
4.25	0.05	0.30	0.00	0.45	0.05	0.30
4.75	0.15	0.15	0.10	2.00	0.65	0.15
5.25	0.20	0.35	0.00	0.10	0.30	0.30
5.75	0.35	0.30	0.00	0.10	0.30	0.10
6.50	0.07	0.05	0.35	0.55	0.00	0.35
7.50	0.05	0.15	0.20	0.25	0.30	0.15
8.50	0.10	0.05	0.05	0.10	0.10	0.05
9.50	0.05	0.45	0.15	0.35	0.10	0.30
10.50	0.00	0.55	0.10	0.00	0.45	0.45
11.50	0.01	0.30	0.10	0.15	0.05	0.40
12.50	0.00	0.30	0.05	0.10	0.60	0.15
13.50	0.00	0.20	0.15	0.15	0.25	0.05
14.50	0.00	0.12	0.20	0.00	0.30	0.30
15.50	0.03	0.21	0.20	0.20	0.30	0.15
16.50	0.02	0.20	0.02	0.15	0.55	0.20
17.50	0.01	0.14	0.04	0.20	0.55	0.45
18.50	0.01	0.13	0.05	0.05	0.30	0.45
19.50	0.05	0.03	0.00	0.05	0.20	0.40

Table 4.12: Differences (in cycles of 60 Hz) between the operating times of the simulated CO-9 overcurrent relay and the published times for time dial settings of 6.0, 7.0, 8.0, 9.0, 10.0 and 11.0.

Current multiple	Differences at time dial settings of					
	6.0	7.0	8.0	9.0	10.0	11.0
2.75	0.00	0.90	0.00	0.00	0.00	0.00
3.25	0.90	0.15	0.45	0.20	1.10	0.00
3.75	0.70	0.00	0.30	0.25	0.20	0.45
4.25	0.45	0.05	0.05	0.10	1.00	0.70
4.75	0.05	0.10	0.10	0.05	0.85	0.20
5.25	0.45	0.05	0.25	0.10	0.50	0.05
5.75	0.05	0.05	0.05	0.10	0.40	0.15
6.50	0.15	0.05	0.25	0.05	0.60	0.25
7.50	1.20	0.10	0.30	0.15	0.15	0.45
8.50	0.25	0.55	0.45	0.35	0.40	1.05
9.50	0.00	0.10	0.15	0.10	0.05	1.70
10.50	0.05	0.55	0.10	0.25	0.40	0.15
11.50	0.30	0.15	0.45	0.15	0.35	0.15
12.50	0.45	0.10	0.10	0.30	0.20	0.25
13.50	0.10	1.10	0.20	0.01	0.25	0.35
14.50	0.50	0.20	0.20	0.35	0.35	0.20
15.50	0.30	0.20	0.15	0.10	0.30	0.15
16.50	0.05	0.05	0.10	0.10	0.25	0.00
17.50	0.05	0.00	0.40	0.35	0.25	0.05
18.50	0.10	0.30	0.15	0.15	0.25	0.00
19.50	0.05	0.25	0.30	0.05	0.15	0.35

5. PROPOSED ALGORITHMS FOR TRANSFORMER WINDING PROTECTION - VERSION-I

5.1. Introduction

Previously proposed algorithms to detect transformer winding faults are described in Chapter 3. Some of these algorithms use harmonic components of differential currents to restrain trippings during magnetizing inrush conditions. The algorithms based on the harmonic-restraint principle can restrain relay operation even for some internal faults. A previously proposed algorithm [13] uses flux-restraint instead of harmonic-restraint. The use of differential equation models of transformers have also been suggested [14, 15, 16]. These algorithms use currents in the transformer phase windings to make relaying decisions.

This chapter proposes algorithms that can detect winding faults in single-phase and three-phase transformers [46, 47]. The algorithms for protecting three-phase transformers are suitable for situations where it is possible or not possible to measure winding currents; for example, in delta-wye transformers in which the terminals of each phase of a delta winding are not brought out of the tank separately. The non-linearity and hysteresis of the transformer core are considered but do not explicitly become part of the algorithms. B-H curve data of the transformer core are not required. A number of cases similar to those encountered in practice were simulated on a digital computer; the data obtained from the simulations was used to test the algorithms. Some results showing the performance of the algorithms are also included in this chapter.

The proposed algorithms use the electro-magnetic equations of a transformer for detecting winding faults. These differential equations express voltages as functions of currents and mutual flux linkages. The equations are valid during magnetizing inrush, normal operation, and external faults. However, they are not valid during internal faults. The proposed algorithms exploit this feature to detect internal faults.

While describing the algorithms, it is assumed that the transformation ratio is one. Also, currents and voltages at the power system level are used in the equations. These considerations prevent the equations from becoming unnecessarily complicated. In practice, the relays use voltages and currents from potential and current transformer secondaries. Therefore, the turns ratio of the transformer and instrument transformers were taken into consideration while implementing the algorithms.

5.2. Detecting Faults in a Single-Phase Transformer

Consider a two-winding single-phase transformer as shown in Figure 5.1. In this figure, voltages, currents and the parameters of the transformer are as follows.

v_1 and v_2 are the voltages of the primary and secondary windings respectively,

i_1 and i_2 are the currents in the primary and secondary windings respectively,

r_1 and r_2 are the resistances of the primary and secondary windings respectively,

l_1 and l_2 are the leakage inductances of the primary and secondary windings respectively, and

λ_m are the mutual flux linkages.

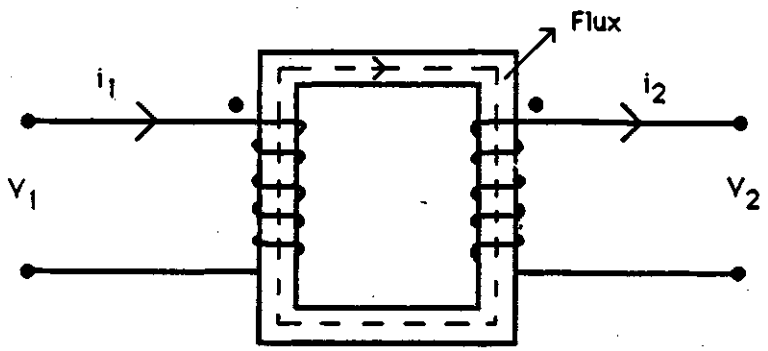

Figure 5.1: A circuit diagram of a two-winding single-phase transformer.

The following differential equation expresses the primary voltage as a function of the primary current and the mutual flux linkages.

$$v_1 = r_1 i_1 + l_1(di_1/dt) + (d\lambda_m/dt) \tag{5.1}$$

Similarly, the following equation expresses the secondary voltage as a function of the secondary current and the mutual flux linkages.

$$v_2 = -r_2 i_2 - l_2(di_2/dt) + (d\lambda_m/dt) \tag{5.2}$$

A rearrangement of this equation provides

$$d\lambda_m/dt = v_2 + r_2 i_2 + l_2(di_2/dt). \tag{5.3}$$

This equation expresses the mutual flux linkages as a function of the secondary current and voltage. The term, $d\lambda_m/dt$, includes the effects of the non-linearity and hysteresis of the B-H curve. Eliminating $d\lambda_m/dt$ from Equation 5.1 by using Equation 5.3 provides

$$v_1 = r_1 i_1 + l_1(di_1/dt) + v_2 + r_2 i_2 + l_2(di_2/dt). \tag{5.4}$$

Integrating both sides of Equation 5.4 provides the following equation.

$$\int_{t_1}^{t_2} v_1 dt = r_1 \int_{t_1}^{t_2} i_1 dt + l_1\{i_1(t_2)-i_1(t_1)\} + \int_{t_1}^{t_2} v_2 dt +$$

$$r_2 \int_{t_1}^{t_2} i_2 dt + l_2\{i_2(t_2)-i_2(t_1)\} \qquad (5.5)$$

Applying the trapezoidal rule for performing the integrations in this equation yields

$$(t_2-t_1)[v_1(t_1)+v_1(t_2)]/2 = r_1(t_2-t_1)[i_1(t_1)+i_1(t_2)]/2 +$$
$$l_1[i_1(t_2)-i_1(t_1)] + (t_2-t_1)[v_2(t_1)+v_2(t_2)]/2 +$$
$$r_2(t_2-t_1)[i_2(t_1)+i_2(t_2)]/2 + l_2[i_2(t_2)-i_2(t_1)]. \qquad (5.6)$$

Digital relays sample voltages and currents at a selected rate. The intersampling time, ΔT, is known. Consider that the proposed algorithm receives samples of v_1, v_2, i_1 and i_2 at ΔT intervals. If n is an integer, t_1 and t_2 can be replaced by $(n-1)\Delta T$ and $n\Delta T$ respectively. Making these substitutions in Equation 5.6 provides

$$\Delta T\{v_1(n\Delta T)+v_1[(n-1)\Delta T]\}/2 = r_1\Delta T\{i_1(n\Delta T)+i_1[(n-1)\Delta T]\}/2 +$$
$$l_1\{i_1(n\Delta T)-i_1[(n-1)\Delta T]\} + \Delta T\{v_2(n\Delta T)+v_2[(n-1)\Delta T]\}/2 +$$
$$r_2\Delta T\{i_2(n\Delta T)+i_2[(n-1)\Delta T]\}/2 + l_2\{i_2(n\Delta T)-i_2[(n-1)\Delta T]\}. \qquad (5.7)$$

Dividing both sides of this equation by $\Delta T/2$ and then rearranging yields

$$v_1(n\Delta T) = (r_1+2l_1/\Delta T)i_1(n\Delta T) + (r_1-2l_1/\Delta T)i_1[(n-1)\Delta T] +$$
$$v_2(n\Delta T) + v_2[(n-1)\Delta T] + (r_2+2l_2/\Delta T)i_2(n\Delta T) +$$
$$(r_2-2l_2/\Delta T)i_2[(n-1)\Delta T] - v_1[(n-1)\Delta T]. \qquad (5.8)$$

This equation expresses the present sample of the primary voltage as a function of the secondary voltage, the primary and secondary currents, and the previous sample of the primary voltage. If the parameters, r_1, r_2, l_1 and l_2 of the transformer are known, it becomes possible to calculate the right hand side of Equation 5.8 after taking the $(n-1)th$ and $n-th$ samples of the transformer voltages and currents. The computed value is the estimate of

$v_1(n\Delta T)$ whereas the left hand side is measured value. The estimated and measured values are equal during normal operation, overexcitation, magnetizing inrush and external fault conditions. However, these values are not equal during internal faults.

It is clear from Equation 5.8 that the samples of the transformer voltages and currents only are needed to estimate $v_1(n\Delta T)$. No data of the B-H or magnetizing curve are needed.

5.2.1. The algorithm

This section describes an algorithm that is suitable for microprocessor-based protection of single-phase transformers. The algorithm uses the technique described in the previous section. It also assumes that the primary and secondary voltages, and primary and secondary currents are sampled at a pre-specified rate. The algorithm performs the following steps.

1. Initialize a trip index, TRIP, to zero.

2. Sample the voltages and currents of the primary and secondary windings.

3. Estimate the value of $v_1(n\Delta T)$ using the right hand side of Equation 5.8 and samples of the primary and secondary currents and secondary voltage taken at $n\Delta T$ and $(n-1)\Delta T$ s, and sample of the primary voltage taken at $(n-1)\Delta T$ s.

4. Subtract the value of the primary voltage sampled at $n\Delta T$ s from the value estimated in step 3. The absolute value of this difference is referred as ERROR.

5. Check if the point, (|Measured value of the primary voltage|, ERROR) lies in the fault region of the relay characteristic shown in Figure 5.2. If it does, add two to the trip index, TRIP; otherwise subtract one from TRIP.

6. Check if TRIP is negative. If it is, reset it to zero and revert to step 2. Otherwise, proceed to step 7.

7. Check if TRIP is greater than a prespecified threshold. If it is,

the algorithm concludes that an internal fault exists and starts a tripping procedure. Otherwise, the algorithm reverts to step 2.

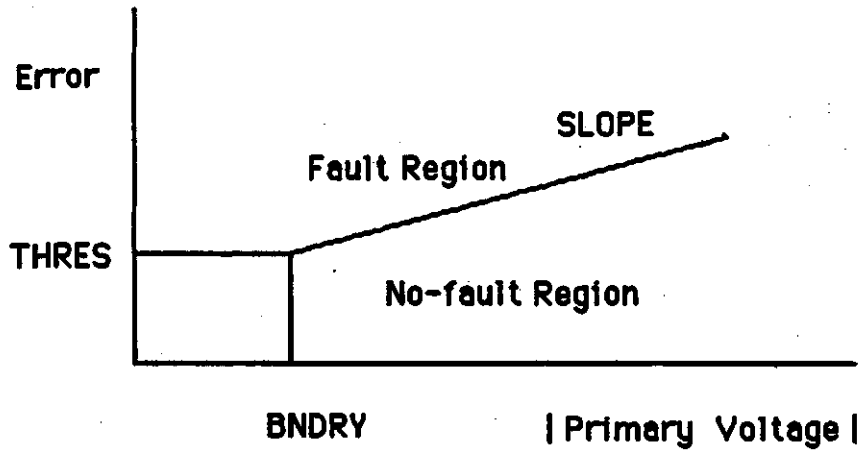

Figure 5.2: The proposed error vs primary-volts characteristic of the relay.

5.3. Detecting Faults in Three-Phase Transformers

Consider a three-phase transformer whose primary windings are a, b, and c and the secondary windings are A, B and C. Also consider that the parameters of the transformer are as follows:

r_a, r_b and r_c are the resistances of the primary windings a, b and c respectively,

l_a, l_b and l_c are the leakage inductances of the primary windings a, b and c respectively,

r_A, r_B and r_C are the resistances of the secondary windings A, B and C respectively,

l_A, l_B and l_C are the leakage inductances of the secondary windings A, B and C respectively,

λ_{aA} are the mutual flux linkages of windings a and A,

λ_{bB} are the mutual flux linkages of windings b and B, and

λ_{cC} are the mutual flux linkages of windings c and C.

The following sections develop the techniques for detecting winding faults in three-phase wye-wye and delta-wye transformers. The digital algorithms suitable for detecting winding faults in three-phase transformers are then described.

5.3.1. Wye-wye tranformers

Figure 5.3 shows the primary and secondary windings of a three-phase wye-wye connected transformer. The following differential equations express the phase-voltages of the primary windings as functions of the primary currents and the mutual flux linkages.

$$v_a = r_a i_a + l_a(di_a/dt) + (d\lambda_{aA}/dt) \tag{5.9}$$

$$v_b = r_b i_b + l_b(di_b/dt) + (d\lambda_{bB}/dt) \tag{5.10}$$

$$v_c = r_c i_c + l_c(di_c/dt) + (d\lambda_{cC}/dt) \tag{5.11}$$

where:

v_a, v_b and v_c are voltages of the a, b and c-phase windings respectively, and

i_a, i_b and i_c are currents in the a, b and c-phase windings respectively.

Similary, the following equations express the voltages of the secondary windings as functions of the secondary currents and the mutual flux linkages.

$$v_A = -r_A i_A - l_A(di_A/dt) + (d\lambda_{aA}/dt) \tag{5.12}$$

$$v_B = -r_B i_B - l_B(di_B/dt) + (d\lambda_{bB}/dt) \tag{5.13}$$

$$v_C = -r_C i_C - l_C(di_C/dt) + (d\lambda_{cC}/dt) \tag{5.14}$$

where:

v_A, v_B and v_C are the voltages of the A, B and C-phase windings respectively, and

i_A, i_B and i_C are the currents in the A, B and C-phase windings respectively.

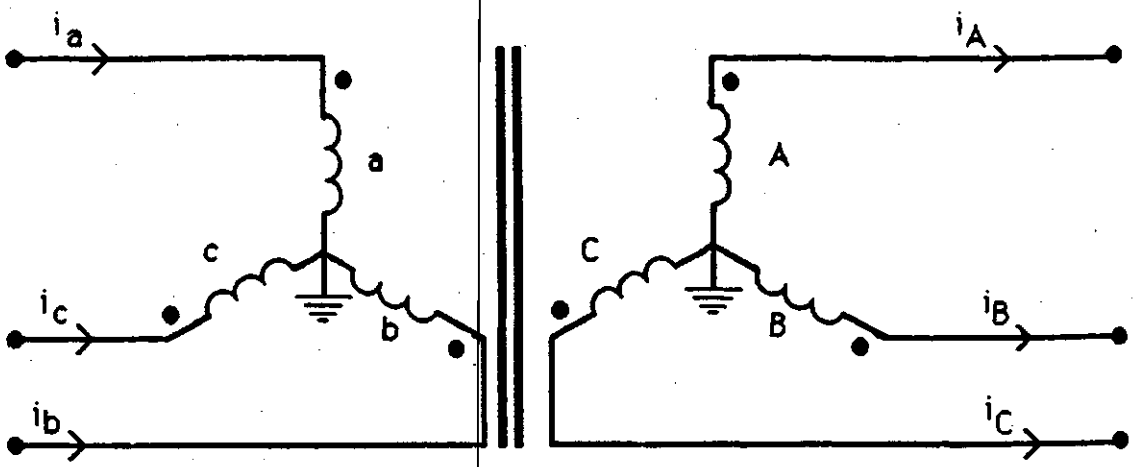

Figure 5.3: A circuit diagram of a two-winding three-phase wye-wye transformer.

Processing Equations 5.9 and 5.12 using the technique described in Section 5.2 provides Equation 5.15. The procedure involves eliminating the term, $d\lambda_{aA}/dt$, from Equation 5.9 by using Equation 5.12, applying rectangular rule to integrate both sides of the resulting equation and then rearranging it. A similar procedure provides Equations 5.16 and 5.17.

$$v_a(n\Delta T) = (r_a+2l_a/\Delta T)i_a(n\Delta T) + (r_a-2l_a/\Delta T)i_a[(n-1)\Delta T] +$$
$$v_A(n\Delta T) + v_A[(n-1)\Delta T] + (r_A+2l_A/\Delta T)i_A(n\Delta T) +$$
$$(r_A-2l_A/\Delta T)i_A[(n-1)\Delta T] - v_a[(n-1)\Delta T] \qquad (5.15)$$

$$v_b(n\Delta T) = (r_b+2l_b/\Delta T)i_b(n\Delta T) + (r_b-2l_b/\Delta T)i_b[(n-1)\Delta T] +$$
$$v_B(n\Delta T) + v_B[(n-1)\Delta T] + (r_B+2l_B/\Delta T)i_B(n\Delta T) +$$
$$(r_B-2l_B/\Delta T)i_B[(n-1)\Delta T] - v_b[(n-1)\Delta T] \quad (5.16)$$

$$v_c(n\Delta T) = (r_c+2l_c/\Delta T)i_c(n\Delta T) + (r_c-2l_c/\Delta T)i_c[(n-1)\Delta T] +$$
$$v_C(n\Delta T) + v_C[(n-1)\Delta T] + (r_C+2l_C/\Delta T)i_C(n\Delta T) +$$
$$(r_C-2l_C/\Delta T)i_C[(n-1)\Delta T] - v_c[(n-1)\Delta T] \quad (5.17)$$

If the parameters of the transformer are known, it becomes possible to calculate the right hand sides of Equations 5.15, 5.16 and 5.17 after taking two consecutive samples of voltages and currents. The right hand side of Equation 5.15 provides an estimate of $v_a(n\Delta T)$ whereas the left hand side of the equation is the measured value. Similarly, the right hand sides of Equations 5.16 and 5.17 provide the estimated values of $v_b(n\Delta T)$ and $v_c(n\Delta T)$ respectively. The left hand sides of these equations are their measured values. As in the case of single-phase transformers, the estimated and measured values are equal during normal operation, overexcitation, magnetizing inrush and external fault conditions. However, for internal transformer faults, these values are not equal.

5.3.1.1. The algorithm

The algorithm for the protection of three-phase wye-wye conntected transformers uses the technique described in Section 5.3.1 and performs the following steps.

1. Initialize the three trip indices, TRIPA, TRIPB and TRIPC to zero.
2. Samples the primary and secondary voltages, and line currents.
3. Compute the estimated values of $v_a(n\Delta T)$, $v_b(n\Delta T)$ and $v_c(n\Delta T)$

by using the voltage and current samples and the right hand sides of Equations 5.15, 5.16 and 5.17 respectively.

4. Subtract the measured value of $v_a(n\Delta T)$ from its estimated value. Let the absolute difference be ERRORA.

5. Subtract the measured value of $v_b(n\Delta T)$ from its estimated value. Let the absolute difference be ERRORB.

6. Subtract the measured value of $v_c(n\Delta T)$ from its estimated value. Let the absolute difference be ERRORC.

7. Check if the point, (|Measured value of the primary voltage of phase A|, ERRORA) lies in the fault region of the relay characteristic shown in Figure 5.2. If it does; add two to the trip index, TRIPA; otherwise subtact one from TRIPA.

8. Check if TRIPA is negative. If it is, reset it to zero and proceed to step 9. Otherwise proceed to step 9 without modifying TRIPA.

9. Check if the point, (|Measured value of the primary voltage of phase B|, ERRORB) lies in the fault region of the relay characteristic shown in Figure 5.2. If it does; add two to the trip index, TRIPB; otherwise subtact one from TRIPB.

10. Check if TRIPB is negative. If it is, reset it to zero and proceed to step 11. Otherwise proceed to step 11 without modifying TRIPB.

11. Check if the point, (|Measured value of the primary voltage of phase C|, ERRORC) lies in the fault region of the relay characteristic shown in Figure 5.2. If it does; add two to the trip index, TRIPC; otherwise subtact one from TRIPC.

12. Check if TRIPC is negative. If it is, reset it to zero and proceed to step 13. Otherwise proceed to step 13 without modifying TRIPC.

13. Test the criteria of Table 5.1 to determine the condition of the transformer. Issue a trip command if the trip indices satisfy one of the conditions listed in the table. Otherwise, the algorithm reverts to step 2.

Table 5.1: Values of the trip indices during internal faults in a wye-wye transformer.

Condition no.	Value of the trip index TRIPA	TRIPB	TRIPC	Diagnosis
1.	TRIPA >T	TRIPB <T	TRIPC <T	Internal fault in phase A
2.	TRIPA <T	TRIPB >T	TRIPC <T	Internal fault in phase B
3.	TRIPA <T	TRIPB <T	TRIPC >T	Internal fault in phase C
4.	TRIPA >T	TRIPB >T	TRIPC <T	Internal fault in phases A and B
5.	TRIPA >T	TRIPB <T	TRIPC >T	Internal fault in phases A and C
6.	TRIPA <T	TRIPB >T	TRIPC >T	Internal fault in phases B and C
7.	TRIPA >T	TRIPB >T	TRIPC >T	Internal fault in phases A, B and C

T = Threshold

5.3.2. Delta-wye transformers

Figure 5.4 shows the winding connections of a three-phase delta-wye connected transformer. The following equations express the voltages of the delta connected windings as functions of the primary currents and the mutual flux linkages.

$$v_a = r_a[i_a+i_{pp}] + l_a[d(i_a+i_{pp})/dt] + (d\lambda_{aA}/dt) \quad (5.18)$$

$$v_b = r_b[i_b+i_{pp}] + l_b[d(i_b+i_{pp})/dt] + (d\lambda_{bB}/dt) \quad (5.19)$$

$$v_c = r_c[i_c+i_{pp}] + l_c[d(i_c+i_{pp})/dt] + (d\lambda_{cC}/dt) \quad (5.20)$$

where:

v_a, v_b and v_c are voltages of the a, b and c-phase windings respectively,

i_a+i_{pp} is the current in the winding of phase a,

i_b+i_{pp} is the current in the winding of phase b,

i_c+i_{pp} is the current in the winding of phase c and

i_{pp} is the curent that circulates in the delta connected winding.

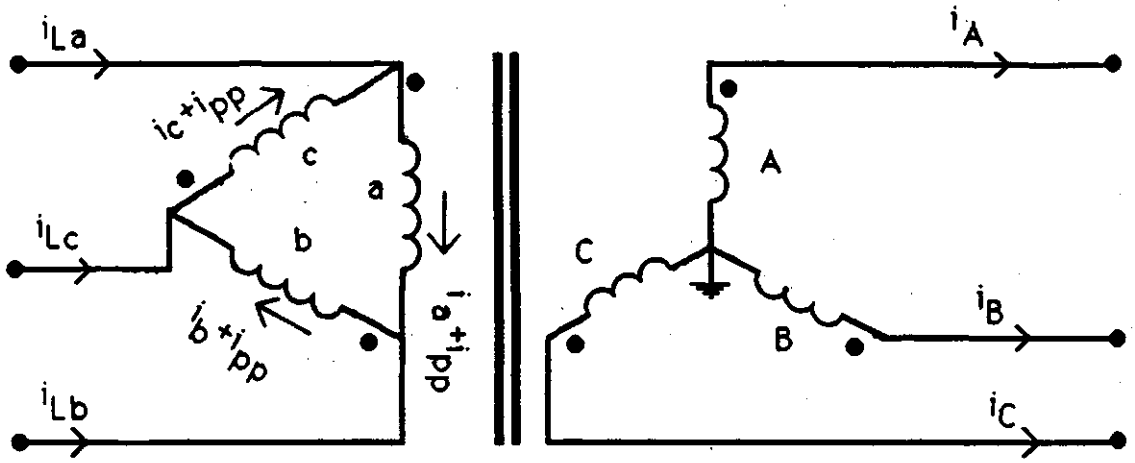

Figure 5.4: A circuit diagram of a two-winding three-phase delta-wye transformer.

Similarly, the following equations express the voltages of the secondary windings as functions of the secondary currents and mutual flux linkages.

$$v_A = -r_A i_A - l_A(di_A/dt) + (d\lambda_{aA}/dt) \tag{5.21}$$

$$v_B = -r_B i_B - l_B(di_B/dt) + (d\lambda_{bB}/dt) \tag{5.22}$$

$$v_C = -r_C i_C - l_C(di_C/dt) + (d\lambda_{cC}/dt) \tag{5.23}$$

where:

v_A, v_B and v_C are voltages of the A, B and C-phase windings respectively and

i_A, i_B and i_C are currents in the A, B and C-phase windings respectively.

Applying the procedure used in the previous sections, Equations 5.24, 5.25 and 5.26 are obtained.

$$\begin{aligned} v_a(n\Delta T) = {} & (r_a+2l_a/\Delta T)i_a(n\Delta T) + (r_a-2l_a/\Delta T)i_a[(n-1)\Delta T] + \\ & (r_a+2l_a/\Delta T)i_{pp}(n\Delta T) + (r_a-2l_a/\Delta T)i_{pp}[(n-1)\Delta T] + \\ & v_A(n\Delta T) + v_A[(n-1)\Delta T] + (r_A+2l_A/\Delta T)i_A(n\Delta T) + \\ & (r_A-2l_A/\Delta T)i_A[(n-1)\Delta T] - v_a[(n-1)\Delta T] \end{aligned} \tag{5.24}$$

$$\begin{aligned} v_b(n\Delta T) = {} & (r_b+2l_b/\Delta T)i_b(n\Delta T) + (r_b-2l_b/\Delta T)i_b[(n-1)\Delta T] + \\ & (r_b+2l_b/\Delta T)i_{pp}(n\Delta T) + (r_b-2l_b/\Delta T)i_{pp}[(n-1)\Delta T] + \\ & v_B(n\Delta T) + v_B[(n-1)\Delta T] + (r_B+2l_B/\Delta T)i_B(n\Delta T) + \\ & (r_B-2l_B/\Delta T)i_B[(n-1)\Delta T] - v_b[(n-1)\Delta T] \end{aligned} \tag{5.25}$$

$$\begin{aligned} v_c(n\Delta T) = {} & (r_c+2l_c/\Delta T)i_c(n\Delta T) + (r_c-2l_c/\Delta T)i_c[(n-1)\Delta T] + \\ & (r_c+2l_c/\Delta T)i_{pp}(n\Delta T) + (r_c-2l_c/\Delta T)i_{pp}[(n-1)\Delta T] + \\ & v_C(n\Delta T) + v_C[(n-1)\Delta T] + (r_C+2l_C/\Delta T)i_C(n\Delta T) + \\ & (r_C-2l_C/\Delta T)i_C[(n-1)\Delta T] - v_c[(n-1)\Delta T] \end{aligned} \tag{5.26}$$

The right hand sides of Equations 5.24, 5.25 and 5.26 can not be computed because the currents i_a, i_b, i_c and i_{pp} are not known. Since, the currents, i_a, i_b and i_c, are the non-circulating components of the winding currents, their sum must be zero. Equation 5.27 expresses this situation as a mathematical equation. Also, Equation 5.28 defines the current circulating in the delta winding.

$$i_a + i_b + i_c = 0 \tag{5.27}$$

$$i_{pp} = [(i_a+i_{pp}) + (i_b+i_{pp}) + (i_c+i_{pp})]/3 \tag{5.28}$$

The following equations express the line currents as functions of the currents in the delta windings.

$$i_{La} = i_a - i_c \tag{5.29}$$

$$i_{Lb} = i_b - i_a \tag{5.30}$$

$$i_{Lc} = i_c - i_b \tag{5.31}$$

Subtracting Equation 5.30 from Equation 5.29, replacing i_b+i_c with $-i_a$ and rearranging gives Equation 5.32. A similar procedure provides Equations 5.33 and 5.34.

$$i_a = (i_{La} - i_{Lb})/3 \tag{5.32}$$

$$i_b = (i_{Lb} - i_{Lc})/3 \tag{5.33}$$

$$i_c = (i_{Lc} - i_{La})/3 \tag{5.34}$$

The circulating current, i_{pp}, has two components. One component is the zero sequence current to balance the flow of zero sequence currents in the wye connected windings. The second component is the in-phase component of the magnetizing current flowing in the delta connected windings. If the value of i_{pp} is known, the right hand sides of Equations 5.24, 5.25 and 5.26 can be computed.

Option 1

One possible alternative is to use Equation 5.24 to estimate the terms containing the circulating current and use Equations 5.25 and 5.26 for detecting faults. For this purpose, Equation 5.24 can be rearranged as

$$(r_a+2l_a/\Delta T)i_{pp}(n\Delta T) + (r_a-2l_a/\Delta T)i_{pp}[(n-1)\Delta T] =$$
$$v_a(n\Delta T) + v_a[(n-1)\Delta T] - (r_a+2l_a/\Delta T)i_a(n\Delta T) -$$
$$(r_a-2l_a/\Delta T)i_a[(n-1)\Delta T] - v_A(n\Delta T) - v_A[(n-1)\Delta T] -$$
$$(r_A+2l_A/\Delta T)i_A(n\Delta T) - (r_A-2l_A/\Delta T)i_A[(n-1)\Delta T]. \quad (5.35)$$

Multiplying both sides of this equation with $[(r_b+2l_b/\Delta T)/(r_a+2l_a/\Delta T)]$ provides

$$[(r_b+2l_b/\Delta T)/(r_a+2l_a/\Delta T)](r_a+2l_a/\Delta T)i_{pp}(n\Delta T) +$$
$$[(r_b+2l_b/\Delta T)/(r_a+2l_a/\Delta T)](r_a-2l_a/\Delta T)i_{pp}[(n-1)\Delta T] =$$
$$[(r_b+2l_b/\Delta T)/(r_a+2l_a/\Delta T)](\textit{R.H.S of Equation } 5.35). \quad (5.36)$$

Since the X/R ratios of the three phases of a transformer are approximately equal and large, and ΔT is small, the following is a valid aproximation:

$$[(r_b+2l_b/\Delta T)/(r_a+2l_a/\Delta T)] \approx$$
$$[(r_b-2l_b/\Delta T)/(r_a-2l_a/\Delta T)]$$

Substituting this expression into the second term of the left hand side of Equation 5.36 provides

$$(r_b+2l_b/\Delta T)i_{pp}(n\Delta T) + (r_b-2l_b/\Delta T)i_{pp}[(n-1)\Delta T] =$$
$$[(r_b+2l_b/\Delta T)/(r_a+2l_a/\Delta T)](\textit{R.H.S. of Equation } 5.35). \quad (5.37)$$

A similar procedure provides

$$(r_c+2l_c/\Delta T)i_{pp}(n\Delta T) + (r_c-2l_c/\Delta T)i_{pp}[(n-1)\Delta T] =$$
$$[(r_c+2l_c/\Delta T)/(r_a+2l_a/\Delta T)](\textit{R.H.S. of Equation } 5.35). \quad (5.38)$$

It is possible to compute the right hand sides of Equations 5.37 and 5.38 immediately after taking the latest samples of voltages and currents. These

values are the estimates of the terms containing the circulating current which can be used in Equations 5.25 and 5.26 to compute their right hand sides. As stated earlier, the right hand sides provide the estimates of $v_b(n\Delta T)$ and $v_c(n\Delta T)$ respectively. The left hand sides are the measurements. The estimated and measured values are equal for magnetizing inrush, overexcitation, external faults and normal operating conditions. However, they are not equal for faults in the transformer protection zone.

In the above procedure, Equation 5.35 estimates the terms involving the circulating current from the measurements of voltages and currents of windings a and A. The measurements from the remaining windings provide enough information to decide whether an internal fault exists or not.

Option 2

It is also possible to use the measurements from windings b and B to estimate the circulating current terms. For this purpose, Equation 5.25 is rearranged as

$$(r_b+2l_b/\Delta T)i_{pp}(n\Delta T) + (r_b-2l_b/\Delta T)i_{pp}[(n-1)\Delta T] =$$
$$v_b(n\Delta T) + v_b[(n-1)\Delta T] - (r_b+2l_b/\Delta T)i_b(n\Delta T) -$$
$$(r_b-2l_b/\Delta T)i_b[(n-1)\Delta T] - v_B(n\Delta T) - v_B[(n-1)\Delta T] -$$
$$(r_B+2l_B/\Delta T)i_B(n\Delta T) - (r_B-2l_B/\Delta T)i_B[(n-1)\Delta T]. \qquad (5.39)$$

It is possible to calculate the right-hand side of Equation 5.39 immediately after taking samples of voltages and currents. By following a procedure similar to that used in Option 1, the following equations can be obtained.

$$(r_a+2l_a/\Delta T)i_{pp}(n\Delta T) + (r_a-2l_a/\Delta T)i_{pp}[(n-1)\Delta T] =$$
$$[(r_a+2l_a/\Delta T)/(r_b+2l_b/\Delta T)](\textit{R.H.S. of Equation } 5.39) \qquad (5.40)$$

$$(r_c+2l_c/\Delta T)i_{pp}(n\Delta T) + (r_c-2l_c/\Delta T)i_{pp}[(n-1)\Delta T] =$$

$$[(r_c+2l_c/\Delta T)/(r_b+2l_b/\Delta T)](\textit{R.H.S. of Equation } 5.39) \qquad (5.41)$$

It is possible to compute the values of the right hand sides of Equations 5.40 and 5.41. These values are the estimates of the terms containing the circulating current which can be used in Equations 5.24 and 5.26 to compute their right hand sides which provide estimates of $v_a(n\Delta T)$ and $v_c(n\Delta T)$ respectively. The left hand sides are the measured values. The estimated and measured values are equal for magnetizing inrush, overexcitation, external faults and normal operating conditions. However, they are not equal for faults in the transformer protection zone.

Option 3

The measurements from windings c and C can also be used to estimate the circulating current. For this purpose, Equation 5.26 is rearranged as

$$(r_c+2l_c/\Delta T)i_{pp}(n\Delta T) + (r_c-2l_c/\Delta T)i_{pp}[(n-1)\Delta T] =$$

$$v_c(n\Delta T) + v_c[(n-1)\Delta T] - (r_c+2l_c/\Delta T)i_c(n\Delta T) -$$

$$(r_c-2l_c/\Delta T)i_c[(n-1)\Delta T] - v_C(n\Delta T) - v_C[(n-1)\Delta T] -$$

$$(r_C+2l_C/\Delta T)i_C(n\Delta T) - (r_C-2l_C/\Delta T)i_C[(n-1)\Delta T]. \qquad (5.42)$$

The right hand side of Equation 5.42 can be calculated immediately after taking samples of voltages and currents. It is possible to obtain the following equations by using a procedure similar to that used in Option 1.

$$(r_a+2l_a/\Delta T)i_{pp}(n\Delta T) + (r_a-2l_a/\Delta T)i_{pp}[(n-1)\Delta T] =$$

$$[(r_a+2l_a/\Delta T)/(r_c+2l_c/\Delta T)](\textit{R.H.S. of Equation } 5.42) \qquad (5.43)$$

$$(r_b+2l_b/\Delta T)i_{pp}(n\Delta T) + (r_b-2l_b/\Delta T)i_{pp}[(n-1)\Delta T] =$$

$$[(r_b+2l_b/\Delta T)/(r_c+2l_c/\Delta T)](\textit{R.H.S. of Equation } 5.42) \qquad (5.44)$$

The values of the right hand sides of these equations can be computed. These values provide the estimates of the terms containing the circulating current which can be used in Equations 5.24 and 5.25 to compute their right hand sides which are the estimated values of $v_a(n\Delta T)$ and $v_b(n\Delta T)$ respectively. The left hand sides are the measured values. As stated earlier in this section, the estimated and measured values are equal for magnetizing inrush, overexcitation, external faults and normal operating conditions. However, they are not equal for faults in the transformer protection zone.

The phase whose measurements are used to estimate the terms containing the circulating current is classified as the "Reference Phase" in this work.

5.3.2.1. The algorithm

The algorithm for the protection of a delta-wye transformer uses the technique described in Section 5.3.2. It consists of four modules; the first, second, and third modules estimate the primary voltages and the fourth module is a decision-making module.

The first computing module uses phase A as the "Reference Phase" and performs the following steps.

1. Initialize the trip indices, TRIPB1, TRIPC1, TRIPA2, TRIPC2, TRIPA3 and TRIPB3 to zero.
2. Sample the primary and secondary voltages and line currents.
3. Compute the value of the non-circulating currents, i_a, i_b and i_c, by using Equations 5.32, 5.33 and 5.34 respectively.
4. Calculate the value of the right hand side of Equation 5.35.
5. Estimate the values of $(r_b+2l_b/\Delta T)i_{pp}(n\Delta T) + (r_b-2l_b/\Delta T)i_{pp}[(n-1)\Delta T]$ and $(r_c+2l_c/\Delta T)i_{pp}(n\Delta T) + (r_c-2l_c/\Delta T)i_{pp}[(n-1)\Delta T]$ by using Equations 5.37 and 5.38 respectively.

6. Estimate the values of $v_b(n\Delta T)$ and $v_c(n\Delta T)$ by using the right hand sides of Equations 5.25 and 5.26 respectively.

7. Subtract the measured value of $v_b(n\Delta T)$ from its estimated value. Let the absolute difference be ERRORB1.

8. Subtract the measured value of $v_c(n\Delta T)$ from its estimated value. Let the absolute differnce be ERRORC1.

9. Check if the point (|Measured value of the primary voltage of phase B|, ERRORB1) lies in the fault region of the relay characteristic shown in Figure 5.2. If it does, add two to the trip index, TRIPB1; otherwise subtract one from TRIPB1.

10. Check if the trip index, TRIPB1, is negative. If it is, reset it to zero and proceed to step 11. Otherwise, proceed to step 11 without modifying TRIPB1.

11. Check if the point (|Measured value of the primary voltage of phase C|, ERRORC1) lies in the fault region of the relay characteristic shown in Figure 5.2. If it does, add two to the trip index, TRIPC1; otherwise subtract one from TRIPC1.

12. Check if the trip index, TRIPC1, is negative. If it is, reset it to zero and proceed to step 1 of the second computing module. Otherwise, proceed to step 1 of the second computing module without modifying TRIPC1.

The second computing module uses phase B as the "Reference Phase" and performs the following steps.

1. Calculate the value of the right hand side of Equation 5.39.

2. Estimate the values of $(r_a+2l_a/\Delta T)i_{pp}(n\Delta T) + (r_a-2l_a/\Delta T)i_{pp}[(n-1)\Delta T]$ and $(r_c+2l_c/\Delta T)i_{pp}(n\Delta T) + (r_c-2l_c/\Delta T)i_{pp}[(n-1)\Delta T]$ by using Equations 5.40 and 5.41 respectively.

3. Estimate the values of $v_a(n\Delta T)$ and $v_c(n\Delta T)$ by using the right hand sides of Equations 5.24 and 5.26 respectively.

4. Subtract the measured value of $v_a(n\Delta T)$ from its estimated value. Let the absolute difference be ERRORA2.

5. Subtract the measured value of $v_c(n\Delta T)$ from its estimated value. Let the absolute difference be ERRORC2.

6. Check if the point (|Measured value of the primary voltage of phase A|, ERRORA2) lies in the fault region of the relay characteristic shown in Figure 5.2. If it does, add two to the trip index, TRIPA2; otherwise subtract one from TRIPA2.

7. Check if the trip index, TRIPA2, is negative. If it is, reset it to zero and proceed to step 8. Otherwise, proceed to step 8 without modifying TRIPA2.

8. Check if the point (|Measured value of the primary voltage of phase C|, ERRORC2) lies in the fault region of the relay characteristic shown in Figure 5.2. If it does, add two to the trip index, TRIPC2; otherwise subtract one from TRIPC2.

9. Check if the trip index, TRIPC2, is negative. If it is, reset it to zero and proceed to step 1 of the third computing module. Otherwise, proceed to step 1 of the third computing module without modifying TRIPC2.

The third computing module uses phase C as the "Reference Phase" and performs the following steps.

1. Calculate the value of the right hand side of Equation 5.42.

2. Estimate the values of $(r_a+2l_a/\Delta T)i_{pp}(n\Delta T) + (r_a-2l_a/\Delta T)i_{pp}[(n-1)\Delta T]$ and $(r_b+2l_b/\Delta T)i_{pp}(n\Delta T) + (r_b-2l_b/\Delta T)i_{pp}[(n-1)\Delta T]$ by using Equations 5.43 and 5.44 respectively.

3. Estimate the values of $v_a(n\Delta T)$ and $v_b(n\Delta T)$ by using the right hand sides of Equations 5.24 and 5.25 respectively.

4. Subtract the measured value of $v_a(n\Delta T)$ from its estimated value. Let the absolute difference be ERRORA3.

5. Subtract the measured value of $v_b(n\Delta T)$ from its estimated value. Let the absolute difference be ERRORB3.

6. Check if the point (|Measured value of the primary voltage of phase A|, ERRORA3) lies in the fault region of the relay characteristic shown in Figure 5.2. If it does, add two to the trip index, TRIPA3; otherwise subtract one from TRIPA3.

7. Check if the trip index, TRIPA3, is negative. If it is, reset it to zero and proceed to step 8. Otherwise, proceed to step 8 without modifying TRIPA3.

8. Check if the point (|Measured value of the primary voltage of phase B|, ERRORB3) lies in the fault region of the relay characteristic shown in Figure 5.2. If it does, add two to the trip index, TRIPB3; otherwise subtract one from TRIPB3.

9. Check if the trip index, TRIPB3, is negative. If it is, reset it to zero and proceed to step 1 of the decision-logic module. Otherwise, proceed to step 1 of the decison-logic module without modifying TRIPB3.

The decision-logic module uses the trip indices generated by the three computing modules to determine the condition of the transformer. It performs the following steps to accomplish this task.

1. Obtain the trip indices, TRIPB1, TRIPC1, TRIPA2, TRIPC2, TRIPA3 and TRIPB3 generated by the three computing modules.

2. Test the criteria of Table 5.2 to determine the condition of the transformer. Issue a trip command if the trip indices generated by any two of the three computing modules satisfy one of the conditions listed in Table 5.2. Otherwise, revert to step 2 of the first computing module.

5.4. Testing of Algorithms

The proposed algorithms were tested using a microVAX 3600 digital computer that is available at the University of Saskatchewan. The voltages and currents needed for evaluating the performance of the algorithms were generated using the Electro-Magnetic Transient Program (EMTP) [48]. The EMTP was directed to provide discrete values of voltages and currents at a sampling rate of 24000 Hz. Raw data were processed by digital equivalents of low-pass filters. The outputs of these filters were converted to data at 1200 Hz. The discrete data were then presented to FORTRAN programs that simulated the proposed algorithms. The algorithms used a relay characteristic similar to that of Figure 5.2. THRES and BNDRY were set at 7.5% and 20% of the rated primary voltage of the transformer. SLOPE was set at 0.03 and the threshold for the trip indices was set at 20. The selection of these values require a compromise between speed, sensitivity and security of the algorithm and were arrived at by analysing the response of the algo-

Table 5.2: Criteria used by the decision-logic module for detecting internal faults.

Condition no.	Trip indices computed by 1st computing module	2nd computing module	3rd computing module	Diagnosis
1.	TRIPB1 >T TRIPC1 >T	TRIPA2 >T TRIPC2 <T	TRIPA3 >T TRIPB3 <T	Internal fault in phase A
2.	TRIPB1 >T TRIPC1 <T	TRIPA2 >T TRIPC2 >T	TRIPA3 <T TRIPB3 >T	Internal fault in phase B
3.	TRIPB1 <T TRIPC1 >T	TRIPA2 <T TRIPC2 >T	TRIPA3 >T TRIPB3 >T	Internal fault in phase C
4.	TRIPB1 >T TRIPC1 >T	TRIPA2 >T TRIPC2 >T	TRIPA3 >T TRIPB3 >T	Two or three phase internal fault

T = Threshold

rithm to different operating conditions of the transformer. A threshold of 20 means that the algorithm has to wait for a minimum of one half cycle (of 60 Hz) after the inception of a fault before a decision is made by the relay. This makes the algorithm secure by not allowing trippings on transients.

Using the settings and thresholds specified in the previous paragraph, the algorithms were tested for several operating conditions of the transformers. This section discusses the results obtained from those tests. Before presenting the results, the procedures for generating signals and simulating low-pass filters are described.

5.4.1. Generating input signals

Input signals needed for evaluating the performance of the algorithms were generated using the EMTP and models of a single-phase and a three-phase transformer. The voltage and current waveforms sampled at 24000 Hz were obtained from the EMTP for magnetizing inrush, overexcitation and external and internal faults. The sampled values of the waveforms were recorded in data files. The procedures used to simulate the transformers are given in Appendix C. The parameters of the transformers are also listed.

5.4.2. Simulating low-pass filters

Low-pass filters are used in digital relays to band-limit the inputs. The cut-off frequency of the low-pass filters should be less than one half the sampling frequency to minimize the effects of aliasing. Fourth-order Bessel, low-pass filters with a cut-off frequency of 200 Hz were selected for this application because they provide a constant time delay for the pass-band frequencies. This is necessary because the proposed algorithms are based on the relationship between instantaneous voltages and currents of transfomers instead of their single-frequency phasors. Appendix D reviews the procedure for converting the transfer function of a fourth-order analog low-pass Bessel filter to an equivalent digital filter [49]. The procedure provided the following transfer function.

$$H(z) = \frac{2.1862\times10^{-6}(1+4z^{-1}+6z^{-2}+4z^{-3}+z^{-4})}{1-3.7554z^{-1}+5.2929z^{-2}-3.3180z^{-3}+0.7806z^{-4}} \tag{5.45}$$

Since $H(z)$ is $Y(z)/X(z)$, Equation 5.45 can be rearranged as

$$Y(z)(1 - 3.7554z^{-1} + 5.2929z^{-2} - 3.3180z^{-3} + 0.7806z^{-4}) = 2.1862\times10^{-6}(1 + 4z^{-1} + 6z^{-2} + 4z^{-3} + z^{-4})X(z). \tag{5.46}$$

This equation rewritten in terms of the time delay of n sampling intervals and rearranged is

$$y(n) = 2.1862\times10^{-6}[x(n) + 4x(n-1) + 6x(n-2)$$
$$+ 4x(n-3) + x(n-4)] + 3.7554y(n-1) - 5.2929y(n-2)$$
$$+ 3.3180y(n-3) - 0.7806y(n-4). \quad (5.47)$$

This equation was implemented on the microVAX 3600 digital computer to simulate low-pass filters. The magnitude and phase responses of these filters are shown in Figures 5.5 and 5.6 respectively.

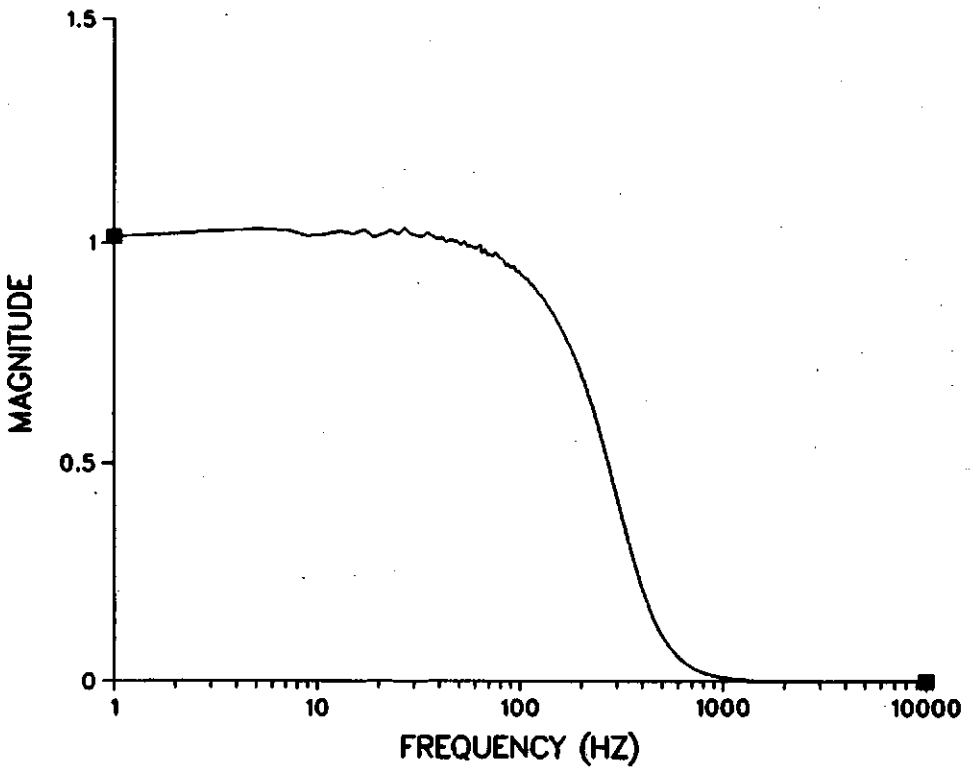

Figure 5.5: Magnitude response of the low-pass filter.

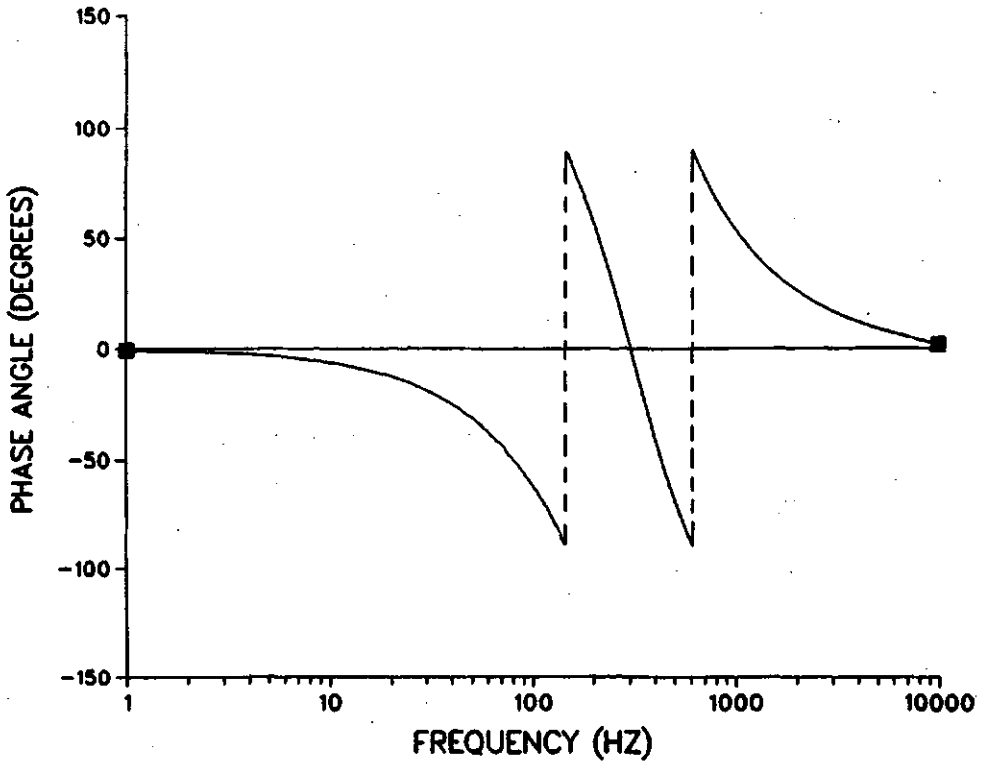

Figure 5.6: Phase response of the low-pass filter.

5.4.3. Test results - a single-phase transformer

The algorithm for protecting single phase transformers was tested using simulated data. The conditions simulated included one magnetizing inrush, an external fault, and two internal faults. The program simulating the proposed algorithm computed the value of ERROR and TRIP.

Figure 5.7 shows the instantaneous values of the primary and secondary voltages, and the primary current for a magnetizing inrush condition. Figure 5.8 shows the performance of the algorithm for this case. The figure depicts the value of ERROR and the trip index, TRIP. The trip index does not exceed the threshold and, therefore, the algorithm did not issue a trip command.

Figure 5.9 shows the performance of the algorithm for an external fault. The figure depicts the error and the trip index and shows that the trip index remains well below the threshold value and, therefore, no trip command is issued.

Figure 5.10 shows the performance of the algorithm for a ground fault on the primary winding of the transformer. This figure shows the values of ERROR as a function of the primary voltage and TRIP as a function of time. The figure also shows that the trip index exceeds the threshold in about 8 ms when the algorithm issues a trip signal.

Figure 5.11 shows the performance of the proposed algorithm for a fault that short circuits 20% of the secondary winding. The value of TRIP does not increase as rapidly as in the case of a high level fault (e.g. Figure 5.10). However, the algorithm issues a trip command in 12 ms. This case demonstrates that the algorithm can detect low-level internal faults.

5.4.4. Test results - three-phase transformers

The proposed algorithms for protecting three-phase transformers were tested using simulated data. The conditions simulated include magnetizing inrush, overexcitation and, external and internal faults including ground faults and inter-turn short circuits. Table 5.3 lists the simulated conditions. The results of the tests are presented in this section.

5.4.4.1. A wye-wye transformer

The algorithm for protecting a wye-wye transformer computed one trip index for each phase and issued a trip command if the trip indices satisfy any of the conditions listed in Table 5.1. Tables 5.4 and 5.5 summarize the results showing the performance of the algorithm for different conditions. Table 5.4 shows the maximum values of the trip indices for magnetizing inrush and external fault conditions. Table 5.5 shows the time taken by the trip indices to exceed the threshold for internal faults and provide the time

Table 5.3: List of transformer conditions used to test the performance of the proposed algorithms.

Case No.	Description
1.	Magnetizing inrush - I.
2.	Magnetizing inrush - II.
3.	External fault involving phase A and ground.
4.	External fault involving phase B and C.
5.	Three phase external fault.
6.	Overexcitation.
7.	Internal fault on sec. side that short-circuits 20% of winding of phase B.
8.	Internal fault on sec. side that short-circuits 50% of windings of phase A.
9.	Transformer switched-on with an internal fault that involves sec. winding of phase C and the ground.
10.	Internal fault on pri. side that short circuits winding phases A and C.
11.	Transformer switched-on with an internal fault that short-circuits 20% of secondary windings of phases B and C.
12.	Transformer switched on with an internal fault that involves primary winding of phase B and ground.

Table 5.4: Maximum values of the trip indices for magnetizing inrush, overexcitation and external fault conditions in the wye-wye transformer.

Case No.	Maximum value of		
	TRIPA	TRIPB	TRIPC
1.	0	0	0
2.	0	0	0
3.	8	0	0
4.	0	8	8
5.	6	8	8
6.	0	0	0

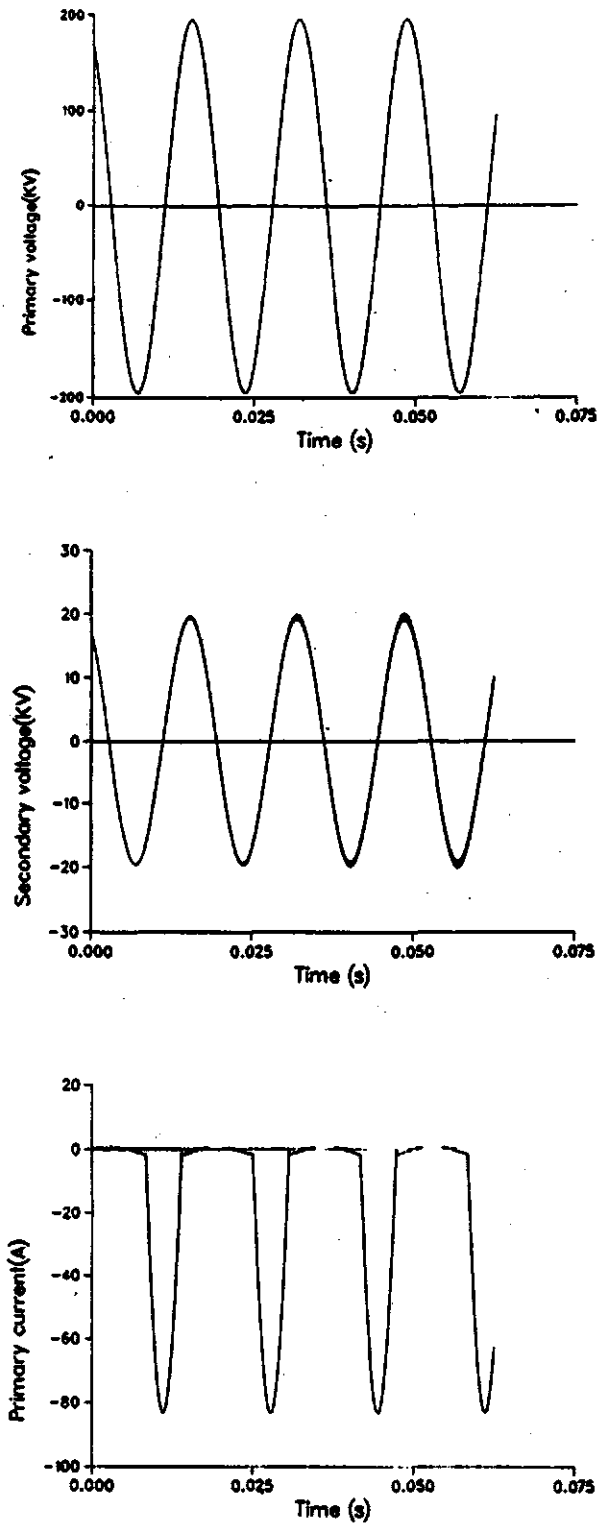

Figure 5.7: Instantaneous values of the primary and secondary voltages and the primary current for a magnetizing inrush condition in the single-phase transformer. The transformer was connected to the supply at time 0.0 s.

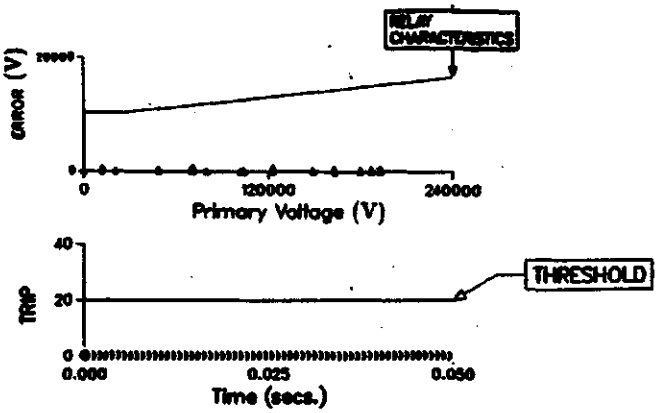

Figure 5.8: Errors and values of the trip index for a magnetizing inrush condition in the single-phase transformer. The transformer was connected to the supply at time 0.0 s.

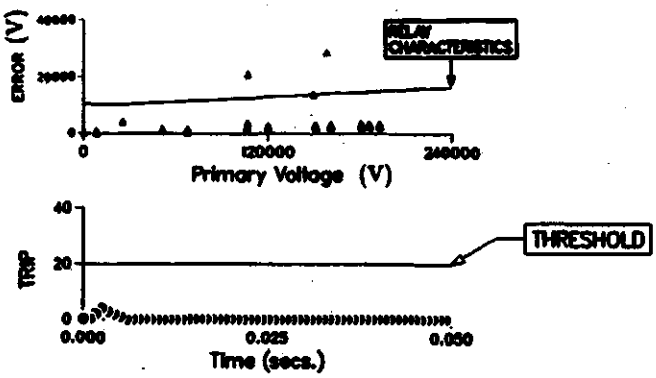

Figure 5.9: Errors and values of the trip index for an external fault condition in the single phase transformer. The fault was applied at time 0.0 s.

taken to issue a trip command. An examination of these tables indicates that the trip indices remain well below the threshold for magnetizing inrush, overexcitation and external faults. However, for internal faults, some trip indices exceed the threshold in relatively short times. It is also observed that the trip time varies from about 8 ms to 15 ms depending on the type and severity of the fault.

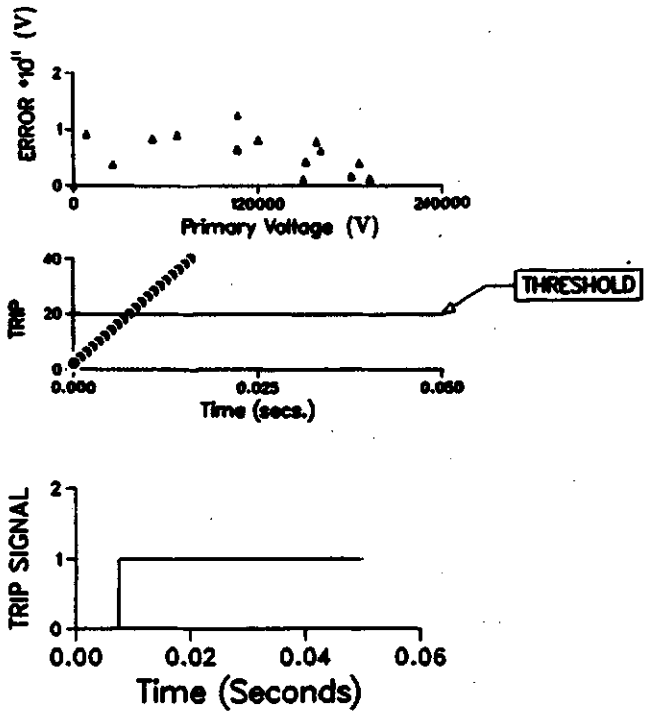

Figure 5.10: Errors, values of the trip index and the trip command for a ground fault in the primary windings of the single-phase transformer. The fault was applied on time 0.0 s.

Figure 5.12 shows the instantaneous values of the primary currents for a magnetizing inrush condition. Figure 5.13 shows the instantaneous values of the primary and secondary voltages and Figure 5.14 shows the performance of the algorithm for this condition. Figure 5.14(a) shows the values of ERRORA as a function of primary voltage of phase A and TRIPA as a function of time. Figures 5.14(b) and 5.14(c) show the values of ERRORB and TRIPB, and ERRORC and TRIPC respectively. These indices do not exceed the threshold indicating that the algorithm blocked tripping during magnetizing inrush.

Figure 5.15 shows the performance of the algorithm for a phase A to ground external fault. Figures 5.15(a), 5.15(b) and 5.15(c) depict the errors and the trip indices for phases A, B and C respectively. These figures in-

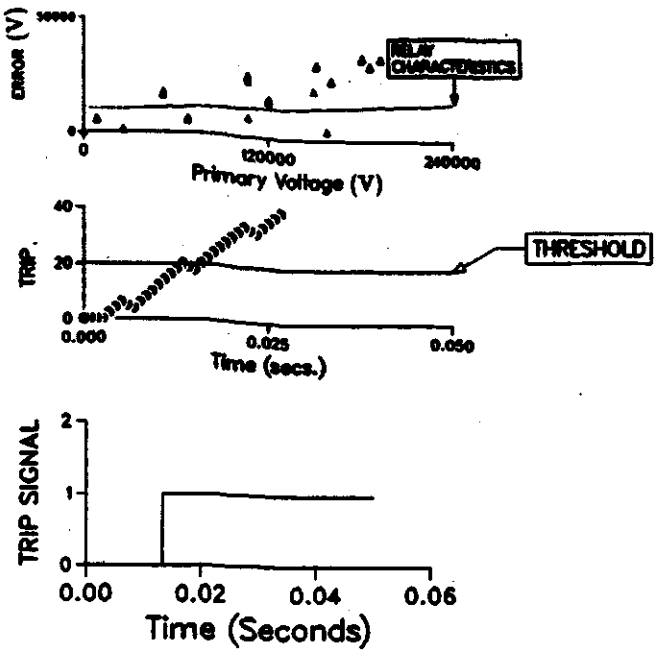

Figure 5.11: Errors, values of the trip index and the trip command for a low-level fault in the secondary windings of the single-phase transformer. The fault was applied on time 0.0 s.

dicate that the trip indices remain well below the threshold value and, therefore, no trip command is issued.

Figure 5.16 shows the performance of the proposed algorithm when the transformer is switched-on and an internal fault short circuiting twenty percent of the secondary windings of phases B and C exists. Figures 5.16(a), 5.16(b) and 5.16(c) depict the errors and the trip indices for phases A, B and C respectively. The trip indices TRIPB and TRIPC exceeded the threshold and the algorithm issued a trip command in about 15 ms after the inception of the fault as shown in Figure 5.16(d).

Table 5.5: Time required by the trip indices to exceed the threshold for internal fault conditions in a wye-wye transformer.

Case No.	Time required by the trip index			
	TRIPA (s)	TRIPB (s)	TRIPC (s)	Trip time (s)
7.	******	0.0108	******	0.0108
8.	0.0092	******	0.0083	0.0083
9.	******	******	0.0108	0.0108
10.	0.0075	******	0.0075	0.0075
11.	******	0.0142	0.015	0.0142
12.	******	0.0075	******	0.0075

****** signifies that the trip index remains below the threshold.

5.4.4.2. A delta-wye transformer

The algorithm for protecting a delta-wye transformer computed two trip indices for each phase used as reference. The decision-logic module received these indices and made trip/no-trip decisions using the criteria of Table 5.2. Tables 5.6 and 5.7 summarize the performance of the algorithm for different conditions. Table 5.6 shows the maximum value of the trip indices for magnetizing inrush and external fault conditions. Table 5.7 shows the time taken by each trip index to exceed threshold for internal faults and the time taken to issue a trip command. An examination of these tables indicates that the trip indices remain well below the threshold for magnetizing inrush, overexcitation and external faults. However, for internal faults, some trip indices exceed the threshold in relatively short times. The trip time varies from about 8 ms to 14 ms depending on the type and severity of the fault.

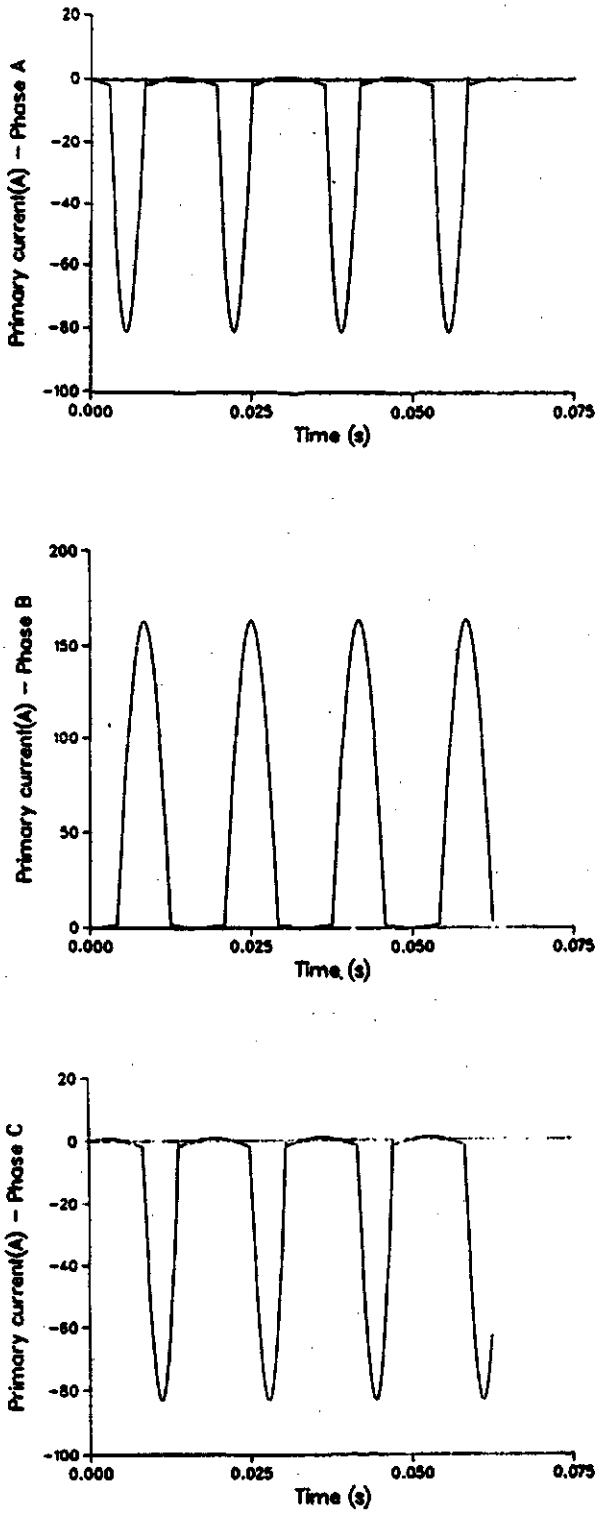

Figure 5.12: Instantaneous values of the primary currents for a magnetizing inrush condition in the wye-wye transformer. The transformer was connected to the supply at time 0.0 s.

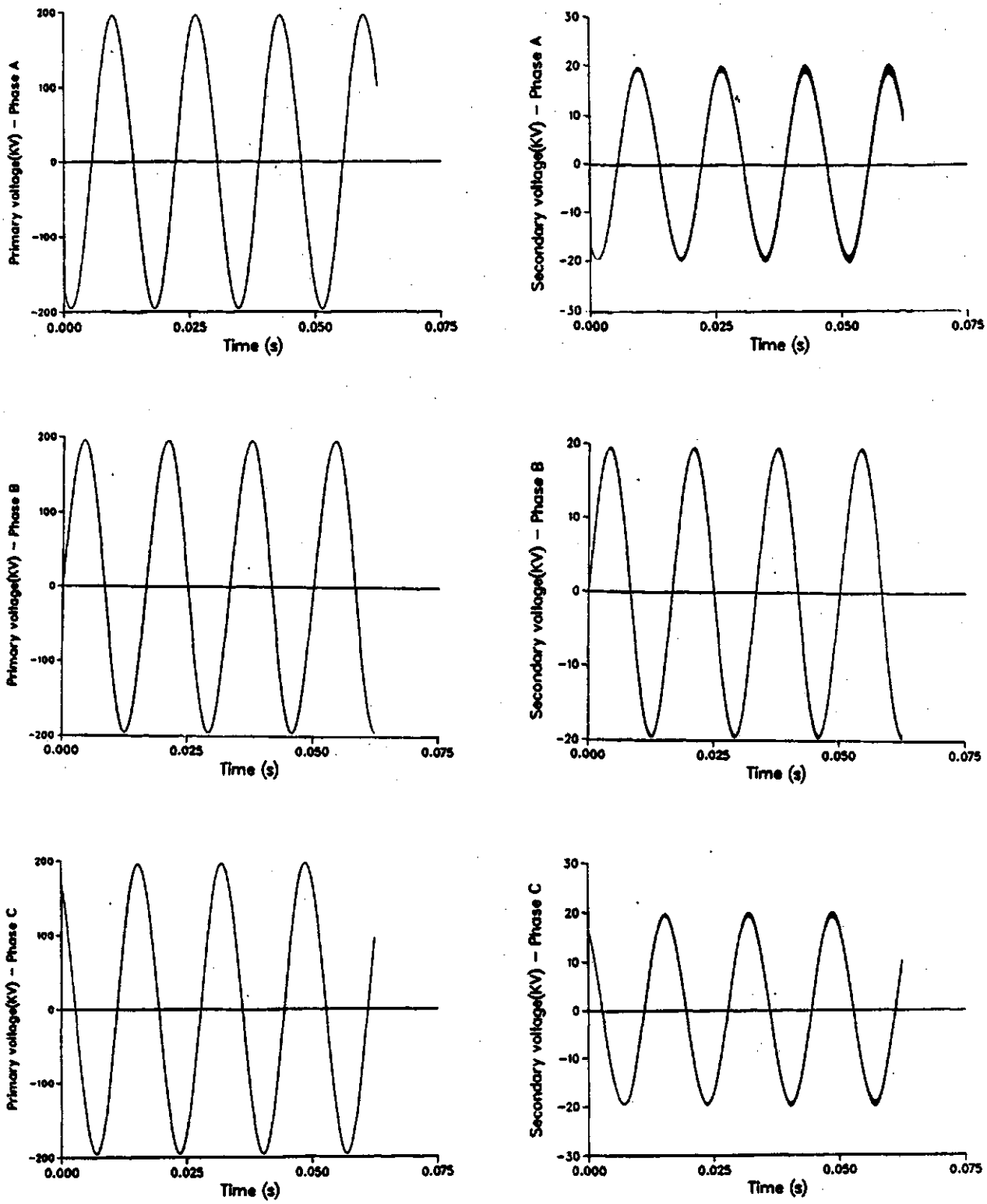

Figure 5.13: Instantaneous values of the primary and secondary voltages for a magnetizing inrush condition in the wye-wye transformer. The transformer was connected to the supply at time 0.0 s.

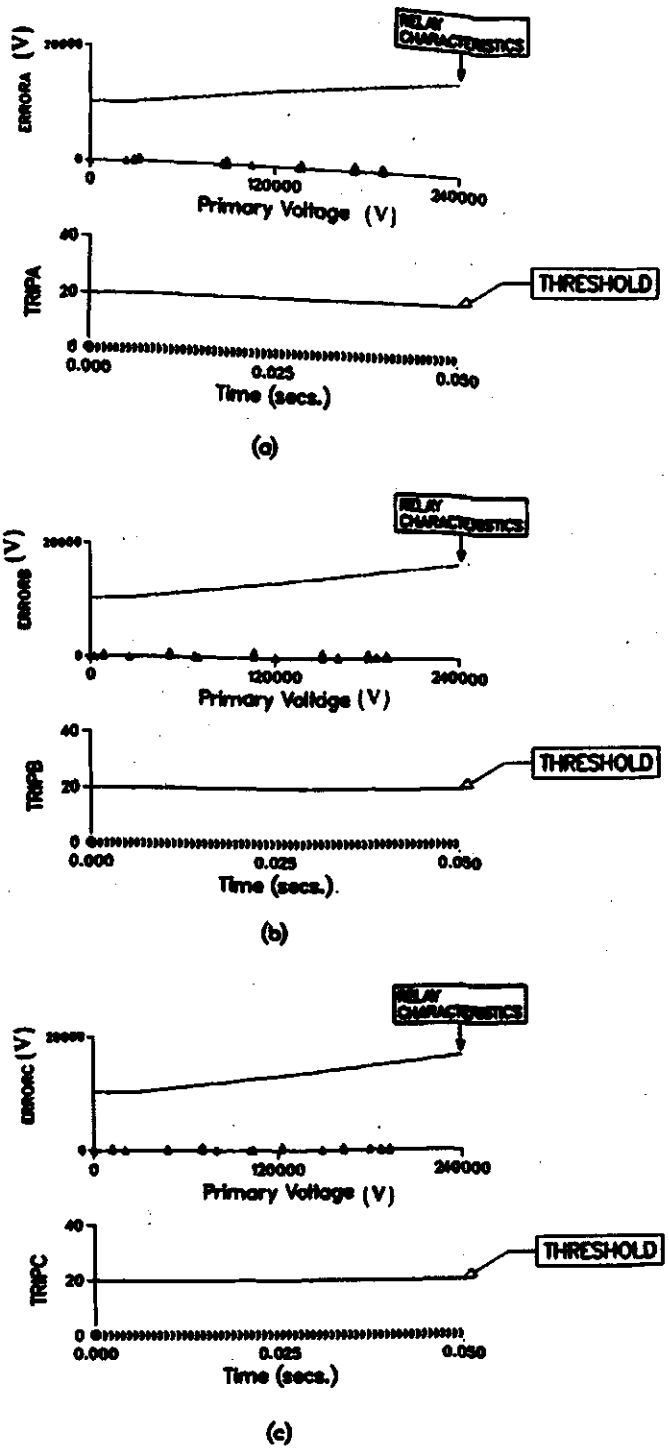

Figure 5.14: Errors and values of the trip indices for (a) phase A, (b) phase B and (c) phase C during a magnetizing inrush condition in the wye-wye transformer. The transformer was connected to the supply at time 0.0 s.

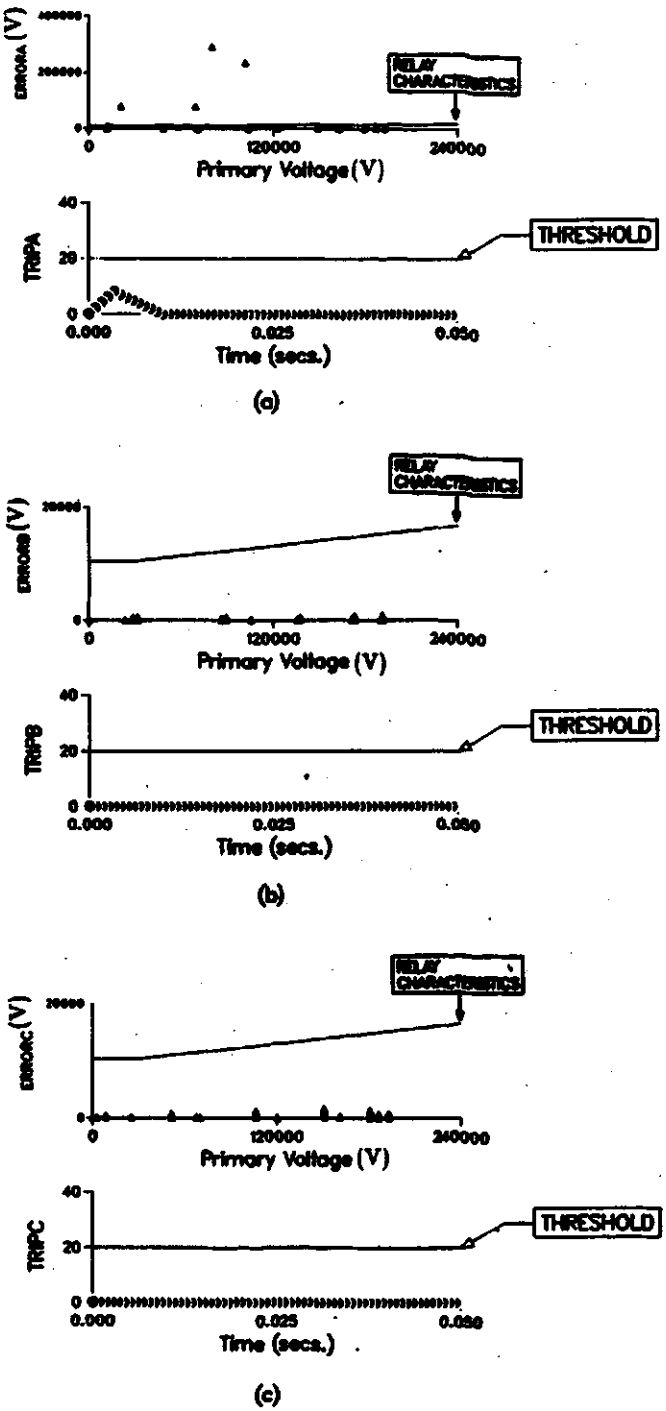

Figure 5.15: Errors and values of the trip indices for (a) phase A, (b) phase B and (c) phase C during a fault external to the wye-wye transformer. The fault was applied at time 0.0 s.

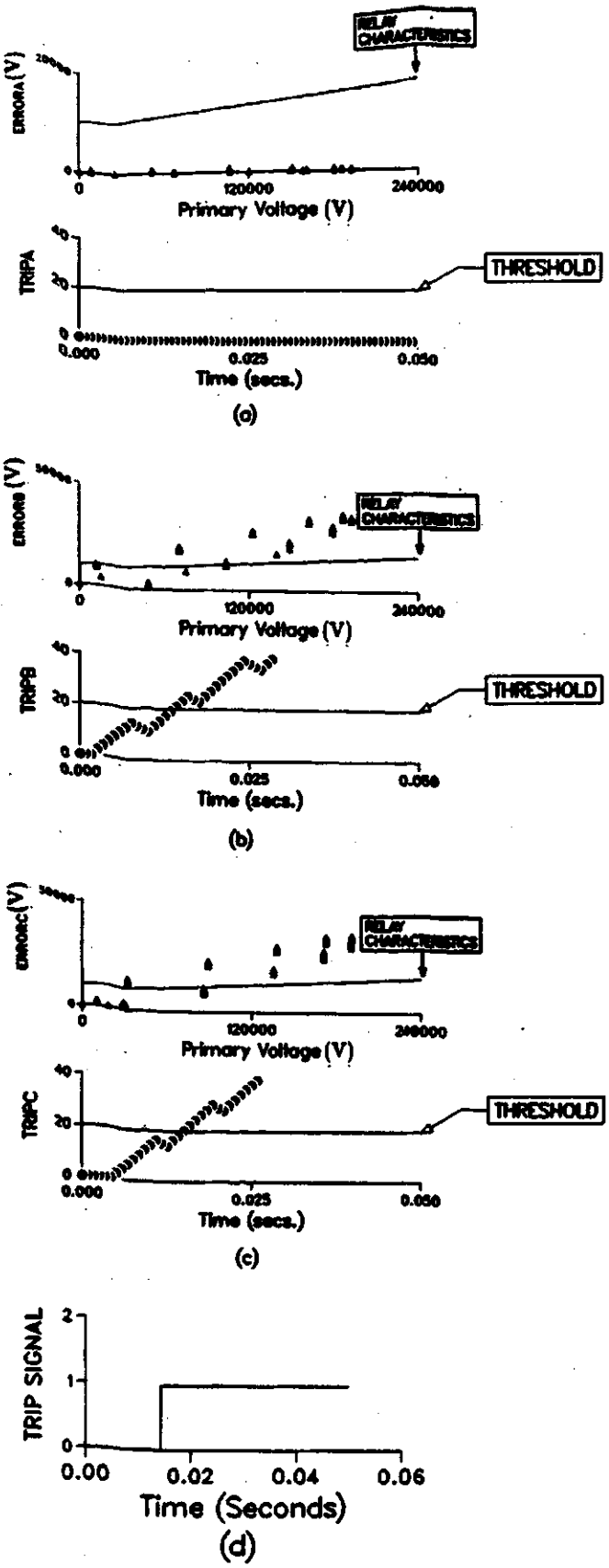

Figure 5.16: Errors and values of the trip indices for (a) phase A, (b) phase B and (c) phase C. during an internal fault in the wye-wye transformer. (d) Trip command issued by the algorithm vs time. The fault was applied at time 0.0 s.

Table 5.6: Maximum values of the trip indices for magnetizing inrush, overexcitation and external fault conditions in the delta-wye transformer.

Case No.	Maximum value of					
	TRIPB1	TRIPC1	TRIPA2	TRIPC2	TRIPA3	TRIPB3
1.	0	0	0	0	0	0
2.	0	0	0	0	0	0
3.	4	6	4	0	6	0
4.	8	8	8	10	8	10
5.	8	6	8	10	6	8
6.	0	0	0	0	0	0

Table 5.7: Time required by the trip indices to exceed the threshold for internal fault conditions in the delta-wye transformer.

Case No.	Time required by the trip index						
	TRIPB1 (s)	TRIPC1 (s)	TRIPA2 (s)	TRIPC2 (s)	TRIPA3 (s)	TRIPB3 (s)	Trip time (s)
7.	0.0083	******	0.0083	0.0083	******	0.0083	0.0083
8.	0.0100	0.0083	0.0100	0.0108	0.0083	0.0108	0.0100
9.	******	0.0083	******	0.0083	0.0083	0.0083	0.0083
10.	0.0075	0.0075	0.0075	0.0075	0.0075	0.0075	0.0075
11.	0.0133	0.0150	0.0150	0.0133	0.0158	0.0142	0.0133
12.	0.0075	0.0075	0.0075	0.0075	0.0075	0.0075	0.0075

****** signifies that the trip index remains below the threshold.

Figure 5.17 shows the instantaneous values of the primary currents for a magnetizing inrush condition. Figure 5.18 shows the instantaneous values of the primary and secondary voltages and Figure 5.19 shows the performance of the algorithm for this condition. Figure 5.19(a) shows the values of ERRORB1, ERRORC1, TRIPB1 and TRIPC1 when phase A is the "Reference Phase". Figures 5.19(b) and 5.19(c) show the values of ERRORA2, TRIPA2, ERRORC2 and TRIPC2, and ERRORA3, TRIPA3, ERRORB3 and TRIPB3. These indices do not exceed the threshold and, therefore, no trip command was issued as the transformer experienced magnetizing inrush.

Figure 5.20 shows the performance of the algorithm for a phase B to C external fault. Figures 5.20(a), 5.20(b) and 5.20(c) depict the errors and corresponding trip indices when phase A, B or C is used as the "Reference Phase". These figures indicate that trip indices remain well below the threshold and, therefore, no trip command is issued.

Figure 5.21 demonstrates the performance of the algorithm for a phase A and C to ground fault on the primary winding of the transformer. Figure 5.21(a) shows the values of ERRORB1, ERRORC1, TRIPB1 and TRIPC1 when phase A is the "Refereence Phase". Figures 5.21(b) and 5.21(c) show the values of ERRORA2, TRIPA2, ERRORC2 and TRIPC2, and ERRORA3, TRIPA3, ERRORB3 and TRIPB3. The decision-logic module correctly identified it as an internal fault and issued a trip command in about 8 ms. Figure 5.21(d) shows the trip signal generated by the decision-logic module.

5.5. Summary

Digital algorithms that can detect winding faults in single-phase and three-phase transformers are presented in this chapter. The algorithms are based on non-linear models of transformers instead of using the harmonic components of differential currents to avoid trippings during magnetizing inrush conditions. The non-linearity and hysteresis of the transformer core are

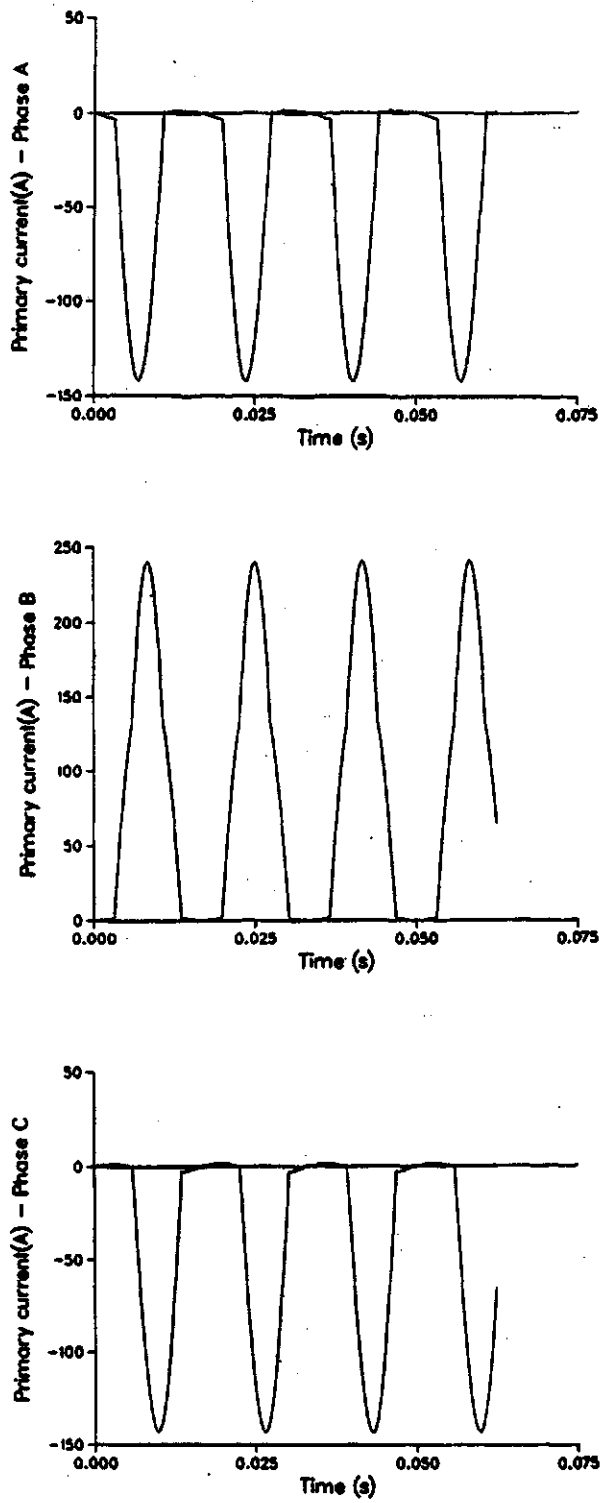

Figure 5.17: Instantaneous values of the primary currents for a magnetizing inrush condition in the delta-wye transformer. The transformer was connected to the supply at time 0.0 s.

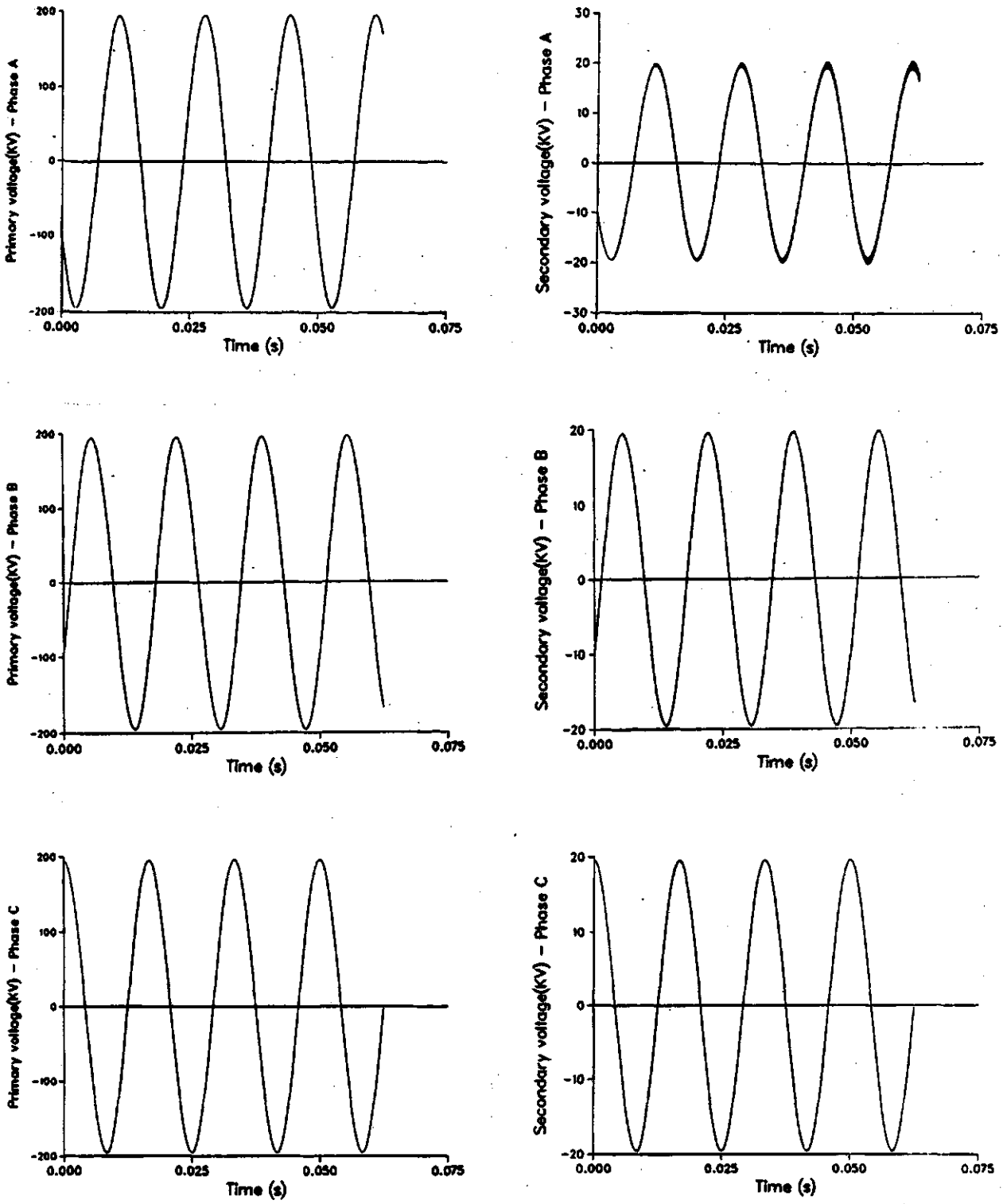

Figure 5.18: Instantaneous values of the primary and secondary voltages for a magnetizing inrush condition in the delta-wye transformer. The transformer was connected to the supply at time 0.0 s.

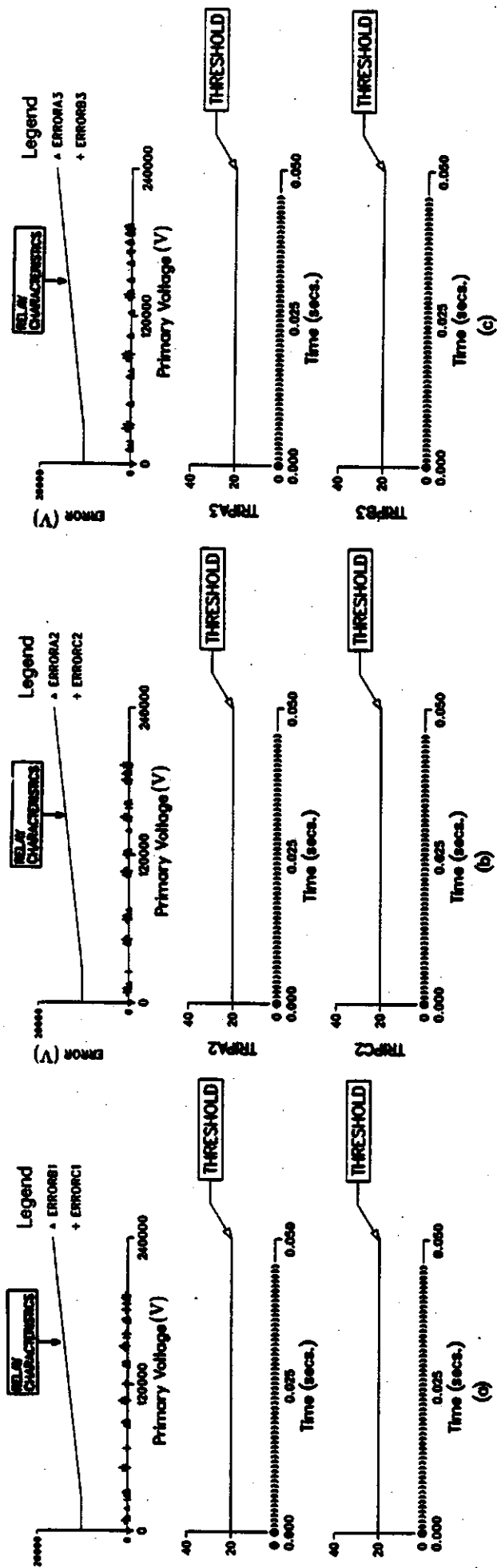

Figure 5.19: Errors and values of the trip indices for a magnetizing inrush condition in the delta-wye transformer when (a) phase A, (b) phase B or (c) phase C is used as the "Reference Phase". The transformer was connected to the supply at time 0.0 s.

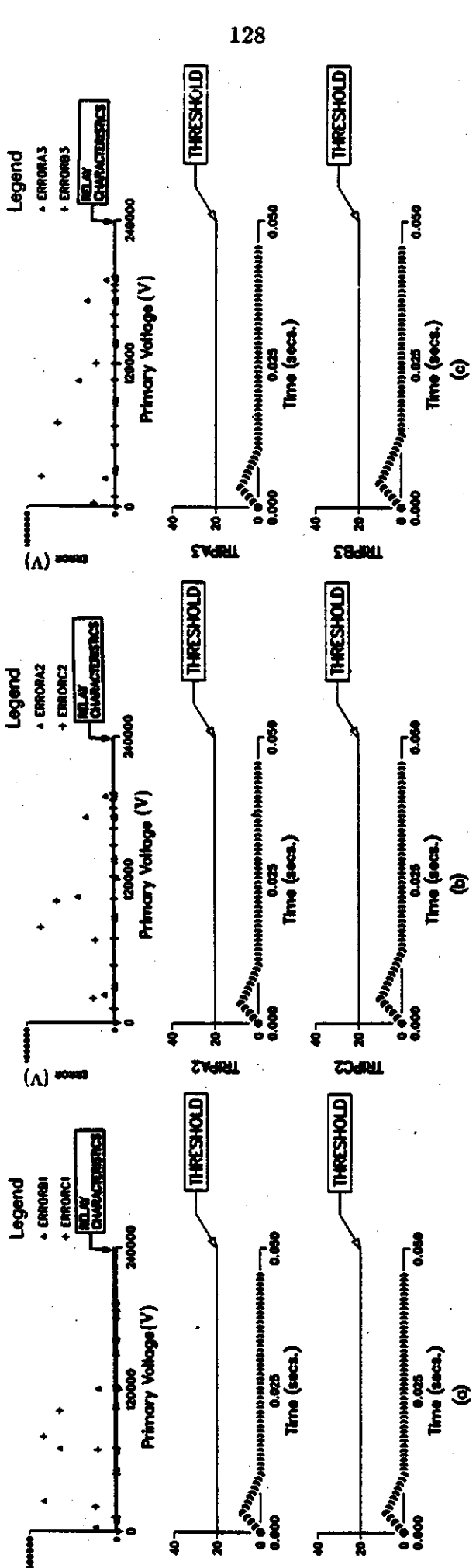

Figure 5.20: Errors and values of the trip indices for a fault external to the delta-wye transformer when (a) phase A, (b) phase B or (c) phase C is used as the "Reference Phase". The fault was applied at time 0.0 s.

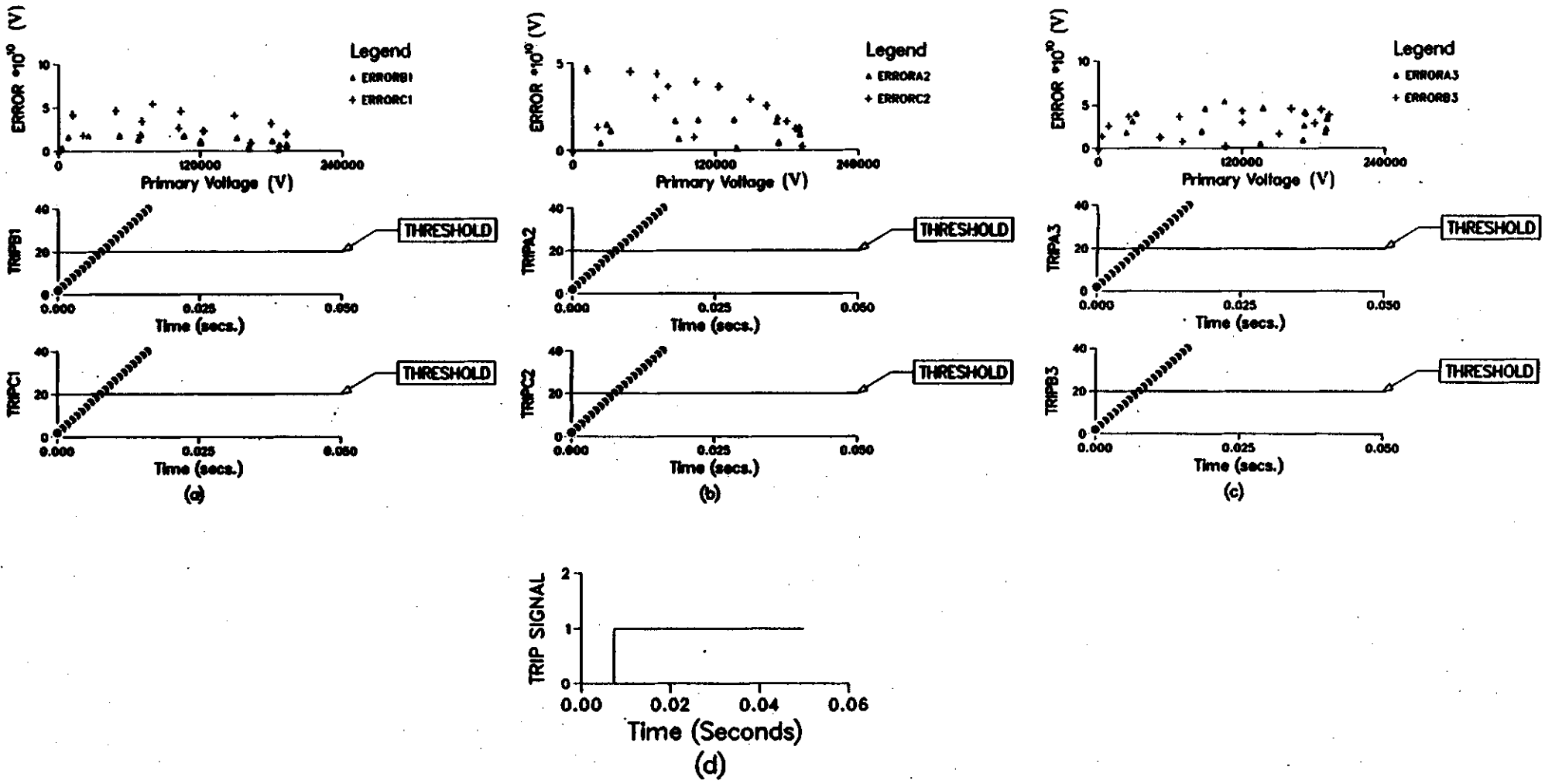

Figure 5.21: Errors and values of the trip indices for an internal fault in a delta-wye transformer when (a) phase A, (b) phase B or (c) phase C is used as the "Reference Phase". (d) Trip command issued by the algorithm vs time. The fault was applied at time 0.0 s.

taken into account but they do not explicitly become part of an algorithm. The algorithms can protect three-phase delta-wye transformers even if the winding currents can not be measured.

The algorithms were tested for a variety of operating conditions that were simulated using the EMTP on a digital computer. The test results are presented in this chapter. The results indicate that the algorithms do not issue trip commands during magnetizing inrush, overexcitation and external fault conditions. However, the algorithms issue trip commands for internal faults. The trip times are from about 8 ms to 15 ms depending on the type and severity of the fault.

6. PROPOSED ALGORITHMS FOR TRANSFORMER WINDING PROTECTION - VERSION-II

6.1. Introduction

Version-I of the digital relaying algorithms that can detect winding faults in single-phase and three-phase transformers are described in Chapter 5. Those algorithms use the trapezoidal rule to perform numerical integrations and do not neglect the effect of the resistances of the windings. The resistances of the transformer windings are small compared to their leakage reactances and, therefore, can be neglected. Also, numerical integrations can be performed using the rectangular rule. Version-II of the algorithms incorporate these features [47, 50].

While describing the algorithms the transformation ratio is assumed to be one. Also, currents and voltages at the power system level are used. These considerations prevent the equations from becoming unnecessarily complicated. Protective relays use voltages and currents from potential and current transformer secondaries. Therefore, the turns ratio of the transformer and instrument transformers were taken into consideration while implementing the algorithms.

This chapter describes the development of Version-II of the digital algorithms for protecting single-phase and three-phase transformers. Some test results demonstrating the performance of the algorithms are also presented. The algorithms were tested by using the signals used to test Version-I of the algorithms. This provides a direct comparison of the two versions of the al-

gorithms. The results from the comparisons are also included in this chapter.

6.2. Detecting Faults in a Single-Phase Transformer

Consider a two-winding single-phase transformer shown in Figure 5.1. The effects of the resistances of the windings on the transformer operation are neglegible compared to the effects of the inductances. The primary and secondary voltages expressed as functions of the primary and secondary currents and mutual flux linkages are

$$v_1 = l_1(di_1/dt) + (d\lambda_m/dt) \text{ and} \tag{6.1}$$

$$v_2 = -l_2(di_2/dt) + (d\lambda_m/dt). \tag{6.2}$$

Eliminating $d\lambda_m/dt$ from Equation 6.1 by using Equation 6.2 provides

$$v_1 = l_1(di_1/dt) + v_2 + l_2(di_2/dt). \tag{6.3}$$

Integrating both sides of this equation from time t_1 to t_2 provides

$$\int_{t_1}^{t_2} v_1 dt = l_1\{i_1(t_2)-i_1(t_1)\} + \int_{t_1}^{t_2} v_2 dt + l_2[i_2(t_2)-i_2(t_1)]. \tag{6.4}$$

Applying the rectangular rule for performing integrations yields

$$(t_2-t_1)[v_1\{(t_1+t_2)/2\}] = l_1[i_1(t_2)-i_1(t_1)]$$

$$+ (t_2-t_1)\{v_2[(t_1+t_2)/2]\} + l_2[i_2(t_2)-i_2(t_1)]. \tag{6.5}$$

Digital relays sample voltages and currents at time intervals, say ΔT seconds. If n is an integer, t_1, t_2 and $[t_1+t_2]/2$ can be replaced by $(n-1)\Delta T$, $n\Delta T$ and $(n-0.5)\Delta T$ respectively. Making these substitutions in Equation 6.5 provides

$$\Delta T\{v_1[(n-0.5)\Delta T]\} = l_1\{i_1(n\Delta T)-i_1[(n-1)\Delta T]\} +$$

$$\Delta T\{v_2[(n-0.5)\Delta T]\} + l_2\{i_2(n\Delta T)-i_2(n-1)\Delta T]\}. \tag{6.6}$$

Dividing both sides of this equation by ΔT provides

$$v_1[(n-0.5)\Delta T] = (l_1/\Delta T)i_1(n\Delta T) - (l_1/\Delta T)i_1[(n-1)\Delta T] +$$
$$(l_2/\Delta T)i_2(n\Delta T) - (l_2/\Delta T)i_2[(n-1)\Delta T] + v_2[(n-0.5)\Delta T]. \quad (6.7)$$

This equation expresses the primary voltage as a function of the secondary voltage and the primary and secondary currents. Consider that the leakage inductances, l_1 and l_2 are known. It is possible to calculate the right hand side of Equation 6.7 after taking samples of currents at $(n-1)\Delta T$ and $n\Delta T$ seconds and the samples of the voltages at $(n-0.5)\Delta T$ seconds. The value of the right hand side of the equation is the estimate of $v_1[(n-0.5)\Delta T]$. The left hand side is the measured value of $v_1[(n-0.5)\Delta T]$. The estimated and measured values are equal during normal operation, overexcitation, magnetizing inrush and external fault conditions. However, they are not equal during internal faults.

6.2.1. The algorithm

The algorithm for microprocessor-based protection of single-phase transformers uses the technique described in Section 6.2. It assumes that the primary and secondary voltages, and primary and secondary currents are sampled at a pre-specified rate. The algorithm requires that the sampling instants of voltages and currents be offset by one half of an intersampling time. The algorithm performs the functions similar to those of Version-I of the algorithm described in Section 5.2.1 but uses the equations decribed in Section 6.2.

6.3. Detecting Faults in Three-Phase Transformers

Consider a three-phase transformer whose primary windings are a, b, and c and the secondary windings are A, B and C whose parameters are described in Section 5.3. The following sections develop the techniques for detecting winding faults in three-phase transformers when their primary and secondary windings are either wye or delta connected. The digital algorithms for detecting transformer winding faults are then described.

6.3.1. Wye-wye tranformers

Figure 5.3 shows the circuit diagram of a wye-wye connected three-phase transformer. If the winding resistances are neglected, the following differential equations expressing the primary and secondary voltages as functions of the primary and secondary currents and the mutual flux linkages can be written.

$$v_a = l_a(di_a/dt) + (d\lambda_{aA}/dt) \tag{6.8}$$

$$v_b = l_b(di_b/dt) + (d\lambda_{bB}/dt) \tag{6.9}$$

$$v_c = l_c(di_c/dt) + (d\lambda_{cC}/dt) \tag{6.10}$$

$$v_A = -l_A(di_A/dt) + (d\lambda_{aA}/dt) \tag{6.11}$$

$$v_B = -l_B(di_B/dt) + (d\lambda_{bB}/dt) \tag{6.12}$$

$$v_C = -l_C(di_C/dt) + (d\lambda_{cC}/dt) \tag{6.13}$$

Applying the procedure described in Section 6.2 to Equations 6.8 and 6.11 provides Equation 6.14. A similar approach provides Equations 6.15 and 6.16.

$$v_a[(n-0.5)\Delta T] = (l_a/\Delta T)i_a(n\Delta T) - (l_a/\Delta T)i_a[(n-1)\Delta T] + v_A[(n-0.5)\Delta T] + (l_A/\Delta T)i_A(n\Delta T) - (l_A/\Delta T)i_A[(n-1)\Delta T] \tag{6.14}$$

$$v_b[(n-0.5)\Delta T] = (l_b/\Delta T)i_b(n\Delta T) - (l_b/\Delta T)i_b[(n-1)\Delta T] + v_B[(n-0.5)\Delta T] + (l_B/\Delta T)i_B(n\Delta T) - (l_B/\Delta T)i_B[(n-1)\Delta T] \tag{6.15}$$

$$v_c[(n-0.5)\Delta T] = (l_c/\Delta T)i_c(n\Delta T) - (l_c/\Delta T)i_c[(n-1)\Delta T] + v_C[(n-0.5)\Delta T] + (l_C/\Delta T)i_C(n\Delta T) - (l_C/\Delta T)i_C[(n-1)\Delta T] \tag{6.16}$$

If the leakage inductances of the transformer windings are known, the right

hand sides of Equations 6.14, 6.15 and 6.16 can be calculated after taking two samples of voltages and currents. The right hand side of Equation 6.14 is the estimate of $v_a[(n-0.5)\Delta T]$ whereas the left hand side is the measured value. As in the case of single-phase transformers, the estimated and measured values are equal during normal operation, overexcitation, magnetizing inrush and external faults. However, for internal faults involving winding a or A, these values are not equal. Similarly, the right hand side of Equation 6.15 provides the estimated value of $v_b[(n-0.5)\Delta T]$ whereas the left hand side is the measured value. The estimated and measured values are equal except when winding b or B is faulted. Similarly, the values of the left and right hand sides of the Equation 6.16 can be compared to detect internal faults in windings c or C.

6.3.1.1. The algorithm

The algorithm for the protection of three-phase wye-wye conntected transformers uses the technique described in Section 6.3.1. It performs the functions similar to those of Version-I of the algorithm described in Section 5.3.1.1 but uses the equations decribed in Section 6.3.1.

6.3.2. Delta-wye transformers

Figure 5.4 shows the winding connections of a delta-wye transformer. The following equations express the voltages of the transformer windings as functions of currents and the mutual flux linkages if the winding resistances are neglected.

$$v_a = l_a[d(i_a+i_{pp})/dt] + (d\lambda_{aA}/dt) \tag{6.17}$$

$$v_b = l_b[d(i_b+i_{pp})/dt] + (d\lambda_{bB}/dt) \tag{6.18}$$

$$v_c = l_c[d(i_c+i_{pp})/dt] + (d\lambda_{cC}/dt) \tag{6.19}$$

$$v_A = -l_A(di_A/dt) + (d\lambda_{aA}/dt) \tag{6.20}$$

$$v_B = -l_B(di_B/dt) + (d\lambda_{bB}/dt) \tag{6.21}$$

$$v_C = -l_C(di_C/dt) + (d\lambda_{cC}/dt) \tag{6.22}$$

Applying the procedure described in the previous sections to these equations provides Equations 6.23, 6.24 and 6.25.

$$\begin{aligned} v_a[(n-0.5)\Delta T] &= (l_a/\Delta T)i_a(n\Delta T) - (l_a/\Delta T)i_a[(n-1)\Delta T] + \\ &(l_a/\Delta T)i_{pp}(n\Delta T) - (l_a/\Delta T)i_{pp}[(n-1)\Delta T] + v_A[(n-0.5)\Delta T] + \\ &(l_A/\Delta T)i_A(n\Delta T) - (l_A/\Delta T)i_A[(n-1)\Delta T] \end{aligned} \tag{6.23}$$

$$\begin{aligned} v_b[(n-0.5)\Delta T] &= (l_b/\Delta T)i_b(n\Delta T) - (l_b/\Delta T)i_b[(n-1)\Delta T] + \\ &(l_b/\Delta T)i_{pp}(n\Delta T) - (l_b/\Delta T)i_{pp}[(n-1)\Delta T] + v_B[(n-0.5)\Delta T] + \\ &(l_B/\Delta T)i_B(n\Delta T) - (l_B/\Delta T)i_B[(n-1)\Delta T] \end{aligned} \tag{6.24}$$

$$\begin{aligned} v_c[(n-0.5)\Delta T] &= (l_c/\Delta T)i_c(n\Delta T) - (l_c/\Delta T)i_c[(n-1)\Delta T] + \\ &(l_c/\Delta T)i_{pp}(n\Delta T) - (l_c/\Delta T)i_{pp}[(n-1)\Delta T] + v_C[(n-0.5)\Delta T] + \\ &(l_C/\Delta T)i_C(n\Delta T) - (l_C/\Delta T)i_C[(n-1)\Delta T] \end{aligned} \tag{6.25}$$

The currents i_a, i_b and i_c, are the non-circulating components of the winding currents and i_{pp} is the current circulating in the delta winding. The non-circulating components can be computed by using Equations 5.32, 5.33 and 5.34 respectively but the circulating current is not known. As in Version-I of the algorithms, it is possible to use Equation 6.23 to estimate the terms containing the circulating current and use Equations 6.24 and 6.25 for detecting faults. For this purpose, Equation 6.23 is rearranged as follows.

$$\begin{aligned} &(l_a/\Delta T)i_{pp}(n\Delta T) - (l_a/\Delta T)i_{pp}[(n-1)\Delta T] = \\ &v_a[(n-0.5)\Delta T] - (l_a/\Delta T)i_a(n\Delta T) + (l_a/\Delta T)i_a[(n-1)\Delta T] - \\ &v_A[(n-0.5)\Delta T] - (l_A/\Delta T)i_A(n\Delta T) + (l_A/\Delta T)i_A[(n-1)\Delta T]. \end{aligned} \tag{6.26}$$

It is possible to evaluate its right hand side immediately after taking the

latest samples of the voltages and currents. The value of $(l_b/\Delta T)i_{pp}(n\Delta T) - (l_b/\Delta T)i_{pp}[(n-1)\Delta T]$ is required to compute the right hand side of Equation 6.24. This value can be estimated by multiplying Equation 6.26 with (l_b/l_a) which provides

$$(l_b/\Delta T)i_{pp}(n\Delta T) - (l_b/\Delta T)i_{pp}[(n-1)\Delta T] = (l_b/l_a)(\textit{R.H.S. of Equation } 6.26). \quad (6.27)$$

Similarly multiplying Equation 6.26 with (l_c/l_a) provides

$$(l_c/\Delta T)i_{pp}(n\Delta T) - (l_c/\Delta T)i_{pp}[(n-1)\Delta T] = (l_c/l_a)(\textit{R.H.S. of Equation } 6.26). \quad (6.28)$$

It is possible to compute the right hand sides of Equations 6.27 and 6.28 which are the estimates of the terms containing the circulating current in Equations 6.24 and 6.25. Now, it becomes possible to compute the right hand sides of Equations 6.24 and 6.25. which provide the estimated values of $v_b[(n-0.5)\Delta T]$ and $v_c[(n-0.5)\Delta T]$ respectively. The left hand sides are the measurements. The estimated and measured values are equal for magnetizing inrush, overexcitation, external faults and normal operating conditions. However, they are not equal for faults in the transformer protection zone.

In the above procedure, Equation 6.26 estimates the terms involving the circulating current from the measurements of voltages and currents of windings a and A. The measurement from the remaining windings provide enough information to decide whether an internal fault exists or not.

It is also possible to use the measurements from windings b and B to estimate the circulating current terms. For this purpose, Equation 6.24 is rearranged as follows:

$$\begin{aligned}(l_b/\Delta T)i_{pp}(n\Delta T) - (l_b/\Delta T)i_{pp}[(n-1)\Delta T] = \\ v_b[(n-0.5)\Delta T] - (l_b/\Delta T)i_b(n\Delta T) + (l_b/\Delta T)i_b[(n-1)\Delta T] - \\ v_B[(n-0.5)\Delta T] - (l_B/\Delta T)i_B(n\Delta T) + (l_B/\Delta T)i_B[(n-1)\Delta T]. \end{aligned} \quad (6.29)$$

It is possible to evaluate the right-hand side of Equation 6.29 immediately after taking the samples of voltages and currents. The following equations can be obtained by multiplying Equation 6.29 with (l_a/l_b) and (l_c/l_b) respectively.

$$(l_a/\Delta T)i_{pp}(n\Delta T) - (l_a/\Delta T)i_{pp}[(n-1)\Delta T] =$$
$$(l_a/l_b)(\textit{R.H.S. of Equation } 6.29) \tag{6.30}$$

$$(l_c/\Delta T)i_{pp}(n\Delta T) - (l_c/\Delta T)i_{pp}[(n-1)\Delta T] =$$
$$(l_c/l_b)(\textit{R.H.S. of Equation } 6.29) \tag{6.31}$$

It is possible to compute the values of the right hand sides of these equations which are the estimates of the terms containing the circulating current in Equations 6.23 and 6.25 respectively. After calculating these values, it becomes possible to compute the right hand sides of Equations 6.23 and 6.25 which are the estimated values of $v_a[(n-0.5)\Delta T]$ and $v_c[(n-0.5)\Delta T]$ respectively. The left hand sides are the measurements. The estimated and measured values are equal for magnetizing inrush, overexcitation, external faults and normal operating conditions. However, they are not equal for faults in the transformer protection zone.

The measurements from windings c and C can also be used to estimate the circulating current. For this purpose, Equation 6.25 is rearranged as follows:

$$(l_c/\Delta T)i_{pp}(n\Delta T) - (l_c/\Delta T)i_{pp}[(n-1)\Delta T] =$$
$$v_c[(n-0.5)\Delta T] - (l_c/\Delta T)i_c(n\Delta T) + (l_c/\Delta T)i_c[(n-1)\Delta T] -$$
$$v_C[(n-0.5)\Delta T] - (l_C/\Delta T)i_C(n\Delta T) + (l_C/\Delta T)i_C[(n-1)\Delta T]. \tag{6.32}$$

The right hand side of Equation 6.32 can be evaluated immediately after taking samples of voltages and currents. It is possible to obtain Equations 6.33 and 6.34 by multiplying Equation 6.32 with (l_a/l_c) and (l_b/l_c) respectively.

$$(l_a/\Delta T)i_{pp}(n\Delta T) - (l_a/\Delta T)i_{pp}[(n-1)\Delta T] =$$

$$(l_a/l_c)(\textit{R.H.S. of Equation } 6.32) \tag{6.33}$$

$$(l_b/\Delta T)i_{pp}(n\Delta T) - (l_b/\Delta T)i_{pp}[(n-1)\Delta T] =$$

$$(l_b/l_c)(\textit{R.H.S. of Equation } 6.32) \tag{6.34}$$

The right hand sides of these equations provide the estimates of the terms containing the circulating current which can be computed. The computed values can be used in Equations 6.24 and 6.25 respectively. Now, it becomes possible to estimate the values of the right hand sides of Equations 6.24 and 6.25 which are the estimated values of $v_a[(n-0.5)\Delta T]$ and $v_b[(n-0.5)\Delta T]$ respectively. The left hand sides are the measurements. As previously, the estimated and measured values are equal for magnetizing inrush, overexcitation, external faults and normal operating conditions. However, they are not equal for faults in the transformer protection zone.

The phase whose measurements are used to estimate the circulating current is classified as the "Reference Phase".

6.3.2.1. The algorithm

The algorithm for the protection of a delta-wye transformer uses the technique described in Section 6.3.2. It consists of four modules; the first, second, and third computing modules and a decision-logic module. The modules perform functions similar to the modules of Version-I of the algorithm as described in Section 5.3.2.1. However, they use the equations described in the Section 6.3.2.

6.4. Testing the Algorithms

The algorithms were tested using a microVAX 3600 digital computer which is available at the University of Saskatchewan. The signals needed for evaluating the performance of the algorithms were generated by the Electro-Magnetic Transient Program (EMTP) [48] and were the same as used to test Version-I of the algorithms. Raw data were processed by digital filters described in Section 5.4.2. The outputs of the filters were converted to data of 1200 Hz sampling rate. A sampling skew of 1/2400 s was introduced between the voltage and current samples. The discrete data were then presented to FORTRAN programs that simulated the proposed algorithms which used a relay characteristics similar to that of Figure 5.2. The values of THRES and BNDRY were set at 7.5% and 20% of the rated primary voltage of the transformer. SLOPE was set at 0.03 and the trip index threshold was set at 20. This section discusses the results obtained from the simulated tests.

6.4.1. Test results - a single-phase transformer

The algorithm for protecting single phase transformers was tested using the simulated data for magnetizing inrush, an external fault and internal faults including ground faults and inter-turn short circuits. The program computed the values of ERROR and TRIP for these conditions.

Figure 6.1 shows the performance of the algorithm for a magnetizing inrush condition. The figure depicts the values of ERROR as a function of primary voltage and TRIP as a function of time. The trip index does not exceed the threshold indicating that the algorithm does not issue a trip command during magnetizing inrush.

Figure 6.2 shows the performance of the algorithm for an external fault. The figure shows that the trip index remains well below the threshold and no trip command is issued.

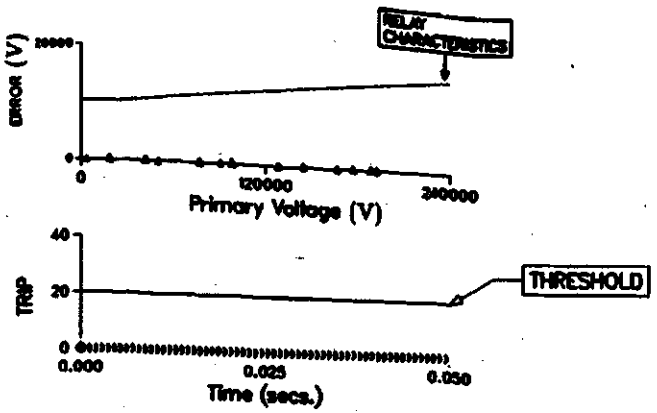

Figure 6.1: Errors and values of the trip index for a magnetizing inrush condition in the single-phase transformer. The transformer was connected to the supply at time 0.0 s.

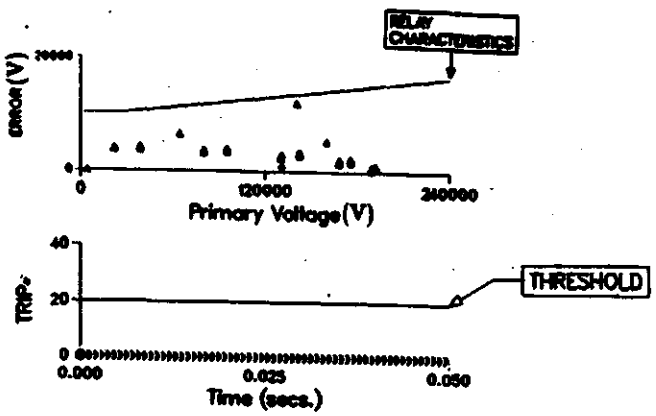

Figure 6.2: Errors and values of the trip index for a fault external to the single phase transformer. The fault was applied at time 0.0 s.

Figure 6.3 shows the performance of the algorithm for a ground fault on the primary winding of the transformer. This figure shows that the trip index exceeds the threshold in about 8 ms when the algorithm issues a trip command.

Figure 6.4 shows the performance of the proposed algorithm for a fault that short circuits 20% of the secondary winding. The trip index does not increase as rapidly as it did in the case of a high level fault reported in Figure 6.3. However, the algorithm issues a trip command in about 20 ms as shown in Figure 6.4. This case demonstrates that the algorithm can detect low-level internal faults.

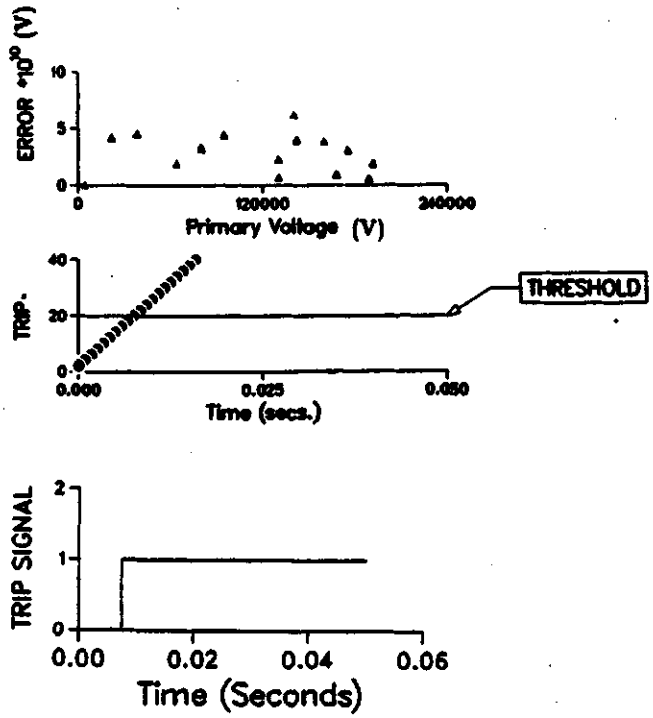

Figure 6.3: Errors, values of the trip index and the trip command for a ground fault in the primary windings of the single-phase transformer. The fault was applied at time 0.0 s.

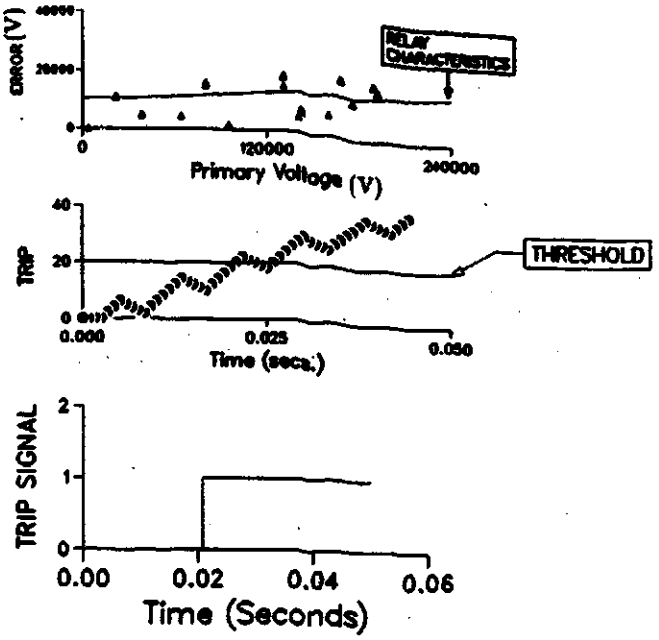

Figure 6.4: Errors, values of the trip index and the trip command for a low-level fault on the secondary windings of the single-phase transformer. The fault was applied at time 0.0 s.

6.4.2. Test results - three-phase transformers

The proposed algorithms for protecting three-phase transformers were tested using the simulated data. The conditions simulated included magnetizing inrush, overexcitation and, external and internal faults including ground faults and inter-turn short circuits. Table 5.3 lists the conditions for which the performance of the algorithms was tested. The results of these tests are presented in this section.

6.4.2.1. A wye-wye transformer

The algorithm for protecting a wye-wye transformer computed one trip index for each phase and issues a trip command if the trip indices satisfy one of the conditions listed in Table 5.1. Tables 6.1 and 6.2 list the results showing the performance of the algorithm for different conditions. Table 6.1

shows the maximum value of the trip indices for magnetizing inrush and external fault conditions. Table 6.2 shows the time taken by the trip indices to exceed the threshold for internal faults and the time taken to issue trip commands. An examination of the tables indicates that all trip indices remain well below the threshold for magnetizing inrush, overexcitation and external faults. However, for internal faults, some trip indices exceed the threshold value in relatively short times. The trip time varies from about 8 ms to 23 ms depending on the severity of the fault.

Table 6.1: Maximum values of the trip indices for magnetizing inrush, overexcitation and external fault conditions in the wye-wye transformer.

Case No.	Maximum value of		
	TRIPA	TRIPB	TRIPC
1.	0	0	0
2.	0	0	0
3.	8	0	0
4.	0	8	8
5.	0	8	8
6.	0	0	0

Figure 6.5 shows the performance of the algorithm for a magnetizing inrush condition. Figure 6.5(a) shows the values of ERRORA as a function of the primary voltage of phase A and TRIPA as a function of time. Figures 6.5(b) and 6.5(c) show the values of ERRORB and TRIPB, and ERRORC and TRIPC respectively. The indices do not exceed the threshold and the algorithm does not issue a trip command.

Figure 6.6 shows the performance of the algorithm for a phase A to

Table 6.2: Time required by the trip indices to exceed the threshold for internal fault conditions in the wye-wye transformer.

Case No.	Time required by the trip index			
	TRIPA (s)	TRIPB (s)	TRIPC (s)	Trip time (s)
7.	******	0.0133	******	0.0133
8.	0.0125	******	0.0083	0.0083
9.	******	******	0.0108	0.0108
10.	0.0075	******	0.0075	0.0075
11.	******	0.0225	0.025	0.0225
12.	******	0.0075	******	0.0075

****** signifies that the trip index remains below the threshold.

ground external fault. Figures 6.6(a), 6.6(b) and 6.6(c) depict the errors and the trip indices for phases A, B and C respectively. These figures indicate that all trip indices remain well below the threshold value and no trip command is issued.

Figure 6.7 shows the performance of the proposed algorithm for a condition when the transformer is switched on with an internal fault that short circuits 20% of the secondary windings of phases B and C. Figures 6.7(a), 6.7(b) and 6.7(c) depict the errors and trip indices for phases A, B and C respectively. The trip indices TRIPB and TRIPC exceeded the threshold and the algorithm issued a trip command in 23 ms as shown in Figure 6.7(d).

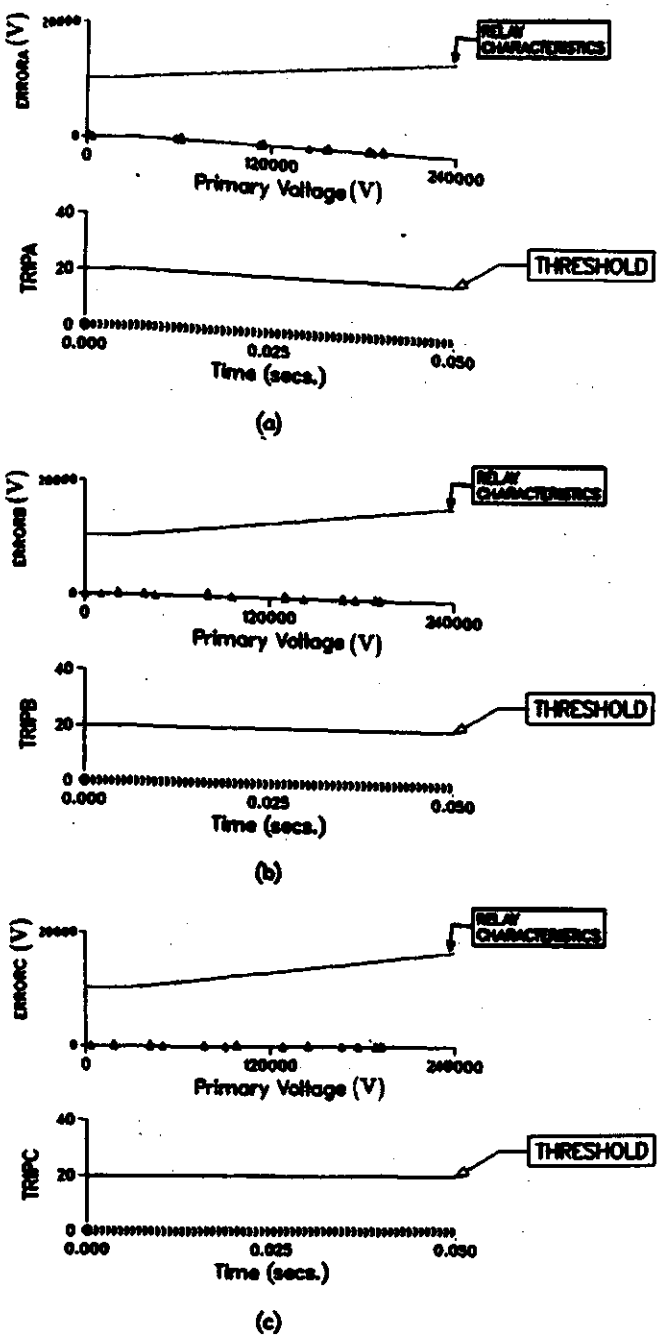

Figure 6.5: Errors and values of the trip indices for (a) phase A, (b) phase B and (c) phase C during a magnetizing inrush condition in the wye-wye transformer. The transformer was connected to the supply at time 0.0 s.

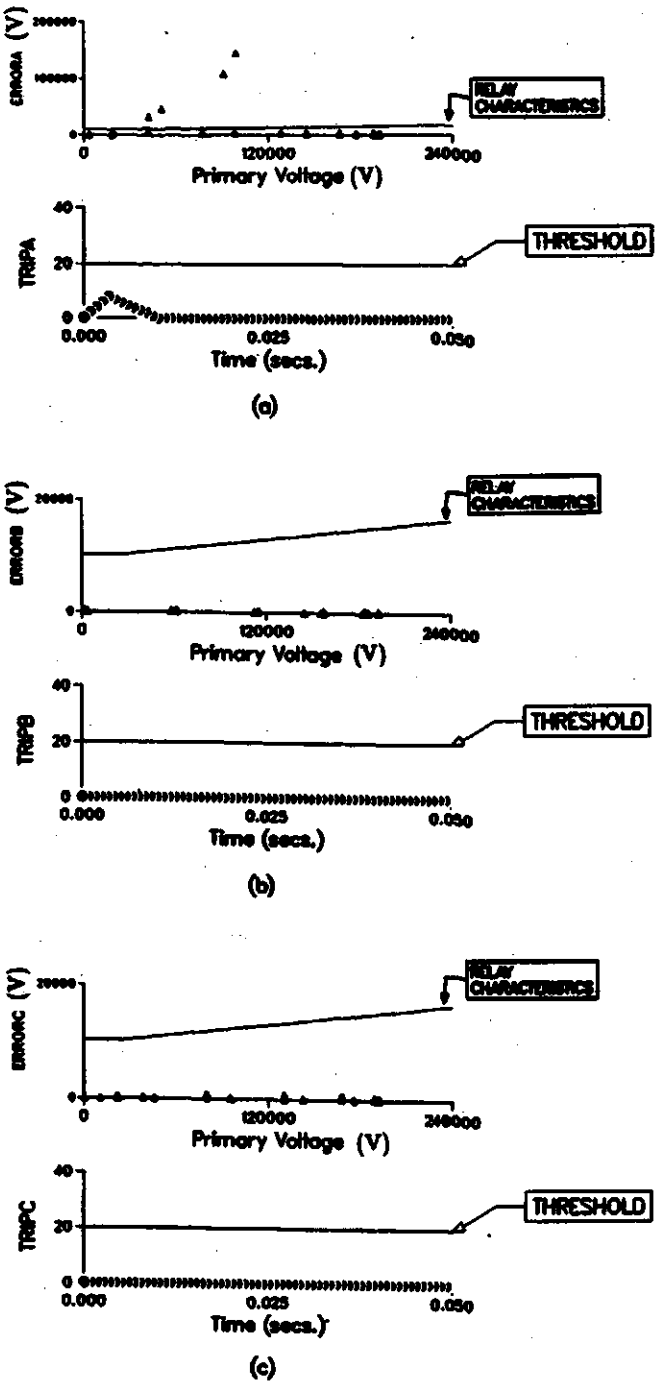

Figure 6.6: Errors and values of the trip indices for (a) phase A, (b) phase B and (c) phase C during a fault external to the wye-wye transformer. The fault was applied at time 0.0 s.

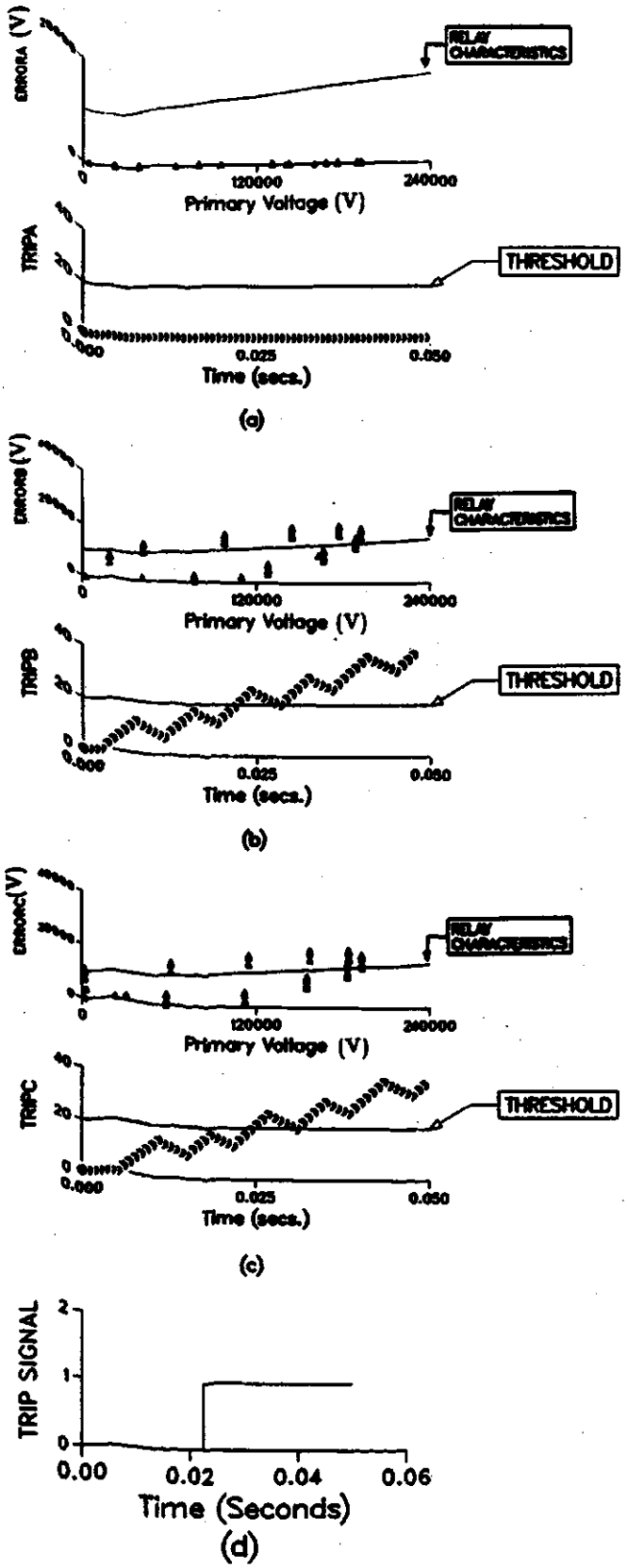

Figure 6.7: Errors and values of the trip indices for (a) phase A, (b) phase B and (c) phase C during an internal fault in the wye-wye transformer. (d) Trip command issued by the algorithm vs time. The fault was applied at time 0.0 s.

6.4.2.2. A delta-wye transformer

The algorithm for protecting a delta-wye transformer computed two trip indices by using each phase as a reference phase. The decision-logic module received these indices and made trip/no-trip decisions using the criteria of Table 5.2. Tables 6.3 and 6.4 summarize the results showing the performance of the algorithm for different conditions. Table 6.3 shows the maximum value of the trip indices for magnetizing inrush and external fault conditions. Table 6.4 shows the time taken by each trip index to exceed the threshold for internal faults and the time taken to issue a trip command. An examination of Tables 6.3 and 6.4 indicates that all trip indices remain well below the threshold for magnetizing inrush, overexcitation and external faults. However, for internal faults, some trip indices exceed the threshold in relatively short times. The trip time varies from about 8 ms to 23 ms depending on the type and severity of the fault.

Table 6.3: Maximum values of the trip indices for magnetizing inrush, overexcitation and external fault conditions in the delta-wye transformer.

Case No.	Maximum value of					
	TRIPB1	TRIPC1	TRIPA2	TRIPC2	TRIPA3	TRIPB3
1.	0	0	0	0	0	0
2.	0	0	0	0	0	0
3.	0	2	0	0	0	0
4.	8	8	8	8	8	8
5.	8	4	8	8	4	8
6.	0	0	0	0	0	0

Table 6.4: Time required by the trip indices to exceed the threshold for internal fault conditions in the delta-wye transformer.

Case No.	Time required by the trip index						Trip time (s)
	TRIPB1 (s)	TRIPC1 (s)	TRIPA2 (s)	TRIPC2 (s)	TRIPA3 (s)	TRIPB3 (s)	
7.	0.0083	******	0.0083	0.0083	******	0.0083	0.0083
8.	0.0100	0.0108	0.0108	0.0108	0.0092	0.0150	0.0108
9.	******	0.0108	******	0.0108	0.0108	0.0108	0.0108
10.	0.0075	0.0075	0.0075	0.0075	0.0075	0.0075	0.0075
11.	0.0242	0.0267	0.0234	0.0150	0.0258	0.0167	0.0234
12.	0.0075	0.0075	0.0075	0.0075	0.0075	0.0075	0.0075

****** signifies that the trip index remains below the threshold.

Figure 6.8 shows the performance of the algorithm for a magnetizing inrush condition. Figure 6.8(a) shows the values of ERRORB1, ERRORC1, TRIPB1 and TRIPC1 when phase A is the "Reference Phase". Figures 6.8(b) and 6.8(c) show the values of ERRORA2, TRIPA2, ERRORC2 and TRIPC2, and ERRORA3, TRIPA3, ERRORB3 and TRIPB3. The indices do not exceed the threshold and, therefore, no trip command is issued.

Figure 6.9 shows the performance of the algorithm for a phase B to C external fault. Figures 6.9(a), 6.9(b) and 6.9(c) depict the errors and the corresponding trip indices when the phase A, B or C is used as the "Reference Phase". These figures show that all trip indices remain well below the threshold value and, therefore, no trip command is issued.

Figure 6.10 shows the performance of the algorithm for a phase A and C to ground fault on the primary side of the transformer. Figure 6.10(a) shows the values of ERRORB1, ERRORC1, TRIPB1 and TRIPC1 when phase A is the "Reference Phase". Figures 6.10(b) and 6.10(c) show the values of ERRORA2, TRIPA2, ERRORC2 and TRIPC2, and ERRORA3,

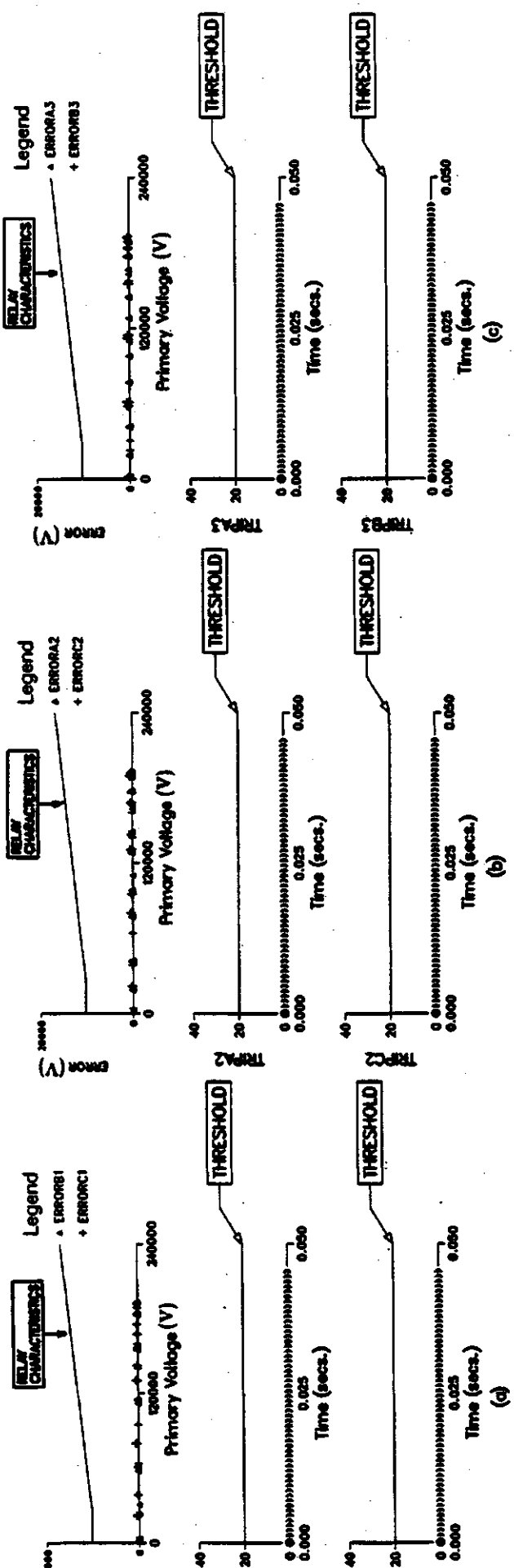

Figure 6.8: Errors and values of the trip indices for a magnetizing inrush condition in the delta-wye transformer when (a) phase A, (b) phase B or (c) phase C is used as the "Reference Phase". The transformer was connected to the supply at time 0.0 s.

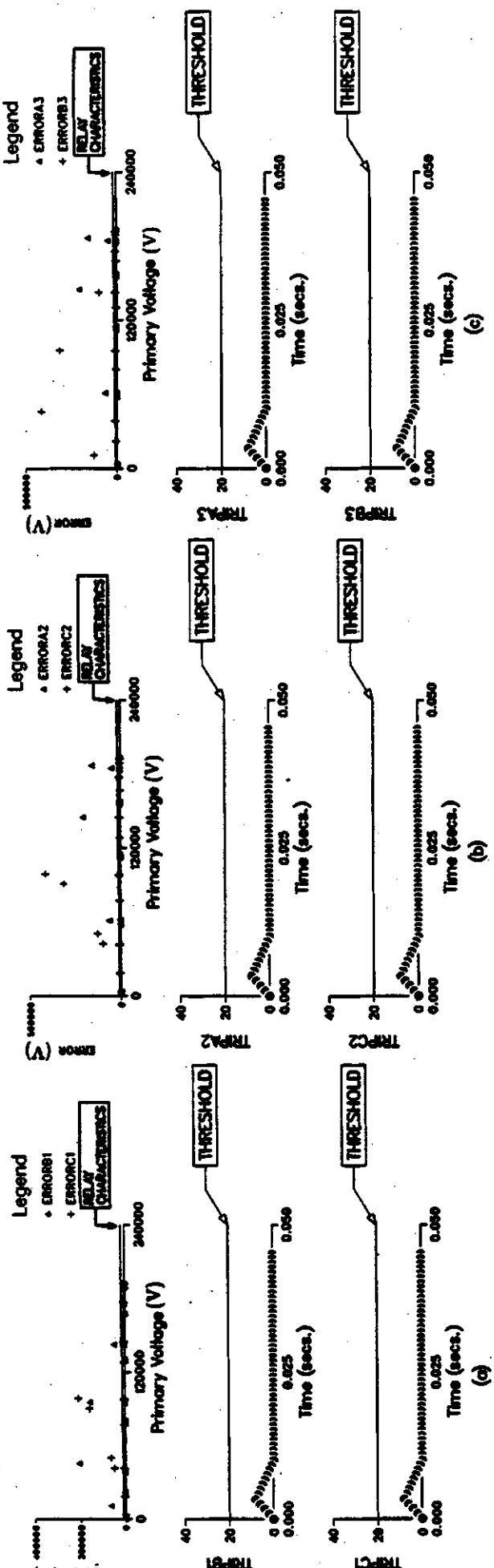

Figure 6.9: Errors and values of the trip indices for a fault external to the delta-wye transformer when (a) phase A, (b) phase B or (c) phase C is used as the "Reference Phase". The fault was applied at time 0.0 s.

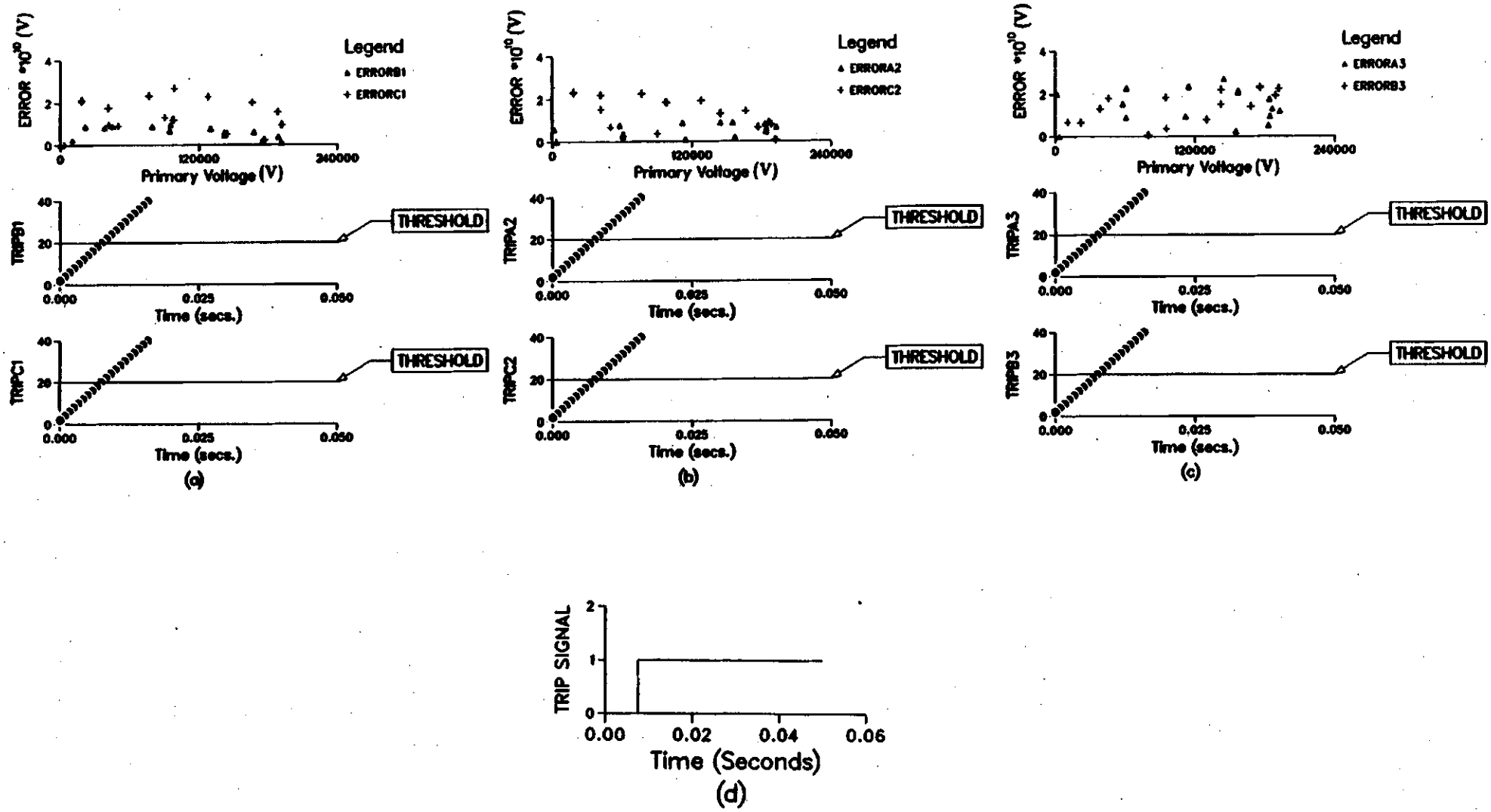

Figure 6.10: Errors and values of the trip indices for an internal fault in the delta-wye transformer when (a) phase A, (b) phase B or (c) phase C is used as the "Reference Phase". (d) Trip command issued by the algorithm vs time. The fault was applied at time 0.0 s.

TRIPA3, ERRORB3 and TRIPB3. The decision-logic module correctly identified it as an internal fault and issued a trip command in about 8 ms as shown in Figure 6.10(d).

6.5. Comparison of Version-I and Version-II

Version-I and Version-II of the algorithms were compared for two aspects, the performance of the algorithms and the computations required for implementing the algorithms on a microprocessor.

Both versions of the algorithms were tested using the same test data. Also, the relay settings while testing the algorithms were the same. Therefore, it is reasonable to compare the results and draw conclusions.

The test results from Version-I and Version-II of the algorithms for a single-phase transformer are presented in Sections 5.4.3 and 6.4.1 respectively. The results show that in both versions, the trip indices remain well below the threshold for magnetizing inrush and external fault conditions. For internal faults, Version-I issued a trip command in about 8 ms to 14 ms whereas Version-II took about 8 ms to 21 ms.

The test results from Version-I and Version-II of the algorithms for a three-phase wye-wye transformer are summarized in Tables 5.4 and 5.5, and 6.1 and 6.2 respectively. These tables show that in both versions, all trip indices remain well below the threshold for magnetizing inrush, overexcitation and external faults. For internal faults, Version-I issued a trip command in about 8 ms to 15 ms whereas Version-II took about 8 ms to 23 ms.

The test results from Version-I and Version-II of the algorithms for a three-phase delta-wye transformer are summarized in Tables 5.6 and 5.7, and 6.3 and 6.4 respectively. These tables indicate that for both versions, all trip indices remain well below the threshold for magnetizing inrush, overexcitation and external faults. For internal faults, Version-I issued a trip

command in about 8 ms to 14 ms whereas Version-II took about 8 ms to 24 ms.

The performance of both versions is comparable for magnetizing inrush, overexcitation, external fault and heavy internal faults. For low-level internal faults, Version-II of the algorithms took more time than Version-I.

The number of additions/subtractions and multiplications required to implement Version-I and Version-II of the algorithms are listed in Table 6.5. This does not include the number of arithmetic operations required to form the trip index/indices and the computations required by the decision-logic module which are identical in both versions. Table 6.5 shows that Version-II requires fewer computations compared to Version-I for protecting single-phase and three-phase transformers. However, if the algorithms are implemented on a faster microprocesor, such as TMS32025, the larger number of additions/subtractions and multiplications in Version-I of the algorithms will not significantly increase the computation time compared to the time which the computations will take if Version-II is implemented.

6.6. Summary

This chapter presents Version-II of the algorithms that can detect winding faults in single-phase and three-phase transformers. These algorithms are conceptually similar to those of Version-I except that the resistances of the transformer windings are neglected while developing these algorithms. Also, the rectangular rule is used to perform numerical integrations.

The algorithms were tested using the data used to test Version-I. The test results are presented in the chapter. The results show that the algorithms do not issue trip commands during magnetizing inrush, overexcitation and external faults. However, the algorithms issue trip commands for internal faults in about 8 ms to 23 ms depending on the type and severity of the fault.

Table 6.5: Number of arithmetic operations required to implement Version-I and Version-II of the algorithms.

Algorithm for protection of	No. of add/subtract operations for		No. of multiply operations for	
	Version-I	Version-II	Version-I	Version-II
Single-phase transformer	7	5	8	6
Three-phase wye-wye transformer	21	15	24	18
Three-phase delta-wye transformer	42	30	48	36

A comparison of Version-I and Version-II of the algorithms shows that their performances are comparable for magnetizing inrush, overexcitation, external faults and heavy internal faults. However, for low-level faults Version-II takes more time than Version-I. The computation requirements of Version-I are more than the requirements of Version-II. However, if the algorithms are implemented on a faster microprocessor, the computation time requirements of both versions will be approximately equal.

7. DESIGN, IMPLEMENTATION AND TESTING OF THE PROTECTION AND MONITORING SYSTEM

Microprocessor relays for protecting transformers previously reported in the literature are briefly described in Chapter 3. A digital overcurrent relaying algorithm [42, 43] is proposed in Chapter 4. It is demonstrated that the algorithm correctly emulates the time-current characteristics of inverse-time overcurrent relays. Digital algorithms for protecting windings of transformers [46, 47, 50] are proposed in Chapters 5 and 6.

In this work, the proposed algorithms were implemented on a microprocessor-based system for protecting transformers. This chapter describes the design, implementation and testing of the microprocessor-based system for protecting and monitoring single-phase and three-phase transformers [51, 52, 53]. The system includes facilities for detecting winding faults in power transformers and emulates overcurrent relays to protect the transformer in cases of sustained external faults. The system also has spare input channels that can be used to monitor transformer parameters. The performance of the system was tested in the laboratory. Some test results are included in this chapter.

The design requirements of the proposed system are first identified. The design of the hardware and software that meets the specified requirements is then presented. This is followed by a description of implementation and testing procedures.

7.1. Design Requirements

The following design requirements for the system were identified.

1. The system should be suitable for protecting single-phase as well as three-phase transformers without major hardware modification.

2. The hardware should be suitable for implementing the selected algorithms for overcurrent and winding protection of single-phase and three-phase transformers.

3. The system should include a man-machine interface (MMI) for modifying the software and for changing relay settings.

4. The system hardware should be isolated and protected from power system transients.

5. The hardware should be modular permitting replacement of a faulty module in the event of a failure.

7.2. Design Of the System Hardware

The system hardware was designed keeping in mind the requirements outlined in the previous section. Figure 7.1 shows the block diagram of the proposed hardware. It consists of the following three functional blocks.

- Isolation and analog scaling block
- Data acquisition block
- Microcomputer

The isolation and analog scaling block consists of six identical modules for processing voltages and six identical modules for processing currents. A module for processing voltage accepts a signal from an analog type potential transducer. It electrically isolates the system from the power system and scales down the voltage to a level suitable for use in the data acquisition block. A module for processing current accepts a signal from an analog type current transducer. It electrically isolates the system from the power system and scales down the current signal. These modules also convert currents to

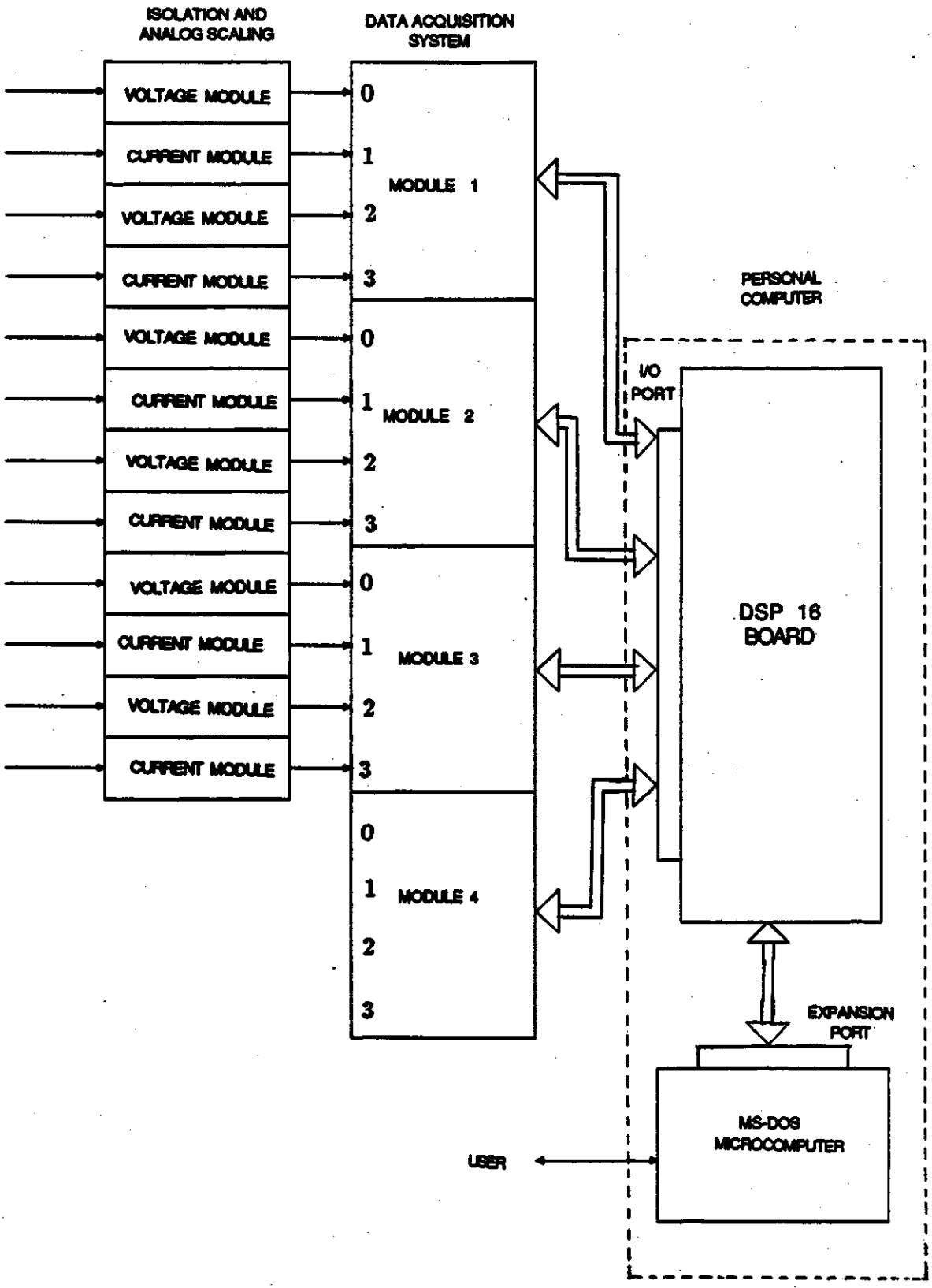

Figure 7.1: A block diagram of the microprocessor-based protection system.

equivalent voltages of levels suitable for use in the data acquisition block because this block accepts voltage inputs only.

The data acquisition block of the system consists of hardware that samples and quantizes signals at a specified rate. This block consists of four identical modules. Each module samples and digitizes four signals; two representing voltages and two representing currents. For three phase transformers, the system is required to sample and digitize six voltages and six currents; therefore, three data acquisition modules are used. The fourth module is spare and, if needed, can be used to monitor transformer parameters, such as, zero sequence current, tap settings, oil level, oil temprature etc.

The microcomputer block of the system consists of a microprocessor board, MS-DOS personal computer, an input/output port and a clock. The input/output port in association with a clock is used to control the data acquisition process. The microprocessor board implements the digital algorithm by processing the acquired signals to determine the condition of the protected transformer. The microprocessor board is interfaced to an MS-DOS personal computer which provides the user interface facility.

This section describes the design of the isolation and analog scaling, data acquisition and microcomputer blocks of the system.

7.2.1. Isolation and analog scaling

Figure 7.2 shows the schematic diagram of a voltage module of the isolation and analog scaling block (I &AS). The hardware includes an auxiliary transformer which performs two functions; it reduces the level of the voltage signal provided by the potential transformer and electrically isolates the hardware from the high voltage power system. The auxiliary transformer used is manufactured by Hammond [54] and can be mounted on a printed circuit board. The transformer can be used for connecting the

primary windings to either 115V or 230V. The output of the transformer is 12.6V. This voltage is further reduced by a potentiometer which is adjusted to provide 3V rms when the input is equal to the rated voltage. A metal oxide varistor (MOV) provided at the input of the auxiliary transformer protects the system hardware from transients in the voltage signals. The MOV (product no. SIOV-S20K250) used in this design is manufactured by Siemens [55]. The varistor has a maximum allowable operating voltage of 250V and a cut-off voltage of 390V. These ratings are compatible with the ratings of the auxiliary transformer.

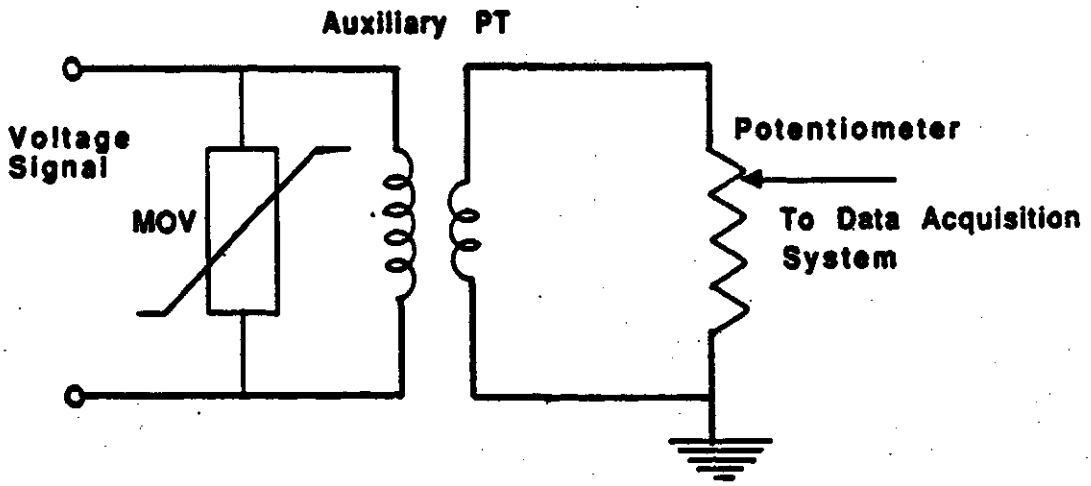

Figure 7.2: The isolation and analog scaling circuit for an input voltage signal.

Figure 7.3 shows the circuit diagram of a module used for processing a current signal. During abnormal operating conditions, a current transformer (ct) can experience primary currents up to 40 times the nominal rating. For 5A ct's, the secondary current could be 200A which corresponds to a peak value of 500A including a full dc offset. Auxiliary ct's with a ratio 100/1 are used. The maximum output of the auxiliary ct is, therefore, 5A. The secondary winding of the auxiliary ct is connected to a one ohm resistor that converts the current signal to an equivalent voltage. A metal oxide varistor connected across the resistor prevents high energy transients from entering

the data acquisition system. The MOV (product no. SIOV-S07K14) used in this design is also manufactured by Siemens [55] and has a maximum allowable operating voltage of 14 volts and a cut-off voltage of 22 volts. These ratings are suitable for protecting the data acquisition system which can withstand up to 15V.

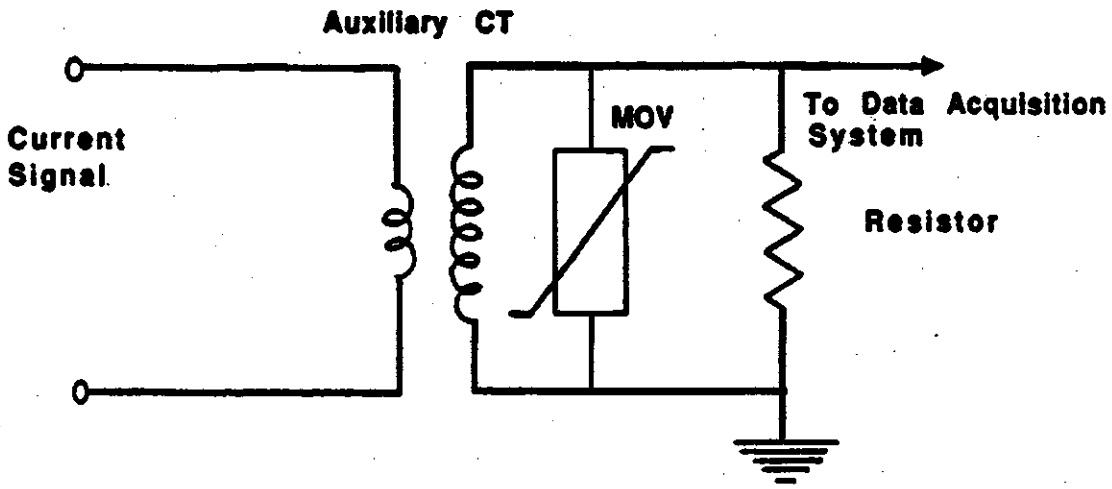

Figure 7.3: The isolation, analog scaling and conversion circuit for an input current signal.

7.2.2. Data acquisition system

The data acquisition system (DAS) is designed as four identical modules. Each module has four input channels for sampling analog signals and converting them to equivalent numbers. The functional blocks of a module of the data acquisition system are shown in Figure 7.4. It consists of four identical channels; each channel has a buffer, an analog filter and a sample and hold amplifier, a multiplexer, another buffer and an analog to digital converter. The four buffers match the impedances of the isolation and analog scaling, and data acquisition blocks. The analog filters attenuate the high frequency components in the inputs. The sample and hold (S/H) amplifiers simultaneously sample the signals. The multiplexer selects under program control the output from one channel at a time and routes it to the

analog to digital (A/D) converter for quantization. The module uses commercially available integrated circuits. This section describes the components used in a module. The control signals required to control the functioning of the data acquisition system are also identified.

The buffer (product no. HA 5033) used in the design is a unity gain buffer manufactured by Harris Corporation [56]. It has an input resistance of 1.5 MΩ and an output resistance of only 5.0 Ω. The filters are National Semiconductor's switched capacitor type (product No. MF10) [57]. These filters do not require external capacitors and inductors. Also, it is possible to select the type of filter (i.e. Butterworth, Bessel, Chevychev etc.) by changing the values of the external resistors. The cut-off frequency of the filters can be set with an accuracy of 3% by changing the frequency of an external clock. Mounts are provided on the board to change the external resistors. The sample and hold unit (S/H) (product No. HA 5320) used in the design is manufactured by Harris Corporation [56]. The unit has a maximum drift rate of 0.5 $\mu V/\mu s$ and a maximum acquisition time of 1.5 μs. The drift rate is important because the signals must be held for the maximum time required to sequentially convert several signals. A short acquisition time and drift rate is selected to ensure that a signal does not change appreciably during acquisition.

The selected analog multiplexer (product N0. HI 508L) is also manufactured by Harris Corporation [56]. The multiplexer can be controlled to route a selected input to the A/D converter. A unity gain buffer (HA5033) is placed between the output of the multiplexer and the input of the A/D converter. This matches the impedances and, thus, avoids the output of the S/H amplifier from collapsing. The A/D converter is of the successive approximation type (product No. HI 774A) manufactured by the Harris Corporation [56]. It provides 12-bit resolution and has a maximum conversion time of 6 μs. It also has the capability of latching the converter output until it is read. This feature is important because the outputs of a number of A/D converters are read into the microcomputer through a single input port.

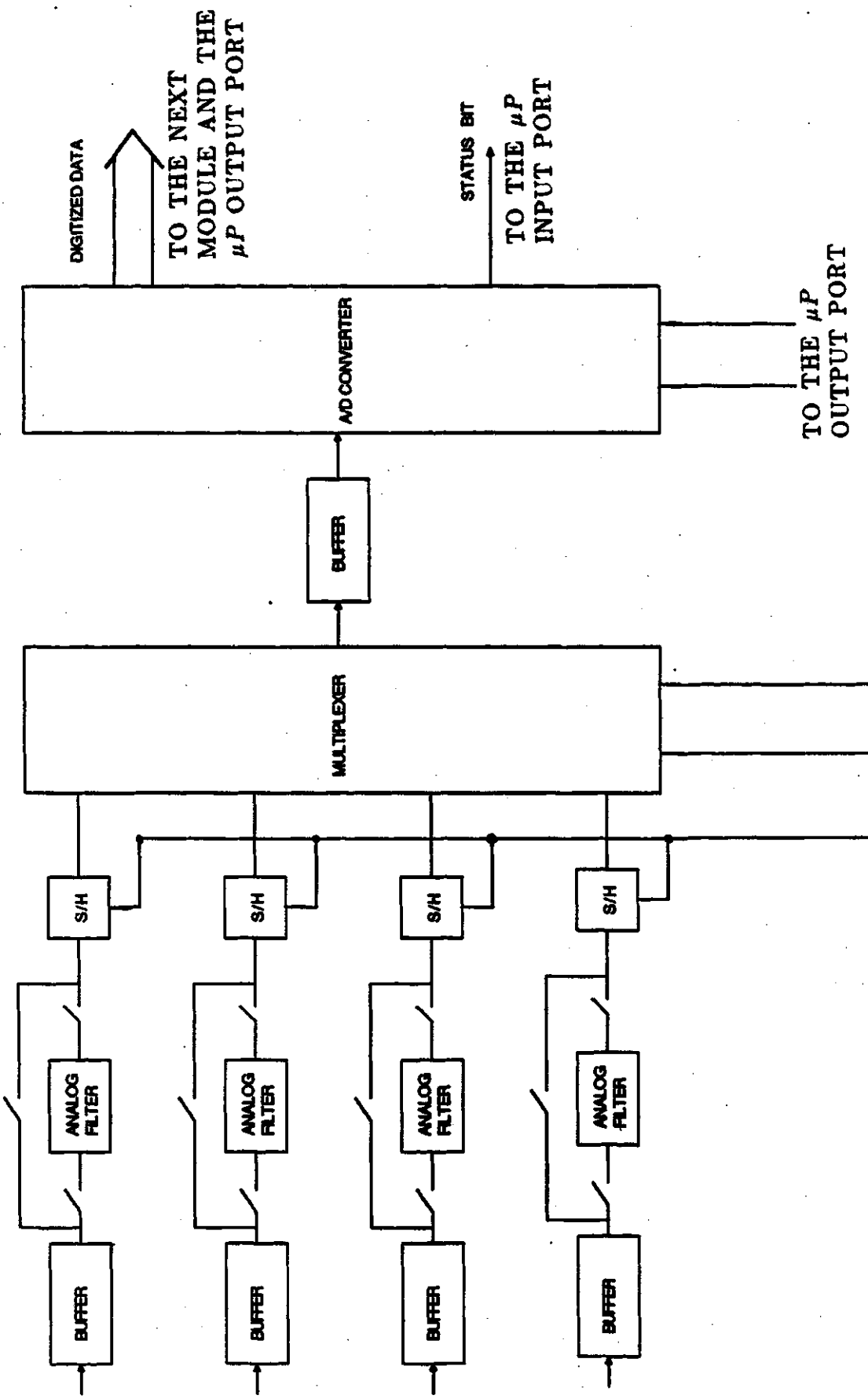

Figure 7.4: A block diagram of the data acquisition module.

The components described above were connected together to form a module of the data acquisition system. A circuit diagram showing the connections of the components in a channel of the module are shown in Figure 7.5. The connections of the multiplexer and the A/D converter of a module of the data acquisition system are shown in Figure 7.6.

The components used in the data acquisition system are controlled by sending signals from an output port of the microprocessor. Also, the status of the A/D converter of each module and the digitized output can be read via an input port. The signals for controlling a module of the data acquisition system are indicated in Figure 7.4. The operation of the S/H amplifiers of a module is controlled by one bit of the output port. This makes sure that all the signals of the module are sampled simultaneously. The multiplexer of a module routes one of the four input signals to the A/D converter, therefore, two bits of the output port are required to select the desired input. The control of the selected A/D converter also requires two bits of the output port; one for starting the analog to digital conversion and the other for enabling the transfer of the quantized data to the input port.

The data acquisition system has four modules and, therefore, sixteen S/H amplifiers, four multiplexers and four A/D converters are to be controlled. All the S/H amplifiers are controlled by one bit of the output port. This makes sure that all the signals are sampled simultaneously. Two bits of the output port are used to control the four multiplexers. The control of A/D converters requires eight bits of the output port, two bits for each A/D converter. This was necessary so that the outputs of the A/D converters can be read sequentially via the input port. Twelve lines of the input port are required to read the digitized data into the microprocessor memory. One line is required to monitor the status of an A/D converter. Since there are four A/D converters in the data acquisition system, four lines of the input port are needed to monitor the A/D converters. The I/O signals requirements of the data acquisition system are summarized in Table 7.1. These

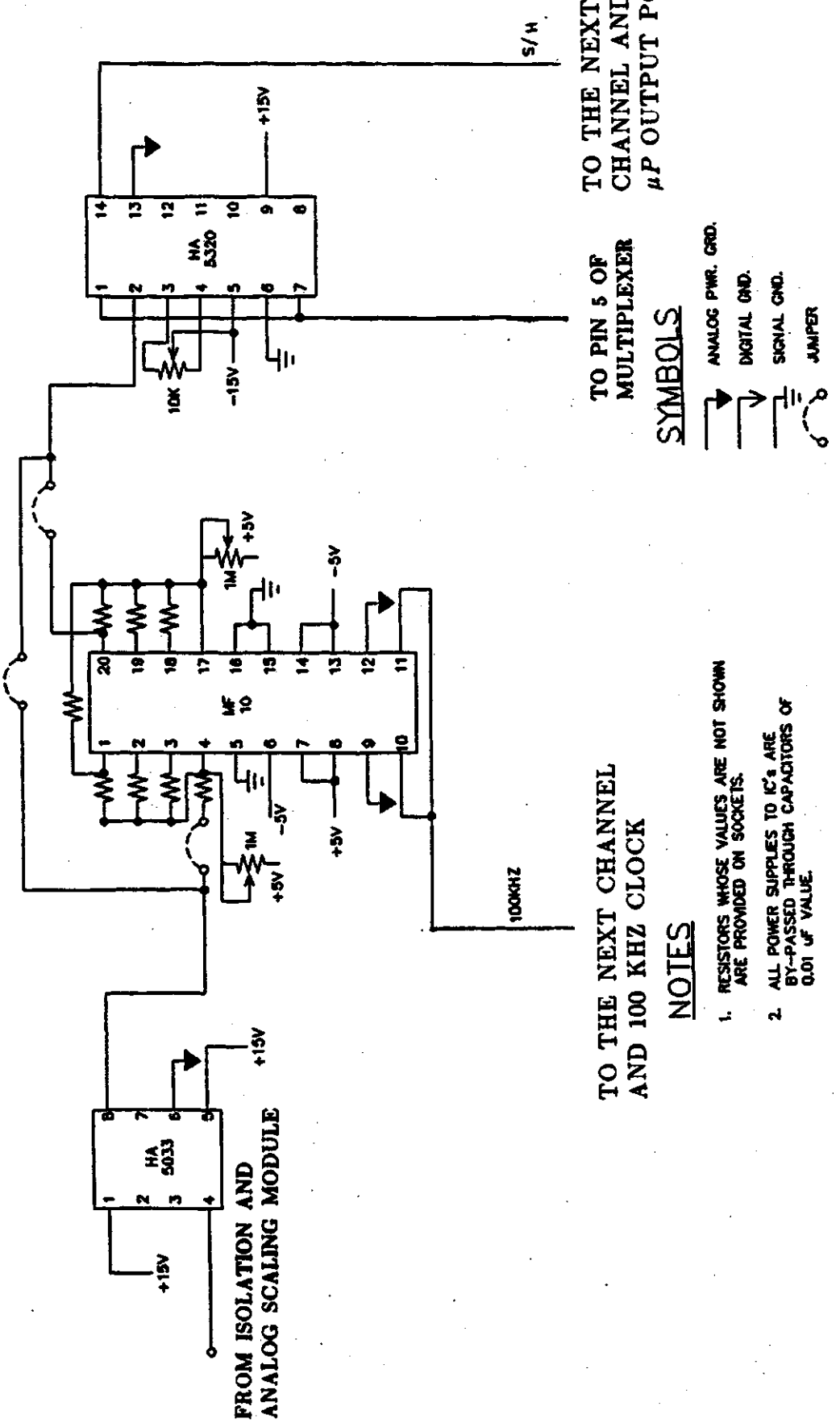

Figure 7.5: A circuit diagram showing the connections of the buffer, analog filter and sample and hold components of a channel of the data acquisition system.

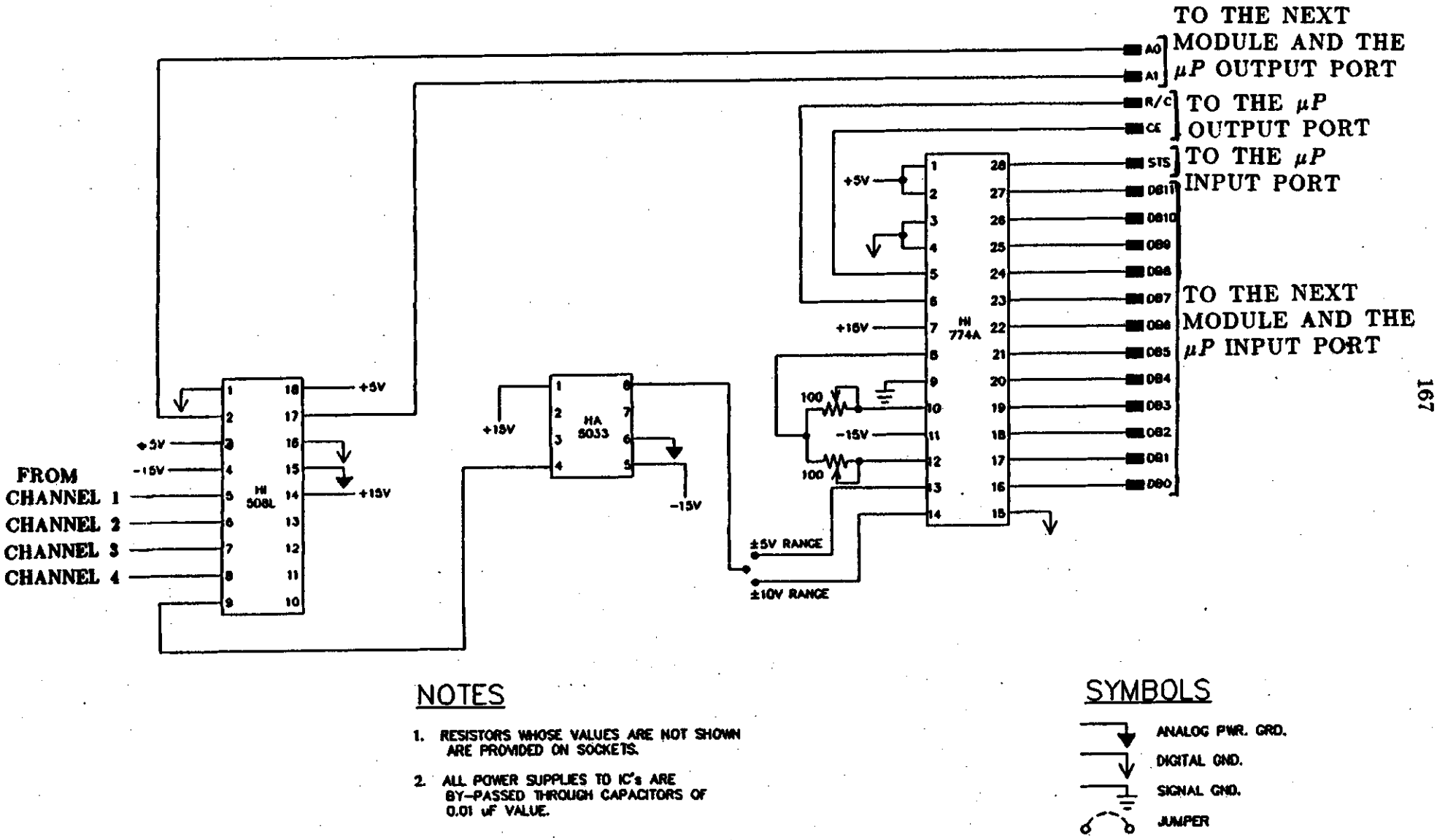

Figure 7.6: A circuit diagram showing the connections of the multiplexer and A/D converter of a module.

requirements indicate that it is possible to control the data acquisition system using a 16-bit input/output port.

Table 7.1: A list of the Input/Output signals for the data acquisition system.

Control signal	Component	Number of bits
Signals from the output port	S/H Amplifiers	1
	Multiplexers	2
	A/D converters	2x4
Signals to the input port	A/D converter output	12
	A/D converter status	1x4

7.2.3. Microcomputer

A DSP-16 microcomputer board [58] based on the Texas Instruments digital signal processor, TMS32025, [59] was selected for use in this design. In addition to its digital signal processing capabilities, the DSP-16 provides the following facilities.

- A program development system
- 16 K-words of zero wait state program/data memory
- A 16-bit programmable timer

Also, the control and data buses of the DSP-16 are accessible for interfacing other peripherals to the board. In this work, a piggy back input/output (I/O) board was designed for interfacing the DSP-16 board with the data acquisition system and the power system. Appendix E gives a circuit diagram of the I/O board and details of its interconnection with the DSP-16 board

and the data acquisition system. The output port of the I/O board controls the operation of the data acquisition system and outputs the trip signal generated by the relay. The input port is used to bring the A/D converter outputs into the memory of the DSP-16 board. A 16-bit programmable timer provided in the DSP-16 is used to control the sampling of the input signals. The DSP-16 board is interfaced to the expansion port of an MS-DOS personal computer. This provides

1. control of the operation of the DSP-16 board from the personal computer,

2. access to the program development system of the DSP-16 board through the personal computer and

3. a man-machine interface to the system for modifying the software, providing relay settings and uploading the relay signals for further analysis.

7.3. The System Software

The software used in the system is divided into two parts, namely the user-interface software and the relaying software. The user interface software is written in the Lattice-C programming language. It runs on an MS-DOS personal computer to which the DSP-16 board is interfaced. The user-interface

1. controls the operation of the DSP-16 board by placing appropriate signals on the expansion port of the personal computer.

2. downloads the relaying software and relay settings into the memory of the DSP-16 microcomputer and

3. uploads data (results of the computations by the relaying software) from the memory of the DSP-16 board to the memory of the personal computer for further analysis.

The relaying software is written in the assembly language of the TMS32025 digital signal processor. This software is divided into two parts; data acquisition software and application software. This section describes the functions performed by the data acquisition and application software.

7.3.1. Data acquisition software

The data acquisition software controls the operation of the data acquisition system which samples and quantizes voltage and current signals at a prespecified rate. When the system is used to protect a single-phase transformer, the data acquisition system acquires only four signals; two voltages and two currents. However, for three-phase transformers, it acquires twelve signals; six voltages and six currents. The data acquisition software is in two packages. The first package is used to acquire signals when Version-I of the algorithms is used for winding protection of transformers. The second package is used if Version-II of the algorithms is used. The first package performs the following functions.

1. Enable the software interrupt capability of the TMS32025 timer.
2. Load the timer with a number to produce interrupts at specified intervals of time.
3. Wait for the timer to generate an interrupt. Proceed to step 4 on the generation of an interrupt.
4. Send a signal to the S/H amplifiers to hold their input signals.
5. Wait for about 5 μs to allow settling of the charge on the capacitors of the S/H amplifiers.
6. Send a control signal to the multiplexers to select the first channel for providing inputs to the A/D converters.
7. Start A/D conversion by sending a start pulse to the A/D converters.
8. Poll the A/D converters to which start pulse was given to determine if they have completed the conversions.
9. If they have, proceed to step 10, otherwise revert to step 8.
10. Enable the outputs of the A/D converter of the first module. Read and store the digital output in the memory of the DSP-16 board. Proceed to step 11.
11. Enable the outputs of the A/D converter of the second and third

modules respectively. Read the digital outputs and store the numbers in the memory of the DSP-16 board.

12. Select the second channel of the multiplexers for input to the A/D converters and repeat steps 7 to 11.

13. Perform the operations listed in step 12 using the third and then the fourth channel of the multiplexers.

14. Send a signal to the S/H amplifiers to track their input signals.

15. Revert to step 3.

In this manner, the data acquisition software acquires signals at a specified rate and stores them in specified memory locations of the DSP-16 board for use by the application software.

Version-II of the algorithms requires that the voltages and currents should be sampled in such a way that their sampling instants are offset from each other by one half sampling interval. The second package of the data acquisition software performs the following functions to achieve this.

1. Enable the software interrupt capability of the TMS32025 timer.

2. Load the timer with a number to get interrupts at intervals equal to one half of intersampling time.

3. Set the value of a variable, FLAG to one.

4. Wait for the timer to generate an interrupt. Proceed to step 5 on the generation of an interrupt.

5. Send a signal to the S/H amplifiers to hold their input signals.

6. Wait for about 5 μs to allow the signals held by S/H amplifiers to settle.

7. Check if FLAG is one; if it is, proceed to step 8, otherwise proceed to step 17.

8. Send a control signal to the multiplexers to select the first channel for providing inputs to the A/D converters.

9. Start A/D conversion by sending a start pulse to the A/D converters.

10. Poll the A/D converters to determine if they have completed the conversions.

11. If they have, proceed to step 12, otherwise revert to step 10.

12. Enable the outputs of the A/D converter of the first module. Read and store the digital output in the memory of the DSP-16 board. Proceed to step 13.

13. Enable the outputs of the A/D converter of the second and third modules respectively. Read the digital outputs and store the numbers in the memory of the DSP-16 board.

14. Select the third channel of the multiplexers for input to the A/D converters and repeat steps 9 to 13.

15. Send a signal to the S/H amplifiers to track their input signals.

16. Reset the variable, FLAG to zero and revert to step 4.

17. Send a control signal to the multiplexers to select the second channel for providing inputs to the A/D converters.

18. Start A/D conversion by sending a start pulse to the A/D converters.

19. Poll the A/D converters to determine if they have completed the conversions.

20. If they have, proceed to step 21, otherwise revert to step 19.

21. Enable the outputs of the A/D converter of the first module. Read and store the digital output in the memory of the DSP-16 board. Proceed to step 22.

22. Enable the outputs of the A/D converter of the second and third modules respectively. Read the digital outputs and store the numbers in the memory of the DSP-16 board.

23. Select the fourth channel of the multiplexers for input to the A/D converters and repeat steps 18 to 22.

24. Send a signal to the S/H amplifiers to track their input signals.

25. Set the variable, FLAG to one and revert to step 4.

In this manner, the data acquisition software acquires signals at a specified rate and stores them in specified memory locations of the DSP-16 board for use by the application software.

7.3.2. Application software

The application software includes two packages. The first package is the overcurrent relaying software that implements the overcurrent relay algorithm of Chapter 4 and protects the transformer in cases of external faults. The second is the transformer winding protection software that implements the digital algorithms described in Chapters 5 and 6 for detecting winding faults in power transformers. The software uses quantized samples of voltages and currents acquired by the data acquisition system. The description and functions performed by the overcurrent relaying software and the transformer winding protection software are given in this section.

7.3.2.1. Overcurrent relaying software

This software implements the overcurrent relaying algorithm described in Chapter 4. The software consists of two programs. The first program performs off-line functions listed in Section 4.4.4.1 and the second program performs on-line functions listed in Section 4.4.4.2.

The program that performs off-line functions calculates the operating time, t_r, of the selected relay at a specified time dial setting and different current multiples by using Equation 4.1 and the information stored in the microprocessor memory. The stored information includes the modelling coefficients of the selected relay and the time dial settings. The modelling coefficients and time dial setting are stored as equivalent integers by multiplying a_0 by 1024, a_1 by 4096, a_2 by 32768, a_3 by 262144, a_4 by 1048576, a_5 by 2097152 and time dial setting by 2. Therefore, Equation 4.1 was implemented by modifying it to

$$t_r = a_0+(1/8)TDS\{a_1+(1/16)TDS[a_2+(1/16)TDS\{a_3 +(1/8)TDS[a_4+(1/4)TDS(a_5)]\}]\}. \quad (7.1)$$

The program calculates the operating time by evaluating Equation 4.1 backwards. This means that value of $a_5 \times TDS$ is first computed and the result is divided by 4. The resultant value is added to a_4. This procedure is continued until the operating time is obtained. The procedure avoids the division by large numbers. After calculations of the operating time, the program computes the values of $K\Delta T/t_r$ and stores them in a look-up table for use by the program that performs on-line computations. The values of K and ΔT used in this work were 70,562,000 and 1/1200 s respectively.

The program that performs on-line computations has two packages. The first package is used for protection of single-phase transformers. It uses the look-up table of $K\Delta T/t_r$ values, the user-specified value of the pick-up current and the quantized samples of the primary current. It performs steps 1 to 12 described in Section 4.4.4.2. The second package is applicable for protection of three-phase transformers. It contains three modules. The first module uses the look-up table of $K\Delta T/t_r$ values and the quantized samples of the primary current of phase A. It performs steps 1 to 12 described in Section 4.4.4.2. The second and third modules use line currents of phases B and C and perform functions similar to those performed by the first computing module.

7.3.2.2. Winding protection software

This software implements the proposed digital algorithms for protecting power transformers. The details of the algorithms are provided in Chapters 5 and 6. The software uses quantized samples of voltages and currents acquired by the data acquisition system. The software contains three packages, one each for protecting single-phase, three-phase wye-wye and three-phase delta-wye transformers.

The software for the protection of a single-phase transformer performs the steps listed in Section 5.2.1. The software for protecting a three-phase wye-wye connected transformer performs the steps listed in Section 5.3.1.1. The organization of the software for protecting a three-phase delta-wye transformer is shown in Figure 7.7. It consists of four modules, the first, second and third computing modules and a decision-logic module. Each module performs the steps described in Section 5.3.2.1.

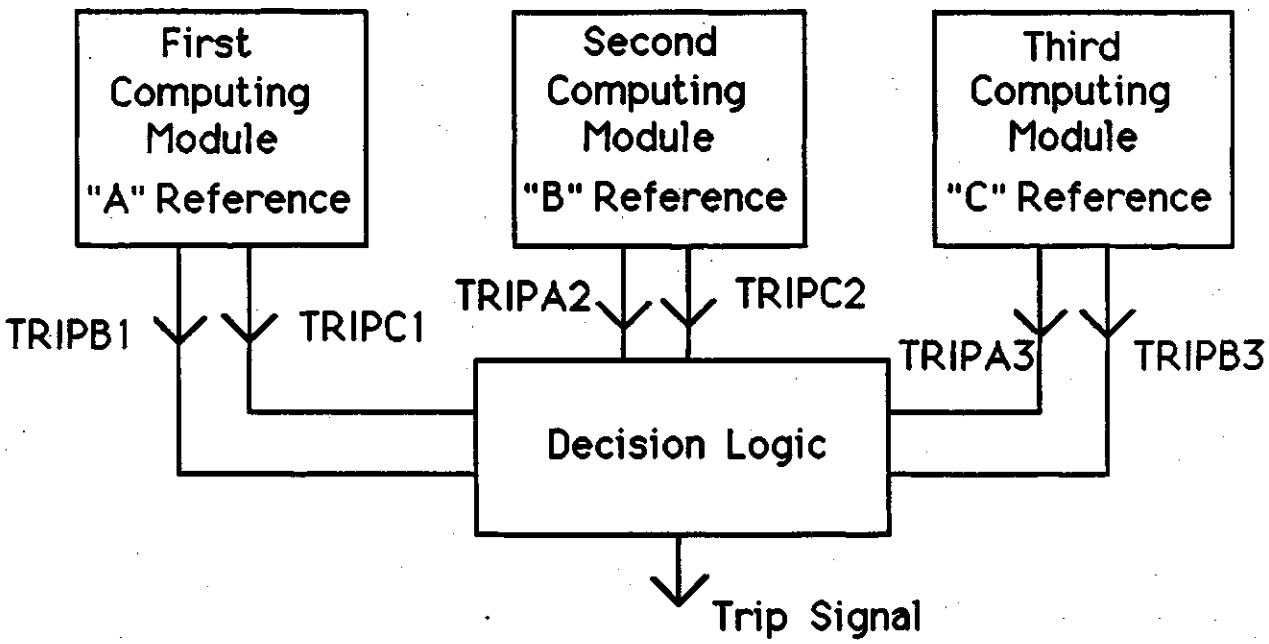

Figure 7.7: Organization of the application software.

7.4. Testing the Protection System

The proposed microprocessor-based system was implemented and tested in the laboratory. The isolation and analog scaling and data acquisition system were implemented on printed circuit boards. Isolation and analog scaling and data acquisition blocks, and the microcomputer were connected together to form the system. The isolation and analog scaling block and the data acquisition block of the relay were calibrated and their transformation ratios were determined. For a voltage channel, a voltage signal of known

magnitude was applied to the voltage processing module of the isolation and analog scaling block and its output was measured to verify that the voltage processing module functions properly. This output signal was applied to the corresponding channel of the data acquisition system and a test program converted it to an equivalent digital number and recorded it. This procedure was repeated to calibrate all voltage channels of the relay.

For a current channel, a current signal of 100A obtained from F1 Test System manufactured by the Doble Engineering Company [60] was injected into the current processing module of the isolation and analog scaling block and its output was measured to verify that the current processing module functions properly. This output signal was then applied to the corresponding channel of the data acquisition system and a test program converted it to an equivalent digital number and recorded it. This procedure was repeated to calibrate all current channels of the relay. Table 7.2 lists the calibration results for the voltage and current channels of the relay.

In the software, the digital numbers representing voltages and currents are brought to a common level by using the primary voltage of phase A as the base value, the information from Table 7.2 and the turns ratio of the protected transformer. The resulting numbers are also multiplied by 100 to reduce the effect of truncation errors. This means that 1V is represented by 1048 in the software. The functioning of the hardware and software, and their coordination was checked by using the program development system of the DSP-16 board.

The microprocessor-based system was tested in the laboratory. The performance of the system for providing overcurrent and winding protection was checked. The test procedure and results are described in the following sections.

Table 7.2: Calibration of the isolation and analog scaling, and data acquisition blocks.

Channel description	Value of input signal	Output of I & AS block	Output of DAS block
PHASE A:			
Pri. Voltage	120.2V	3.07V	1258
Current	100.0A	0.239V	98
Sec. Voltage	242.0V	3.04V	1245
Current	100.0A	0.990V	405
PHASE B:			
Pri. Voltage	119.8V	3.00V	1229
Current	100.0A	0.245V	100
Sec. Voltage	241.0V	3.08V	1261
Current	100.0A	0.961V	394
PHASE C:			
Pri. Voltage	120.0V	3.05V	1249
Current	100.0A	0.245V	100
Sec. Voltage	241.0V	3.01V	1232
Current	100.0A	0.941V	385

7.4.1. Testing overcurrent relays

The ability of the system to correctly emulate the characteristics of the Westinghouse CO-7 and CO-9 relays was tested in the laboratory. The testing involved determining the operating times provided by the system and comparing them with the published times. The operating times were determined for six current multiples and different time dial settings. The current multiples were selected to cover the entire range of the relay characteristics.

In this work, F1 Test System manufactured by the Doble Engineering Company [60] was used. This system can provide a maximum of 160A rms

current. The maximum current for which the characteristic of a Westinghouse CO-7 or CO-9 relay is specified is 20 times the pick-up current. The pick-up current was, therefore, set at 8A. The module designated to input the secondary current of phase A was used for applying current to the relay. The output of the DAS was 33 for the current equal to the pick-up value. This number was further multiplied by 32 to reduce the effects of truncations in the relay software.

The relay type, time dial setting and value of the target number, K were input through the user-interface. In the first test, CO-7 relay type, 0.5 time dial setting and a target number 70562000 were selected. A 20A rms current (2.5 times the pick-up value) was applied to the system. The data acquisition software quantized the input at 1200 Hz. The software program used this information to perform on-line functions of the algorithm. The program emulated the selected relay characteristics and issued a trip command after a delay of several sampling intervals after the application of the current. This program recorded the number of sampling intervals which was converted to time by dividing by 1200. The procedure was repeated to determine the operating times for currents of 4.0, 7.0, 10.0, 15.0 and 20.0 times the pick-up value. The operating times were also determined for time dial settings of 1.0, 2.0, 3.0, 4.0, 5.0, 6.0, 7.0, 8.0, 9.0, 10.0 and 11.0. The entire procedure was repeated for the Westinghouse CO-9 relay.

The relay operating times obtained from the tests were compared with the corresponding values read from the published curves and their absolute differences were computed. Tables 7.3, 7.4 and 7.5 list the published operating time, the operating time of the microprocessor-based system, their absolute differences in cycles of 60 Hz and differences as a percentage of the published operating times for the Westinghouse CO-7 relay. Similarly, Tables 7.6, 7.7 and 7.8 list the the published operating time, the operating time of the microprocessor-based system, their absolute differences in cycles of 60 Hz and the differences as a percentage of the published operating time

for the Westinghouse CO-9 overcurrent relay. An analysis of Tables 7.3 to 7.8 indicates that the operating times provided by the designed system are either within two cycles of 60 Hz or within five percent of the corresponding time read from the published curves. This demonstrates that the microprocessor-based overcurrent relays correctly emulate the selected time-current curves.

7.4.2. Testing the transformer protection scheme

The performance of the transformer protection scheme was tested in the laboratory by using a 15 kVA, delta-wye connected 240/480V three-phase transformer. The system used the software developed for protecting three-phase delta-wye transformers. The values of resistances and inductances of the transformer windings were determined experimentally. The procedure and the values are given in Appendix F. The winding resistances are comparable to their inductive reactances and, therefore, can not be neglected. It was, therefore, decided to use the software that implements Version-I of the algorithm for protecting a delta-wye transformer. Also, the analog filters of the data acquisition system were by-passed because it was observed that voltages and currents do not contain significant amounts of high frequency components. However, in actual practice, analog filters will be used to avoid problems due to aliasing.

The designed system sampled the primary and secondary currents and voltages at 4800 Hz. This was done for twenty-three operating conditions that included magnetizing inrush, external fault, internal fault and simultaneous magnetizing inrush and internal fault conditions. Table 7.9 lists the description of each case. The acquired data were converted to data at 1200 Hz by taking every fourth sample. This data was processed by the software. The values of THRES, SLOPE and BNDRY were set at 18340, 0.03 and 52400 respectively. The threshold for the trip indices was set at 20.

Figures 7.8 and 7.9 show the primary line currents, and primary and

Table 7.3: The published operating times, emulated operating times and their differences for the Westinghouse CO-7 relay when the relay current is 2.5 and 4.0 times the pick-up value.

Time dial setting	Operating times and differences for a current multiple of 2.5				Operating times and differences for a current multiple of 4.0			
	PUBT	EMUT	DIFFC	DIFFP	PUBT	EMUT	DIFFC	DIFFP
0.5	0.300	0.310	0.60	3.33	0.200	0.211	0.66	5.50
1.0	0.590	0.592	0.12	0.34	0.395	0.386	0.54	2.28
2.0	1.100	1.152	3.12	4.73	0.750	0.753	0.18	0.40
3.0	1.625	1.676	3.06	3.14	1.095	1.138	2.58	3.93
4.0	2.180	2.212	1.92	1.47	1.500	1.527	1.62	1.80
5.0	2.720	2.765	2.70	1.65	1.875	1.888	0.78	0.69
6.0	3.260	3.340	4.80	2.45	2.250	2.267	1.02	0.76
7.0	3.850	3.941	5.46	2.36	2.630	2.654	1.44	0.91
8.0	4.510	4.574	3.84	1.42	3.020	3.060	2.40	1.32
9.0	5.100	5.236	8.16	2.67	3.430	3.500	4.20	2.04
10.0	5.815	5.929	6.84	1.96	3.950	3.968	1.08	0.46
11.0	6.500	6.646	8.76	2.25	4.450	4.552	6.12	2.29

PUBT - Published operating time in seconds.

EMUT - Emulated operating time in seconds.

DIFFC - Absolute difference between PUBT and EMUT in cycles of 60 Hz.

DIFFP - Absolute difference between PUBT and EMUT in %age of PUBT.

Table 7.4: The published operating times, emulated operating times and their differences for the Westinghouse CO-7 relay when the relay current is 7.0 and 10.0 times the pick-up value.

Time dial setting	Operating times and differences for a current multiple of 7.0				Operating times and differences for a current multiple of 10.0			
	PUBT	EMUT	DIFFC	DIFFP	PUBT	EMUT	DIFFC	DIFFP
0.5	0.165	0.162	0.18	1.82	0.145	0.144	0.06	0.69
1.0	0.300	0.312	0.72	4.00	0.260	0.268	0.48	3.08
2.0	0.580	0.574	0.36	1.03	0.490	0.483	0.42	1.43
3.0	0.825	0.832	0.42	0.85	0.700	0.703	0.18	0.43
4.0	1.070	1.103	1.98	3.08	0.900	0.931	1.86	3.44
5.0	1.370	1.373	0.18	0.22	1.180	1.177	0.18	0.25
6.0	1.670	1.690	1.20	1.20	1.430	1.442	0.72	0.84
7.0	1.950	1.956	0.36	0.31	1.695	1.697	0.12	0.12
8.0	2.250	2.241	0.54	0.40	1.920	1.933	0.78	0.68
9.0	2.530	2.529	0.06	0.04	2.180	2.175	0.30	0.23
10.0	2.850	2.833	1.02	0.59	2.460	2.440	1.20	0.81
11.0	3.225	3.202	1.38	0.71	2.800	2.774	1.56	0.93

PUBT - Published operating time in seconds.

EMUT - Emulated operating time in seconds.

DIFFC - Absolute difference between PUBT and EMUT in cycles of 60 Hz.

DIFFP - Absolute difference between PUBT and EMUT in %age of PUBT.

Table 7.5: The published operating times, emulated operating times and their differences for the Westinghouse CO-7 relay when the relay current is 15.0 and 20.0 times the pick-up value.

Time dial setting	Operating times and differences for a current multiple of 15.0				Operating times and differences for a current multiple of 20.0			
	PUBT	EMUT	DIFFC	DIFFP	PUBT	EMUT	DIFFC	DIFFP
0.5	0.110	0.110	0.00	0.00	0.100	0.105	0.30	5.00
1.0	0.200	0.205	0.30	2.50	0.200	0.205	0.30	2.50
2.0	0.400	0.403	0.18	0.75	0.395	0.393	0.12	0.51
3.0	0.595	0.598	0.18	0.50	0.560	0.579	1.14	3.39
4.0	0.790	0.803	0.78	1.65	0.746	0.776	1.80	4.02
5.0	1.000	1.027	1.62	2.70	0.950	0.983	1.98	3.47
6.0	1.250	1.236	0.84	1.12	1.120	1.172	3.12	4.64
7.0	1.430	1.432	0.12	0.21	1.285	1.333	2.88	3.74
8.0	1.650	1.668	1.08	1.09	1.495	1.503	0.50	0.56
9.0	1.875	1.853	1.32	1.17	1.680	1.778	4.88	4.17
10.0	2.120	2.090	1.80	1.42	1.925	1.983	3.48	3.01
11.0	2.425	2.382	2.58	1.77	2.175	2.271	5.76	4.41

PUBT - Published operating time in seconds.

EMUT - Emulated operating time in seconds.

DIFFC - Absolute difference between PUBT and EMUT in cycles of 60 Hz.

DIFFP - Absolute difference between PUBT and EMUT in %age of PUBT.

Table 7.6: The published operating times, emulated operating times and their differences for the Westinghouse CO-9 relay when the relay current is 2.5 and 4.0 times the pick-up value.

Time dial setting	Operating times and differences for a current multiple of 2.5				Operating times and differences for a current multiple of 4.0			
	PUBT	EMUT	DIFFC	DIFFP	PUBT	EMUT	DIFFC	DIFFP
0.5	0.370	0.333	2.22	10.0	0.165	0.193	1.68	16.9
1.0	0.840	0.883	2.58	5.15	0.330	0.317	0.78	3.94
2.0	1.600	1.610	0.60	0.63	0.660	0.664	0.24	0.61
3.0	2.400	2.382	1.08	0.75	1.000	1.014	0.84	1.40
4.0	3.300	3.221	4.75	2.39	1.360	1.377	1.00	1.23
5.0	4.200	4.109	5.46	2.17	1.710	1.750	2.40	2.34
6.0	5.150	5.168	1.05	0.35	2.100	2.098	0.12	0.09
7.0	6.150	6.183	2.00	0.54	2.490	2.483	0.45	0.30
8.0	7.000	7.124	7.44	1.77	2.850	2.897	2.80	1.64
9.0	*****	*****	****	****	3.300	3.349	2.94	1.48
10.0	*****	*****	****	****	3.800	3.823	1.35	0.59
11.0	*****	*****	****	****	4.250	4.323	4.35	1.71

PUBT - Published operating time in seconds.

EMUT - Emulated operating time in seconds.

DIFFC - Absolute difference between PUBT and EMUT in cycles of 60 Hz.

DIFFP - Absolute difference between PUBT and EMUT in %age of PUBT.

Table 7.7: The published operating times, emulated operating times and their differences for the Westinghouse CO-9 relay when the relay current is 7.0 and 10.0 times the pick-up value.

Time dial setting	Operating times and differences for a current multiple of 7.0				Operating times and differences for a current multiple of 10.0			
	PUBT	EMUT	DIFFC	DIFFP	PUBT	EMUT	DIFFC	DIFFP
0.5	0.090	0.102	0.72	13.3	0.056	0.058	0.12	3.57
1.0	0.180	0.218	2.25	20.8	0.120	0.116	0.24	3.33
2.0	0.340	0.345	0.30	1.47	0.250	0.244	0.36	1.67
3.0	0.500	0.513	0.80	2.60	0.400	0.396	0.24	1.00
4.0	0.690	0.697	0.42	1.01	0.550	0.551	0.06	0.18
5.0	0.880	0.892	0.72	1.36	0.710	0.702	0.48	1.27
6.0	1.075	1.092	1.02	1.58	0.860	0.851	0.54	1.05
7.0	1.290	1.313	1.38	1.78	1.010	1.016	0.36	0.59
8.0	1.500	1.519	1.14	1.27	1.160	1.183	1.38	1.98
9.0	1.750	1.746	0.24	0.23	1.350	1.354	0.24	0.29
10.0	1.950	1.928	1.32	1.13	1.530	1.578	2.88	3.14
11.0	2.200	2.131	4.14	3.14	1.725	1.773	2.88	2.78

PUBT - Published operating time in seconds.

EMUT - Emulated operating time in seconds.

DIFFC - Absolute difference between PUBT and EMUT in cycles of 60 Hz.

DIFFP - Absolute difference between PUBT and EMUT in %age of PUBT.

Table 7.8: The published operating times, emulated operating times and their differences for the Westinghouse CO-9 relay when the relay current is 15.0 and 20.0 times the pick-up value.

Time dial setting	Operating times and differences for a current multiple of 15.0				Operating times and differences for a current multiple of 20.0			
	PUBT	EMUT	DIFFC	DIFFP	PUBT	EMUT	DIFFC	DIFFP
0.5	0.049	0.058	0.54	18.4	0.048	0.050	0.12	4.17
1.0	0.097	0.092	0.30	5.15	0.094	0.091	0.18	3.19
2.0	0.210	0.203	0.42	3.33	0.196	0.198	0.12	1.02
3.0	0.330	0.333	0.18	0.91	0.300	0.319	1.14	6.33
4.0	0.470	0.467	0.18	0.64	0.430	0.445	0.90	3.49
5.0	0.600	0.596	0.24	0.67	0.540	0.572	1.92	5.93
6.0	0.720	0.718	0.12	0.28	0.650	0.693	2.58	6.62
7.0	0.850	0.844	0.36	0.71	0.770	0.818	2.88	6.23
8.0	0.975	0.976	0.06	0.10	0.900	0.942	2.52	4.67
9.0	1.100	1.117	1.02	1.55	1.000	1.048	2.85	4.75
10.0	1.270	1.264	0.36	0.47	1.150	1.167	1.02	1.48
11.0	1.400	1.437	2.22	2.64	1.290	1.302	0.72	0.93

PUBT - Published operating time in seconds.

EMUT - Emulated operating time in seconds.

DIFFC - Absolute difference between PUBT and EMUT in cycles of 60 Hz.

DIFFP - Absolute difference between PUBT and EMUT in %age of PUBT.

Table 7.9: A list of conditions used to test the performance of transformer winding protection system.

Case No.	Description	Test Result (Figure No.)
1-6	Magnetizing inrush.	7.10, G.1-G.5
7.	Internal fault on sec. side that short-circuits phases A and C through a resistance of approx. 1.2 ohms.	7.14
8.	Internal fault on sec. side that short-circuits phase B through a resistance of approx. 1.2 ohms.	7.18
9.	Internal fault on sec. side that short-circuits phases A, B and C through a resistance of approx. 1.2 ohms.	G.6
10.	Transformer switched on with an internal fault on sec. side that short-circuits phase A and B through a resistance of approx. 1.2 ohms.	G.7
11.	Transformer switched on with an internal fault on sec. side that short-circuits phase C through a resistance of approx. 1.2 ohms.	7.17
12.	Transformer switched on with an internal fault on sec. side that short-circuits phases A, B and C through a resistance of approx. 1.2 ohms.	G.8
13.	Internal fault on pri. side that short-circuits phase A through a resistance of approx. 1.2 ohms.	G.9
14.	Internal fault on pri. side that short-circuits phase A and C through a resistance of approx. 1.2 ohms.	G.10
15.	Transformer switched on with an internal fault on pri. side that short-circuits phases A and B through a resistance of approx. 1.2 ohms.	G.11
16.	Internal fault on pri. side that short-circuits phases A and B through a resistance of app. 1.2 ohms.	G.12
17.	Internal fault on sec. side that short-circuits phases B and C through a resistance of app. 1.2 ohms.	G.13
18.	Internal fault on sec. side that short-circuits phase A through a resistance of approx. 1.2 ohms.	G.14
19.	External fault that involves phases A and C.	7.11
20.	External fault that involves phase A and ground.	G.15
21.	Three phase external fault.	G.16
22.	Transformer switched on with an external fault that involves phases A and B.	G.17
23.	Transformer switched on with an external fault that involves phase C and ground.	G.18

secondary voltages recorded by the system during a magnetizing inrush condition. Figure 7.10 shows the performance of the system for this condition. Figures 7.10(a), 7.10(b) and 7.10(c) show the errors and the corresponding trip indices when phase A, B or C is used as the "Reference Phase" respectively. The trip indices do not exceed the threshold and, therefore, the relay does not issue a trip command.

Figure 7.11 demonstrates the performance of the relay for an external fault involving phases A and C. Figures 7.11(a), 7.11(b) and 7.11(c) show the errors and trip indices when phase A, B or C is used as the "Reference Phase" respectively. All trip indices remain less than the threshold value and, therefore, no trip command is issued.

Figures 7.12 and 7.13 show the primary and secondary voltages, and primary line currents for an internal fault on the secondary side that short-circuits phases A and C through a resistance of 1.2 ohms. An examination of the figures show that the secondary voltages of phases A and C drop as soon as the fault is applied. Figure 7.14 shows the performance of the relay for this operating condition. Figures 7.14(a), 7.14(b) and 7.14(c) show the errors and the corresponding trip indices when phase A, B or C is used as the "Reference Phase". The decision-logic module of the relay issued a trip command in about 12 ms after the inception of the fault as shown in Figure 7.14(d).

Figures 7.15 and 7.16 show the primary and secondary voltages, and primary line currents respectively when the transformer is switched on with an internal fault on the secondary side that short-circuits phase C through a resistance of 1.2 ohms. These figures show that primary currents of phases A and C include the fault and magnetizing inrush currents. However, the primary current of phase B has magnetizing inrush current only. Figure 7.17 shows the performance of the relay for this operating condition. Figures 7.17(a), 7.17(b) and 7.17(c) show the errors and the corresponding trip in-

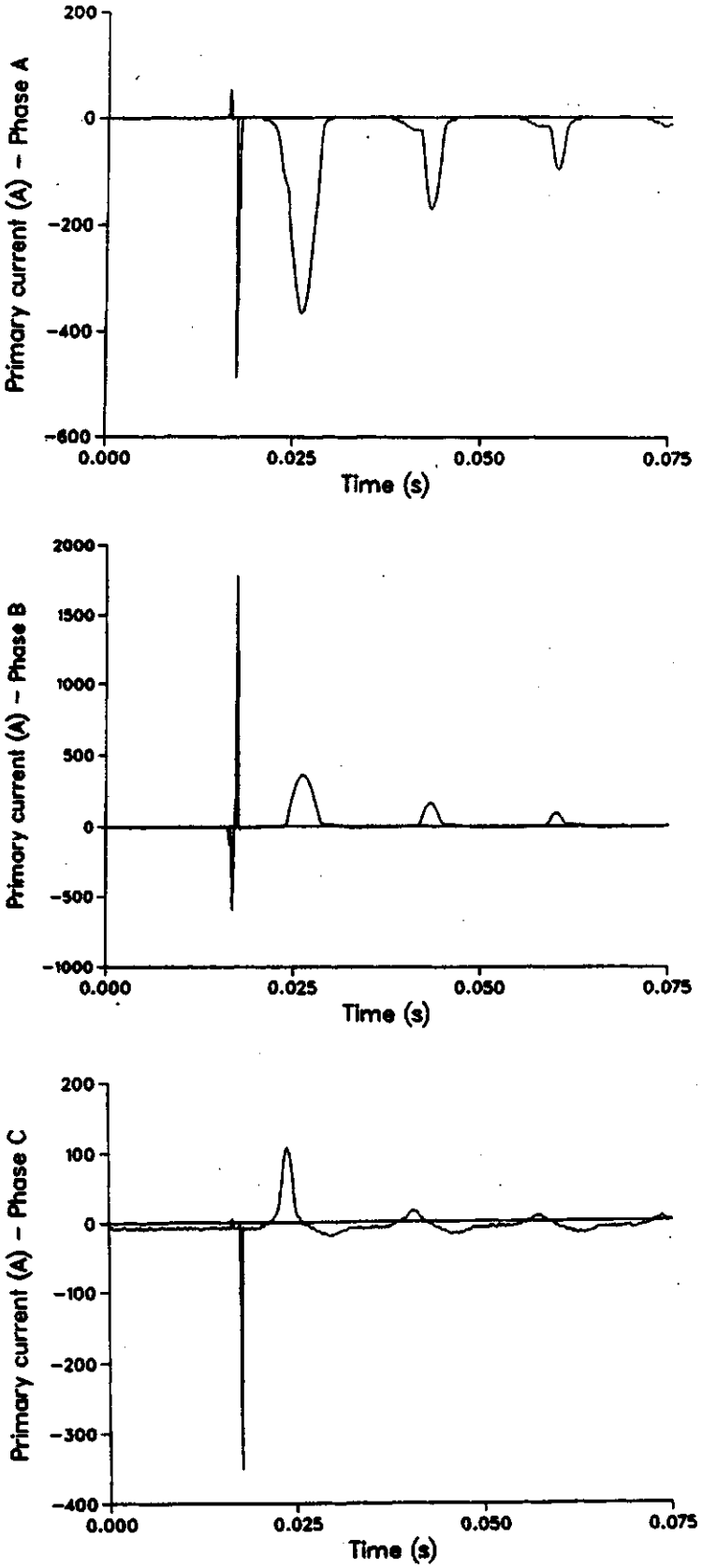

Figure 7.8: Magnetizing inrush currents recorded by the microprocessor-based system. The transformer was connected to the supply at 0.0167 s.

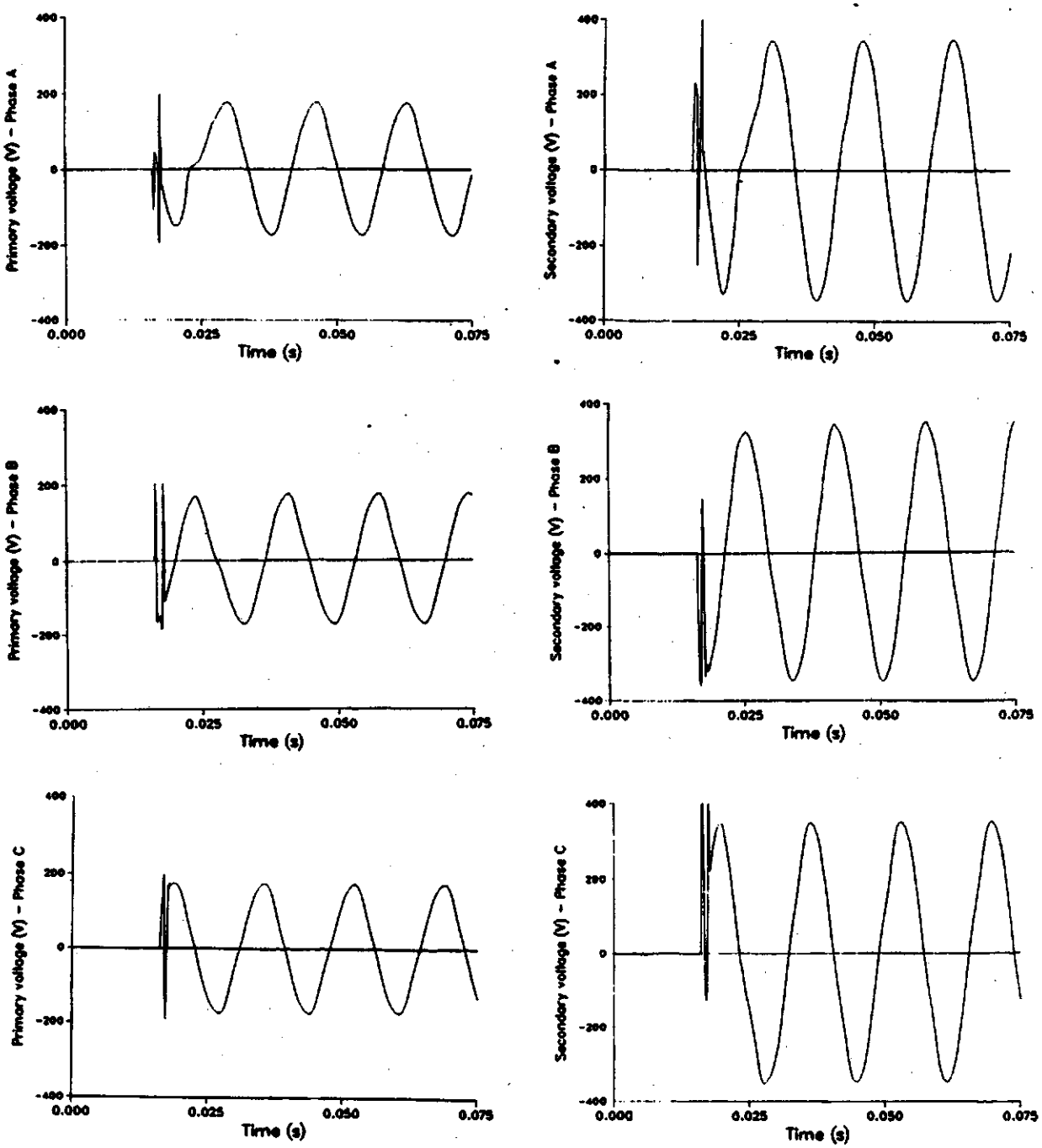

Figure 7.9: The primary and secondary voltages recorded by the microprocessor-based system during a magnetizing inrush condition. The transformer was connected to the supply at 0.0 s.

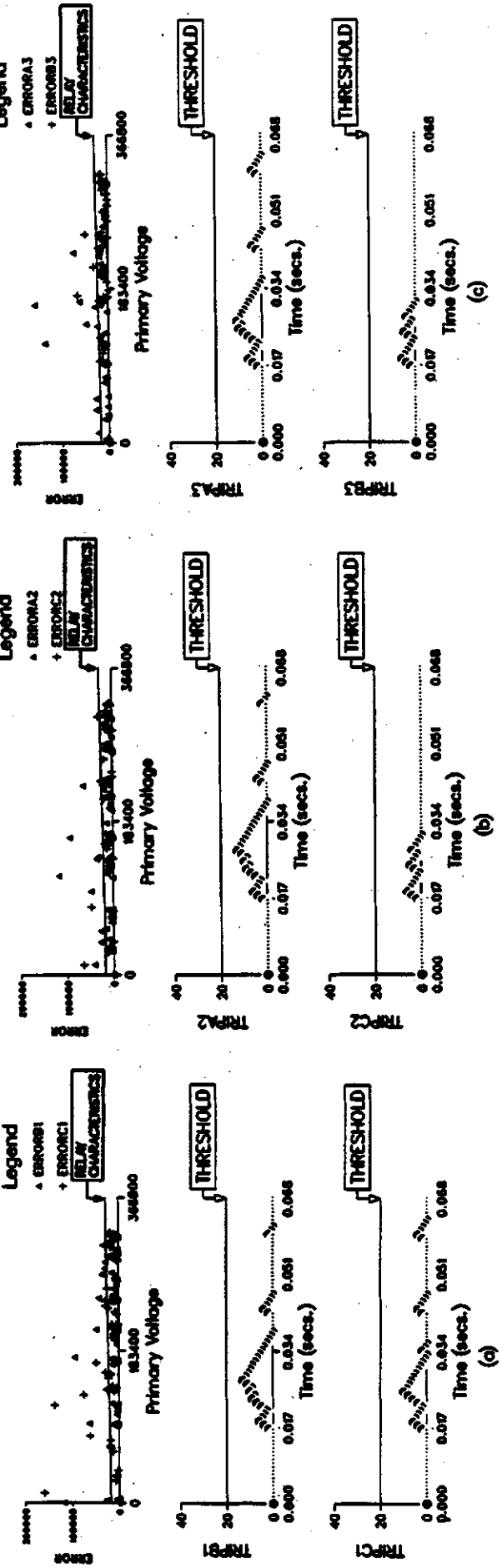

Figure 7.10: Errors and values of the trip indices for a magnetizing inrush condition when (a) phase A, (b) phase B or (c) phase C is used as the "Reference Phase". The transformer was connected to the supply at time 0.0167 s.

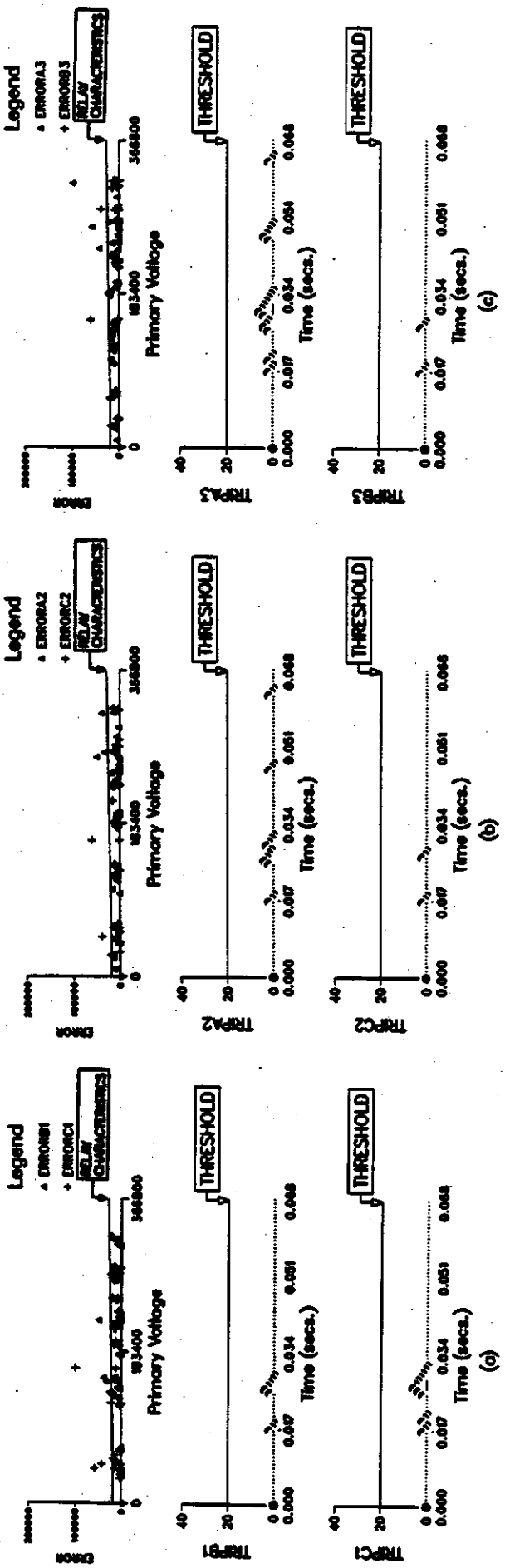

Figure 7.11: Errors and values of the trip indices for an external fault involving phases A and C when (a) phase A, (b) phase B or (c) phase C is used as the "Reference Phase". The fault was applied at 0.0167 s.

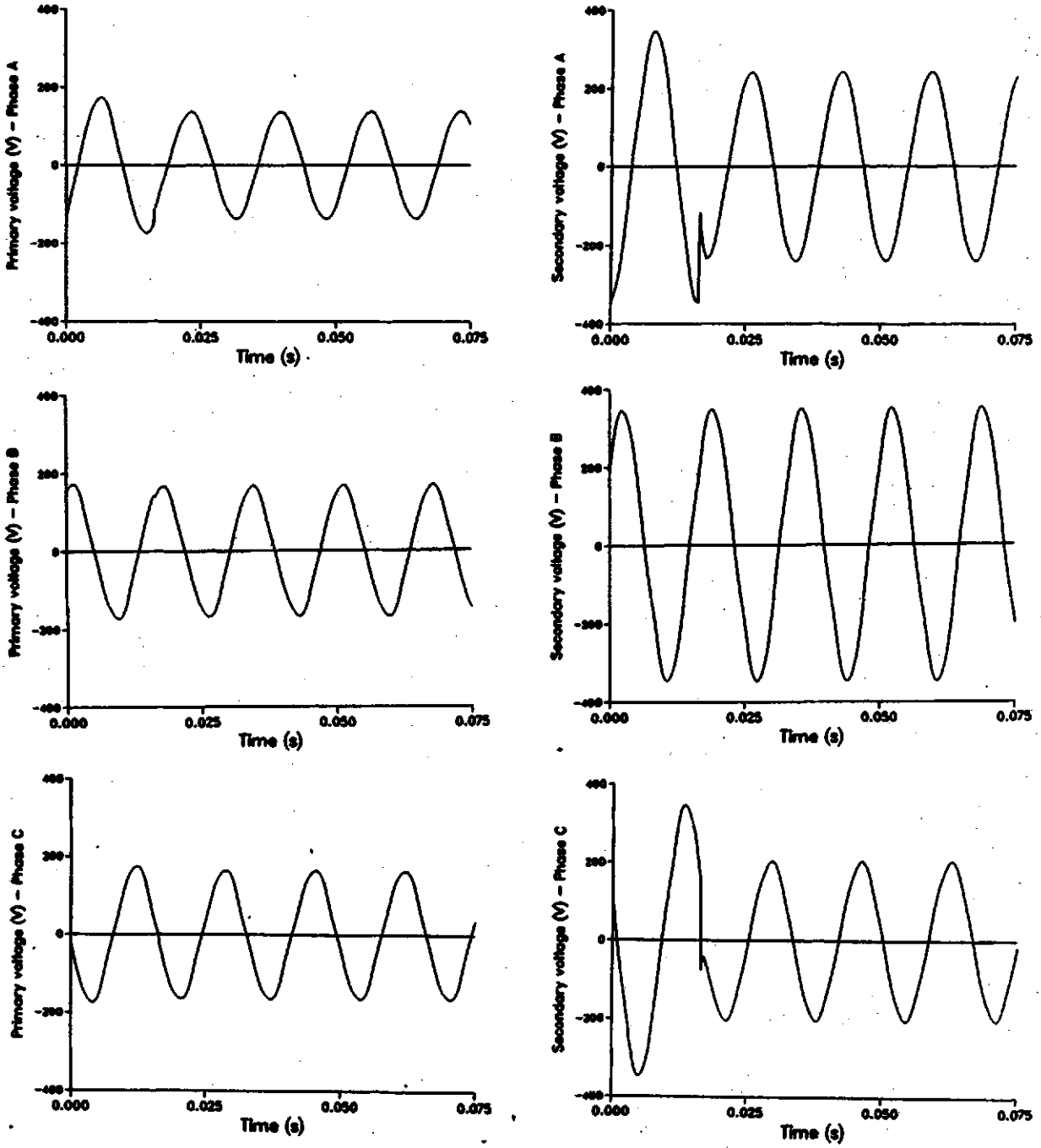

Figure 7.12: The primary and secondary voltages recorded by the microprocessor-based system for an internal fault on the secondary side involving phases A and C. The transformer was connected to the supply at 0.0 s and the fault was applied at 0.0167 s.

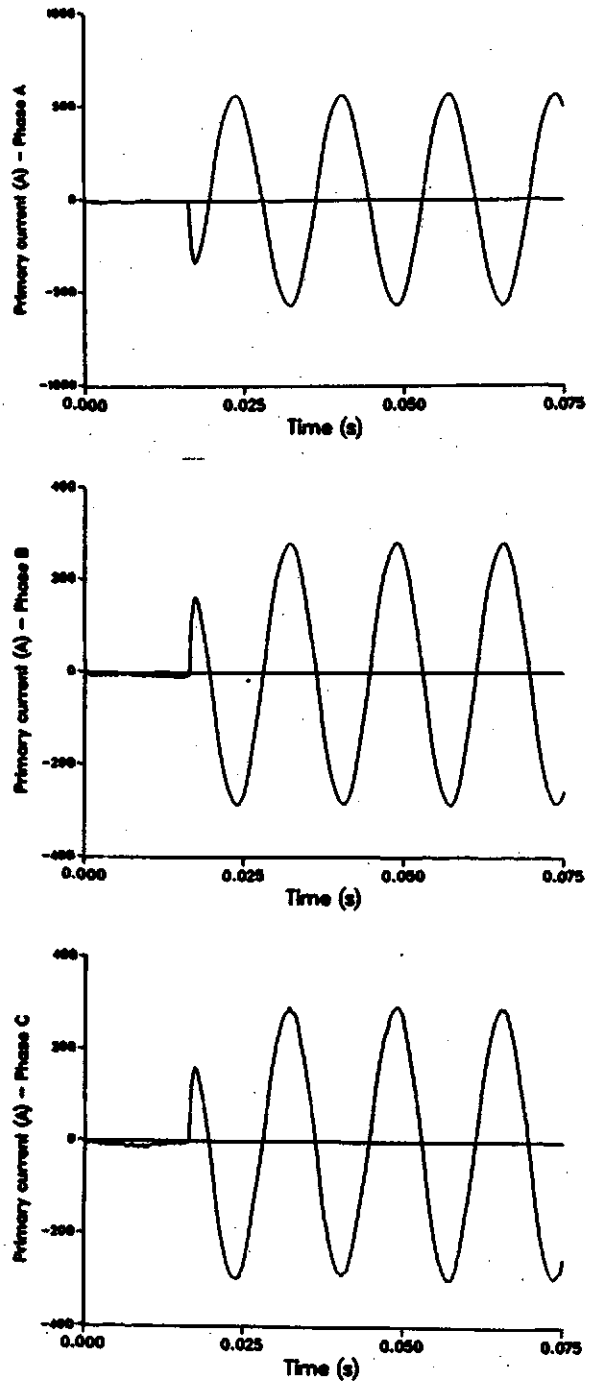

Figure 7.13: The primary currents recorded by the microprocessor-based system for an internal fault on the secondary side involving phases A and C. The transformer was connected to the supply at 0.0 s and the fault was applied at 0.0167 s.

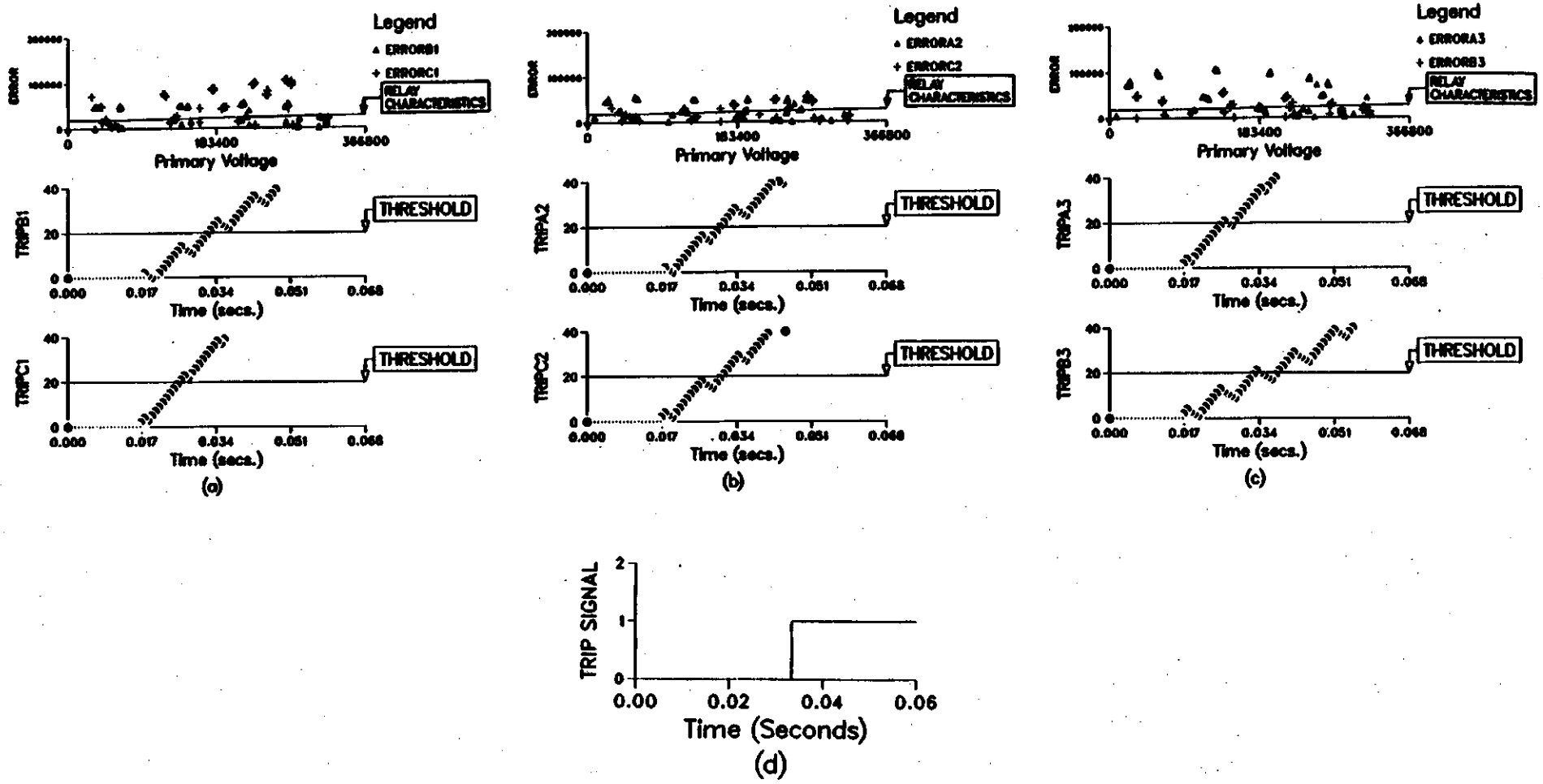

Figure 7.14: Errors and values of the trip indicies for a two-phase internal fault when (a) phase A, (b) phase B or (c) phase C is used as the "Reference Phase". The fault was applied at 0.0167 s.

dices when phase A, B or C is used as the "Reference Phase". The decision-logic module of the relay issued a trip command in about 20 ms after the occurrence of the fault as shown in Figure 7.17(d). This case demonstrates that the system is able to issue trip commands when the transformer is switched on and an internal fault exists.

Figure 7.18 shows the performance of the relay for an internal fault that short circuits the secondary winding of phase B through a resistance of approximately 1.2 ohms. Figures 7.18(a), 7.18(b) and 7.18(c) show the errors and the corresponding trip indices when phase A, B or C is used as the "Reference Phase". The decision-logic module of the relay issued a trip command in about 20 ms after the occurrence of the fault as shown in Figure 7.18(d).

The figures showing the errors, the trip indices and the trip commands for the remaining cases of Table 7.9 are included in Appendix G. An analysis of these figures indicates that all trip indices remain less than the threshold value for magnetizing inrush and external faults. However, for internal faults, some trip indices exceed the threshold value and the software issues trip commands in all cases. The results also demonstrate that the microprocessor-based system also detects faults correctly when internal faults and magnetizing inrush are experienced simultaneously. The average trip time for internal faults varies from about 10 ms to 20 ms depending on the type and severity of the fault.

7.5. Summary

This chapter describes the design, implementation and testing of a microprocessor-based system that detects winding faults in power transformers and emulates overcurrent relays for protecting a transformer from external faults. The transformer winding protection scheme uses digital algorithms that are based on non-linear models of the transformer. It provides fast and accurate detection of internal transformer faults and is suitable for situations

in which it is not possible to measure phase currents in delta connected windings.

Some results obtained from the laboratory testing of the proposed system are presented in this chapter. The results obtained from the testing of the overcurrent protection scheme indicate that the system correctly emulates the Westinghouse CO-7 and CO-9 relays. The winding protection scheme successfully blocks tripping during magnetizing inrush and external faults. It, however, issues a trip command on the occurrence of an internal fault. The trip time for an internal fault varies from 10 to 20 ms depending on the severity and type of the fault.

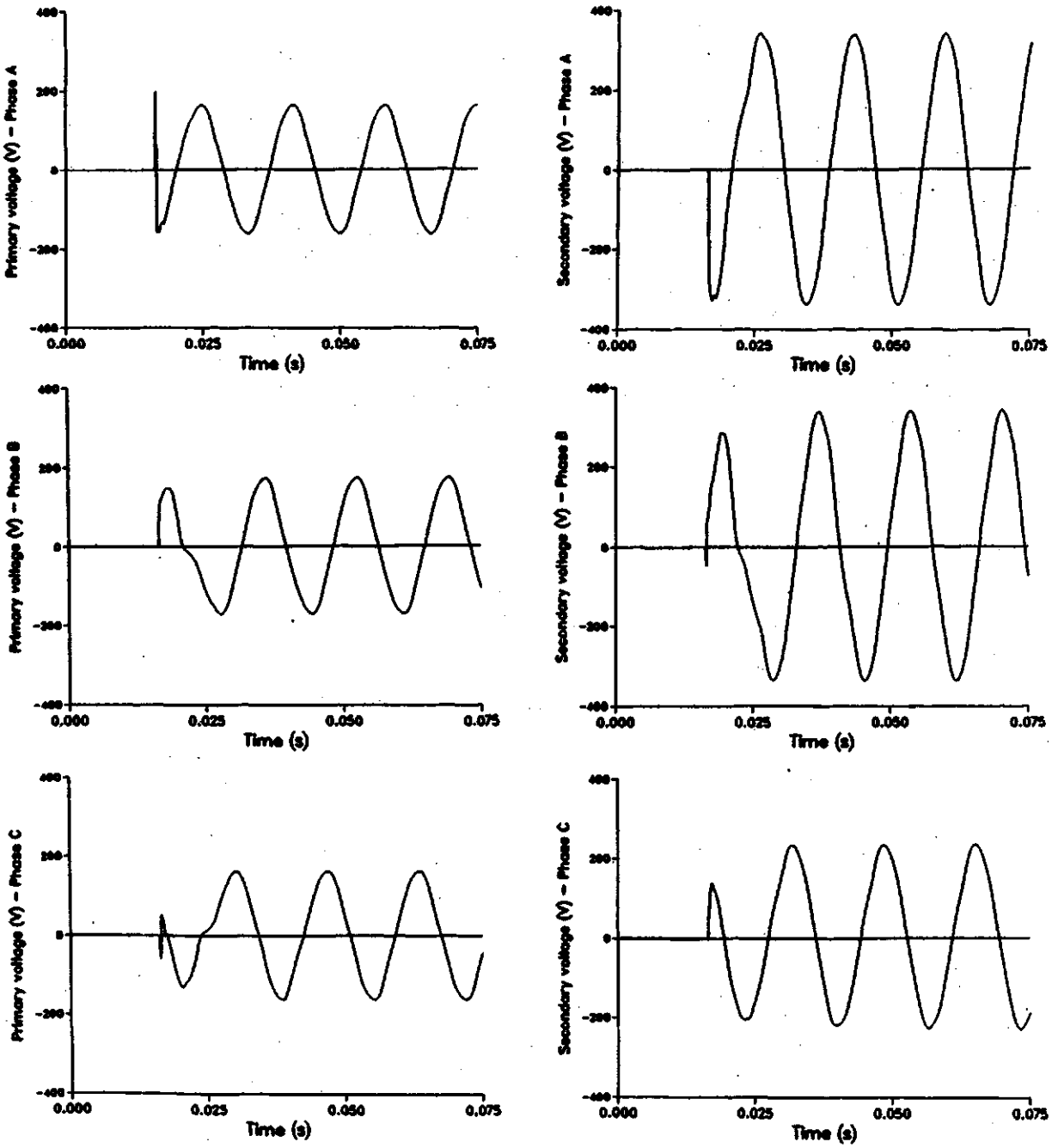

Figure 7.15: The primary and secondary voltages recorded by the microprocessor-based system when the transformer is switched with an internal fault on the secondary side that involves phase C. The transformer was connected to the supply at 0.0167 s.

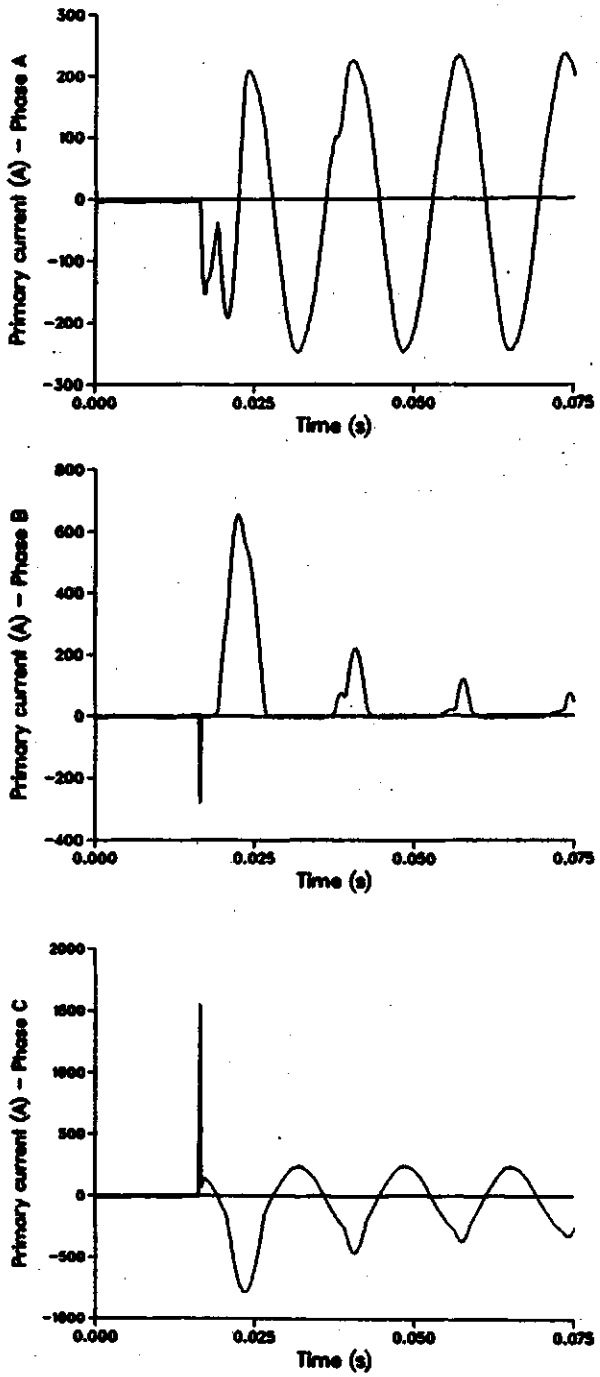

Figure 7.16: The primary currents recorded by the microprocessor-based system when the transformer is switched with an internal fault on the secondary side that involves phase C. Transformer was connected to the supply at 0.0167 s

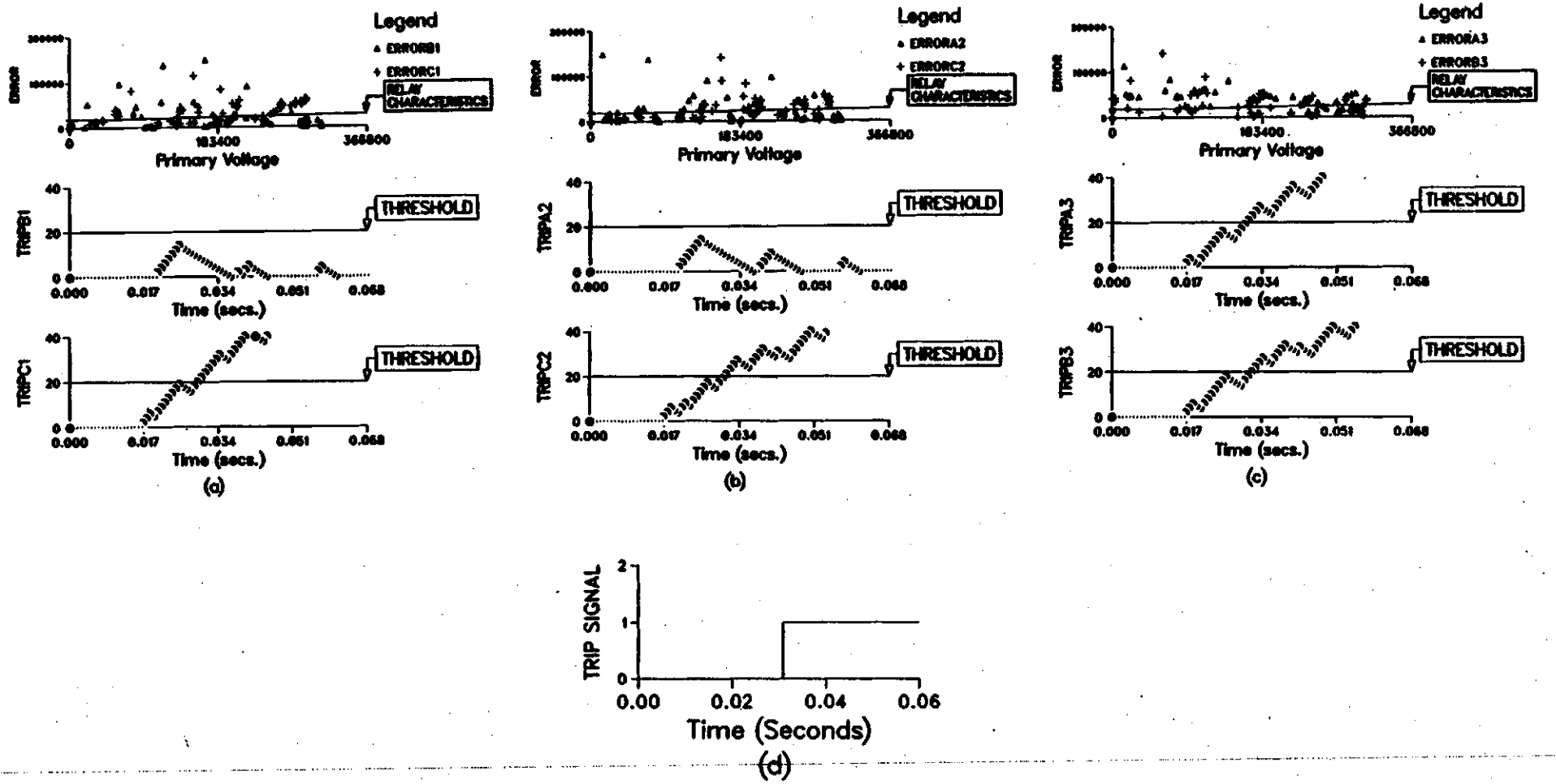

Figure 7.17: Errors and values of the trip indicies when the transformer is switched on with a single phase internal fault when (a) phase A, (b) phase B or (c) phase C is used as the "Reference Phase". The transformer was connected to the supply at time 0.0167 s.

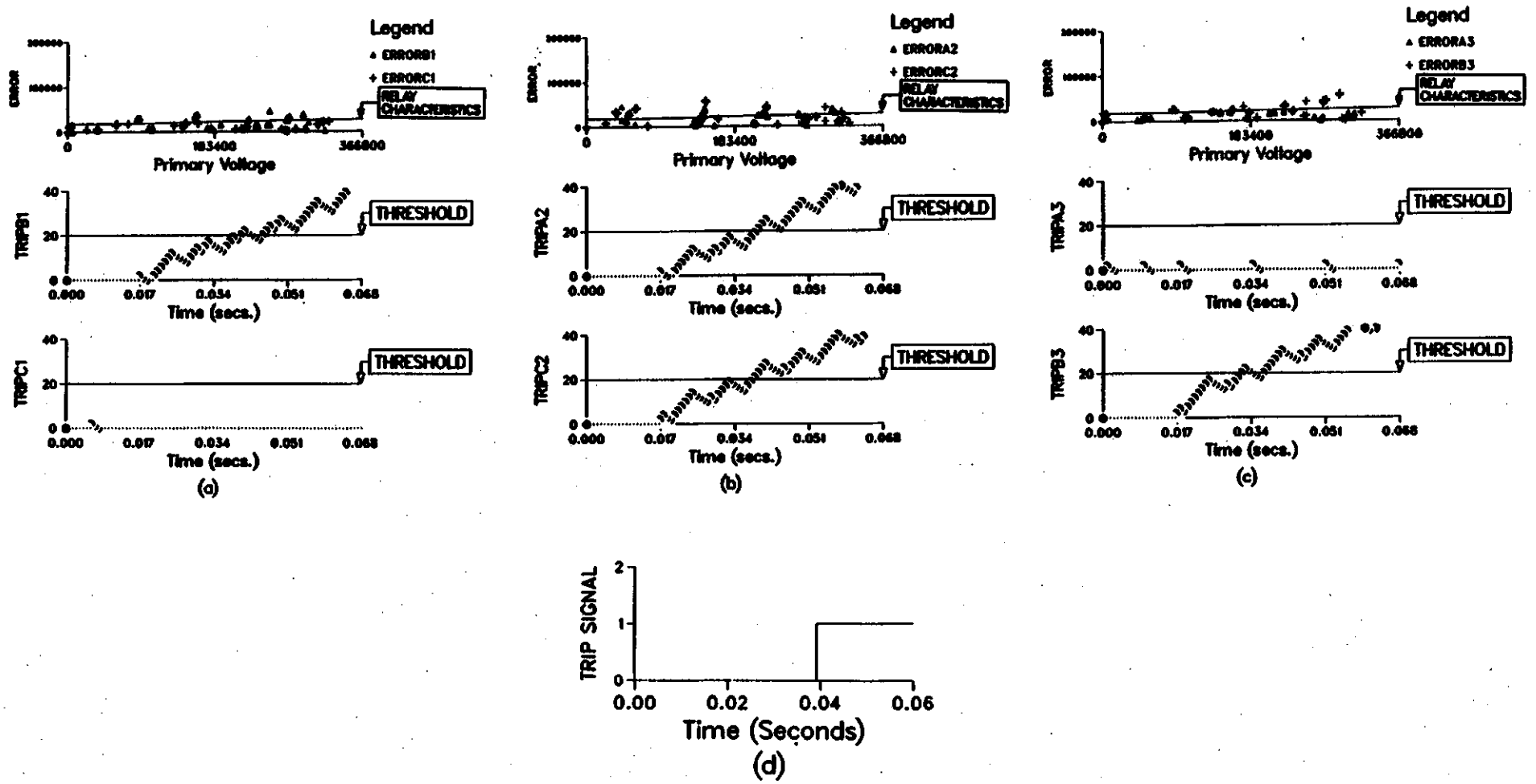

Figure 7.18: Errors and values of the trip indicies for a single phase internal fault when (a) phase A, (b) phase B or (c) phase C is used as the "Reference Phase". The fault was applied at 0.0167 s.

8. SUMMARY AND CONCLUSIONS

8.1. Summary and Conclusions

A power system occasionally experiences faults and abnormal operating conditions. This can cause extensive damage to the equipment in a power system and can result in system instability resulting in major outages to customers. To minimize these effects, the equipment of a power system must be monitored and protected adequately. The first chapter of the thesis has described power system protection concepts and developments leading up to and including the use of microprocessors for monitoring and protection of power system elements. The developments in the area of transformer monitoring and protection using microprocessors has been discussed. Major objectives of the work reported in this thesis were to design, implement and test a microprocessor-based system for the protection of single-phase and three-phase transformers.

Faults affecting transformers are reviewed in Chapter 2. Relays used to detect these faults have also been described. The phenomenon of magnetizing inrush is also described to illustrate the significance of including a restraint feature in a transformer protection relay to avoid trippings during magnetizing inrush conditions. The instruments generally used for measuring and monitoring transformer parameters have also been described in Chapter 2. The present practice of the utilities is to use differential, overcurrent and ground fault relays for protecting transformers. These relays are of either the electro-mechanical or solid-state type. For monitoring transformer parameters, the utilities use electro-mechanical type instruments.

Researchers and designers have made progress in applying microprocessors for protecting and monitoring transformers. A number of digital algorithms for differential, overcurrent and ground fault protection of transformers have been suggested in the past. These algorithms and their limitations are reviewed in Chapter 3. Three microprocessor-based relays for protecting transformers and a recent development in the application of microprocessors for monitoring transformer parameters have also been reviewed in that chapter.

The initial designs of digital algorithms for differential protection of transformers were conceptually similar to that of conventional relays. They used the harmonic components of differential currents to block trippings during magnetizing inrush. The operating voltages of power systems and lengths of transmission lines have increased during the last thirty years. Because of these factors, the differential currents can contain large harmonic components even during internal faults. Therefore, algorithms using harmonic restraint may, in some cases, block trippings during internal faults. Also, if a transformer is energised with an internal fault, the fault currents and magnetizing inrush currents are experienced simultaneously. The harmonic components of the inrush currents can prevent trippings until the inrush currents decay sufficiently. This reduces the speed of the relay in these situations. Major concerns regarding the performance of these algorithms are, therefore, their security and speed.

Recently, some algorithms have been presented that do not rely on the presence of harmonic components in the differential currents to avoid trippings during magnetizing inrush conditions. However, their use requires that the winding currents be known. These currents can not be measured in some situations, for example, in delta connected windings of a three phase transformer where the terminals of the phase windings are not brought out of the tank. Also, some of these algorithms use data of the B-H curve which, generally, are not available and, therefore, must be determined experimentally.

Three algorithms for overcurrent protection have been described in Chapter 3. These algorithms are conceptually similar to each other, however, they use different techniques to model the relay characteristics and to determine the rms value of the fundamental frequency component of the relay current. The implementation of these algorithms on a microprocessor requires considerable on-line computations.

An improved technique for modelling of overcurrent relay characteristics has been proposed and described in Chapter 4. The technique is simple and requires only a modest amount of computer memory. The proposed technique was evaluated. It is demonstrated that the technique accurately models the relay characteristics and is suitable for use in a digital algorithm. The proposed technique has been used to develop an overcurrent digital relaying algorithm which has also been described in Chapter 4. The performance of the proposed algorithm was evaluated using simulations. Some results have been reported in this thesis. The results show that the proposed algorithm accurately emulates the selected relay characteristics.

The fifth chapter of the thesis has described digital algorithms that can detect winding faults in single-phase and three-phase transformers. These algorithms use a non-linear model of a transformer, instead of using the harmonic components of the differential currents, to avoid trippings during magnetizing inrush conditions. The algorithms take the non-linearity and hysteresis of the transformer into account but they do not become part of the algorithms. The algorithms are also suitable for protecting transformers whose winding currents can not be measured from their terminals. The performance of the algorithms were studied for a variety of operating conditions. These were simulated on a digital computer using the EMTP. Some test results have been presented in Chapter 5. The studies presented in that chapter show that the proposed algorithms block trippings during magnetizing inrush conditions and do not issue trip commands for overexcitation and external faults. The algorithms detect internal faults and issue trip com-

mands. The trip times vary from about 8 ms to 15 ms depending on the type and the severity of the fault.

Version-II of the digital algorithms for detecting winding faults in transformers has been presented in the sixth chapter. These algorithms are conceptually similar to those of Chapter 5 except that the resistances of the transformer windings are neglected and integrations are performed using the rectangular rule. The algorithms were tested using the data used for testing Version-I of the algorithms. Test results have also been reported in this chapter. The results indicate that the proposed algorithms do not issue trip commands for magnetizing inrush, overexcitation and external faults. However, trip commands are issued for internal faults. The trip times vary from about 8 ms to 23 ms depending on the type and severity of the fault.

The performance of Version-I and Version-II of the algorithms has been compared in Chapter 6. The comparison shows that the performance of both versions is similar for magnetizing inrush, overexcitation, external faults and heavy internal faults. However, for low-level internal faults, Version-II of the algorithms takes more time to issue a trip command as compared to Version-I of the algorithms.

Chapter 7 has described the design, implementation and testing of a microprocessor-based system for protecting power transformers. The system implements the digital algorithms of Chapters 4, 5 and 6 to protect the transformers from external and internal faults respectively. The system includes a man-machine interface for changing relay settings and relay software. The system also has spare input channels that can be used for monitoring transformer parameters. The hardware and software of the system has been described in Chapter 7. The implementation and testing procedures have also been described in that chapter. The performance of the system was checked in the laboratory and some results have been presented. The tests show that the winding protection scheme of the system successfully

blocks tripping during magnetizing inrush conditions and external faults. However, for internal faults, the system issues trip commands; the trip times vary from 10 ms to 20 ms depending on the severity and the type of the fault. It has also been demonstrated that the system issued trip commands without delay for the situations where the transformer was switched on with an internal fault. The overcurrent protection scheme of the system was also tested in the laboratory. The test results indicate that the system correctly emulates the characteristics of the selected relays.

The studies reported in this thesis have demonstrated that

1. the proposed technique for modelling of overcurrent relay characteristics can accurately represent the characteristics in a computer. The technique can be used to develop a digital algorithm that performs most of the computations in an off-line mode and, therefore, requires very few on-line computations.

2. the proposed digital algorithms for detecting winding faults in single phase and three phase transformers can block trippings during magnetizing inrush conditions without relying on the harmonics of the differential currents. The algorithms can provide tripping on the occurrence of winding faults in the transformers in about 8 ms to 20 ms depending on the type and severity of the fault.

3. the microprocessor-based system described in the thesis can be successfully used for protecting and monitoring single phase and three phase transformers.

8.2. Suggestions for Future Work

It has been demonstrated in this thesis that the proposed microprocessor-based system is capable of protecting and monitoring single phase and three phase transformers. The laboratory testing of the system has provided satisfactory results. Future work would be to check the performance of the system for a utility transformer. Faults in utility transformers occur infrequently. Therefore, the system software should include facilities to record data and other relevant information in the event of a fault. This

would facilitate the analysis of the response of the microprocessor-based system during faults.

Also, utility transformers are often equipped with tap changers. The proposed system can be modified to monitor tap positions using one of its spare input channels. This information can then be used to dynamically adjust the turns ratio of the transformer in the system software. This will avoid errors due to ratio mismatch if a tap position changes.

REFERENCES

1. Blackburn, J. L., *Protective Relaying - Principles and Applications* , Marcel Dekker Inc., New York and Basel, 1987.

2. Westinghouse Electric Corporation, *Applied Protective Relaying,* Relay Instrument Division, Pittsburgh, PA, 1979.

3. Madhava Rao, T. S., *Power System Protection - Static Relays,* McGraw Hill Book Company, New York, 1981.

4. Sachdev, M.S. (Coordinator), *Microprocessor Relays and Protection Systems,* IEEE Tutorial Course Text, Publication No. 88 EM0269-1-PWR, 1988.

5. Sachdev, M.S. (Coordinator), *Computer Relaying,* IEEE Tutorial Course Text, Publication No. 79 EH0148-7-PWR, 1979.

6. Last, F. H. and Stalewski, A., "Protective Gear as a Part of Automatic Power System Control", *Symp. on Automatic Control in Electricity Supply, Manchester, IEE Conf. Publication 16, Part I,* Mar. 1966.

7. Rockefeller, G. D., "Fault Detection With a Digital Computer", *IEEE Transactions on Power Apparatus and Systems,* Vol. PAS-88, April 1969, pp. 438-464.

8. Malik, O. P., Dash, P. K., and Hope, G. S., "Digital Protection of Power Transformers", *IEEE PES Winter Meeting, New York, Paper No. A76 191-7,* Jan. 1976.

9. Schweitzer, E. O., Larson, R. R., and Flechsig, A., "An Efficient Inrush Detection Algorithm for Digital Computer Relay Protection of Transformers", *IEEE PES Summer Meeting, Mexico City, Paper No. 77 510-1,* July 1977.

10. Sachdev, M. S. and Shah, D. V., "Transformer Differential and Restricted Earth Fault Protection Using a Digital Processor", *Transactions of the Engineering and Operating Division of the Canadian Electrical Association,* Vol. 20, Part 4, March 1981, pp. 1-11.

11. Thorp, J. S., and Phadke, A. G., "A Microprocessor Based Three-

Phase Transformer Differential Relay", *IEEE Transactions on Power Apparatus and Systems*, Vol. PAS-101, Feb. 1982, pp. 426-432.

12. Murty, Y. V.V. S., and Smolinski, W. J., "A Kalman Filter Based Digital Percentage Differential and Ground Fault Relay for a 3-Phase Power Transformer", *IEEE PES Winter Meeting, New York, Paper No. 88 WM 121-6*, Jan./Feb. 1988.

13. Phadke, A. G. and Thorp, J. S., "A New Computer-Based Flux-Restrained Current-Differential Relay for Power Transformer Protection", *IEEE Transactions on Power Apparatus and Systems*, Vol. PAS-102, Nov. 1983, pp. 3624-3628.

14. Sykes, J. A., "A New Technique for High Speed Transformer Fault Protection Suitable for Digital Computer Implementation", *IEEE PES Summer Meeting, San Francisco, Paper No. C72 429-9*, July 1972.

15. Jin, Y. S. and Sachdev, M. S., "An Algorithm for Digital Differential Protection of Transformers Using a Non-Linear Model", *Proceedings of the IEEE Electronicom'85, Paper No. 85155*, Dec. 1985, pp. 366-369.

16. Inagaki, K., Higaki, M., Matsui, Y., Suzuki, M., Yoshida, K. and Maeda, T., "Digital Protection Method for Power Transformers Based on An Equivalent Circuit Composed of Inverse Inductance", *IEEE Transactions on Power Delivery*, Vol. 3, Oct. 1988, pp. 1501-1510.

17. Degens, A. J. and Langedijk, J. J. M., "Integral Approach to the Protection of Power Transformers by Means of a Microprocessor", *International Journal of Electrical Power and Energy Systems*, Vol. 7, Jan. 1985, pp. 37-47.

18. Singh, J., Sachdev, M.S., Fleming, R.J. and Krause, A., "Digital IDMT Directional Overcurrent Relays", *Developments in Power System Protection, IEE Conference Publication No. 185*, April 1980, pp. 84-87.

19. Schweitzer, E. O. and Aliaga, A., "Digital Programmable Time-Parameter Relay Offers Versatility and Accuracy", *IEEE Transactions on Power Apparatus and Systems*, Vol. PAS-99, Jan. 1980, pp. 152-157.

20. Burton, P.J., Graham, J., Hall, A.C., Laver, J.A. and Oliver, A.J., "Recent Developments by CEGB to Improve the Perdiction and Monitoring of Transformer Performance", *CIGRE 1984, Paper 12-09*1984, pp. 1-10.

21. Tsukioka, H., Sugawara, K. and Mori, E., "New Apparatus for Detecting Hydrogen, Carbon Monoxide and Methane Dissolved in Transformer Oil", *IEEE Transactions on Electrical Insulation*, Vol. EI-18, pp. 409-419.

22. Poyser, T. D., "An On-Line Microprocessor Based Transformer

Analysis System to Improve the Availability and Utilization of Power Transformers", *IEEE Transactions on Power Apparatus and Systems*, Vol. PAS-102, April 1983, pp. 957-962.

23. Poyser, T. D., Yannucci, D.A., Templeton, J.B. and Lenderking, B.N., "On-Line Monitoring of Power Transformers", *IEEE Transactions on Power Apparatus and Systems*, Vol. PAS-104, Jan. 1985, pp. 207-211.

24. Larson, R. R., Flechsig, A. J. and Schweitzer, E. O., "The Design and Test of a Digital Relay for Transformer Protection", *IEEE Transactions on Power Apparatus and Systems*, Vol. PAS-98, May/June 1979, pp. 795-804.

25. Sonnemann, W. K., Wagner, C. L. and Rockefeller, G. D., "Magnetizing Inrush Phenomena in Transformer Banks", *Transactions of the AIEE, Part III - Power Apparatus and Systems*, Vol. 77, Oct. 1958, pp. 884-892.

26. Specht, T. R., "Transformer Inrush and Rectifier Transient Currents", *IEEE Transactions on Power Apparatus and Systems*, Vol. PAS-88, No. 4April, 1969, pp. 269-276.

27. Warrington, A. R. van C., *Protective Relays, Their Theory and Practice* , Chapman and Hall Ltd., London, Vol. I, 1968.

28. Stiganant, S. A. and Franklin, A. C., *The J & P Transformer Book,* John Wiley and Sons, Vol. I, 1973.

29. American National Standards Institute, New York, NY., *ANSI/IEEE C37.91, IEEE Guide for Protective Relay Applications to Power Transformers,* 1985.

30. Luckett, R.G., Munday, P.J., and Murray, B.E., "Substation Based Computer for Control and Protection", *Developments in Power System Protection, IEE Conference Publication No. 125, London*, March 1975.

31. Brooks, A. E., "Distance Relaying using Least Error Squares Estimates of Voltage, Current and Impedance", *Proceeding of 10th Power Industry Computer Application Conference, IEEE Publication No. 77CH 1131-2-PWR*, May 1977.

32. Sachdev, M. S. and Baribeau, M. A., "A New Algorithm for Digital Impedence Relays", *IEEE Transactions on Power Apparatus and Systems*, Vol. PAS-98, Nov./Dec. 1979, pp. 2232-2240.

33. Sykes, J. A. and Morrison, I. F., "A Proposed Method of Harmonic Restraint Differential Protection of Transformers By Digital Computer", *IEEE Transactions on Power Apparatus and Systems*, Vol. PAS-91, May/June 1977, pp. 1266-1272.

34. Sachdev, M. S., Wood, H. C. and Johnson, N. G., "Kalman Filtering

Applied to Power System Measurements for Relaying", *IEEE Transactions on Power Apparatus and Systems*, Vol. PAS-104, Dec. 1985, pp. 3565-3573.

35. Murty, Y. V. V. S., and Smolinski, W. J., "Design and Implementation of a Digital Differential Relay for a 3-Phase Power Transformer Based on Kalman Filtering Theory", *IEEE Transactions on Power Delivery*, Vol. 3, April 1988, pp. 525-533.

36. Elect. Engg. Staff of MIT, *Magnetic Circuits and Transformers*, John Wiley and Sons Inc., New York, 1943.

37. Westinghouse Electric Corporation, Relay Instrument Division, Newark, NJ, U.S.A., *Instructions, Type CO Overcurrent Relays, IL 41-101P*, 1976.

38. IEC Standard, Publication No. 255-4., *Single Input Energising Quantity Measuring Relays With Dependent Specified Time*, 1976.

39. Radke, G. E., "A Method for Calculating Time-Overcurrent Relay Settings by Digital Computer", *IEEE Transactions on Power Apparatus and Systems*, Vol. 82, 1963, pp. 1501-1510.

40. Albrecht, R. E., Nisja, M.J., Peero, W.E., Rockefeller, G.D. and Wagner, C.L., "Digital Computer Protective Device Coordination Program I - General Program Description", *IEEE Transactions on Power Apparatus and Systems*, Vol. PAS-83, 1964, pp. 402-411.

41. Sachdev, M. S., Singh, J. and Fleming, R. J., "Mathematical Models Representing Time-Current Characteristics of Overcurrent Relays for Computer Applications", *IEEE PES Winter Meeting, New York, Paper No. A78 131-5*, Jan.-Feb. 1978.

42. Sidhu, T. S., Sachdev, M. S. and Wood, H. C., "Application of Virtual Digital Relays", *Conference Record of the IEEE Industry Applications Society Annual Meeting, Atlanta, Paper No. 59021*, Oct. 19-23, 1987, pp. 1744-1749.

43. Wood, H. C., Sachdev, M. S. and Sidhu, T. S.,, "Tools for Computer-Aided Development of Microprocessor Based Power System Relays", *Conference Record of the IEEE Industry Applications Society Annual Meeting, Atlanta, Paper No. 59013*, Oct. 19-23, 1987, pp. 1733-1738.

44. Singh J., *Overcurrent Relays: Modelling of Characteristics and Feasibility of a Computer Based Design*, M.Sc. Thesis, University of Saskatchewan, Saskatoon, Canada, 1978.

45. Sidhu, T. S., *Computer-Aided Design and Performance Evaluation of Digital Relays*, M.Sc. Thesis, University of Saskatchewan, Saskatoon, Canada, 1985.

46. Sachdev, M. S., Sidhu, T. S. and Wood, H. C., "A Digital Relaying Algorithm for Detecting Transformer Winding Faults", *IEEE Transactions on Power Delivery*, Vol. 4, July 1989, pp. 1638-1648.

47. Sachdev, M. S., Sidhu, T. S. and Wood, H. C., "A Non-Linear Modelling Approach for Detecting Winding Faults in Power Transformers", *Transactions of the Engineering and Operating Division of the Canadian Electrical Association*, Vol. 28, 1989, pp. 1-16.

48. Mayer, W. S. and Liu, T. H., *EMTP Rule Book*, Bonneville Power Administration, Portland, Oregon, 1982.

49. Oppenheim, A. V. and Schafer, R. W., *Digital Signal Processing*, Prentice Hall Inc., Englewood Cliffs, N.J., 1978.

50. Sidhu, T. S., Sachdev, M. S. and Wood, H. C., "Detecting Transformer Winding Faults Using Non-Linear Models of Transformers", *Fourth International Conference on Developments in Power System Protection, IEE Publication No. 302*, April 11-13, 1989, pp. 70-74.

51. Sidhu, T. S., Sachdev, M. S. and Wood, H. C., "Design, Implementation and Testing of A Microprocessor-Based High-Speed Relay for Detecting Transformer Winding Faults", submitted for publication in IEEE Transactions on Power Delivery

52. Sidhu, T. S., Sachdev, M. S. and Wood, H. C., "Design and Testing of a Microprocessor Based Relay for Detecting Transformer Winding Faults", *Conference Proceedings of the International Conference on Power System Protection'89, Singapore*, Sept. 13 - 14, 1989, pp. 365-381.

53. Wood, H. C., Sidhu, T. S., Sachdev, M. S. and Nagpal, M., "A General Purpose Hardware for Microprocessor Based Relays", *Conference Proceedings of the International Conference on Power System Protection'89, Singapore*, Sept. 13 - 14, 1989, pp. 43-59.

54. Hammond Manufacturing Company, Guelph, Ontario, Canada, *Low Profile Power Transformers - Technical Data Product Section 50*, 1988.

55. Siemens Electric Limited, Downsview, Ontario, Canada., *Electronic Components*, 1980/81.

56. Harris Corporation, Melbourne, Florida, U.S.A., *Analog and Telecommuniciations Product Data Book*, 1984.

57. National Semiconductor Corporation, Santa Clara, California, U.S.A., *Linear Applications Data Book*, 1986.

58. Ariel Corporation, New York, New York, U.S.A., *DSP-16, Real Time Data Acquisition Processor*, 1988.

59. Texas Instruments Inc., Houston, Texas, U.S.A., *Second-Generation TMS320 User's Guide,* 1987.

60. Doble Engineering Company, Watertown, MA, U.S.A., *Model F1 Single-Phase Test System,* 1981.

61. Strang, G., *Linear Algebra and Its Applications,* Academic Press Inc., New York, ISBN 0-12-673660-X, 1980.

62. Van Valkenburg, M.E., *Analog Filter Design,* Holt, Riehart and Winston, New York, 1982.

A. DETERMINATION OF MODELLING COEFFICIENTS

This appendix describes a procedure to compute the coefficients of the polynomial described by Equation 4.1. The procedure uses the data read from the published time-current characteristics of an overcurrent relay. The procedure is illustrated by calculating the modelling coefficients of the Westinghouse CO-7 relay at a current multiple of 5.0. The operating time of the CO-7 relay for different time dial settings at a current multiple of 5.0 is as follows:

Time Dial Setting (TDS)	Relay Operating Time (in seconds)
0.5	0.180
1.0	0.345
2.0	0.650
3.0	0.960
4.0	1.300
5.0	1.630
6.0	1.960
7.0	2.300
8.0	2.650
9.0	3.020
10.0	3.425
11.0	3.850

If the relay characteristics is modelled in the form of Equation 4.1, the first time dial setting and operating time relationship provides

$$a_0 + a_1(0.5) + a_2(0.5)^2 + a_3(0.5)^3 + a_4(0.5)^4 + a_5(0.5)^5 = 0.18. \quad (A.1)$$

Completing the arithmetic provides

$$a_0 + 0.5a_1 + 0.25a_2 + 0.125a_3 + 0.0625a_4 + 0.03125a_5 = 0.18. \quad (A.2)$$

Similarly, the second time dial setting and operating time relationship provides

$$a_0 + a_1 + a_2 + a_3 + a_4 + a_5 = 0.345. \quad (A.3)$$

Continuing the procedure, the following equations are obtained.

1.0	0.50	0.250	0.1250	0.06250	0.031250	a_0		0.180
1.0	1.00	1.000	1.0000	1.00000	1.000000	a_1		0.345
1.0	2.00	4.000	8.0000	16.0000	32.00000	a_2		0.650
1.0	3.00	9.000	27.000	81.0000	243.0000	a_3	=	0.960
1.0	4.00	16.00	64.000	256.000	1024.000	a_4		1.300
1.0	5.00	25.00	125.00	625.000	3125.000	a_5		1.630
1.0	6.00	36.00	216.00	1296.00	7776.000			1.960
1.0	7.00	49.00	343.00	2401.00	16807.00			2.300
1.0	8.00	64.00	512.00	4096.00	32768.00			2.650
1.0	9.00	81.00	729.00	6561.00	59049.00			3.020
1.0	10.0	100.0	1000.0	10000.0	100000.0			3.425
1.0	11.0	121.0	1331.0	14641.0	161051.0			3.850

which can be written as

$$[A][X] = [b] \quad (A.4)$$

It is possible to find the values of the coefficients, [X], by using least squares curve fitting techniques [61] as follows.

$$[X] = [[A]^T[A]]^{-1}[A]^T[b] \quad (A.5)$$

Applying the above procedure on Equation A.4 provides the value of [X] given as

$$[X] = \begin{matrix} a_0 \\ a_1 \\ a_2 \\ a_3 \\ a_4 \\ a_5 \end{matrix} \begin{matrix} 0.03879516 \\ 0.28733138 \\ 0.01192646 \\ -0.00174806 \\ 0.00012020 \\ -0.00000139 \end{matrix}$$

B. ESTIMATION OF THE RMS VALUE

B.1. Introduction

The rms value of the fundamental frequency component of a relay current can be computed from its real and imaginary parts. This process requires two squaring functions and one square root function to be performed. These functions are computationally inefficient to implement on microprocessors. However, these calculations can be replaced by a piecewise linear approximation [45]. This approximation requires only additions and multiplications by constants and is more efficient than the general purpose multiplication of two unknowns. The error in the estimate can be made arbitrarily small. The method of estimation is described in this appendix.

B.2. Mathematical Background

Consider that I_r and I_i are the real and imaginary components of a phasor having magnitude, P. These components represent a point in a complex plane. The amplitude of the phasor is the distance from the origin to that point. The amplitude is unaffected by the signs of I_r and I_i and points (I_r, I_i) and (I_i, I_r) are equidistant from the origin. Let

$$a = max(|I_r|,|I_i|) \text{ and} \tag{B.1}$$

$$b = min(|I_r|,|I_i|). \tag{B.2}$$

Then, (a,b) is a point in the first octant at a distance, P, from the origin. As a first approximation, let

$$\overline{P} = xa + yb \tag{B.3}$$

where:

$\overline{P}$ is the estimated peak value.

In Equation B.3, x and y are coefficients or the multipliers and their value can be estimated by minimizing the error $(\overline{P}-P)$.

This is the case when only one approximation region is considered. Additional accuracy can be obtained by subdividing the first octant into multiple regions and using different approximations in each region. However, processing time increases as the number of regions is increased. In general, for n regions there will be a set of values of x and y, (x_1,y_1), (x_2,y_2) $\cdots$ (x_n,y_n). Each set of coefficients x and y is valid for a particular range of ratios of b/a. The values of each set of coefficients can be calculated using least error squares fit of the data (of a particular region for which values of x and y are being evaluated) to a linear equation of the form of Equation B.3. If m is the number of data points used to fit the data from the n-th region, then in matrix from it can be written as

$$\underset{(m\times 1)}{[P]} = \underset{(1\times 1)}{[x_n]}\underset{(m\times 1)}{[a]} + \underset{(1\times 1)}{[y_n]}\underset{(m\times 1)}{[b]} \qquad (B.4)$$

Values of unknowns x_n and y_n can be calculated using Equation B.5.

$$\begin{matrix} x_n \\ y_n \end{matrix} = \begin{matrix} \{\alpha[P]-\alpha[b]\beta[P]\}/(1-\alpha[b]\beta[a]) \\ \{\beta[P]-\beta[a]\alpha[P]\}/(1-\beta[a]\alpha[b]) \end{matrix} \qquad (B.5)$$

where:

$\alpha = [[a]^T[a]]^{-1}[a]^T$ and

$\beta = [[b]^T[b]]^{-1}[b]^T$

Reference [45] lists the coefficients that were calculated considering one, two, three, four, five, six, eight, ten and sixteen regions of approximation. The use of these coefficients in Equation B.3 provides the estimated peak value of

the fundamental frequency component. However, it is possible to pre-multiply these coefficients by $\sqrt{2}$ for estimating the rms values.

C. SIMULATION OF TRANSFORMER CONDITIONS

The Electro-Magnetic Transient Program (EMTP) [48] was developed at the Bonneville Power Administration, Portland, Oregon. The EMTP provides pre-programmed models of the power system elements. In this work, the model of an N-winding single-phase transformer, shown in Figure C.1, was used. The important features of the model are as follows:

1. N-1 single-phase two-winding ideal transformers are involved that provide the correct transformation ratio of windings 2, 3, · · · N with respect to winding 1.

2. Each winding has an associated leakage-impedence branch, involving resistance and inductance.

3. Saturation and magnetizing current effects are confined to a single non-linear reactor in the winding 1 circuit.

4. Core losses are confined to a constant linear resistance which is in parallel with the saturation branch.

For the modelling of a three-phase transformer, three single-phase transformers were connected in the desired configuration. Faults on the terminals of the transformers and external faults were simulated by closing the switches provided at the desired fault points. For simulating the magnetizing inrush conditions, the non-linear reactor in winding-1 circuit was replaced with a type-96 hysteresis element. A partial winding fault in the transformer winding was simulated by replacing the short-circuit winding with a combination of two windings. For example, consider a winding that has a resistance of R_2, an inductance of L_2 and a transformation ratio of N_2 with

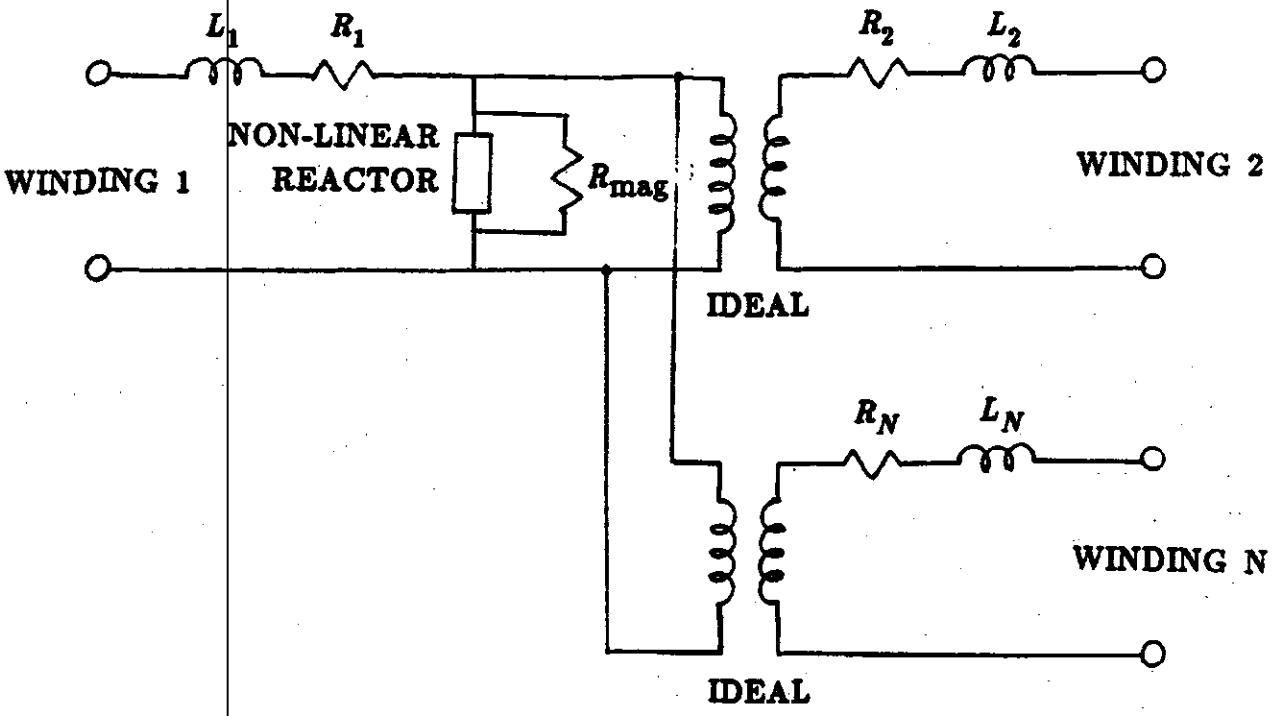

Figure C.1: Model of an N-winding single-phase transformer.

respect to winding 1. Also, consider that x% of this winding is short-circuited. This winding can be replaced by a combination of two windings as shown in Figure C.2.

In the present work the EMTP was used to simulate various conditions in 30 MVA, 138/13.8kV single-phase and three-phase transformers. The parameters of the simulated transformers are shown in Table C.1. The current-flux characteristics of the model transformers are shown in Figure C.3. The core losses of modern transformers are very small and, therefore, were neglected in the simulations. The data obtained from simulations were used for testing winding protection algorithms. Test results were reported in Chapters 5 and 6.

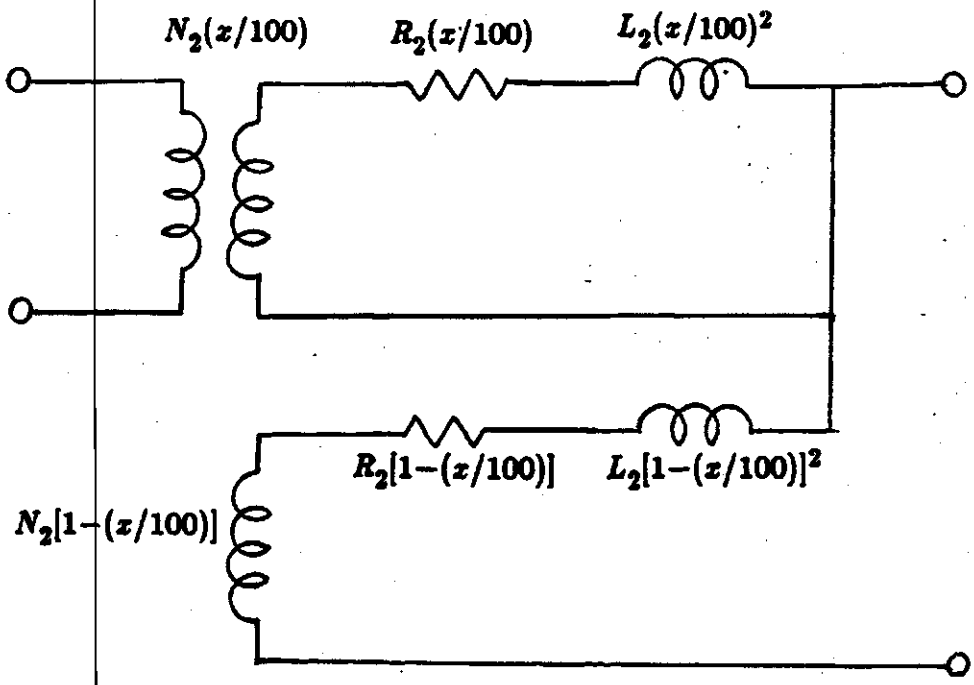

Figure C.2: A combination of windings equivalent to a partly short-circuited winding in the transformer model.

Table C.1: Winding resistance and leakage inductance of a single-phase transformer model.

Parameter		Primary winding	Secondary winding
Resistance	(Ohms)	0.095	0.00095
Inductance	(mH)	12.63	0.1263

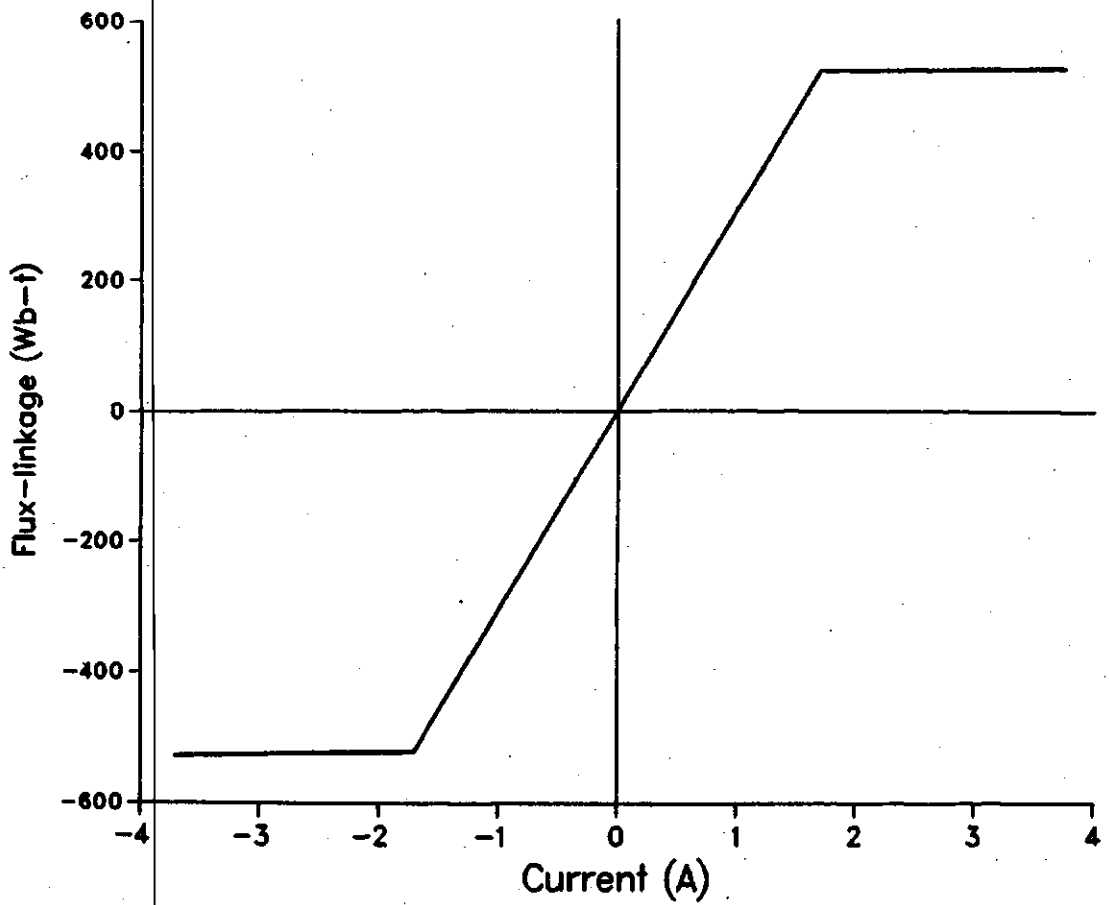

Figure C.3: Current-flux characteristics of the model transformer.

D. DESIGN OF THE LOW-PASS DIGITAL FILTER

The transfer function, $H(s)$, of a fourth order low-pass Bessel type analog filter having a cut-off frequency of ω_c rad/s is defined by the following equation [62].

$$H(s) = \frac{5.255\omega_c^4}{(s^2+2.74\omega_c s+2.045\omega_c^2)(s^2+1.99w_c s+2.57\omega_c^2)} \qquad (D.1)$$

The designed digital filter should have a cut-off frequency of 200 hz. The inter-sampling time used for the design of low pass filter is (1/24000) s. Due to warping effect, the cut-off frequency of a digital filter is some what different than the cut-off frequency of its corresponding analog filter. The cut-off frequency of the equivalent analog filter can be obtained as [49]

$$\omega_c = 2\times 24000\times tan(200\pi/24000) = 1257\ rad/s \qquad (D.2)$$

Substituting the value of ω_c in Equation D.1 provides the following transfer function of the analog filter that has a cut-off frequency of 1257 rad/s.

$$H(s) = \frac{1.3119\times 10^{13}}{(s^2+3444.2s+3231200.2)(s^2+2501.4s+4060725.9)} \qquad (D.3)$$

In this equation, the Laplace operator can be replaced by operator z using Equation D.4.

$$s = (2/\Delta T)[(1-z^{-1})/(1+z^{-1})] \qquad (D.4)$$

Substituting (1/24000) for ΔT, the following equation can be obtained.

$$s = 48000[(1-z^{-1})/(1+z^{-1})] \qquad (D.5)$$

Substitution of Equation D.5 in Equation D.3 provides the following equation.

$$H(z) = \frac{2.1862\times10^{-6}(1+4z^{-1}+6z^{-2}+4z^{-3}+z^{-4})}{1-3.7554z^{-1}+5.2929z^{-2}-3.3180z^{-3}+0.7806z^{-4}} \qquad (D.6)$$

The above equation provides the transfer function of a digital filter equivalent of a low-pass fourth-order Bessel-type analog filter having a cut-off frequency of 200 Hz.

E. CIRCUIT DIAGRAM OF I/O BOARD

The circuit diagram of the piggy-back I/O board is shown in Figure E.1. The design uses two latches (74LS374), two buffers (74LS244), an address decoder (74S138) and an inverter (74LS04). The diagram also identifies the interconnection of the I/O board to the DSP-16 board. The interface details of the input and output ports of the piggy-back board to the data acquisition system are provided in Tables E.1 and E.2 respectively.

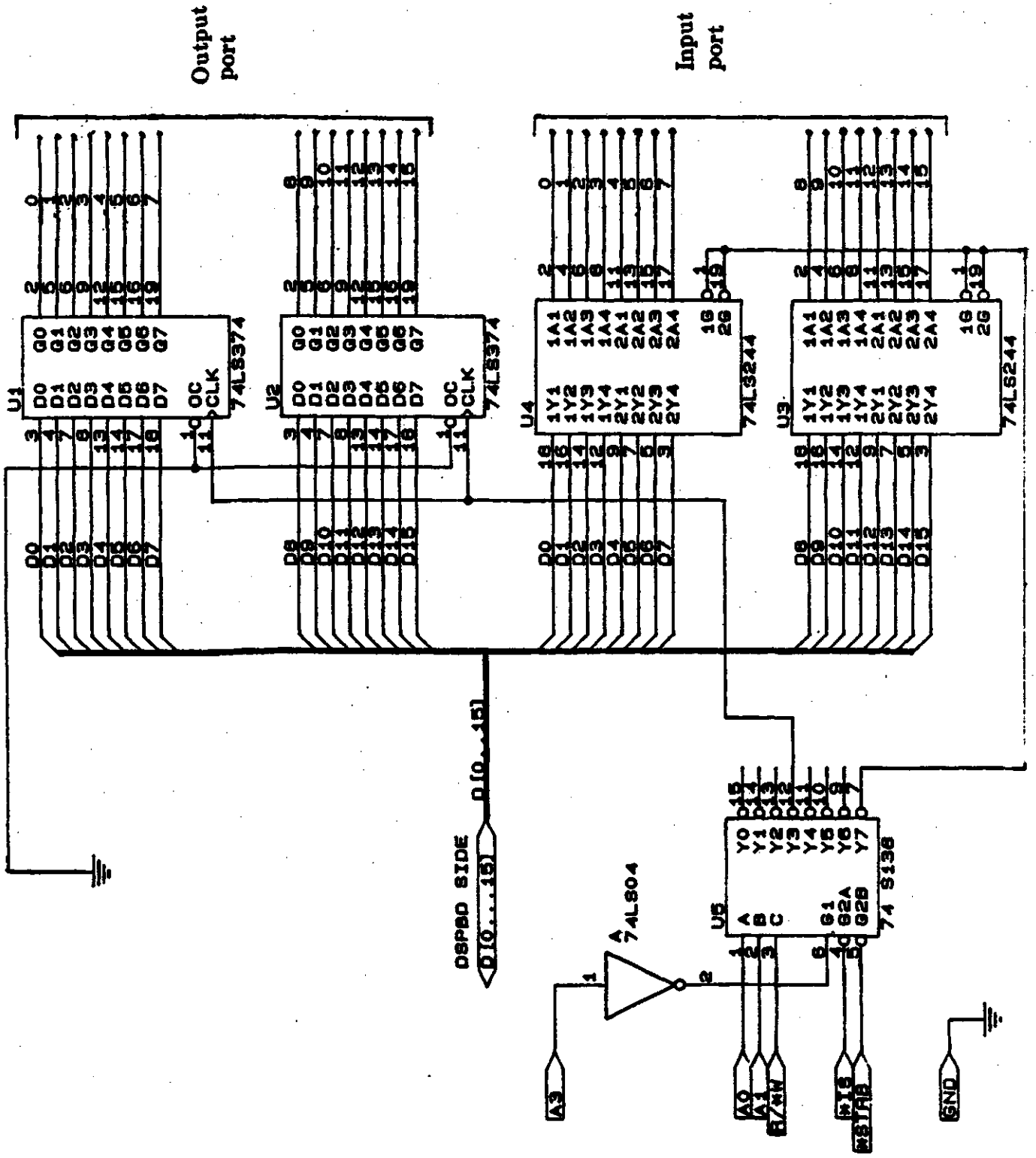

Figure E.1: Circuit diagram of the piggy-back I/O board.

Table E.1: Description of the interconnections between the output port and data acquisition system.

Output port (Bit no.)	Data acquisition system
0	S/H of all modules
1	A0 of all modules
2	A1 of all modules
8	C/E of module 1
9	C/E of module 2
10	C/E of module 3
11	C/E of module 4
12	R/C of module 1
13	R/C of module 2
14	R/C of module 3
15	R/C of module 4

Table E.2: Description of the interconnections between the input port and data acquisition system.

Input port (Bit no.)	Data acquisition system
0 to 11	D0 to D11 of all modules
12	STS of module 1
13	STS of module 2
14	STS of module 3
15	STS of module 4

F. DETERMINATION OF TRANSFORMER WINDING PARAMETERS

The implementation of the winding protection scheme requires that the resistances and inductances of the transformer windings be known. These values can be calculated from the transformer design data and, therefore, are known to the transformer manufacturers. However, in this work, these values were determined experimentally. The procedure and the results are described in this appendix.

F.1. Procedure and Results

The secondary windings of the delta-star transformer were shorted circuited through a resistance of approximately 1.2 ohms. The rated voltage was applied to the primary windings and the transformer voltages and currents were sampled, digitized and recorded at 4800 Hz by using microprocessor-based system. The recorded data from the short-circuit test were transferred to the MicroVAX 3600 digital computer. A FORTRAN program was written to convert the digital samples to the equivalent voltages and currents at the transformer terminals. Also, this program converted the data to a sampling rate of 1200 Hz by taking every fourth sample of the data. The resulting samples were provided to another FORTRAN program that implements the least square filter whose coefficients are listed in Table 4.7. The least error square filter processed the samples and estimated the steady-state value of phasors representing the transformer winding voltages and currents. Table F.0 lists the calculated values of steady-state voltages and currents. All the values in Table F.0 are referred to the primary side of the transformer. These steady-state phasors were used to estimate the

value of winding resistances and inductive reactances. Equation F.1 provided the value of the combined resistance, R_A, of the primary and secondary windings of phase A.

$$R_A = Re[(V_A - V_a)/I_a] \qquad (F.1)$$

where:

R_A is the combined resistance of the primary and secondary windings of phase A,

V_A is the voltage of primary winding of phase A,

V_a is the voltage of secondary winding of phase A,

I_a is the current in the secondary winding of phase A and

Re represents the real part.

Similarly, Equation F.2 provided the value of the combined inductive reactance, X_A, of the primary and secondary windings of phase A.

$$X_A = Im[(V_A - V_a)/I_a] \qquad (F.2)$$

where:

X_A is the combined inductive reactance of the primary and secondary windings of phase A and

Im indicates the imaginary part.

The above equations provided the values of the combined resistance and inductive reactance of the windings of phase A. However, the implementation of the algorithm requires the resistances and inductances of the primary and secondary windings. These were obtained by assuming that resistances and inductive reactances of the primary and secondary windings are equal. Therefore, the total resistance and inductive reactance obtained from Equations F.1 and F.2 respectively were divided by two to obtain the values for

the primary and secondary windings of phase A. A similar procedure was followed to obtain the value of resistances and inductances of windings of phases B and C. Table F.1 lists the calculated values of resistances and inductances of the primary and secondary windings of the transformer.

Table F.1: Transformer voltage and current phasors during the short-circuit test.

Phasor description	Value of the phasor
PHASE A:	
Pri. Voltage (V)	28.8-j245.1
Sec. Voltage (V)	-28.2-j177.0
Current (A)	69.0-j281.5
PHASE B:	
Pri. Voltage (V)	189.0+j172.3
Sec. Voltage (V)	122.5+j116.0
Current (A)	264.3+j81.4
PHASE C:	
Pri. Voltage (V)	-217.9+j72.9
Sec. Voltage (V)	-94.4+j54.37
Current (A)	-344.17+j193.8

Table F.2: Resistance and inductance of the primary and secondary windings of the test transformer.

Winding	Resistance (Ohms)	Inductance (H)
PHASE A:		
Pri. winding	0.140	0.00017
Sec. winding	0.140	0.00017
PHASE B:		
Pri. winding	0.144	0.00016
Sec. winding	0.144	0.00016
PHASE C:		
Pri. winding	0.144	0.00015
Sec. winding	0.144	0.00015

G. RESULTS FROM TESTING OF THE WINDING PROTECTION SCHEME

The test results illustrating the performance of the winding protection scheme for some transformer operating conditions were presented in Chapter 7. This appendix provides the test results demonstrating the performance of the winding protection scheme for the remaining transformer conditions listed in Table 7.9. Figures G.1 to G.5 show the errors and the trip indices for magnetizing inrush conditions. Figures G.6 to G.14 show the errors and trip indices for internal fault conditions. These figures also show the trip commands issued by the system. Figures G.15 to G.18 show the errors and trip indices for external faults.

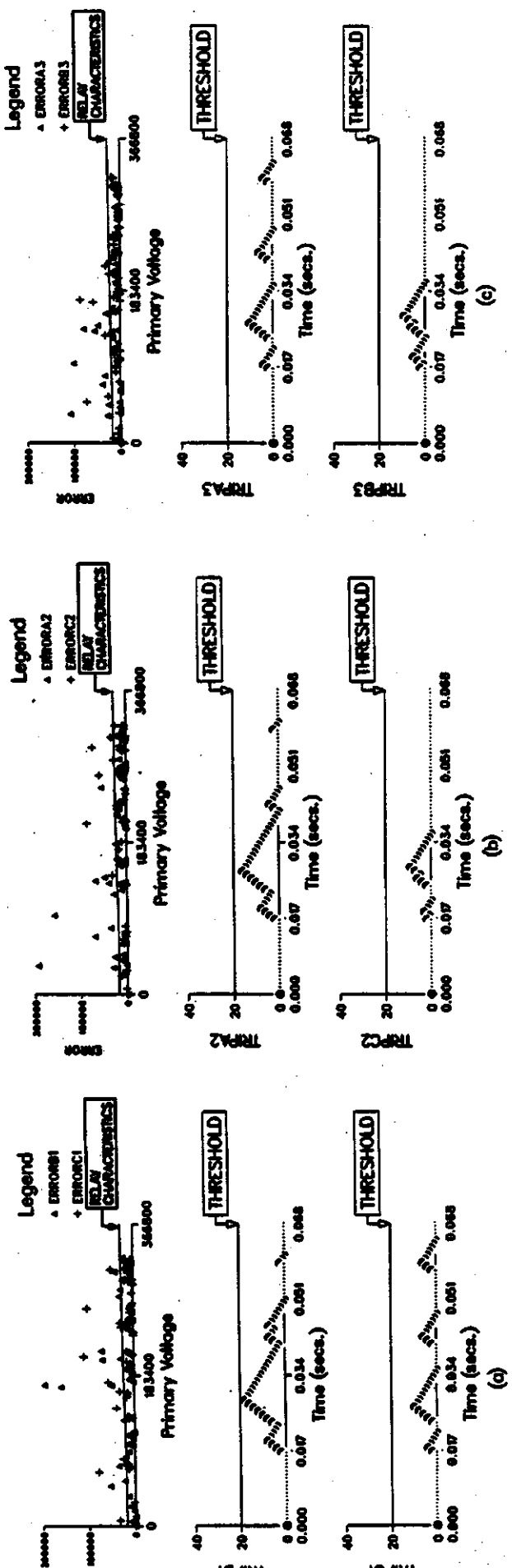

Figure G.1: Errors and values of the trip indices for a magnetizing inrush condition when (a)phase A, (b)phase B or (c)phase C is used as the "Reference phase". The transformer was connected to the supply at 0.0167 s.

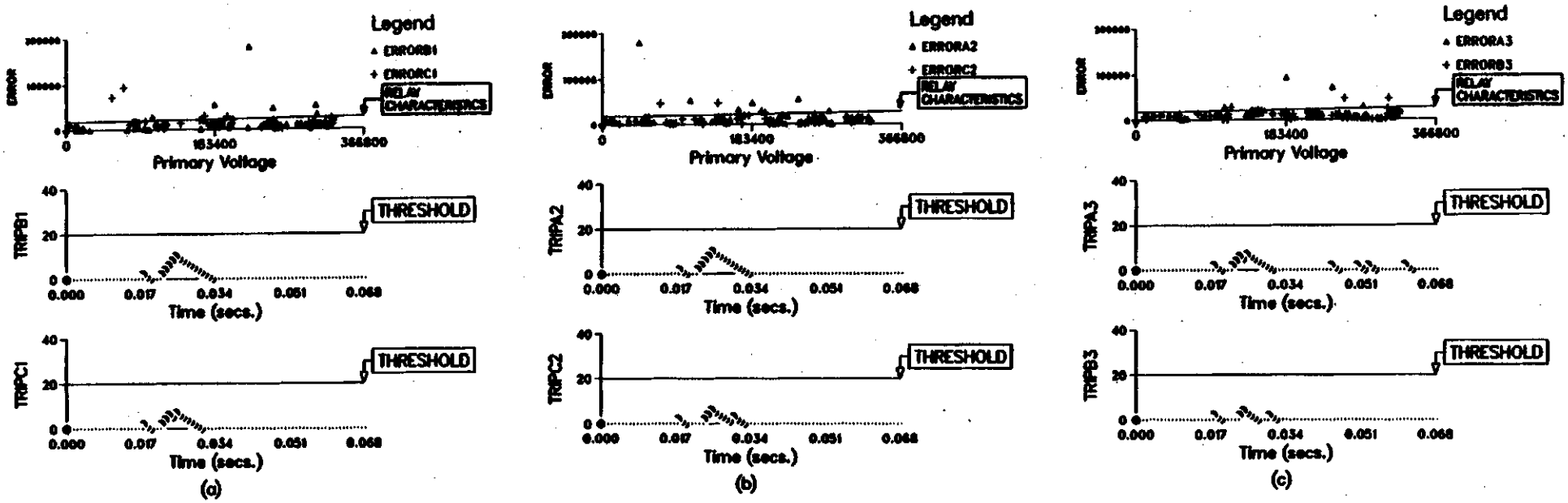

Figure G.2: Errors and values of the trip indices for a magnetizing inrush condition when (a)phase A, (b)phase B or (c)phase C is used as the "Reference phase". The transformer was connected to the supply at 0.0167 s.

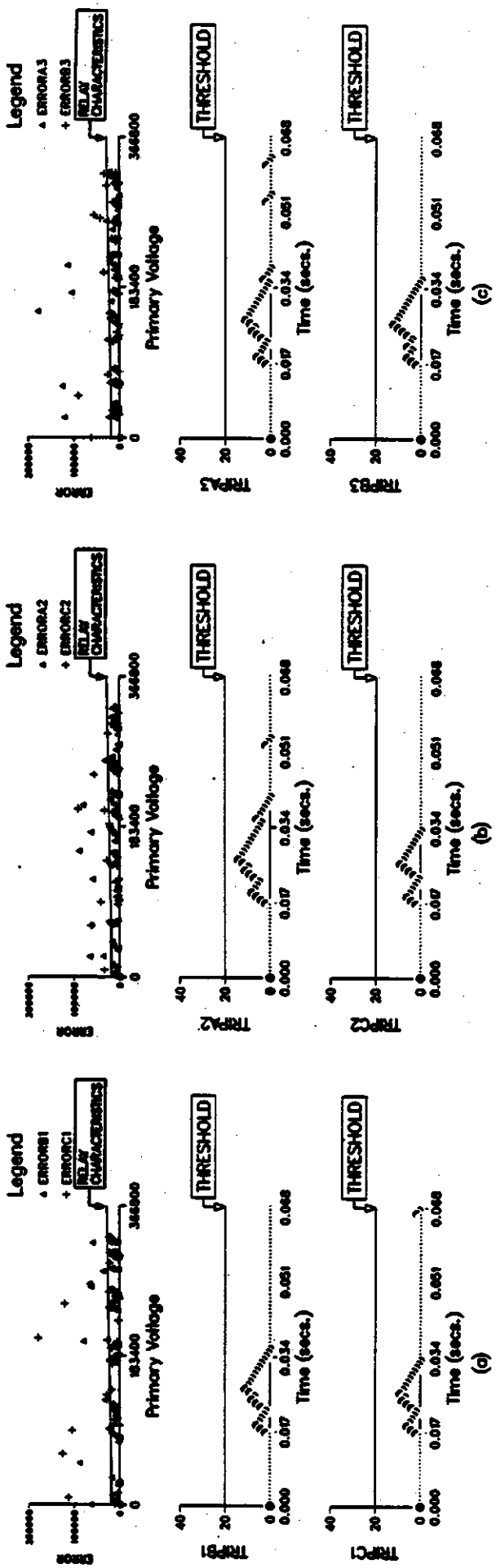

Figure G.3: Errors and values of the trip indices for a magnetizing inrush condition when (a)phase A, (b)phase B or (c)phase C is used as the "Reference phase". The transformer was connected to the supply at 0.0167 s.

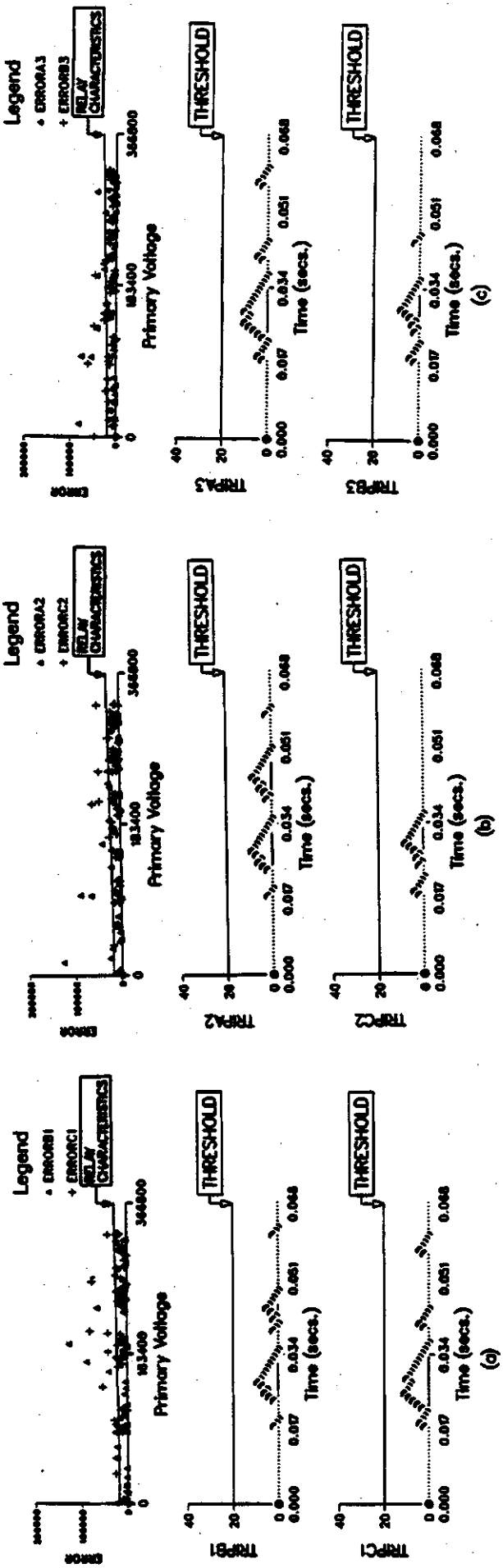

Figure G.4: Errors and values of the trip indices for a magnetizing inrush condition when (a)phase A, (b)phase B or (c)phase C is used as the "Reference phase". The transformer was connected to the supply at 0.0167 s.

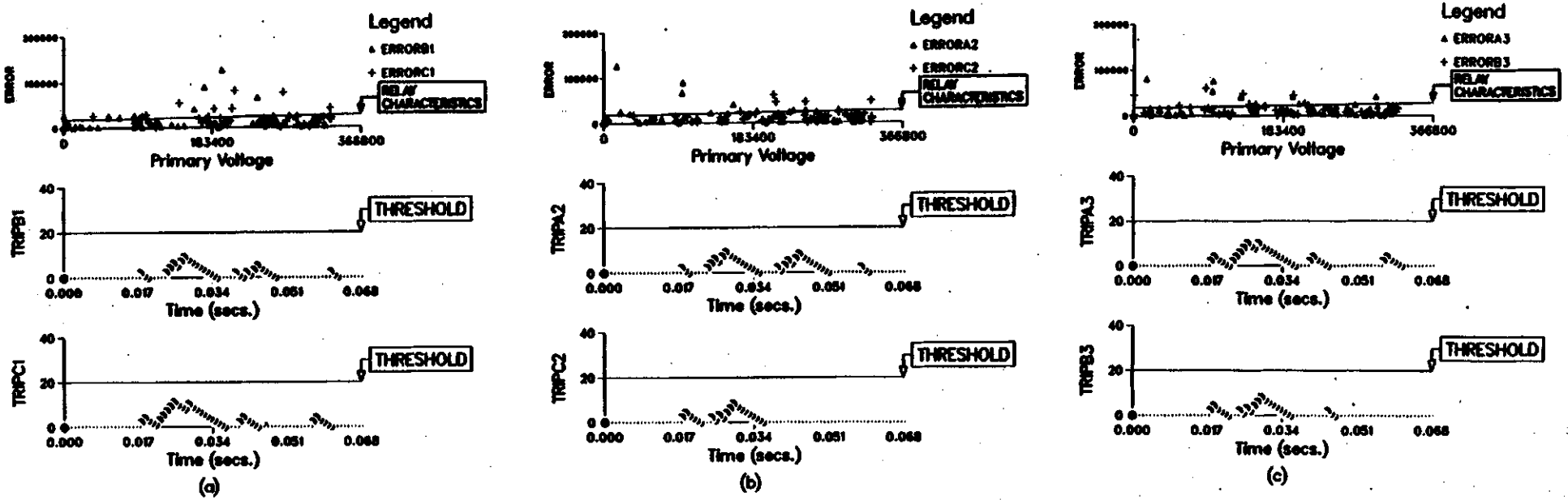

Figure G.5: Errors and values of the trip indices for a magnetizing inrush condition when (a)phase A, (b)phase B or (c)phase C is used as the "Reference phase". The transformer was connected to the supply at 0.0167 s.

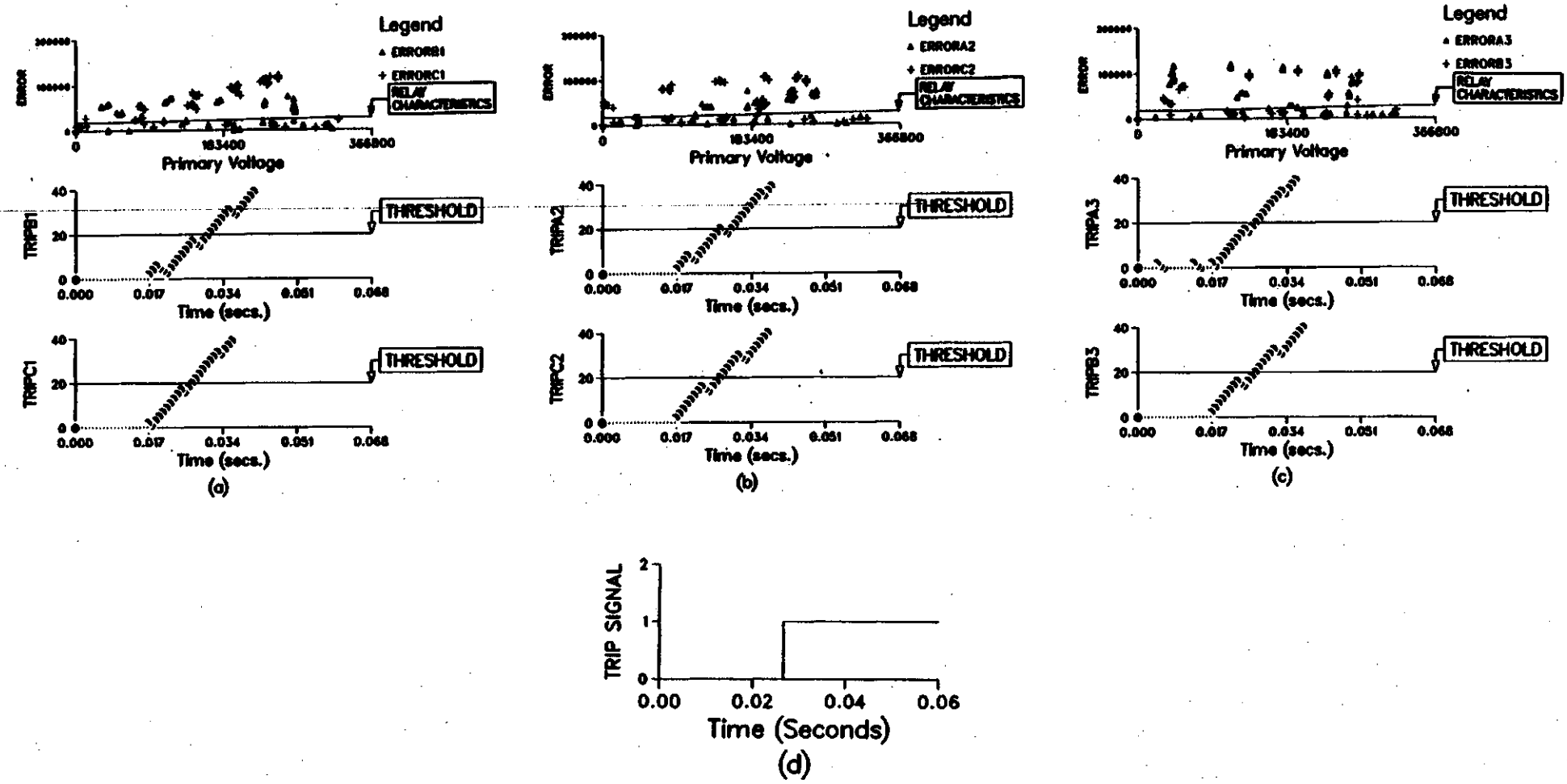

Figure G.6: Errors and values of the trip indices for an internal fault on the secondary side that short circuits phases A, B and C through a resistance of 1.2 ohms and when (a)phase A, (b)phase B or (c)phase C is used as the "Reference phase". Trip command issued by the system is shown in (d). The fault was applied at 0.0167 s.

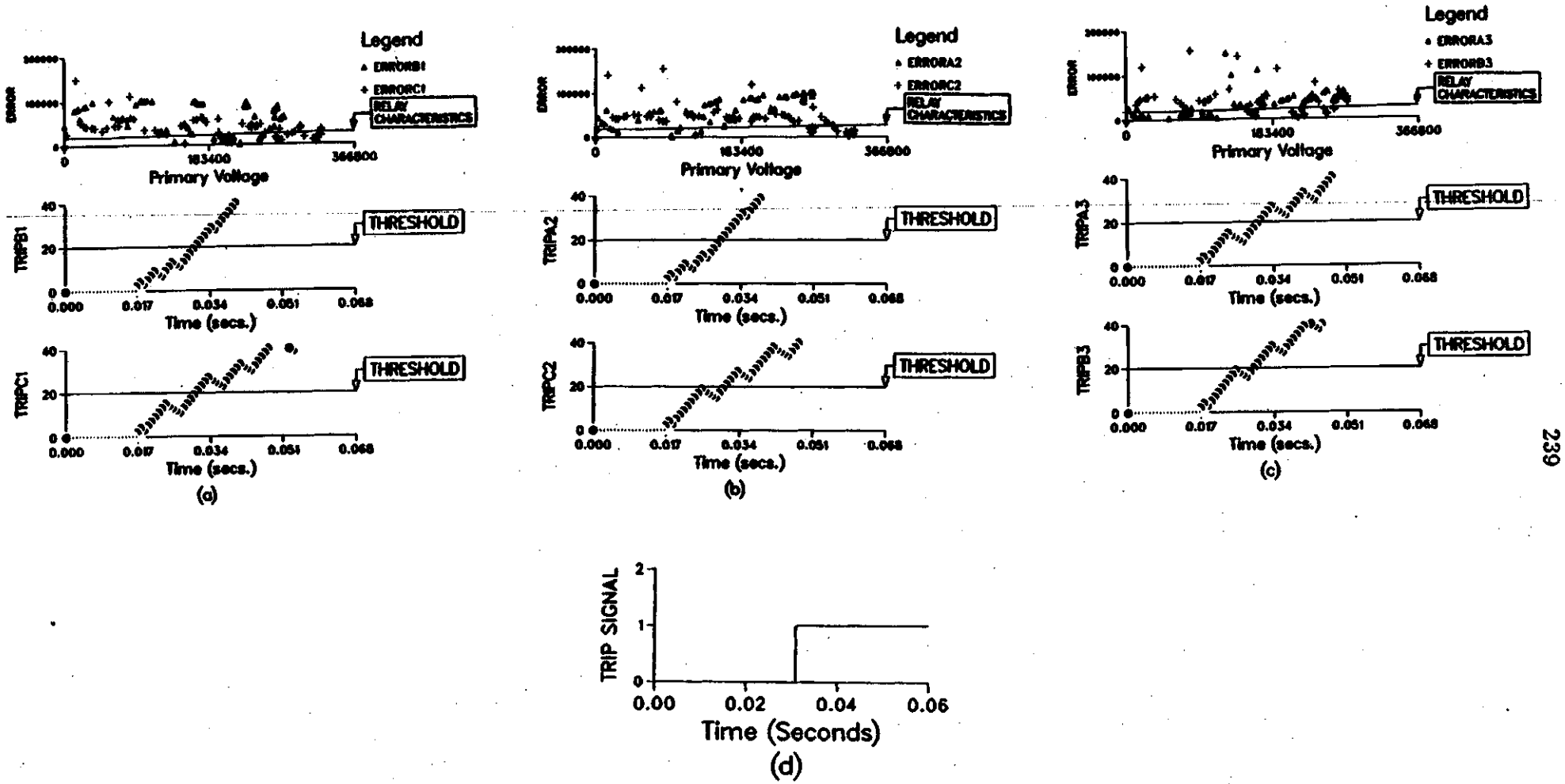

Figure G.7: Errors and values of the trip indices for a condition when the transformer is switched on with an internal fault on secondary side that short circuits phases A and B through a resistance of 1.2 ohms and when (a)phase A, (b)phase B or (c)phase C is used as the "Reference phase". Trip command issued by the system is shown in (d). The transformer was connected to the supply at 0.0167 s.

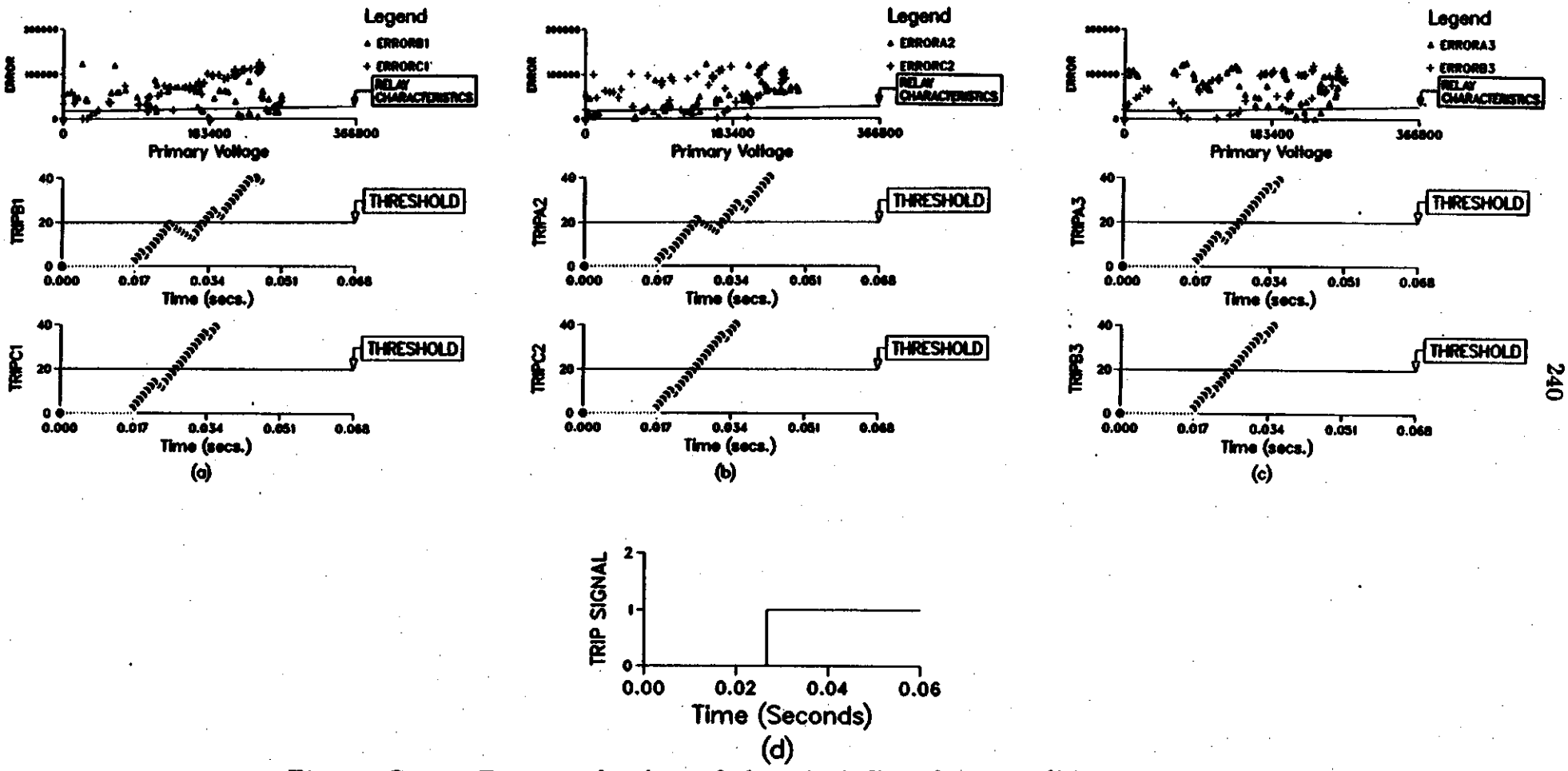

Figure G.8: Errors and values of the trip indices for a condition when the transformer is switched on with an internal fault on secondary side that short circuits phases A, B and C through a resistance of 1.2 ohms and when (a)phase A, (b)phase B or (c)phase C is used as the "Reference phase". Trip command issued by the system is shown in (d). The transformer was connected to the supply at 0.0167 s.

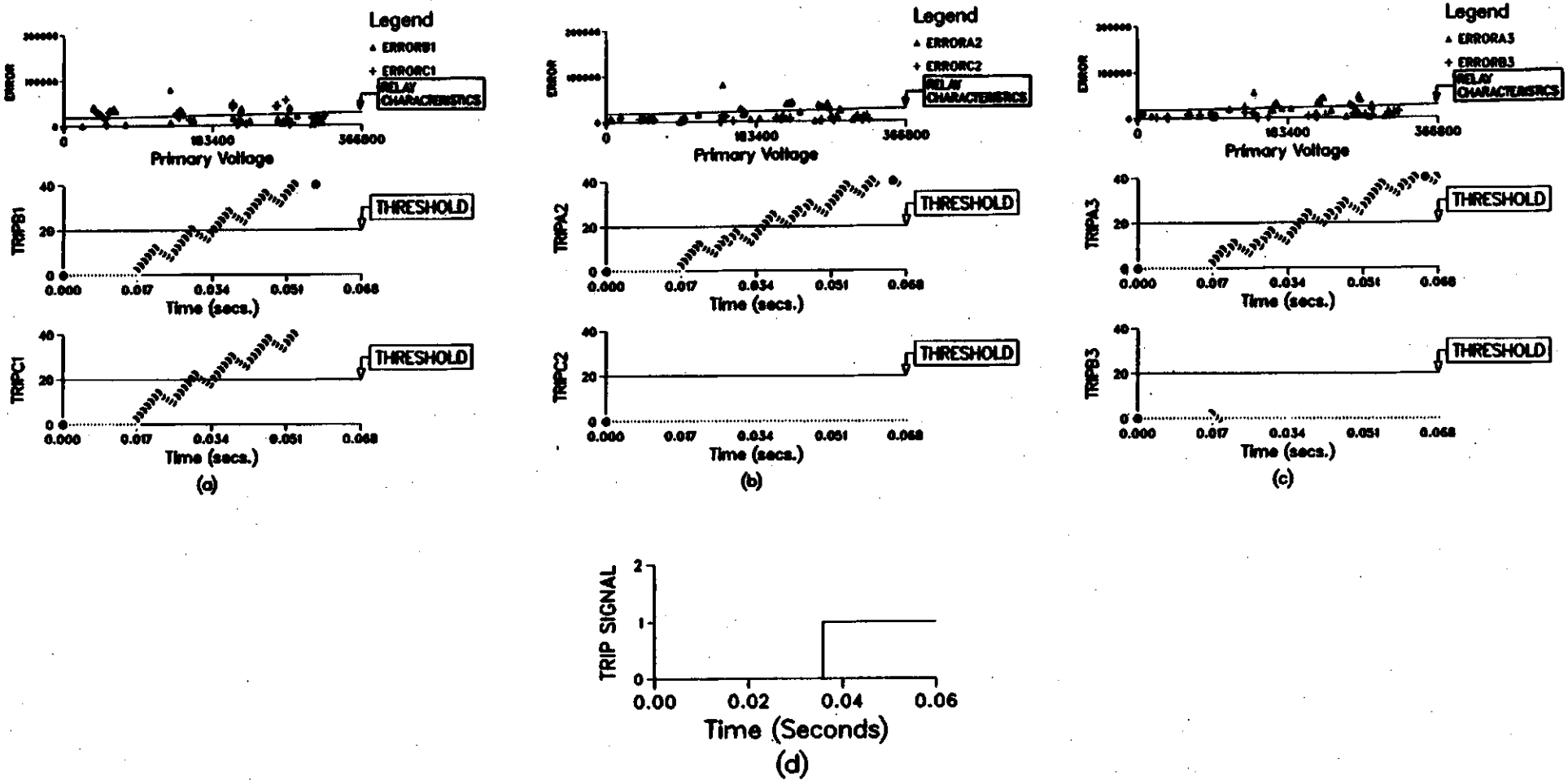

Figure G.9: Errors and values of the trip indices for a condition when the transformer is switched on with an internal fault on primary side that short circuits phase A through a resistance of 1.2 ohms and when (a)phase A, (b)phase B or (c)phase C is used as the "Reference phase". Trip command issued by the system is shown in (d). The transformer was connected to the supply at 0.0167 s.

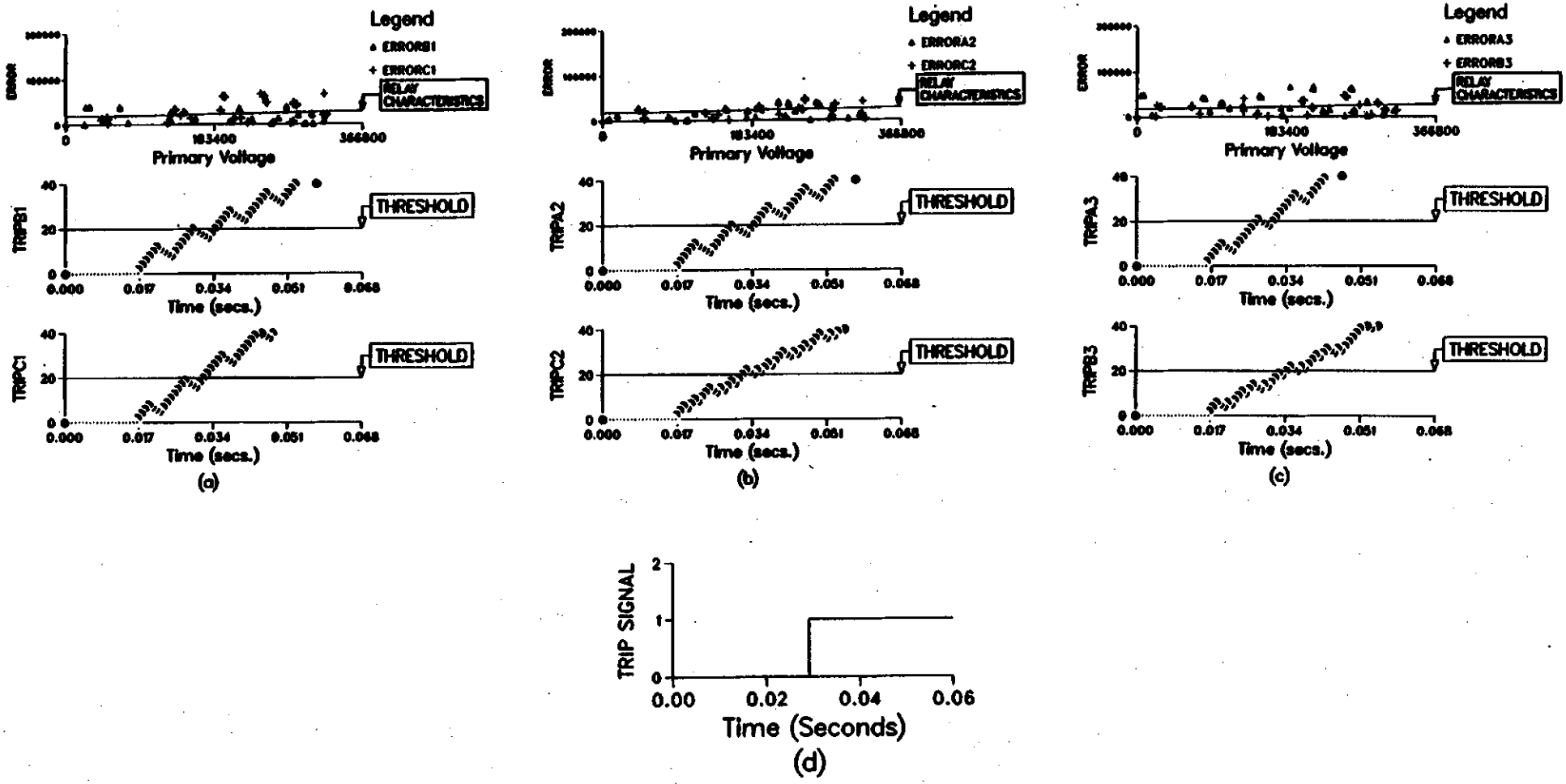

Figure G.10: Errors and values of the trip indices for an internal fault on the primary side that short circuits phases A and C through a resistance of 1.2 ohms and when (a)phase A, (b)phase B or (c)phase C is used as the "Reference phase". Trip command issued by the system is shown in (d). The fault was applied at 0.0167 s.

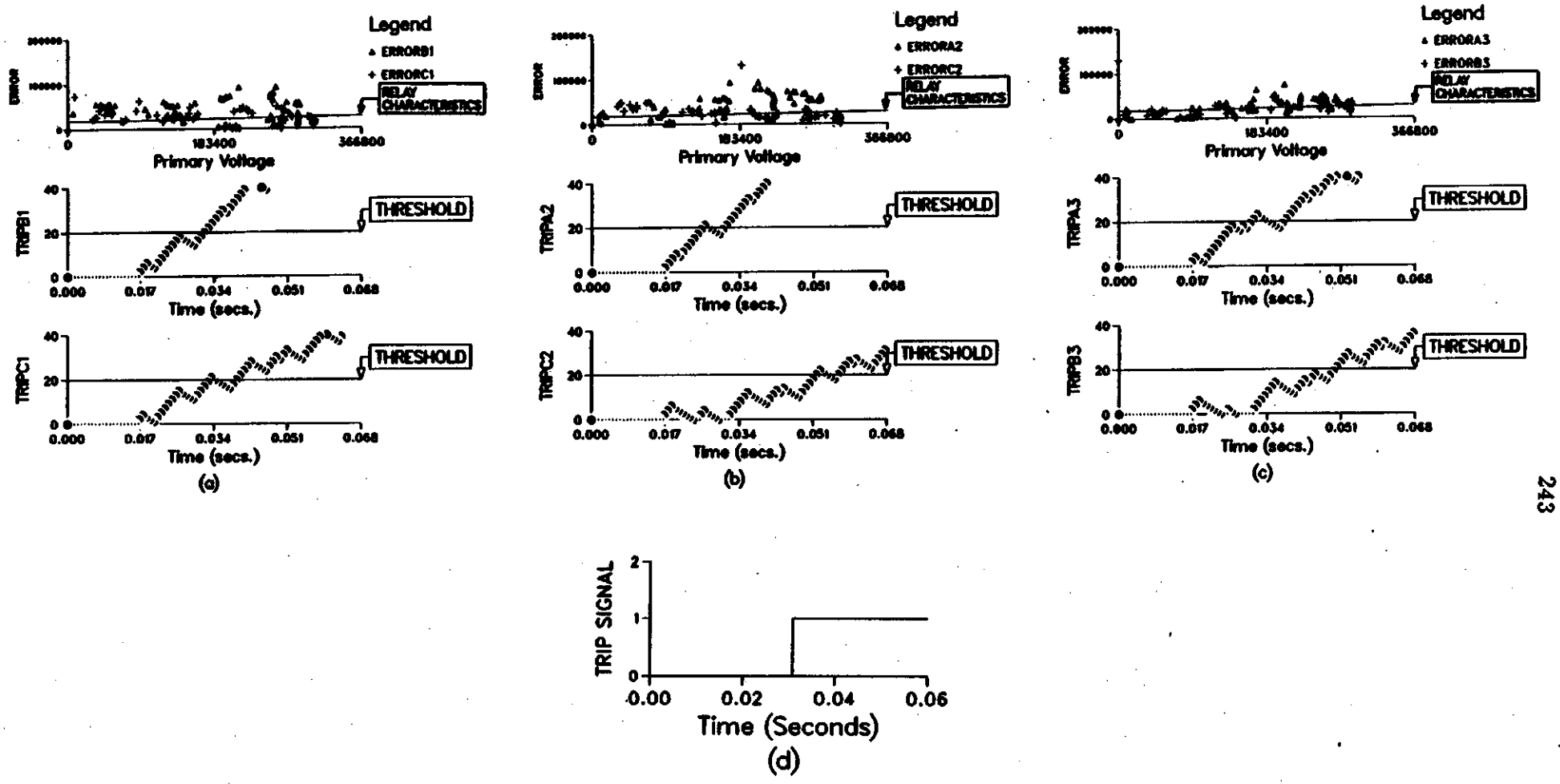

Figure G.11: Errors and values of the trip indices for a condition when the transformer is switched on with an internal fault on the primary side that short circuits phases A and B through a resistance of 1.2 ohms and when (a)phase A, (b)phase B or (c)phase C is used as the "Reference phase". Trip command issued by the system is shown in (d). The transformer was connected to the supply at 0.0167 s.

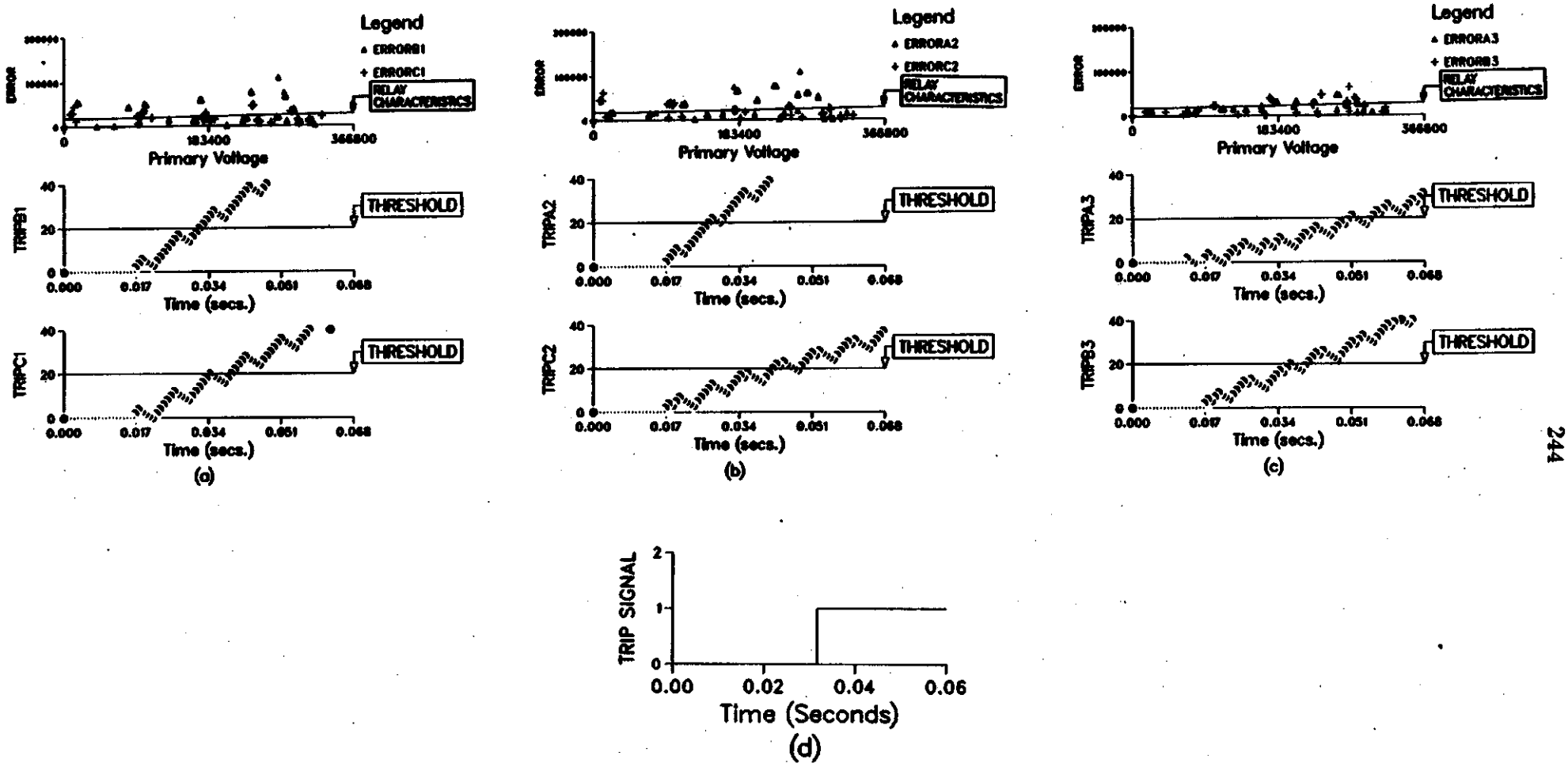

Figure G.12: Errors and values of the trip indices for an internal fault on the primary side that short circuits phases A and B through a resistance of 1.2 ohms and when (a)phase A, (b)phase B or (c)phase C is used as the "Reference phase". Trip command issued by the system is shown in (d). The fault was applied at 0.0167 s.

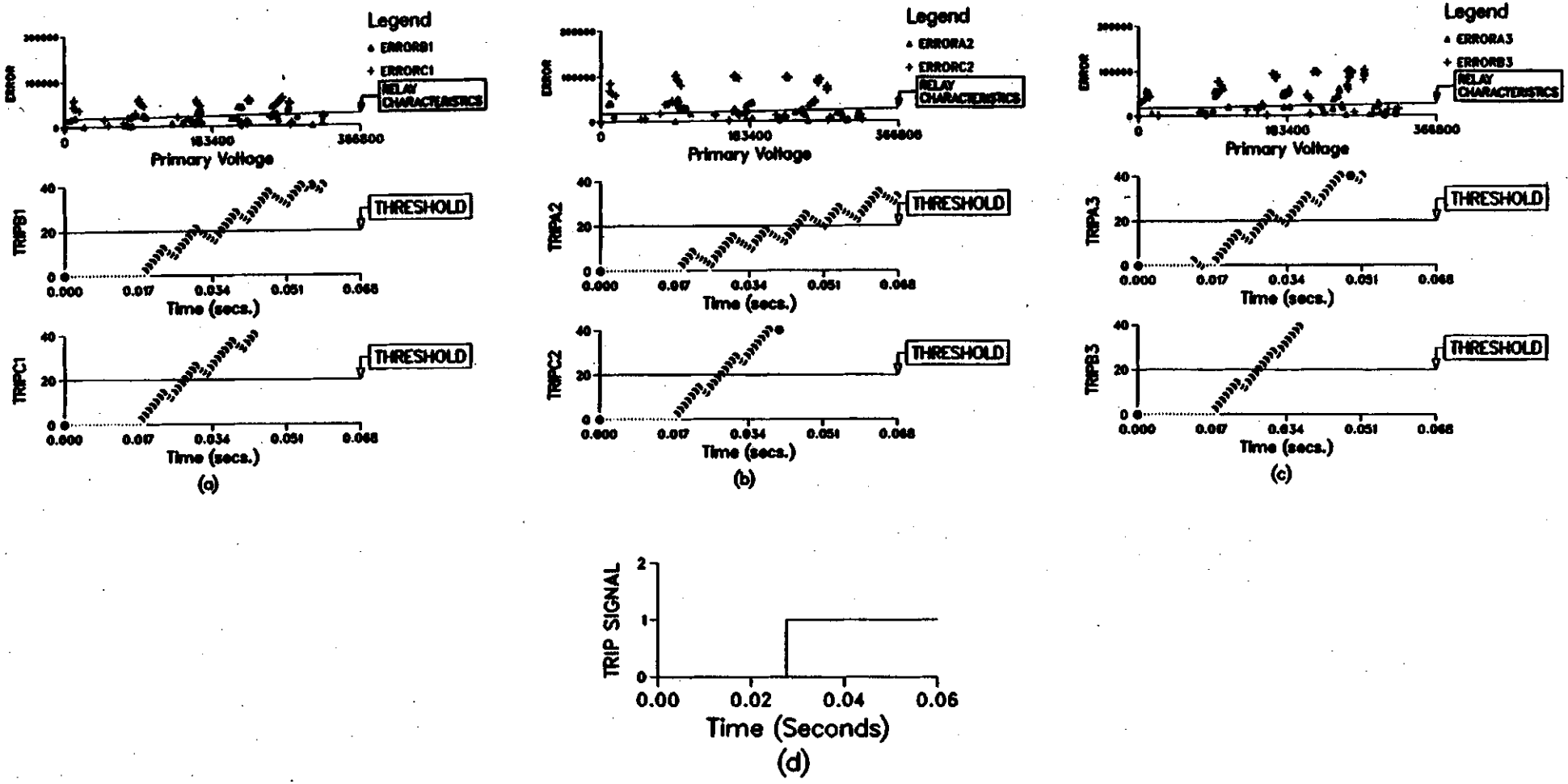

Figure G.13: Errors and values of the trip indices for an internal fault on the secondary side that short circuits phases B and C through a resistance of 1.2 ohms and when (a)phase A, (b)phase B or (c)phase C is used as the "Reference phase". Trip command issued by the system is shown in (d). The fault was applied at 0.0167 s.

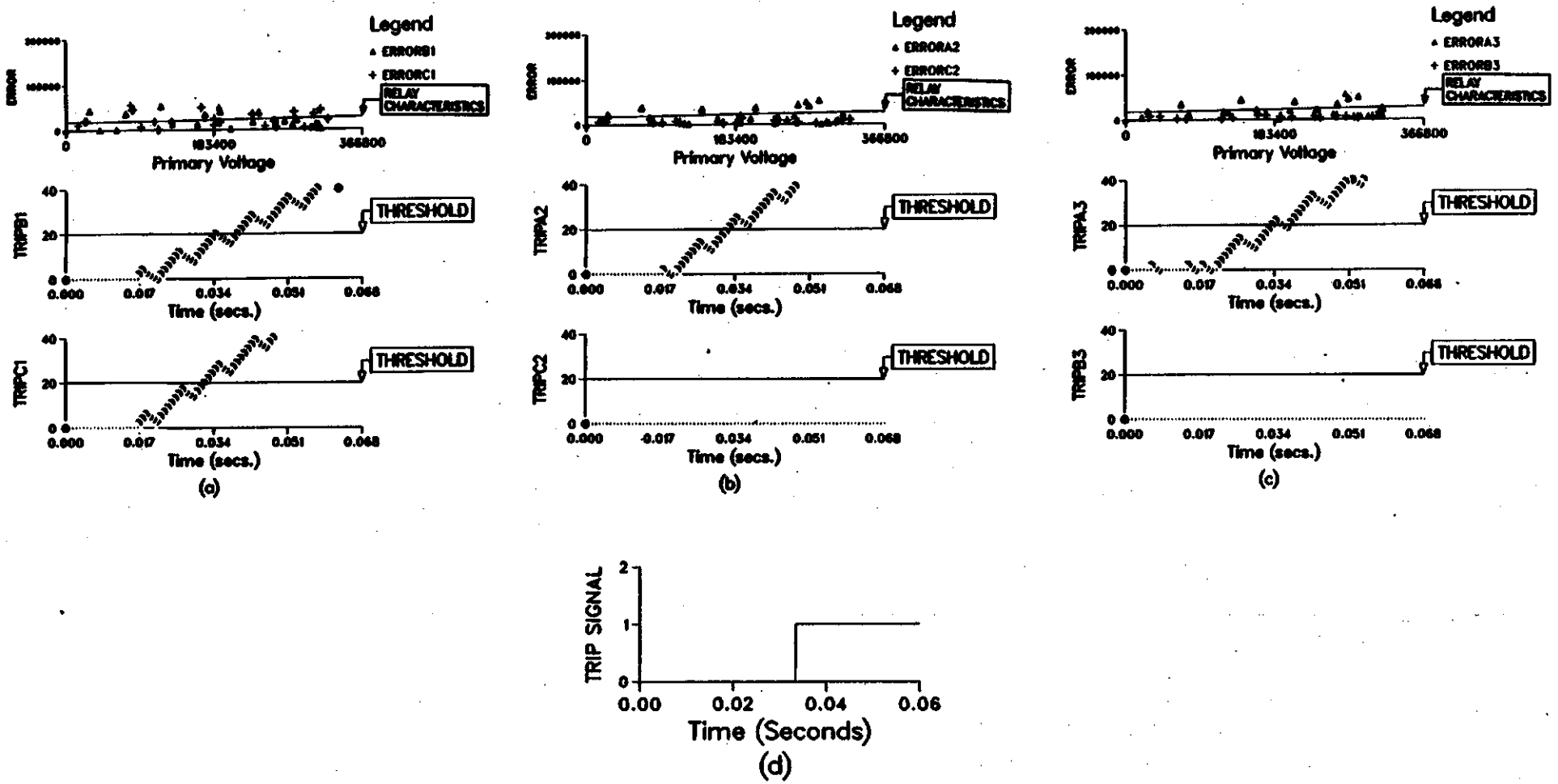

Figure G.14: Errors and values of the trip indices for an internal fault on the secondary side that short circuits phase A through a resistance of 1.2 ohms and when (a)phase A, (b)phase B or (c)phase C is used as the "Reference phase". Trip command issued by the system is shown in (d). The fault was applied at 0.0167 s.

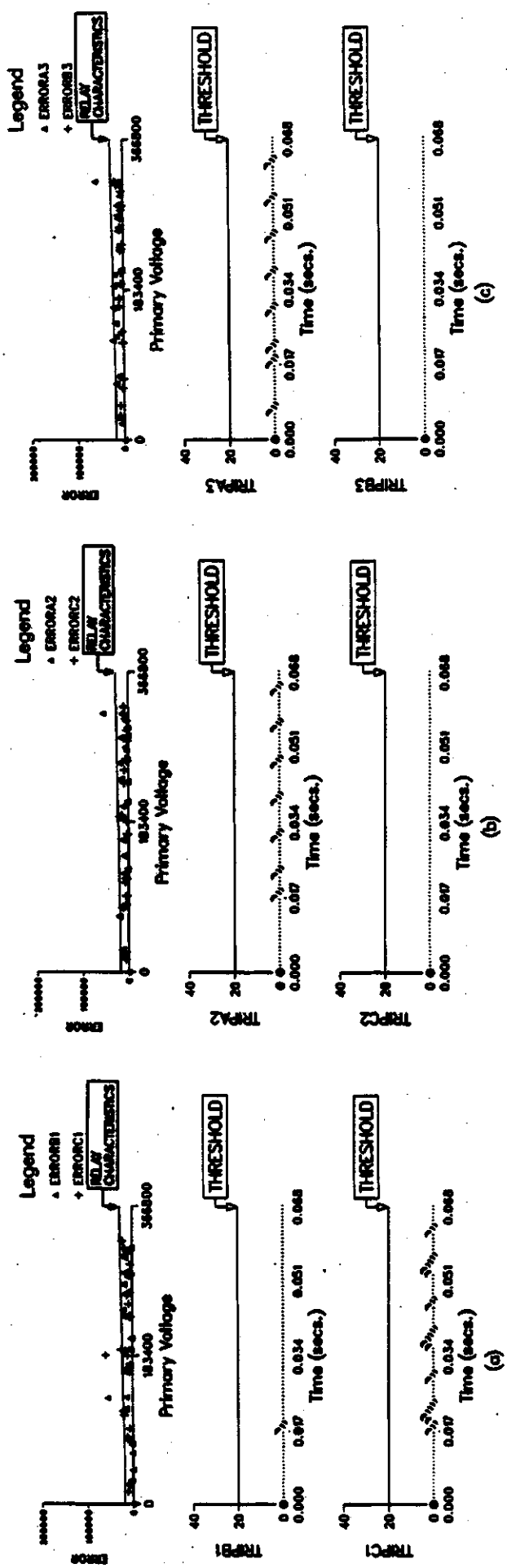

Figure G.15: Errors and values of the trip indices for an external fault that involves phases A and ground when (a)phase A, (b)phase B or (c)phase C is used as the "Reference phase". The fault was applied at 0.0167 s.

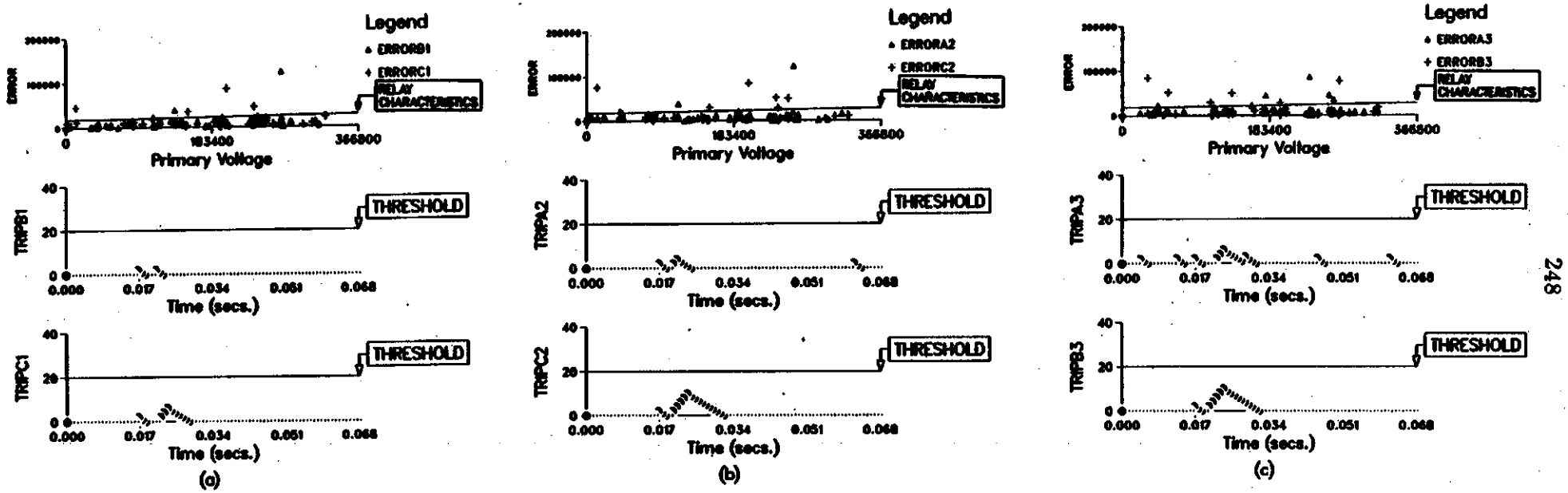

Figure G.16: Errors and values of the trip indices for a three phase external fault when (a)phase A, (b)phase B or (c)phase C is used as the "Reference phase". The fault was applied at 0.0167 s.

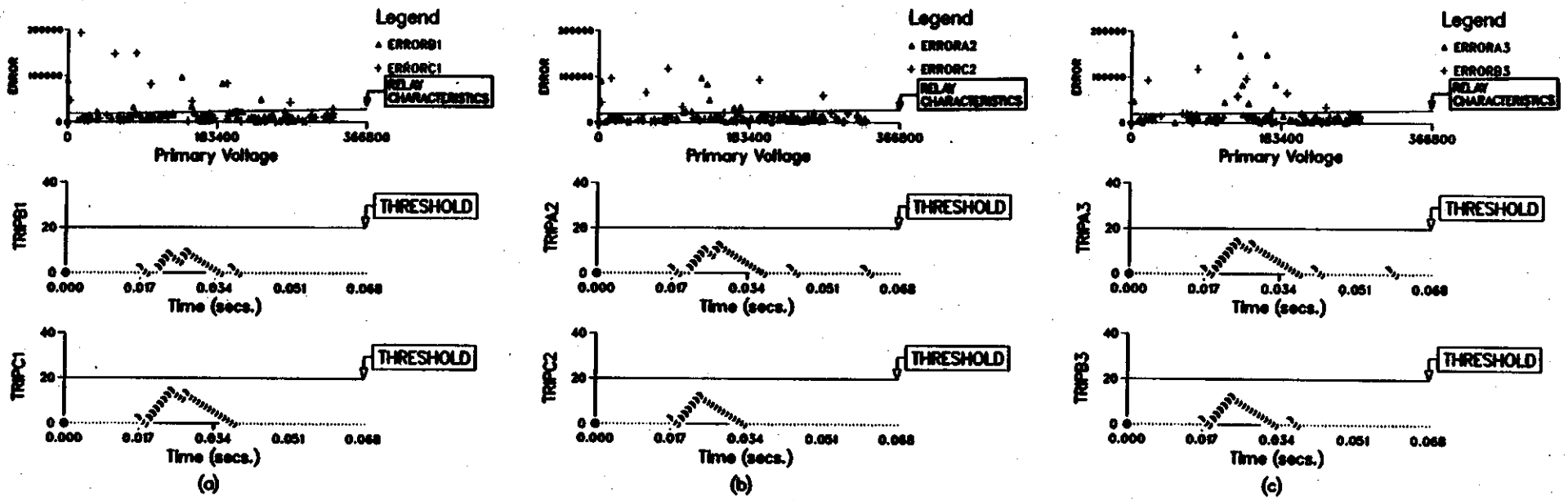

Figure G.17: Errors and values of the trip indices for a condition when the transformer is switched on with an external fault involving phases A and B and when (a)phase A, (b)phase B or (c)phase C is used as the "Reference phase". The transformer was connected to the supply at 0.0167 s.

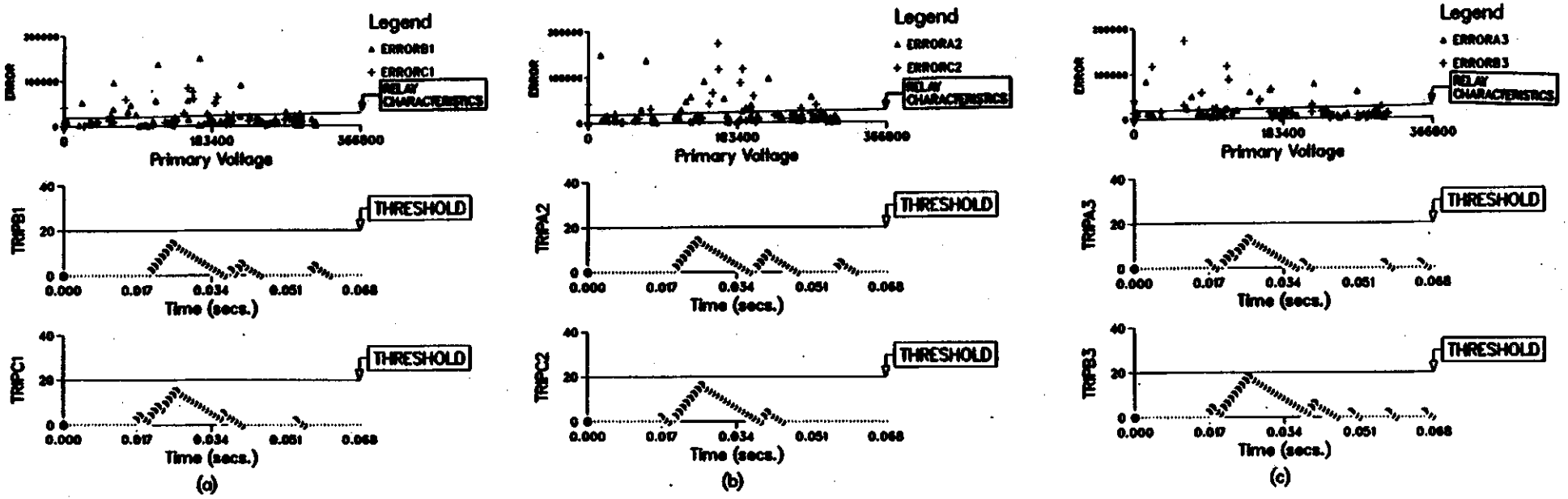

Figure G.18: Errors and values of the trip indices for a condition when the transformer is switched on with an external fault involving phase C and ground and when (a)phase A, (b)phase B or (c)phase C is used as the "Reference phase". The transformer was connected to the supply at 0.0167 s.